IN VIVO DISCOVERIES IN MDM2-MEDIATED P53 REGULATION

Nicole Rae Tackmann

A dissertation submitted to the faculty at the University of North Carolina at Chapel Hill in partial fulfillment of the requirements for the degree of Doctor of Philosophy in the Curriculum in Genetics and Molecular Biology in the School of Medicine.

Chapel Hill
2017

Approved by:

Adrienne Cox

Jeffrey MacDonald

Karen Mohlke

Qing Zhang

Yanping Zhang

ABSTRACT

Nicole Rae Tackmann: DISCOVERIES IN MDM2-MEDIATED P53 REGULATION *IN VIVO*
(Under the direction of Yanping Zhang)

The transcription factor p53 is a stress sensor and tumor suppressor. Its many target genes contribute to tumor suppression through regulation of cell cycle arrest, senescence, apoptosis, and metabolism. Ubiquitously transcribed and translated, p53 regulation is primarily mediated through mouse double minute 2 (MDM2). MDM2 binds to p53, inhibits its transcriptional activation capabilities, and harbors E3 ubiquitin ligase activity to facilitate p53 degradation. Upon cellular stress, upstream signaling transducers modify or bind MDM2 to prevent its inhibition of p53.

Ribosomal proteins (RPs) bind to MDM2 either in the response to ribosomal biogenesis stress or oncogenic overproduction of RPs, which occurs in cancer due to increased proliferation. p19ARF also transduces hyperproliferative signals, inhibiting MDM2 to stabilize p53. Both p19ARF- and RP-MDM2 binding are important for p53 activation following oncogenic c-MYC overexpression, but whether these interactions are interdependent was unknown. We utilized mice bearing the $MDM2^{C305F}$ mutation, which disrupts RPL11- and RPL5-MDM2 binding, crossed them with mice containing deletion of p19ARF, and examined c-MYC-induced tumorigenesis. We found that concomitant disruption of these signals enhanced tumorigenesis, indicating that RP-MDM2 and p19ARF-MDM2 binding are two distinct mechanisms causing c-MYC-induced p53 activation.

Further, we examined whether RP-MDM2 interaction could transduce proliferative signals in cancers driven by other oncogenes. We crossed $MDM2^{C305F}$ mice to mice bearing an $Hras^{G12V}$ transgene or an Apc^{Min} allele, which promote melanoma and colorectal tumor

formation, respectively. We found that in response to RAS stimulation, RPL11 and RPL5 do not participate in MDM2 inhibition. In response to APC deletion, RPL11 and RPL5 expression and MDM2 binding are increased in a colon-specific manner. As a result, $MDM2^{C305F}$ mice experience increased colorectal tumorigenesis and decreased p53 activation. Collectively, these results suggest that RP-MDM2 interaction is important for transducing individual oncogenic stress signals in a p19ARF-independent manner.

We have also examined the role of MDM2 E3 ligase activity in controlling p53 following the overexpression of c-MYC. Using mice bearing the $MDM2^{Y487A}$ mutation, which disrupts MDM2 E3 ligase activity, we found that MDM2 E3 ligase activity is dispensable for regulating p53 following oncogenic c-MYC overexpression and surprisingly that its disruption may provide a survival advantage.

ACKNOWLEDGMENTS

I would like to thank the many people that have contributed to my intellectual, professional, and personal development during my time as a graduate student. Without their guidance, this work would not have been possible.

My mentor, Yanping Zhang for allowing me the freedom to develop my own research, but also encouraging me to collaborate and help others with their own projects. His leadership style encouraged me to think independently but also to seek help when I need it.

Past and current members of the Zhang Lab, who have been integral sources of learning and friendship: Derek Franklin, Shijie Liu, Patrick Leslie, Jing Yang, Hui Tian, Anqun Tang, Laura Rowley, Yizhou He, Yong Liu, Xuan Meng, Tae-Hyung Kim, Fuyuki Sato, Aiwen Jin, and Lishi Zhou. I am particularly indebted to Xuan Meng and Shijie Liu for their essential contributions to this work and investment in my training. I also want to thank Laura Rowley and Derek Franklin for their continued mentorship throughout my professional development.

My committee members, who have been helpful advisors and generous sources of expertise: Adrienne Cox, Qing Zhang, Jeffrey MacDonald, and Karen Mohlke.

My family, for always supporting and encouraging me during my graduate training. To my husband, Jeff, you have always believed in me and given me strength during the toughest times. To my parents, Tim and Sue, you have given me a foundation of love and reassurance. To my brothers, Adam and Torin, I am thankful for your comradery and unrelenting ability to keep me humble. To my “adopted” sisters, Amy, Rose, and Emily, knowing you has been an honor, and you have made me a better person. Finally, all of my friends and colleagues that I have had the privilege to know or work with during my time at UNC. You have made my graduate school experience one of the most transformative periods of my life.

TABLE OF CONTENTS

LIST OF TABLES

LIST OF FIGURES

LIST OF ABBREVIATIONS

4E-BP1	eukaryotic initiation factor 4E-binding protein
4-OHT	4-hydroxytamoxifen
AKT	protein kinase B, PKB
APAF1	apoptotic protease-activating factor 1
APC	adenomatous polyposis coli
ATM	ataxia-telangiectasia mutated
ATP	adenosine triphosphate
B23/NPM1	nucleophosmin/nucleolar phosphoprotein B23
BAX	BCL-2-associated X protein
BCL-2	B-cell lymphoma 2
BCR-ABL	breakpoint cluster region and abelson murine leukemia viral oncogene homolog 1 fusion protein
BOP1	block of proliferation 1
CC-3	cleaved caspase 3
chga	chromogranin A
ChIP	chromatin immunoprecipitation
CHK2	checkpoint kinase 2
CreER	cre recombinase estrogen receptor
DDX5	DEAD-Box Helicase 5
DKC1	dyskerin
DNA	deoxyribonucleic acid
E2F1	E2F transcription factor 1
eIF4e	eukaryotic translation initiation factor 4E
ERK	extracellular signal-regulated kinase

FBL	fibrillarin
G1	gap 1 phase
GADD45α	growth arrest and DNA damage-inducible protein GADD45 alpha
GAPDH	glyceraldehyde 3-phosphate dehydrogenase
GCN5	histone acetyltransferase GCN5
GLS2	glutaminase 2
GLUT1	glucose transporter 1
GLUT4	glucose transporter 4
H&E	hematoxylin and eosin stain
IHC	immunohistochemistry
IP	immunoprecipitation
IR	ionizing radiation
Ki-67	marker of proliferation Ki-67
lgr5	leucine-rich repeat-containing G-protein coupled receptor 5
lyz1	lysozyme 1
MAX	myc-associated factor X
MCD	malonyl-CoA decarboxylase
MDM2	mouse double minute 2
MDMX	mouse double minute 4
MEF	mouse embryo fibroblast
MEK	mitogen-activated protein kinase kinase
mTOR	mammalian target of rapamycin
muc2	mucin 2
MYC	MYC proto-oncogene protein
NCL	nucleolin

NES	nuclear export signal
NLS	nuclear localization signal
NOP56	nucleolar protein 56
NOXA	phorbol-12-myristate-13-acetate-induced protein 1
NRF2	nuclear factor erythroid 2-related factor
$p16^{INK4A}$	cyclin-dependent kinase inhibitor 2A
p19ARF	mouse alternative reading frame tumor suppressor (p14ARF in human)
p300	histone acetyltransferase p300
p53ER	p53 estrogen receptor
PCNA	proliferating cell nuclear antigen
PCR	polymerase chain reaction
PFK2	6-phosphofructo-2-kinase/fructose-2,6-biphosphatase 3
PI3K	phosphoinositide 3-kinase
POLI	RNA polymerase I
POLII	RNA polymerase II
POLIII	RNA polymerase III
PUMA	p53 upregulated modulator of apoptosis
qPCR	quantitative polymerase chain reaction
RAS	RAS proto-oncogene
RE	response element
RING	really interesting new gene
RNA	ribonucleic acid
RP	ribosomal protein
RPL11	60S ribosomal protein L11
RPL23	60S ribosomal protein L23

RPL5	60S ribosomal protein L5
S	synthesis phase (of mitosis)
SEM	standard error of the mean
siRNA	short interfering RNA
SNP	single nucleotide polymorphism
TFIID	transcription factor II D
TIGAR	TP53 induced glycolysis regulatory phosphatase
TIP60	histone acetyltransferase KAT5
TRRAP	transformation/transcription domain-associated protein
TTF-I	RNA polymerase I transcription termination factor
TUNEL	terminal deoxynucleotidyl transferase-mediated dUTP-biotin nick end labeling
Ub	ubiquitin
WB	Western blot
WT	wild-type

CHAPTER 1: INTRODUCTION[1]

Since its discovery almost 40 years ago (DeLeo et al., 1979; Kress et al., 1979; Lane and Crawford, 1979; Linzer and Levine, 1979), the transcription factor tumor protein 53 (TP53, hereafter referred to as p53) has been one of the most highly studied proteins. p53 is famously known as the 'guardian of the genome' (Efeyan and Serrano, 2007; Lane, 1992) due to its participation in the repair of damaged DNA, but it has been appreciated that p53 contributes to a multitude of cellular functions, including but not limited to: cell cycle arrest, programmed cell death (apoptosis), cell senescence, cell differentiation, energy metabolism, angiogenesis, cell communication, organismal fertility and immune response (Menendez et al., 2009). Considering these various functions, p53 is thought to be a master regulator of stress response that plays a crucial role in cancer prevention.

Much of p53 research has focused on the downstream targets that contribute to its function as a stress regulator, but the signals that contribute to p53 activation both at basal levels and in response to stress are also being actively pursued. This introduction will initially explore the known functions of p53 and its role as a tumor suppressor. Next, this introduction will delve into the regulation of p53 *in vivo*, and explore the upstream cancer-associated factors that contribute to p53 activation. Finally, the purpose of this dissertation will be addressed,

[1] Portions of this chapter discussing *in vivo* MDM2 and MDMX studies were adapted from a review article published in Journal of Molecular Cell Biology. I wrote the manuscript, Yanping Zhang and I edited the manuscript, and Yanping Zhang finalized the manuscript. The original citation is as follows: Tackmann, N.R., and Zhang, Y. (2017). Mouse modelling of the MDM2/MDMX-p53 signalling axis. Journal of Molecular Cell Biology *9*, 34-44.

which focuses on clarifying the contributions of the upstream and downstream signals responsible for p53 regulation *in vivo*.

p53 functions

The broadest, most well-studied function of p53 is that of a transcription factor. In the presence of other cofactors p53 binds DNA, typically in the promoter region of a gene, and activates or represses the expression of that gene. There are more than one hundred genes that have been characterized as p53 targets, and new p53 target genes are discovered every year. Broadly, targets of p53 transcriptional activation participate in promoting cell cycle arrest, apoptosis, DNA damage repair, and senescence, as well as controlling cell metabolism. A host of stress signals converge to activate p53, including DNA damage, oxidative stress, nutrient depletion, hypoxia, nucleolar stress, and proliferative signals, most of which are present in the tumor ecosystem.

Although p53 is widely known as a tumor suppressor protein, upon its discovery p53 was originally classified as an oncogene (DeLeo et al., 1979; Kress et al., 1979; Lane and Crawford, 1979; Linzer and Levine, 1979). It is now well known that p53, encoded by *TP53*, is frequently mutated or inactivated in various cancers (Muller and Vousden, 2013). Though p53 mutations are commonly found throughout the length of the protein, the most common p53 mutations occur within the DNA-binding domain of p53 and are thought to render p53 functionally inactive as a transcription factor (Pavletich et al., 1993). However, p53 mutations can confer new oncogenic functions, including novel protein binding partners, increased protein stability, and chemotherapeutic resistance in cells (Blandino et al., 1999; Dittmer et al., 1993; Muller and Vousden, 2014; Olive et al., 2004; Song et al., 2007). These discoveries surrounding the oncogenic properties of p53 mutants clarified the original confusion surrounding the tumor suppressor status of p53.

Interestingly, mice deficient for p53 are viable, but tend to develop tumors (typically lymphomas) and die by 6 months of age (Donehower et al., 1992). Mice with heterozygous p53 deletion, on the other hand, tend to develop a wider range of neoplasms, including sarcomas, carcinomas, and lymphomas. This is similar to the pathology of human patients with Li-Fraumeni syndrome, a dominant familial condition in which patients inherit a mutated or null copy of p53, rendering them susceptible to spontaneous tumor development.

In its role as a transcription factor, p53 binds tightly to specific DNA sequences via its central DNA binding domain. Following binding, p53 recruits other transcription or chromatin-modifying proteins to promote or repress gene transcription. The transactivation domain of p53 binds to two subunits of the TFIID complex, $TAF_{II}40$ and $TAF_{II}60$, as well as several other TATA-binding protein-associated factors, which promote the formation of the transcription preinitiation complex (Farmer et al., 1996; Martin et al., 1993; Seto et al., 1992; Thut et al., 1995). p53 also binds to a number of chromatin modifying factors, including p300, a histone acetyltransferase (Lill et al., 1997). The acetylation of histone lysine residues in enhancer and promoter regions is thought to promote more open chromatin structures that are associated with transcriptional activation of genes (Eberharter and Becker, 2002).

The requirements of p53-mediated gene regulation have been extensively studied using both *in vitro* DNA binding assays and *in vivo* chromatin immunoprecipitation (ChIP). Several groups have described a 20-base-pair consensus p53 response element (RE) (Funk et al., 1992; Wang et al., 1995). The consensus sequence for the p53 RE is RRRCWWGYYY…n…RRRCWWGYYY, where R represents a purine, Y represents a pyrimidine, W represents an A or T, and n represents a 0-13 base pair spacer (Menendez et al., 2009). However, many p53 target genes have mismatches within the consensus sequence, and in fact some validated p53 targets only contain half of the canonical response element, deemed a “half site” (Jordan et al., 2008). The high variability within verified p53 response elements likely provides fine-tuning of the p53 regulatory network, as certain response elements may only

be bound by p53 under certain contexts. However, the heterogeneity of p53 RE sequences has also led to challenges and disagreement within the field. For instance, the distinct differences in RE sequences or protein-protein interactions specifically required for p53-mediated gene suppression are not fully understood.

As stated above, p53 target genes are implicated in a wide range of functions. One of the most well-characterized p53 target genes, *cdkn1a* codes for the cell cycle regulator $p21^{WAF1/CIP1}$ (p21 hereafter) (el-Deiry et al., 1993). Following DNA damage and other stresses, p53 transcriptionally upregulates p21, inducing a G1 to S phase cell cycle arrest. This arrest allows the cells to pause and repair DNA damage before continuing forward with cell division. p53 promotes DNA damage repair by transactivating GADD45α (growth arrest and DNA damage inducible alpha), which stimulates DNA excision repair through increased binding with PCNA (proliferating cell nuclear antigen) (Smith et al., 1994). p53 activation also engages the induction of apoptotic machinery, including target genes such as *bax* (BCL-2-associated X protein), *puma* (p53 upregulated modulator of apoptosis), *apaf1* (apoptotic protease-activating factor 1), and *noxa* (phorbol-12-myristate-13-acetate-induced protein 1) (Moroni et al., 2001; Nakano and Vousden, 2001; Oda et al., 2000; Toshiyuki and Reed, 1995). BAX is a BCL-2 family protein that contributes to the permeabilization of the mitochondrial membrane (Chipuk et al., 2004; Pastorino et al., 1998), while PUMA directs BAX to the mitochondrial membrane (Kim et al., 2009). APAF1 forms a complex with cytochrome c to facilitate the activation of caspase 3 (Li et al., 1997; Zou et al., 1997), while NOXA interacts with other BCL-2 family proteins to promote the release of caspase-9 (Oda et al., 2000). More recently, new p53 targets functioning in the control of cell metabolism have also been discovered, including TIGAR (TP53 induced glycolysis regulatory phosphatase), PFKFB3 (6-phosphofructo-2-kinase/fructose-2,6-biphosphatase 3), MCD (malonyl-CoA decarboxylase), GLS2 (glutaminase 2), GLUT1 (glucose transporter 1), and GLUT4 (glucose transporter 4) (Bensaad et al., 2006; Franklin et al., 2016; Hu et al., 2010; Liu et al., 2014b; Schwartzenberg-Bar-Yoseph et al., 2004). These metabolic

targets are highly varied in their functions. GLUT1 and GLUT4 regulate the import of glucose into the cell, while TIGAR and PFKFB3 regulate the flux of glucose into either glycolysis (producing ATP and pyruvate) or into the pentose phosphate pathway (producing NADPH and nucleotides). MCD participates in fatty acid oxidation, and GLS2 is an important tumor-suppressive regulator of glutamine metabolism (Liu et al., 2014a; Szeliga et al., 2014; Zhang et al., 2013a). Through the transcriptional regulation of all of these targets and others, p53 is thought to control the stress response of a cell, mediating a choice between cell death in the case of irreparable damage, or DNA damage repair and cell survival.

Although the canonical p53 functions in promoting cell cycle arrest, apoptosis, and senescence have long thought to be the primary mechanisms of p53 tumor suppression, recent mouse modeling has revealed that these p53 effectors may not be the primary barriers to tumor formation and progression. For example, Li et al. (2012) recently modeled a p53 mouse in which three lysine residues in the DNA binding domain of p53 were mutated to arginine (known as $p53^{3KR}$ mice), thus preventing the acetylation of those residues, which is important for p53-mediated transcriptional upregulation of the target genes p21, PUMA, and NOXA. Canonical apoptotic targets, senescence targets and other cell cycle arrest targets are unable to be transcriptionally upregulated in the $p53^{3KR}$ mouse. Surprisingly, compared to $p53^{-/-}$ mice, $p53^{3KR}$ mice are resistant to tumor formation. The reciprocal experiment was performed by another group using $p21^{-/-};noxa^{-/-};puma^{-/-}$ triple knockout mice, with similar results (Valente et al., 2013). These studies suggest that the primary tumor suppressive functions of p53 may be contingent on its metabolic targets or other protein interactions. Although canonical p53 targets like p21 can still be used as a barometer for p53 activity, these studies have forced the field to reevaluate its philosophy about p53-mediated tumor suppression.

Overview of MDM2/MDMX-mediated p53 regulation

While p53 transcription and translation are largely believed to occur ubiquitously, basal p53 levels and activity are kept relatively low. In response to various stress-inducing stimuli, p53 becomes stabilized and activated, allowing it to serve as a nuclear transcription factor. In general, p53 post-translational modifications are thought to dictate the stability, localization, and activity of p53. For example, p53 ubiquitination mediates its nuclear export and degradation, while acetylation or phosphorylation of p53 at various residues contributes to its activation or choice of target genes (Barlev et al., 2001).

p53 regulation is multifaceted and two additional proteins are considered critically important for proper control: mouse double minute 2 (MDM2) and mouse double minute 4 (MDM4, also known as MDMX), which cooperate to govern the posttranslational stability, localization, and activity of p53 (Hu et al., 2007; Wade et al., 2010). MDM2 was first discovered in the 3T3DM mouse tumor cell line, in which it was amplified through minute circular chromosomes (Fakharzadeh et al., 1991). MDM2 is widely considered to be the primary negative regulator of p53, and it is theorized to achieve p53 inhibition through two distinct mechanisms. MDM2 harbors E3 ubiquitin ligase activity towards p53 through its RING domain, catalyzing the transfer of ubiquitin to p53 from an E2-conjugating enzyme (Haupt et al., 1997; Honda et al., 1997; Jackson and Berberich, 2000; Kubbutat et al., 1997). The ubiquitination of p53 leads to its export from the nucleus into the cytoplasm, where it can be degraded by the 26S proteasome (Lohrum et al., 2001). MDM2 also inhibits p53 activity by binding to the p53 transactivation domain through its N-terminal p53 binding domain (Chen et al., 1993).

Both MDM2 and MDMX can directly bind to the p53 transactivation domain and inhibit p53-mediated transcription of its target genes (Chen et al., 1993; Shvarts et al., 1996). MDM2 and MDMX are highly homologous, sharing similar p53-binding domains and RING domains (Shvarts et al., 1996). MDM2 and MDMX interact via their RING domains to form a heterodimer, and this heterodimer has been proposed to promote more efficient p53 inhibition than MDM2 or

MDMX alone (Tanimura et al., 1999). In addition to regulating p53 stability and activity, *mdm2* was also discovered to be a p53 target gene (Barak et al., 1993). It is thought that following p53-activation, this feedback loop is important for returning p53 to basal levels and activity.

Although approximately 50% of cancers have a mutation in p53 (Muller and Vousden, 2013), it is less commonly appreciated that WT p53 is often functionally inactivated. This is commonly accomplished through aberrantly expressed MDM2 or MDMX, which reduce total and nuclear p53 levels and activity (Tovar et al., 2006). This trend is supported by *in vivo* data. Transgenic *Mdm2* or *MdmX* overexpression in mice supports increased spontaneous tumor development due to decreased p53 activity (Jones et al., 1998; Xiong et al., 2010). Mice bearing a cancer-associated human SNP contributing to increased *Mdm2* transcription are also susceptible to decreased p53 function and increased tumorigenesis (Bond et al., 2004; Post et al., 2010), suggesting that naturally occurring MDM2 “overexpression” (as opposed to transgenic overexpression) contributes to p53 functional inactivation and cancer.

In general, p53 activation and stabilization is thought to occur two ways. In response to stress, upstream signaling proteins place posttranslational marks on p53 (such as phosphorylation) that prevent its interactions with MDM2 and MDMX. Second, these upstream signaling proteins inhibit MDM2 or MDMX via direct protein interaction or by posttranslational modification. These activities serve to prevent MDM family protein mediated p53 inhibition and degradation.

In vivo **studies of MDM-mediated p53 regulation**

Lessons from knockout mice

In vivo models have furthered our understanding of the physiologic intricacies of p53 regulation by MDM2 and MDMX. Although early *in vitro* work demonstrated that MDM2 could bind to p53 and mask p53 transactivation activity (Chen et al., 1993; Oliner et al., 1993), the degree of MDM2 importance to p53 regulation was not fully appreciated until the creation of

Mdm2 deletion alleles in the mouse (de Oca Luna et al., 1995; Jones et al., 1995). Surprisingly, mice deficient for MDM2 die between embryonic days 4.5−6.5, with pronounced levels of apoptosis throughout the embryo. This embryonic lethality caused by loss of MDM2 is rescued by concomitant loss of p53, suggesting that the primary function of MDM2 during embryogenesis is to inhibit undue p53 activation or accumulation. These studies also established that MDM2 and p53 are expressed ubiquitously during embryonic development.

MDM2-mediated p53 regulation also remains essential in the adult mouse. The p53-dependent embryonic lethality caused by MDM2 deficiency renders the study of MDM2 in p53 regulation difficult *in vivo*. To address this, Christophorou et al. (2005) developed a mouse model expressing the hormone-binding domain of a modified estrogen receptor placed at the 3' end of the *TP53* coding sequence, therefore generating a switchable chimeric p53 protein (p53ER hereafter) that is only active in the presence of tamoxifen or 4-hydroxytamoxifen (4-OHT). The p53ER protein behaves like a null allele in the absence of tamoxifen, which allows for the generation of MDM2-deficient mice and the study of MDM2-dependent p53 regulation in the adult mouse. Ringshausen et al. (2006) then crossed $p53^{ER/-}$ mice with $Mdm2^{+/-}$ mice to generate $Mdm2^{-/-};p53^{ER/-}$ mice. Strikingly, all $Mdm2^{-/-};p53^{ER/-}$ mice died within 5-6 days after a single tamoxifen injection and displayed severe anemia and bone marrow ablation. Several proliferative tissues were also severely atrophied, including small intestine and colon tissue. On the other hand, classically radio-insensitive tissues such as the heart and kidney appeared normal following tamoxifen treatment. However, in all tissues examined, p53 was more transcriptionally active, though not to levels associated with cell death, suggesting that the loss of MDM2 allows for spontaneous p53 activation throughout the body (Ringshausen et al., 2006).

In a similar study, Zhang et al. (2014a) used a conditional *Mdm2* deletion allele ($Mdm2^{FM}$) (Grier et al., 2002) coupled with a whole body, tamoxifen-inducible, Cre-mediated recombination allele (CreER) to study the effects of whole body *Mdm2* loss at various stages of aging, since overall p53 activity has been shown to decline with age (Feng et al., 2007). Similar

to *Mdm2*$^{-/-}$;*p53*$^{ER/-}$ mice, 2-4 month old *Mdm2*$^{FM/-}$;*CreER* mice experience p53-mediated morbidity within a few days after tamoxifen injection. In addition to extensive damage to radio-sensitive tissues, *Mdm2*$^{FM/-}$;*CreER* mice also display extensive levels of apoptosis/atrophy in the kidney and liver, radio-insensitive tissues. It appears that loss of *Mdm2* results in spontaneous p53 stabilization and activation in most organs and that MDM2 is required for viability in mice of all ages.

Several other studies (Table 1.1) have generated tissue-specific deletions of *Mdm2* using conditional *Mdm2* deletion alleles combined with tissue-specific Cre expression, including expression in differentiated intestinal smooth muscle cells, erythroid, and cardiac tissue (Boesten et al., 2006; Grier et al., 2006; Maetens et al., 2007; Xiong et al., 2006). Others have coupled whole body *Mdm2* deletions with tissue-specific reintroduction of p53 (Francoz et al., 2006). Most tissues in which *Mdm2* has been deleted, especially those that are highly proliferative, exhibit substantially increased levels of apoptosis, suggesting that basal MDM2-mediated p53 regulation is critical in nearly all tissues and that too much p53 can be lethal.

Similar to MDM2, loss of MDMX in the mouse is also embryonic lethal, with concomitant *TP53* deletion rescuing the lethality (Parant et al., 2001), suggesting that MDM2 and MDMX play non-redundant roles in the inhibition of p53 activation or stabilization. Interestingly, overexpression of an MDM2 transgene (*Mdm2*$^{Tg/+}$) can rescue MDMX deletion (Steinman et al., 2005), hinting that MDM2 is capable of restraining undue p53 activity *in vivo* but that it may require MDMX for efficient inhibition. From these studies, it is possible to speculate that MDMX serves to either directly enhance MDM2 inhibitory functions or enhance its stability.

It also appears that MDMX is less important to p53 regulation in the adult mouse than MDM2. Garcia et al. (2011) combined *MdmX*$^{+/-}$ mice with the p53ER model to generate *MdmX*$^{-/-}$;*p53*$^{ER/-}$ mice and tested whether, like MDM2, MDMX is critical to p53 suppression in the adult mouse. Surprisingly, *MdmX*$^{-/-}$;*p53*$^{ER/-}$ mice injected with tamoxifen daily live an average of 29 days. Spontaneous p53 activity was also observed in select tissues. Six hours after tamoxifen

injection and in the absence of MDMX, the mRNA expression of p53 cell cycle target gene *cdkn1a* (*p21*) was significantly increased in almost all tissues examined. However, the mRNA expression of *puma*, a p53 apoptotic target, was only significantly increased in radio-sensitive tissues. The expression of *p21* following p53ER restoration correlated with decreased proliferation in tissues, while the expression of *puma* correlated with increased apoptosis. In contrast to *Mdm2*$^{-/-}$;*p53*$^{ER/-}$ mice, *MdmX*$^{-/-}$;*p53*$^{ER/-}$ mice are remarkably tolerant to temporary p53ER restoration. After daily injections of tamoxifen for one week, *MdmX*$^{-/-}$;*p53*$^{ER/-}$ mice displayed significant loss of cell proliferation in the spleen, bone marrow, and thymus tissue, but following withdrawal of tamoxifen, the mice were able to recover without long-term adverse consequences. Tissue-specific p53 restoration studies in *MdmX*$^{-/-}$ mice and tissue-specific deletions of *MdmX* have further indicated that the necessity of MDMX in p53 regulation is context dependent; conversely, many conditional deletion studies support the idea that MDM2 is critical in the suppression of basal p53 in almost all situations.

Consistent with this idea, several groups have suggested that MDMX serves to enhance MDM2-mediated p53 degradation (Badciong and Haas, 2002; Gu et al., 2002; Linke et al., 2008). The relatively better survival of *MdmX*$^{-/-}$;*p53*$^{ER/-}$ mice compared to *Mdm2*$^{-/-}$;*p53*$^{ER/-}$ mice in response to transient p53ER restoration suggests that MDM2 is at least capable of restraining p53 on its own for short periods of time, but it is conceivable that efficient MDM2-mediated p53 inhibition or degradation is required for long-term viability. Indeed, the levels of p53 are increased in *MdmX*$^{-/-}$;*p53*$^{ER/-}$ MEFs compared to MEFs containing MDMX (Garcia et al., 2011), supporting the idea that MDMX plays some role in regulating p53 stability *in vivo*. It is possible that in *MdmX*$^{-/-}$;*p53*$^{ER/-}$ mice p53ER accumulates to levels that could require MDMX enhancement of MDM2-mediated p53 inhibition, indicated by the eventual lethality of continuous tamoxifen injection in *MdmX*$^{-/-}$;*p53*$^{ER/-}$ mice.

Overall, MDM2 and MDMX deletion models have suggested the following notions about MDM2- and MDMX-mediated p53 regulation: (i) MDM2 is the master regulator of p53 and is

necessary to prevent p53-dependent cell death at all stages (ii) MDMX may serve to enhance MDM2-mediated p53 inhibition and/or degradation in a developmental and tissue-specific manner.

Mechanisms of MDM2- and MDMX-mediated p53 regulation: lessons from knockin and transgenic mice

In vitro studies have allowed us to identify mechanisms of MDM2- and MDMX-dependent p53 inhibition, while *in vivo* studies have allowed us delineate the biologically relevant contributions of these mechanisms. In particular, several mouse models (Figure 1.1a and Table 1.2) have helped to clarify p53 regulation *in vivo*.

MDM2/MDMX heterodimer formation and p53 binding

Early *in vitro* studies suggested that the primary mechanism of MDM2- and MDMX-dependent p53 inhibition was mediated through direct MDM2 and MDMX binding to the p53 transactivation domain, causing disruption of p53 activity (Kussie et al., 1996; Oliner et al., 1993; Shvarts et al., 1996). These studies also revealed that MDM2 could act as an E3 ubiquitin ligase towards p53, causing its degradation by the proteasome and suggesting a dual regulatory mechanism (Haupt et al., 1997; Honda et al., 1997). To directly test whether or not MDM2/MDMX-p53 binding alone could restrain p53 activity *in vivo*, Itahana et al. (2007) created mice bearing a mutation in the MDM2 RING domain ($MDM2^{C462A}$) that disrupts MDM2 E3 ligase activity and MDM2-MDMX binding. Homozygous $MDM2^{C462A}$ mutation results in p53-dependent embryonic lethality before embryonic day 7.5, suggesting that MDM2- or MDMX-p53 interaction alone is not sufficient to permit embryonic development and that MDM2-MDMX heterodimer formation and/or MDM2 E3 ligase activity may be the primary mechanisms for MDM2/MDMX-mediated p53 suppression *in vivo*.

Studies in *MdmX* knockin mice also appear to corroborate that MDM2/MDMX-p53 binding is insufficient for p53 inhibition, particularly during embryogenesis. Pant et al. (2011)

generated an allele carrying an in-frame deletion of the MDMX RING domain (*MdmX*$^{\Delta RING}$). At the same time, Huang et al. (2011) generated an allele carrying a point mutation in the MDMX RING domain (*MdmX*^{C462A}). Both of these alleles disrupt MDM2-MDMX interaction without altering MDM2. Mice homozygous for either *MdmX*$^{\Delta RING}$ or *MdmX*^{C462A} exhibit p53-dependent embryonic lethality. Although these two mouse models both disrupt MDM2/MDMX binding and present p53-dependent homozygous embryonic lethality, there have been several observations in apparent contradiction. First, when combined with a *p53*^{neo} allele, which expresses ~15% of WT p53 levels (low enough to permit embryonic development), MEFs containing MDMX$^{\Delta RING}$ appear to display greater p53 activity with no difference in p53 stabilization compared to MEFs containing WT MDMX, suggesting that MDMX does not necessarily contribute to MDM2-mediated p53 degradation. On the other hand, *MdmX*$^{C462A/C462A}$ embryos present both increased p53 abundance and activity. These observations suggest that the MDM2-MDMX interaction is required for efficient p53 activity inhibition, but may or may not be required for p53 degradation during embryogenesis. The discrepancy between these mouse models has challenged the interpretation of in the *in vivo* necessity of MDM2-MDMX binding.

Complicating these observations further, Pant et al. (2011) also generated a Cre-inducible MDMX RING deletion allele (*MDMX*^{flxRING}) and crossed these mice with mice containing a tamoxifen-dependent Cre allele (*CreER*). When adult *MdmX*$^{flxRING/\Delta RING}$*;CreER* mice were injected with tamoxifen to generate recombined *MdmX*$^{\Delta RING/\Delta RING}$ mice, the mice appeared healthy. Most p53 target genes, with the exception of *p21*, showed little change in expression, suggesting that while required for embryogenesis, MDM2-MDMX heterodimer formation is dispensable for the regulation of p53 activity in adult mice. Whether p53 stability is affected by this loss *in vivo* has not been determined and remains an interesting question. From these studies in mice, it appears that MDM2-MDMX heterodimer formation is important for p53 suppression, but the mechanism of this inhibition is still incompletely understood.

MDM2 E3 ligase activity

The recently developed MDM2^{Y487A} mouse model (Tollini et al., 2014) provided insight into the necessity of MDM2 E3 ligase activity in both basal and stress-dependent p53 regulation. As an extension of the MDM2^{C462A} model, in which both MDM2 E3 ligase activity and MDM2-MDMX interaction are disrupted, the MDM2^{Y487A} mutation disrupts MDM2 E3 ubiquitin ligase activity while maintaining MDM2-MDMX interaction. Surprisingly, unlike MDM2^{C462A}, MDMX$^{\Delta RING}$, or MDMX^{C462A} mice, MDM2^{Y487A} mice survive into adulthood, with little phenotypic differences from WT mice under normal, unstressed conditions, clearly indicating that MDM2 E3 ligase activity is not essential for regulating p53 during embryonic development. While no degradation of p53 is observed in MDM2^{Y487A} MEFs, basal p53 activity is slightly increased compared to WT MEFs. This suggests that either MDM2-p53 or MDMX-p53 binding is not sufficient for complete p53 activity suppression, or that without E3 ligase-mediated degradation by MDM2, increased levels of p53 are also spontaneously more active.

Although *Mdm2*$^{Y487A/Y487A}$ mice appear normal under unstressed conditions, these mice are highly sensitive to even sub lethal doses of ionizing radiation (IR), succumbing to p53-dependent hematopoietic failure within about 20 days after exposure, indicating that MDM2 E3 ligase activity is necessary for p53 degradation and suppression during DNA damaging conditions. The relative normalcy of *Mdm2*$^{Y487A/Y487A}$ mice under unstressed conditions suggests that MDM2-MDMX heterodimerization may be particularly important for suppressing chronic, basal levels of p53 activation, such as what might occur during embryogenesis, while MDM2 E3 ligase activity is dispensable under these conditions. However, under stressed conditions where p53 is acutely activated, such as DNA damaging conditions, the MDM2-MDMX heterodimer appears to be insufficient for restraining p53 in the adult mouse. These conditions appear to require the further degradation of p53, mandating the use of MDM2 E3 ligase activity.

Shortly after it was observed to harbor the ability to ubiquitinate p53, MDM2 was also discovered to harbor autoinhibitory ubiquitination activity. In the presence of DNA damage, this

autoubiquitination results in MDM2 destabilization, allowing for further p53 stabilization (Honda and Yasuda, 2000; Stommel and Wahl, 2004). Mutations in the MDM2 RING domain have been shown to increase the stability of overexpressed MDM2 protein (Honda and Yasuda, 2000), but the $MDM2^{C462A}$ and $MDM2^{Y487A}$ mouse models have specifically challenged the notion that MDM2 autoubiquitination occurs *in vivo*. The $MDM2^{C462A}$ and $MDM2^{Y487A}$ mutations disrupt MDM2 E3 ligase activity, yet the half-life and ubiquitination levels of MDM2 do not change, suggesting that in the live mouse MDM2 stability is likely mediated by the activity of other E3 ligases (Itahana et al., 2007; Tollini et al., 2014). These two independent E3 ligase activity-disrupting mutations of MDM2 have shown that MDM2 E3 ligase activity is not required for basal MDM2 degradation *in vivo* (Itahana et al., 2007; Tollini et al., 2014), although whether or not MDM2-MDMX interaction is required for MDM2 ubiquitination is still unclear. *In vitro* MDMX overexpression has been shown to stabilize MDM2, and this stabilization is dependent on the RING domain of each protein (Linares et al., 2003; Tanimura et al., 1999). Conversely, knockdown of MDMX has resulted in reduced MDM2 expression (Gu et al., 2002). Because of this, it was previously proposed that MDMX could redirect MDM2 E3 ligase activity from MDM2 unto itself and stabilize MDM2, but if MDM2 autoubiquitination does not truly occur *in vivo*, this may not be the case. Further, the $MDMX^{C462A}$ mutation disturbs MDM2-MDMX interaction without directly altering MDM2, and in the absence of MDM2-MDMX binding, Huang et al. observed that MDM2 ubiquitination was disrupted *in vivo* (Huang et al., 2011). However, mice containing $MDMX^{\Delta RING}$, which also does not interact with MDM2, display no difference in MDM2 half-life compared to mice containing wild type MDMX (Pant et al., 2011). Resolving these conflicting observations will be important to understanding the regulation of MDM2 stability.

In contrast, *in vivo* models have agreed that MDM2 does control MDMX stability. For example, $Mdm2^{Y487A/Y487A}$ mice lacking MDM2 E3 ligase activity have increased protein levels of MDMX (Tollini et al., 2014), which is in line with *in vitro* studies suggesting that that MDM2 E3 ligase activity acts to ubiquitinate MDMX (Kawai et al., 2003; Pan and Chen, 2003). In addition,

MDMX$^{\Delta RING}$, which does not have the ability to interact with MDM2, is not degraded compared to MDMX in untreated or IR-treated MEFs (Pant et al., 2011).

In vitro studies have suggested that through their respective RING domains (Tanimura et al., 1999), MDMX serves to facilitate MDM2-mediated p53 ubiquitination (Linares et al., 2003). This facilitation could occur indirectly, which has been shown to occur *in vitro,* meaning that MDMX could redirect any possible MDM2 autoinhibitory ubiquitination unto itself, stabilizing MDM2 for p53 ubiquitination (Pan and Chen, 2003). In addition, it is possible that MDMX could directly facilitate p53 ubiquitination, meaning that MDMX could directly enhance the transfer of ubiquitin to p53. However, neither of these hypotheses have been directly tested *in vivo*.

Stress-induced *mdm2* transcription

It is hypothesized that following stress, p53 transactivates *mdm2* to facilitate its own degradation, instituting a regulatory feedback loop. Recently, this idea was directly tested *in vivo*, when Pant and Lozano (2014) generated mice bearing the *Mdm2^{P2}* allele. Point mutations were introduced to two p53 REs within the *Mdm2* promoter region, preventing p53-mediated transactivation. In response to several p53-inducing stresses, p53 stabilization occurred in a similar manner in *Mdm2^{P2}* mice compared to WT mice, but p53 activity persisted longer in *Mdm2^{P2}* mice and MEFs, suggesting that basal levels of MDM2 are sufficient for p53 regulation in unstressed cells, but that the p53-MDM2 feedback loop is required for restraining stress-induced p53 *in vivo*. In addition, the heterozygous deletion of *MdmX* appeared to enhance p53 stability in *Mdm2$^{P2/P2}$;MdmX$^{+/-}$* MEFs, further suggesting the possibility that MDMX may enhance the degradation of stress-induced p53.

Upstream p53 signaling through MDM2 and MDMX - DNA damage

Activation of p53 requires transient inhibition of MDM2 and/or MDMX association, which is mediated through upstream signaling factors. Knockin mouse models have allowed us to appreciate the complex interactions of MDM2 and MDMX in p53 regulation, but they have also been used to delineate the contributions of many upstream signals to overall p53 activation

(Table 2). For instance, *in vitro* studies have shown that in response to DNA damage, ATM phosphorylates MDM2, inhibiting MDM2 E3 ligase activity and RING domain-dependent oligomer formation, thus stabilizing p53 (Cheng et al., 2009; Cheng et al., 2011). To specifically test the importance of ATM-mediated MDM2 phosphorylation at serine 394 (serine 395 in human), Gannon et al. (2012) generated the $MDM2^{S394A}$ mouse, replacing serine 394 with an alanine and disrupting MDM2 phosphorylation *in vivo*. Basal p53 levels and activity were unchanged in these mice, but in response to lethal doses of IR, $MDM2^{S394A}$ mice experience reduced p53 stabilization and activation. This translates to increased survival compared to WT mice, indicating that MDM2 serine 394 phosphorylation is an important event preceding the propagation of p53 stabilization and activation following IR-mediated DNA damage.

MDMX is also phosphorylated following DNA damage, a signal which contributes to its own degradation. ATM phosphorylates MDMX serine 403 (402 in mouse) (Pereg et al., 2005), while CHK2 can phosphorylate serine 342 and serine 367 (341 and 367 in mouse) facilitating MDM2-mediated degradation of MDMX and stabilization of p53 (Chen et al., 2005; LeBron et al., 2006; Okamoto et al., 2005; Pereg et al., 2006). To study the importance of MDMX phosphorylation to p53 activation following DNA damage *in vivo*, Wang et al. (2009) generated $MDMX^{3SA}$ mice, in which serine 341, serine 367, and serine 402 of MDMX are replaced with alanine residues. Upon loss of MDMX phosphorylation capability, $MDMX^{3SA}$ appears to be stabilized at basal levels. Following IR treatment, $MDMX^{3SA}$ remains stable compared to MDMX, and p53 protein levels and transcriptional activity are lower in $MDMX^{3SA}$ MEFs and tissue. In addition, $MDMX^{3SA}$ mice are resistant to lethal IR treatment. These results are in congruence with the reduced basal and DNA damage-induced p53 activity observed in $MDMX^{3SA}$ mice, suggesting that MDMX phosphorylation and subsequent degradation is important for proper p53 activation. These results also suggest that basal MDMX phosphorylation could be required for allowing basal levels of p53 activity.

It is clear from these studies that modification of MDM2 and MDMX by upstream signaling proteins mediates p53 activation in response to DNA damage *in vivo*. Interestingly, $MDM2^{S394A}$ mice are somewhat susceptible to tumor formation, indicating that ATM-mediated MDM2 phosphorylation is likely important for allowing proper p53 activation in response to endogenous, cancer-causing DNA damage events. Other upstream signals contribute to p53 response to cancer-causing events, including the expression of oncogenes, which is described in further detail below.

Oncogene-driven p53 activation

p19ARF-mediated p53 regulation

It is unsurprising that p53, in its role as a stress responder and tumor suppressor, is able to sense hyperproliferative signals mediated by activation or overexpression of oncogenes. Largely, this signaling is thought to be mediated by p19ARF (p14ARF in human), another tumor suppressor protein. Interestingly, p19ARF is named for the fact that it is read from an alternative reading frame of the *Ink4a* locus, from which another tumor suppressor protein, $p16^{Ink4a}$ (cyclin-dependent kinase inhibitor 2A), is also transcribed (Ouelle et al., 1995).

p19ARF has been demonstrated to perform both p53 dependent and independent functions towards overall tumor suppression, but for the purposes of this dissertation, I will focus on discussing the p53 dependent functions of p19ARF (Eischen et al., 1999; Kamijo et al., 1997; Qi et al., 2004). Sustained levels of oncogene activation (by proteins including MYC, BCR-ABL, RAS, and E2F1) activate the transcription of the *Ink4a* locus through as of yet unclear mechanisms (de Stanchina et al., 1998; Palmero et al., 1998; Radfar et al., 1998; Zindy et al., 1998). Following upregulation, p19ARF interacts with MDM2 through its central acidic domain. MDM2-p19ARF interactions have been shown to have multifaceted mechanisms of action towards MDM2 inhibition. For example, p19ARF can sequester MDM2 in the nucleolus, preventing MDM2-p53 interaction (Tao and Levine, 1999; Weber et al., 1999), as well as

promote MDM2 degradation (Zhang et al., 1998). As a result of these interactions, p19ARF prevents MDM2-mediated p53 inhibition (Pomerantz et al., 1998). The current dogma holds that p19ARF is the primary signal from oncogene-induced hyperproliferation to p53 activation.

Like *p53*$^{-/-}$ mice, *p19Arf*$^{-/-}$ mice develop spontaneous tumors, although with a longer latency to eventual death (6 months for *p53*$^{-/-}$ mice versus about 12 months for *p19Arf*$^{-/-}$ mice) (Donehower et al., 1992; Kamijo et al., 1999). In the presence of oncogene expression, this transformation is hastened. For example, when *p19Arf*$^{+/-}$ mice are placed into an *Eμ-Myc* background, lymphoma progression is typically accelerated, and the second *p19Arf* allele tends to be lost with high frequency (Eischen et al., 1999).

There is also evidence to suggest that a feedback loop exists for p19ARF following the activation of p53 (Stott et al., 1998). In the absence of p53, p19ARF levels tend to be elevated in MEFs (Palmero et al., 1998). In addition, mutations in p53 or overexpression of MDM2 tend to be correlated with increased expression of p19ARF, with WT p53 re-expression resulting in decreased p19ARF protein levels and transcription levels (Kamijo et al., 1998; Robertson and Jones, 1998; Stott et al., 1998). Although p19ARF has not been shown to be a p53 target gene and the mechanism of its downregulation is still unclear, p19ARF downregulation following p53 activation likely represents another mechanism through which undue p53 activation is prevented.

Ribosomal protein-mediated MDM2-p53 regulation

Although oncogenes can stimulate p53 activation through p19ARF, it has been recently appreciated that other consequences of oncogene activation can invoke p53 stabilization. Accelerated cell growth and division drive increased assembly of the protein-producing machinery, namely ribosomes, which are important in both cancer progression and p53 activation.

Ribosomes are primarily responsible for translating mRNA to protein. In eukaryotes, the ribosome consists of ribosomal RNA (rRNA) and ribosomal proteins (RPs). During ribosomal biogenesis, RNA polymerase I (POLI) transcribes the 47S precursor rRNA, which is processed into the 5.8S, 18S, and 28S rRNAs. Meanwhile, POLIII transcribes the 5S rRNA, and POLII transcribes the genes coding the 79 ribosomal proteins, which are then translated in the cytoplasm and imported back into the nucleolus. Then, these RPs and rRNAs are assembled in approximately equimolar concentrations, where they form the 40S and 60S ribosomal subunits. The 40S subunit contains 30 unique RPs and a copy of the 18S rRNA, while the 60S subunit contains 49 unique RPs and a copy of each of the 5S, 5.8S and 28S rRNAs (Odintsova et al., 2003; Vladimirov et al., 1996). The subunits are then exported from the nucleolus into the nucleoplasm, and then again exported into the cytoplasm where they form the 80S ribosome.

Ribosome assembly is highly coordinated and essential for cell homeostasis and cell cycle progression. In yeast, it has been estimated that up to 60% of a cell's energy is devoted to producing ribosomes (Warner, 1999). In addition, ribosome production is thought to be tightly coordinated with cell cycle progression. For instance, inhibition of rRNA synthesis via POLI or POLIII inhibition leads to G1 cell cycle arrest (Gomez-Herreros et al., 2013), while downregulation of RPL5 or RPL11 prohibits the translation of cyclins and prohibits cell cycle progression in a p53 independent manner (Teng et al., 2013). Disturbing any step of the assembly can result in what is called "nucleolar stress," which is catastrophic to normal cellular functions.

Ribosome biogenesis dysfunction

Disruption of ribosomal biogenesis can occur in many ways, including the interruption of rRNA synthesis/processing, oncogenic activation, mutation/deletion of RPs, and changes in nutrient abundance. First, disruptions in rRNA synthesis can be produced pharmacologically. For example, in low concentrations Actinomycin D, a DNA damaging chemotherapeutic, inhibits POLI and prevents the transcription of the 47S precursor rRNA (Perry and Kelley, 1970; Sobell

et al., 1971). Similarly, 5-fluorouracil, a nucleotide analog also used as a chemotherapeutic, incorporates into rRNA, disrupting its synthesis and processing (Wilkinson et al., 1975). Ribosome biogenesis is also commonly misregulated in cancer. In particular, the c-MYC oncogene is a master regulator of ribosomal biogenesis and directly upregulates the transcription of many RPs (van Riggelen et al., 2010). MYC-mediated stimulation of ribosomal biogenesis occurs in several ways. First, MYC serves as a transcription factor with its binding partner MAX (myc-associated factor X), directly binding to REs known as E-Box motifs, which are present in the promoters of several RPs. MYC/MAX then recruit histone modifiers and other coregulatory factors, including TRRAP (transformation/transcription domain-associated protein), GCN5 (histone acetyltransferase GCN5), and TIP60 (histone acetyltransferase KAT5) to alter chromatin structure and promote gene transcription (McMahon et al., 2000). As well as promoting the production of RPs, MYC also regulates other factors required for ribosomal biogenesis, including B23 (nucleophosmin or NPM), NCL (nucleoloin), BOP1 (block of proliferation 1), NOP56 (nucleolar protein 56), FBL (fibrillarin), and DKC1 (dyskerin) (Watson et al., 2002). Independent of MAX, MYC can also associate with POLIII and stimulate the transcription of the 5S rRNA (Gomez-Roman et al., 2003). It has been recently appreciated that RP regulation directly contributes to the progression of c-MYC driven cancer. For example, loss of one allele of *rpl24* drastically suppresses MYC driven lymphoma (Barna et al., 2008).

Finally, given the intense energetic demand of ribosome production, it is unsurprising that changes in extracellular nutrient abundance can also drastically alter ribosomal biogenesis (Boulon et al., 2010). A key regulator of this process is the mTOR (mammalian target of rapamycin) complex, a well-characterized sensor of nutrient and growth factor status (Zoncu et al., 2011). Upstream changes in nutrient abundance, including amino acids, dictate mTOR activity (Hara et al., 1998). mTOR has been shown to control the transcription of the precursor 47S and 5S rRNAs through controlling the localization and activity of all three RNA polymerases (Claypool et al., 2004; Hannan et al., 2003; Mahajan, 1994; Mayer et al., 2004). mTOR inhibition

also limits rRNA processing (Iadevaia et al., 2011). Likewise, the transcription of ribosomal protein mRNAs is also under mTOR control, though through unclear mechanisms (Powers and Walter, 1999). Through all of these activities, mTOR plays a direct role in regulating ribosome assembly in response to nutrient status (Li et al., 2006).

Once active, mTOR also directly controls the phosphorylation of S6K (ribosomal protein S6 kinase beta-1) and 4E-BP1 (eukaryotic initiation factor 4E-binding protein) (Gingras et al., 1999; Pullen and Thomas, 1997; Saitoh et al., 2002). Phosphorylated S6K then phosphorylates many other targets, including RPS6 (Ruvinsky and Meyuhas, 2006). The full consequences of RPS6 phosphorylation are poorly understood, but it has been postulated that it facilitates recruitment of the ribosome to the 5' mRNA cap, facilitating translation (Roux et al., 2007). Meanwhile, phosphorylated 4E-BP1 releases eIF4E (eukaryotic translation initiation factor 4E) from inhibitory binding, allowing eIF4E (as part of a multisubunit complex) to recruit 40S ribosomal subunits to the 5' cap of mRNAs and initiate translation. Through all of these activities, mTOR serves to couple nutrient sensing to ribosome biosynthesis and overall protein translation initiation.

It is also important to note that loss of RP function is also associated with several disorders in humans, broadly classified as "ribosomopathies" (Narla and Ebert, 2010). Patients with these disorders tend to present with anemia and bone marrow failure, correlating with increased p53 activity. p53 plays an important role in regulating ribosome biogenesis, discussed below.

p53 monitors ribosome biogenesis

As a stress responder, p53 monitors changes in ribosomal biogenesis. Like p19ARF, several RPs have been found *in vitro* to bind the central zinc finger domain of MDM2, including RPL11, RPL5, and RPL23 (Chen et al., 2007; Dai and Lu, 2004; Dai et al., 2004; Zhang and Lu, 2009; Zhang et al., 2003). In contrast, RPs have not yet been shown to bind to MDMX (Gilkes et al., 2006). It is thought that in the presence of nucleolar stress or altered ribosomal biogenesis,

RPs that are unaffiliated with a ribosome will bind to MDM2 and inhibit MDM2-mediated p53 degradation to stabilize and activate p53 (Dai et al., 2004; Liu et al., 2016b). In this way, p53 is able to monitor that the supply of RPs is balanced and available for the assembly of ribosome machinery. RP-MDM2 binding is hypothesized to occur in two ways. First, it has been shown that disruption of the nucleolus allows RPs to be released into the nucleoplasm, where they can bind MDM2 (Bai et al., 2014; Bhat et al., 2004). Second, it has been shown that in the presence of altered ribosome biogenesis (via *rps6* deletion), the translation of certain ribosomal proteins (specifically RPL11) is increased even in the absence of direct nucleolar disruption (Fumagalli et al., 2009b). An imbalance in RP translation would presumably allow for the production of more non-ribosome affiliated RPs, allowing for increased RP-MDM2 binding and increased p53 activation.

Interestingly, although cancer-associated mutations in MDM2 appear to be rare, several have been shown to occur in the zinc finger domain and disrupt RP-MDM2 interactions (Lindström et al., 2007). One of the more common of these cancer-associated mutations, $MDM2^{C305F}$, resides in the region of RPL11 and RPL5 binding and prevents their interaction with MDM2, but allows other RPs (including RPL23) to maintain binding. In order to directly test the role of RPL11- and RPL5-MDM2 interaction towards p53 activation *in vivo*, Macias et al. (2010) generated the $MDM2^{C305F}$ mouse. Although mice bearing the $MDM2^{C305F}$ mutation present with a normal lifespan, they are highly susceptible to c-MYC induced tumorigenesis, due to reduced p53 activation (Macias et al., 2010). From this study, it was first confirmed that RP-MDM2 interactions could directly translate oncogenic signals to p53 *in vivo*.

It has also become increasingly apparent that RPs serve to regulate p53 in response to nutrient availability. This is not surprising, as p53 regulates cellular energy homeostasis (Vousden and Ryan, 2009; Zhang et al., 2010). Consistently, the $MDM2^{C305F}$ mouse, with its impaired RP-MDM2 binding, is deficient in p53-mediated fatty acid oxidation in response to

fasting (Liu et al., 2014b) and p53-mediated fat storage in response to sustained high-fat diet feeding (Liu et al., 2017).

Though 16 RPs have been shown to bind to MDM2 (Liu et al., 2016b), RPL11 and RPL5 appear to be particularly important for p53 activation due to ribosome biogenesis stress. While RP overexpression has been shown to elicit p53 stress response, others have shown that depletion of RPL5 or RPL11 can abrogate nucleolar stress-induced p53 activation caused by RPS6 downregulation (Fumagalli et al., 2012). The distinct importance of RPL11 and RPL5 towards p53 activation is not completely understood, but several observations point to their importance in ribosome assembly. RPL5 and RPL11 bind with the 5S rRNA to produce a pre-ribosomal complex prior to the formation of the 60S subunit (Donati et al., 2013). In addition, RPL11 and RPL5 reside in the interface of the 60S and 40S ribosome subunits (Ben-Shem et al., 2010), which suggests that their disruption could be particularly harmful to ribosome assembly. Much of RP-MDM2 pathway research has focused on RPL11 and RPL5, and the contributions of other RPs towards p53 activation remain incomplete.

p19ARF participates in the regulation of ribosome biogenesis

Although p19ARF has been shown to interact with and regulate MDM2, it also plays a role ribosome biogenesis, complicating our understanding of the necessities of each of these functions towards the activation of p53. As mentioned previously, p19ARF is often localized to the nucleolus, where ribosome biogenesis occurs. p19ARF appears to exhibit increased nucleolar localization during progression towards replicative senescence, as well as in the presence of increased c-MYC expression (Weber et al., 1999), suggesting that p19ARF may contribute to or enhance RP-mediated p53 activation. Later discoveries clearly suggested this possibility.

For example, nucleolar p19ARF had been found to suppress rRNA transcription by preventing the nucleololar localization of RNA helicase DDX5 and RNA polymerase I

transcription termination factor TTF-I (Lessard et al., 2010; Saporita et al., 2011), as well as to inhibit the processing of the 47S precursor RNA (Sugimoto et al., 2003). p19ARF also interacts with and degrades B23 (Bertwistle et al., 2004; Itahana et al., 2003), a protein that chaperones the import of other auxiliary ribosome biogenesis factors (Lindström, 2010). In addition to degrading B23, p19ARF sequesters B23 in the nucleolus (Brady et al., 2004), preventing it from performing its chaperoning functions.

These studies indicate that p19ARF is intimately linked to ribosome biogenesis, adding another level to its regulation of p53. Importantly, these studies raise the question of whether p19ARF contributes to facilitating RP-MDM2 interaction through its ability to disrupt ribosome assembly and processing. It is evident that RPs and p19ARF play intertwining roles to regulate MDM2, and teasing out the individual contributions of these functions will be important towards understanding the biology of p53 activation.

p53 and cancer therapies

A growing number of studies have suggested targeting mutant p53 or restoring WT p53 as cancer treatment strategy (Burgess et al., 2016; Soragni et al., 2016), and many drugs specifically targeting MDM2-p53 or MDMX-p53 interaction have been developed (Burgess et al., 2016; Vassilev et al., 2004; Wade et al., 2013). Mouse models have supported these strategies in principle. For example, MDMX loss in c-MYC-driven tumors extends survival after p53ER restoration (Garcia et al., 2011), and CreER-mediated *p53*^{neo} restoration in transplanted MDM2-overexpressing tumors also appears to extend survival in mice (Li et al., 2014). However, so far these treatment strategies have enjoyed limited efficacy in the clinic.

In vivo studies have also suggested that other approaches could be taken to restore p53 function in human cancers harboring WT p53, such as inhibiting MDM2-MDMX binding or MDM2 E3 ligase activity. The inhibition of MDM2 E3 ligase activity may be especially attractive as a treatment strategy, because the MDM2^{Y487A} mouse model shows that genetic ablation of

MDM2 E3 ligase activity is tolerated by the adult mouse as well as the developing embryo (Tollini et al., 2014), which suggests that this strategy could avoid toxicity issues. In response to p53-activating stimuli, cells containing MDM2^{Y487A} demonstrate increased p53 stability and activity. Although several inhibitors of MDM2 E3 ligase activity have been identified and shown to stabilize p53 (Herman et al., 2011; Roxburgh et al., 2012; Yang et al., 2005), their activity and specificity may not yet be sufficient for human use. So far, MDM2 E3 ligase inhibitors have not been tested in humans, but several other small-molecule MDM2 antagonists are currently in Phase I trials (Burgess et al., 2016). Mouse models have also suggested that complete restoration of p53 function in the presence of radiation should be used with caution, as abundant p53 activity is toxic to several tissues (Ringshausen et al., 2006; Tollini et al., 2014; Zhang et al., 2014a). Understanding p53 and its regulation in cancer will be important to understand for utilization and the potential repercussions of p53-reactivating therapies.

Dissertation goals

Mouse models of altered MDM2 and MDMX have given us a clearer understanding of the *in vivo* roles of MDM2 and MDMX in p53 regulation (Figure 1) and established that MDM2 and MDMX proteins are master p53 regulators. Broadly, this dissertation will focus on characterizing the *in vivo* roles of RP-MDM2 interaction in p53-mediated tumor prevention. I will also present preliminary data exploring the *in vivo* functional consequences of the loss of MDM2 E3 ligase function (while maintaining MDMX interaction) on p53 activity in response to MYC-driven lymphoma. Below is a more detailed summary of the goals of this dissertation.

First, although RP-MDM2 interaction has been shown to promote p53 activation and tumor suppression in MYC-induced lymphoma (Macias et al., 2010), it was unknown whether these interactions are dependent on p19ARF (Eischen et al., 1999), the canonical oncogene activation signal to p53 that is also heavily involved in nucleolar signaling. Chapter 2 will specifically explore how, in the context of c-MYC-driven lymphoma progression, RPs likely

function independently of p19ARF to induce p53 tumor suppressive functions. To answer this question, this work will rely on the use of the MDM2^{C305F} mouse, in which RPL11- and RPL5-MDM2 interactions are disrupted, coupled with mice containing a p19ARF deletion allele. Likewise, Chapters 3 and 4 will touch on the importance of p19ARF independent RP-MDM2 interactions in other cancer contexts.

Second, although the RP-MDM2-p53 response pathway has been shown to be important for preventing c-MYC driven cancer, it was unknown whether RP-MDM2 interactions could be induced by other cancer drivers. Protein-producing machinery is thought to be critical for supporting uncontrolled proliferation, so it is possible that cancers that are not initiated by c-MYC could still promote p53 activation through RP-MDM2 interactions. Chapters 3 and 4 of this dissertation will explore how the RP-MDM2-p53 pathway is regulated in response to RAS oncogene overexpression and APC deletion, also using the MDM2^{C305F} mouse.

Third, although RP-MDM2 interaction appears to be important for p53 activation in lymphoma, it is possible that this is a tumor- or tissue-specific phenomena. Clearly, different tissue and cancer types will have vastly different cell and genomic architectures. If this knowledge is to be used towards the discovery of new therapies, it is important to determine in which cell/tissue/tumor contexts RP-MDM2 interactions may be the most consequential. Chapters 3 and 4 will explore how RP-MDM2 interactions are differentially important in melanoma, small intestine, and colon cancers.

Finally, Chapter 5 will explore how preventing p53 degradation by genetically manipulating MDM2 E3 ligase activity could allow for increased p53 activity and organismal longevity, suggesting the possibility that MDM2 E3 ligase inhibitors could be used in the future as a safe method of reactivating p53 and allowing it to perform its tumor suppressive functions. Ultimately, the studies presented here aim to understand the intricacies of MDM2/MDMX-p53 regulation in order to facilitate the development of future therapies.

Table 1.1 *Mdm2* and *MdmX* knockout mice

Tissue	MDM model	p53 alleles	Cre transgene	Phenotypes and p53 responses	Refs
Whole Body	*Mdm2*^{puro}	WT	N/A	Decreased body weight, hematopoietic defects, increased apoptosis, increased p53 activity	(Mendrysa et al., 2003)
	MdmX$^{\Delta Ex6}$ (Truncation)	WT	N/A	Embryonic lethality, increased p53 activity on *p53*$^{\Delta P/\Delta P}$ background	(Bardot et al., 2015)
Central Nervous System	*Mdm2*$^{-/-}$	*p53*$^{LSL/-}$	Nestin-Cre	Embryonic lethality, increased p53 protein levels and activity, increased apoptosis	(Francoz et al., 2006)
	MdmX$^{-/-}$	*p53*$^{LSL/-}$	Nestin-Cre	Microcephaly, growth retardation, increased p53 activity and cell cycle arrest	
	Mdm2$^{FM/FM}$	WT	Nestin-Cre	Neonatal lethality, hydrancephaly, increased p53 protein levels and activity, aberrant apoptosis and proliferation	(Grier et al., 2002; Xiong et al., 2006)
	MdmX$^{FX/FX}$	WT	Nestin-Cre	Neonatal lethality, porencephaly, increased p53 activity, aberrant apoptosis and proliferation	
	Mdm2$^{-/-}$	*p53*$^{ER/-}$	N/A	No discernable phenotypes	(Ringshausen et al., 2006)
	MdmX$^{-/-}$	*p53*$^{ER/-}$	N/A	Increased p53 activity, increased apoptosis in subventricular zones	(Garcia et al., 2011)
Bone	*Mdm2*$^{F11-12}$	WT	Col3.6-Cre	E19.5 lethality, skeletal defects, elevated p53 activity but not protein levels, reduced proliferation	(Lengner et al., 2006)
Intestine	*Mdm2*$^{FM/FM}$	WT	Villin-Cre	Normal lifespan, intestinal abnormalities with eventual recovery, increased p53 activity and protein levels	(Valentin-Vega et al., 2008)
	MdmX$^{FX/FX}$	WT	Villin-Cre	No major defects, increased p53-dependent apoptosis and activity in proliferating cells	(Valentin-Vega et al., 2009)
	Mdm2$^{-/-}$	*p53*$^{ER/-}$	N/A	Atrophy of villi and crypts, increased apoptosis	(Ringshausen et al., 2006)
	MdmX$^{-/-}$	*p53*$^{ER/-}$	N/A	Increased apoptosis	(Garcia et al., 2011)
	Mdm2$^{FM/-}$	WT	CAG-Cre (Tamoxifen)	Atrophy in villi and increased apoptosis in crypts of 2-4 month old mice, no phenotypes in 16-18 month old mice	(Zhang et al., 2014a)
Heart	*Mdm2*$^{FM/-}$	WT	αMyhc-Cre	E13.5 lethality, severe defects, increased p53 protein and apoptosis	(Grier et al., 2006)
	MdmX$^{FX/-}$	WT	αMyhc-Cre	Normal, with some premature death at 12 months of age	
	Mdm2$^{FM/-}$	WT	CAG-Cre (Tamoxifen)	Tissue fibrosis, increased p53 activity and protein levels	(Zhang et al., 2014a)
	Mdm2$^{-/-}$	*p53*$^{ER/-}$	N/A	No discernable phenotypes	(Ringshausen et al., 2006)
	MdmX$^{-/-}$	*p53*$^{ER/-}$	N/A	No discernable phenotypes	(Garcia et al., 2011)
Endothelium	*Mdm2*$^{FM/FM}$	WT	Tie2-Cre	Embryonic lethality, severe vascular defects, increased p53 activity	(Zhang et al., 2012)
Skin	*Mdm2*$^{F11-12}$	WT	K5-Cre	Progressive hair loss and decreased skin elasticity, increased p53 protein levels and activity, increased senescence	(Gannon et al., 2011)
Smooth Muscle	*Mdm2*$^{FM/FM}$	WT	Sm22-CreER^{T2}	Death within 12 days after tamoxifen injection, increased p53 protein levels and activity, increased apoptosis	(Boesten et al., 2006)
	MdmX$^{FX/FX}$	WT	Sm22-CreER^{T2}	No discernable phenotypes	
Red Blood Cells	*Mdm2*$^{FM/FM}$	WT	EpoR-GFP-Cre	E13 lethality, defects in erythropoiesis, increased p53 activity	(Maetens et al., 2007)
	MdmX$^{FX/FX}$	WT	EpoR-GFP-Cre	Death between E12.5 and 21 days after birth, anemia, increased p53 activity	
Lens Epithelial Cells	*Mdm2*$^{FM/FM}$	WT	Le-Cre	Defects in lens development, normal birth ratios but hyperglycemia and neonatal lethality (1 week) present, increased p53 levels and apoptosis, decreased cell proliferation	(Zhang et al., 2014b)
	MdmX$^{FX/FX}$	WT	Le-Cre	Eyeless, normal birth ratios and survival into adulthood, increased p53 levels and apoptosis, decreased cell proliferation	

Table 1.2 *Mdm2* and *MdmX* knockin mice

MDM model	Modification	Phenotypes and p53 responses	Refs
Mdm2^{C462A}	Disrupts RING domain and MDMX interaction	Embryonic lethal, increased p53 stability and activity	(Itahana et al., 2007)
Mdm2^{S394A}	Disrupts ATM phosphorylation	Radioresistant, accelerated spontaneous and MYC-induced tumor formation, resistance to radiation-induced lymphoma	(Carr et al., 2016; Gannon et al., 2012)
Mdm2^{C305F}	Disrupts ribosomal protein interaction	Decreased p53 stabilization and activity following ribosomal stress, increased MYC-induced tumors, increased APC loss-induced colon tumors	(Liu et al., 2016a; Macias et al., 2010; Meng et al., 2015b)
Mdm2^{Y487A}	Disrupts E3 ligase function	Increased p53 stability, increased p53 activity after irradiation, increased radiosensitivity	(Tollini et al., 2014)
Mdm2^{SNP309G}	Increases *Mdm2* expression	Increased spontaneous tumorigenesis, reduced p53 levels	(Post et al., 2010)
Mdm2^{P2}	Disrupts p53-mediated *Mdm2* transcription	Prolonged p53 activity after DNA damage, no apparent change in p53 stability, increased radiosensitivity	(Pant and Lozano, 2014)
Mdm2^{2DD}	Mimics constitutive AKT phosphorylation in mammary tissue	Accelerated ERBB2-induced tumors, decreased p53 expression	(Cheng et al., 2010)
MdmX$^{\Delta RING}$	Removes RING domain functions	Embryonic lethal, increased p53 activity	(Pant et al., 2011)
MdmX^{C462A}	Disrupts RING domain and MDM2 binding	Embryonic lethal, increased p53 activity and protein levels	(Huang et al., 2011)
MdmX^{3SA}	Disrupts AKT, ATM, and CHK2 phosphorylation	Radioresistant, accelerated MYC-induced tumor formation, decreased p53 protein levels and activity	(Wang et al., 2009)

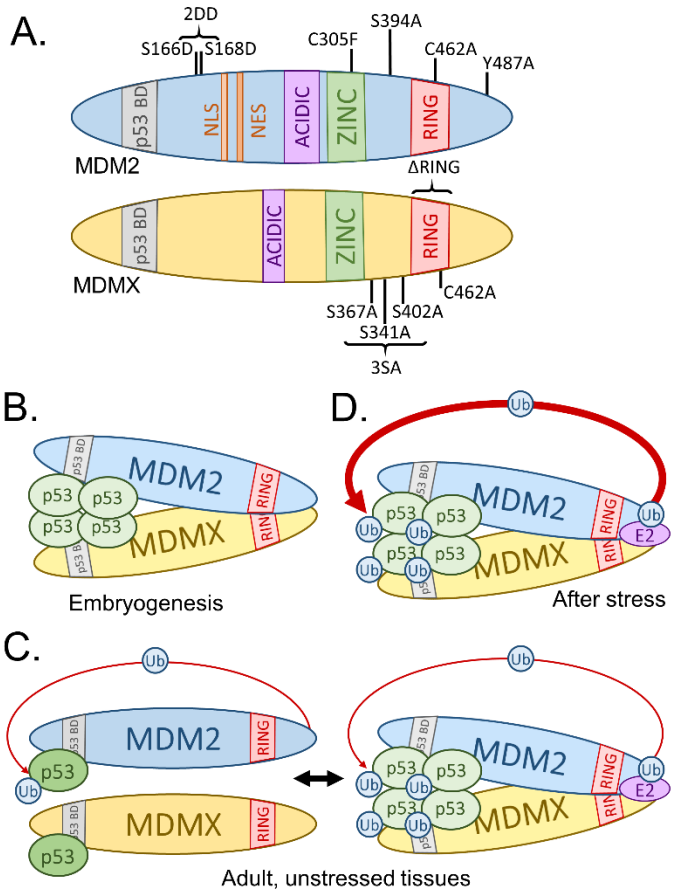

Figure 1. p53 regulation requirements are context dependent

A. Schematic of MDM2 and MDMX protein modifications that have been generated by knockin mouse models.

B. During embryogenesis, both MDM2 and MDMX are required for proper control of p53 activity. The formation of an MDM2-MDMX heterodimer is also required to restrain p53, but MDM2 E3 ligase activity is dispensable at this time.

C. In unstressed adult tissues, the necessity of MDMX or MDM2-MDMX heterodimer formation for proper p53 control is tissue-dependent. MDM2-mediated p53 ubiquitination may still occur in these tissues, which may require MDMX.

D. After stress, such as DNA damage, MDM2 E3 ligase activity is required to return p53 protein to basal levels and control p53 activity. This may or may not require MDM2-MDMX heterodimer formation.

p53 BD=p53 binding domain, NLS=nuclear localization signal, NES=nuclear export signal, ACIDIC=acidic domain, ZINC=zinc finger domain, RING=RING finger domain, Ub=ubiquitin, E2=E2 ubiquitin-conjugating enzyme

CHAPTER 2: ONCOGENIC C-MYC-INDUCED LYMPHOMAGENESIS IS INHIBITED NON-REDUNDANTLY BY THE P19ARF-MDM2-P53 AND RP-MDM2-P53 PATHWAYS[2]

INTRODUCTION

The MYC protein (c-MYC) is a helix-loop-helix leucine zipper transcriptional regulator, which forms specific DNA-binding heterodimers with the MAX protein to control a variety of normal cellular functions (Meyer and Penn, 2008). In addition, c-MYC facilitates the recruitment of POLI to ribosomal DNA promoters (Arabi et al., 2005), promotes the transcription of ribosomal proteins (RPs) by activating POLII (Menssen and Hermeking, 2002) and activates POLIII-mediated transcription of 5S ribosomal RNA and transfer RNA (Gomez-Roman et al., 2003). c-MYC also transactivates many other genes involved in ribosomal biogenesis (De Marval and Zhang, 2011). Increased c-MYC expression is frequently observed in human cancers and it can confer a growth advantage to cells by providing constitutive proliferative signals (Mateyak et al., 1997). However, c-MYC overexpression may also initiate an endogenous apoptotic program (Evan et al., 1992), and through this function trigger a potent tumor surveillance response that effectively opposes hyperproliferation by killing those cells in which c-MYC levels exceed a safe threshold (Packham and Cleveland, 1995).

The p53 transcription factor is a critical tumor suppressor, and when activated it triggers cell cycle arrest, differentiation, apoptosis and senescence. The *TP53* gene is mutated in ~50% of all human tumors and is often referred to as the 'guardian' of the genome (Lane, 1992; Meng

---

[2] This chapter is adapted from a research article originally published in *Oncogene*. Xuan Meng, Yanping Zhang and I designed the study. Xuan Meng performed all of the experiments. Xuan Meng, Yanping Zhang, and I analyzed the data. Xuan Meng, Yanping Zhang and I wrote and edited the manuscript. Jiahong Dong and Yanping Zhang finalized the manuscript. The original citation is as follows: Meng, X., Carlson, N., Dong, J., and Zhang, Y. (2015a). Oncogenic c-Myc-induced lymphomagenesis is inhibited non-redundantly by the p19Arf–Mdm2–p53 and RP–Mdm2–p53 pathways. Oncogene *34*, 5709-5717.

et al., 2014). p53 is primarily regulated by the E3 ubiquitin ligase MDM2, which binds to p53 to both block its transactivation domain and to promote its ubiquitination and degradation. However, p53 enhances *mdm2* transcription, thus forming an autoregulatory feedback loop (Wu et al., 1993). The tumor suppressor p19ARF (p14ARF in human) is transcribed from an alternative reading frame of the INK4a/ARF locus. p19ARF physically binds to MDM2, inhibiting its E3 ligase activity, thereby stabilizing and activating p53, which constitutes a p19ARF-MDM2-p53 signaling pathway (Sherr, 2006). Oncogenic c-MYC-driven tumors receive a selective advantage from inactivation of the p19ARF-MDM2-p53 pathway, diminishing its protective checkpoint function and accelerating normal cell progression to malignancy; this accelerated progression to malignancy is observed in *Eμ-Myc;p19Arf*$^{-/-}$ transgenic mice, a model for Burkitt's lymphoma, which die of lymphoma within a few weeks of birth (Eischen et al., 1999).

Previous evidence has demonstrated that several RPs such as RPL5, RPL11 and RPL23 interact with MDM2 to inhibit its E3 ligase function, thereby stabilizing and activating p53, suggesting an RP-MDM2-p53 pathway (Zhang and Lu, 2009). *In vivo* studies have established the physiological significance of the RP-MDM2 interaction in responding to ribosomal stress to activate p53, providing evidence for a p53 checkpoint mediated by the RP-MDM2 interaction, which is capable of monitoring the integrity of ribosome biogenesis (Macias et al., 2010). Furthermore, with use of the *Eμ-Myc* transgenic mouse model, which constitutively expresses c-MYC in the B-cell lineage and develops B-cell lymphoma at an early age (Adams et al., 1985), we have demonstrated that the RP-MDM2-p53 pathway, similar to the p19ARF-MDM2-p53 pathway, plays a critical role in preventing oncogenic c-MYC-induced lymphomagenesis (Macias et al., 2010).

Previous studies have shown that p19ARF can disturb ribosomal biogenesis by interacting with nucleophosmin (B23/NPM) and inhibiting pre-ribosomal RNA processing (Itahana et al., 2003; Sugimoto et al., 2003). More recently, it has been shown that p19ARF inhibits the function of RNA polymerase I transcription termination factor TTF-I (Lessard et al.,

2010) and DDX5 RNA helicase (Saporita et al., 2011) by preventing their nucleolar localization, thereby inhibiting ribosomal biosynthesis. These studies raise an interesting question as to whether the p19ARF-MDM2-p53 and the RP-MDM2-p53 pathways might function in a linear manner as a p19ARF-RP-MDM2-p53 pathway, where p19ARF additionally activates p53 by inhibiting RP biosynthesis. As such, p19ARF deletion or MDM2^{C305F} mutation, which disrupts RP-MDM2 binding, would result in similar consequences in the context of c-MYC overexpression. To gain insight into the interrelationship and possible cooperative mechanisms between p19ARF-MDM2-p53 and RP-MDM2-p53 pathways, we studied tumorigenesis in mice with disruption of each pathway individually and in combination.

RESULTS

MDM2^{C305F} mutation does not accelerate *p19Arf* deletion initiated spontaneous tumor development

Previous studies have shown that mice with homozygous deletion of *p19Arf* (*p19Arf*$^{-/-}$) are predisposed to spontaneous tumor development (Kamijo et al., 1999), whereas mice with homozygous mutation of *Mdm2*^{C305F} (henceforth referred to as *Mdm2*$^{m/m}$), which prevents MDM2 binding to RPL5 and RPL11 (Lindström et al., 2007), do not develop spontaneous tumors (Macias et al., 2010). Because p19ARF interacts with and inhibits B23/NPM (Itahana et al., 2003; Sugimoto et al., 2003), RNA polymerase I TTF-I (Lessard et al., 2010) and DDX5 (Saporita et al., 2011) and as these factors are all involved in ribosomal biosynthesis, we speculated that the p19ARF-MDM2-p53 and the RP-MDM2-p53 pathways might be functionally interconnected. We crossed *p19Arf*$^{-/-}$ and *Mdm2*$^{m/m}$ mice to generate double-heterozygous *Mdm2*$^{+/m}$*;p19Arf*$^{+/-}$ mice and then intercrossed the *Mdm2*$^{+/m}$*;p19Arf*$^{+/-}$ mice to generate *Mdm2*$^{m/m}$*;p19Arf*$^{-/-}$ compound mice. Of the 186 pups born from intercross of the double-heterozygotes, a predicted Mendelian inheritance was observed (Figure 2.1a, shown are only

three genotypes for simplicity), indicating that concurrent disruption of p19ARF-MDM2-p53 and RP-MDM2-p53 pathways does not affect embryogenesis and early development.

A survival study was carried out to examine the effect of concurrent *p19Arf* deletion and $Mdm2^{C305F}$ mutation on spontaneous tumor formation and lifespan in the mice. Consistent with previous studies, mice heterozygous for $Mdm2^{C305F}$ mutation ($Mdm2^{+/m}$) and *p19Arf* deletion ($p19Arf^{+/-}$) did not show any pathological or physiological changes. In addition, we did not observe any phenotypic changes in double-heterozygous $Mdm2^{+/m}$; $p19Arf^{+/-}$ mice (data not shown). Consistent with previous reports (Kamijo et al., 1999), mice with homozygous deletion of *p19Arf* were predisposed to tumors, mostly lymphomas, and died shortly after the development of disease, resulting in a notably shorter lifespan compared to WT mice (Figure 2.1b). However, mice with homozygous $Mdm2^{C305F}$ mutation did not show observable differences in spontaneous tumor formation and lifespan from the WT littermates. Interestingly, double-homozygous compound mice ($Mdm2^{m/m}$;$p19Arf^{-/-}$) did not show accelerated spontaneous tumor formation compared to mice with only *p19Arf* deletion, instead they displayed slightly decelerated tumor formation (Figure 2.1b; log-rank test P=0.06); the reasons for the deceleration remain unclear. We have noticed that the mean latency for survival of the $p19Arf^{-/-}$ mice in our experiment is 16 months, significantly longer than the previous report of ~ 10 months (Kamijo et al., 1999). One likely reason for the difference is that our mice are in >99% pure C57BL6 background as compared to a mixed 129svj/C57BL6 background in the previous study. It has been reported that C57BL6 mice are more resistant to spontaneous tumor formation than 129svj mice (Hoag, 1963; Smith et al., 1973), and C57BL6 mice are more efficient in total leukocyte recruitment than 129svj mice (White et al., 2002), a function important in preventing lymphomagenesis (Shetty et al., 2012).

Concurrent disruption of the p19ARF-MDM2-p53 and the RP-MDM2-p53 pathways further accelerates oncogenic c-MYC-induced lymphomagenesis

To further investigate the consequence of disruption of the p19ARF-MDM2-p53 and the RP-MDM2-p53 pathways on tumorigenesis, we generated *Eμ-Myc* transgenic mice on $Mdm2^{m/m}$ and $p19Arf^{-/-}$ backgrounds individually and in combination, and compared their tumor-free survival time. *Eμ-Myc;WT* mice died of pre-B/B-cell lymphoma with a mortality curve consistent with previous studies (Figure 2.2) (Adams et al., 1985; Eischen et al., 1999). The median survival of *Eμ-Myc;*$p19Arf^{+/-}$ mice was 15.6 weeks, significantly shorter than *Eμ-Myc;WT* mice (Figure 2.2a, P=0.003), whereas the median survival for *Eμ-Myc;*$Mdm2^{+/m}$ mice was not significantly different from that of *Eμ-Myc;WT* mice (Figure 2.2b, P=0.5). In contrast, homozygous *Eμ-Myc;*$p19Arf^{-/-}$ and *Eμ-Myc;*$Mdm2^{m/m}$ mice developed aggressive, rapid onset pre-B/B-cell lymphoma with a mean survival of 10.1 and 11.6 weeks, respectively (Figures 2.2a-b), indicating that both p19ARF-MDM2 and RP-MDM2 binding function as barriers to oncogenic c-MYC-induced tumorigenesis.

To determine if the RP-MDM2-p53 and p19ARF-MDM2-p53 represent two parallel pathways or a single linear p19ARF-RP-MDM2-p53 pathway against *Eμ-Myc* transgene-induced lymphomas, we generated *Eμ-Myc;*$Mdm2^{m/m}$*;*$p19Arf^{-/-}$ compound mice and evaluated the impact of the double mutation on mouse survival. Remarkably, *Eμ-Myc;*$Mdm2^{m/m}$*;*$p19Arf^{-/-}$ mice demonstrated a median survival of 7.6 weeks, evidently shorter than the lifespan observed in either *Eμ-Myc;*$Mdm2^{m/m}$ or *Eμ-Myc;*$p19Arf^{-/-}$ mice (Figure 2.3a). These data indicate that the p19ARF-MDM2-p53 and the RP-MDM2-p53 interactions likely represent two independent signaling pathways possessing non-overlapping tumor suppression functions. We noticed that the mean survival of *Eμ-Myc;*$p19Arf^{-/-}$ mice is significantly shorter than that of *Eμ-Myc;*$Mdm2^{m/m}$ mice (10.1 vs 11.6 weeks; Figure 2.3a, P=0.0001). This indicates that in addition to directly inhibiting MDM2 and activating p53, p19ARF may also partially exert its function through the RP-MDM2-p53 pathway by inhibiting ribosomal biogenesis (Itahana et al., 2003; Sugimoto et

al., 2003). No significant difference in body weight gain was observed among the genotypes in the early stages of the mouse lifespan (Figure 2.3b). In later stages, however, the *Eμ-Myc;p19Arf*$^{-/-}$ mice grow larger, and the *Eμ-Myc;Mdm2*$^{m/m}$ mice grow smaller than the *Eμ-Myc;WT* control mice. The reason for this discrepancy is unclear. In the final stages of their life, the mice began to lose weight from cancerous cachexia, indicating that these *Eμ-Myc* transgenic mice die of cachexia due to malignant tumor development.

Mdm2$^{m/m}$*;p19Arf*$^{-/-}$ mice demonstrate accelerated c-MYC-induced tumorigenesis and metastasis

Splenomegaly is a common result of infiltration of lymphomas. *Eμ-Myc* transgenic mice typically present with a massive enlargement of the spleen (Sidman et al., 1988). We measured the length of the spleens from mice at 9 weeks of age. As shown in Figure 2.4a, *Eμ-Myc;WT* mice had an average spleen length of 1.6 cm, as compared to 1.1 cm spleen length in *WT*, non-transgenic mice. Both homozygous *Mdm2*^{C305F} mutation and *p19Arf* deletion accelerated splenomegaly, with average spleen size increased in *Eμ-Myc;Mdm2*$^{m/m}$ and *Eμ-Myc;p19Arf*$^{-/-}$ transgenic mice to 2.4 and 2.5 cm, respectively. Compound mice harboring both *Mdm2*^{C305F} mutation and *p19Arf* deletion demonstrated further accelerated splenomegaly, and the average spleen length of *Eμ-Myc;Mdm2*$^{m/m}$*;p19Arf*$^{-/-}$ mice was 3.8 cm at 9 weeks of age.

We next examined the invasive nature of *Eμ-Myc*-induced lymphomas in the spleen, liver, and kidney tissues isolated from 9 week old mice. Spleen metastasis occurred earlier than other organs, and the structure of the spleens in mice harboring *Eμ-Myc* transgene was already destroyed at this age. As shown in Figure 2.4b, expression of the *Eμ-Myc* correlates with an increased number of small lymphocytes within the cords and sinuses, as well as some nodular aggregates surrounding a small vessel, indicative of spleen metastasis. The most significant metastasis was observed in the spleen of *Eμ-Myc;Mdm2*$^{m/m}$*;p19Arf*$^{-/-}$ compound mice. Similar to the spleen, lymphocyte infiltration in the liver can be seen in each of the *Eμ-Myc* transgenic mice, specifically in the region surrounding the central veins. Not surprisingly, the most obvious

liver metastasis was observed in *Eμ-Myc;Mdm2*$^{m/m}$*;p19Arf*$^{-/-}$ compound mice (Figure 2.4b). Kidney metastasis usually occurs in advanced or late-stage lymphomas, and metastatic tumor cells were detected as diffuse and disorganized cells infiltrating between the glomerulus and tubules (Eischen et al., 2004). As shown in Figure 2.4b, in *WT*, *Eμ-Myc;WT*, *Eμ-Myc;Mdm2*$^{m/m}$ and *Eμ-Myc;p19Arf*$^{-/-}$ mice, kidneys revealed no discernible pathological phenotype, and lymphocyte infiltration is only obvious in the compound *Eμ-Myc;Mdm2*$^{m/m}$*;p19Arf*$^{-/-}$ mice. Together, these data indicate that individually disrupting the p19ARF-MDM2-p53 pathway by *p19Arf* deletion or the RP-MDM2-p53 pathway by *Mdm2*^{C305F} mutation augments the invasive nature of *Eμ-Myc*-induced lymphoma. Simultaneous disruption of both pathways, as seen in *Eμ-Myc;Mdm2*$^{m/m}$*;p19Arf*$^{-/-}$ mice, leads to even more malignant and aggressive lymphomagenesis.

To determine if cells in *Eμ-Myc*-expressing spleens retained their proliferative capacity, Ki-67 staining was used to assess cellular proliferation by immunohistochemistry (IHC). As shown in Figure 2.5a, in the absence of the *Eμ-Myc* transgene Ki-67 expression was barely detectable in the spleen of 9 week old *WT* mice (Ki-67 index 0.4). In *Eμ-Myc;WT* mice, we detected increased numbers of Ki-67-positive cells (Ki-67 index 2.8); the number of Ki-67-positive cells was further increased in spleens from *Eμ-Myc;Mdm2*$^{m/m}$ and *Eμ-Myc;p19Arf*$^{-/-}$ mice (Ki-67 index 12.2 and 14.6, respectively). In spleens of *Eμ-Myc;Mdm2*$^{m/m}$*;p19Arf*$^{-/-}$ compound mice the number of Ki-67-positive cells was even further increased (Ki-67 index 53.9).

To examine apoptosis in the spleen tumors of the transgenic mice, TUNEL (terminal deoxynucleotidyl transferase-mediated dUTP-biotin nick end labeling) immunohistochemical analysis was performed. Representative pictures of TUNEL-stained sections are shown in Figure 2.5b. Consistent with previous studies that *Eμ-Myc* induces apoptosis in transgenic spleens, in spleens of 9 week old *Eμ-Myc;WT*, *Eμ-Myc;Mdm2*$^{m/m}$ and *Eμ-Myc;p19Arf*$^{-/-}$ mice, we detected high levels of TUNEL-positive apoptotic cells (14.6, 13.6, and 14.4%, respectively).

However, in spleens of *Eμ-Myc;Mdm2*$^{m/m}$*;p19Arf*$^{-/-}$ compound mice the number of TUNEL positive apoptotic cells decreased to 6.2%.

Local invasion and distant metastasis of lymphomas are commonly observed in *Eμ-Myc* transgenic mice; we therefore analyzed liver tissues from individual mice for signs of metastasis. *Eμ-Myc* transgenic mice were monitored for signs of moribund conditions (Toth et al., 2014), and moribund mice were killed and the livers were collected and examined for sign of metastasis. Tumors were detected in the livers of *Eμ-Myc;WT* transgenic mice at an average age of 22 weeks (Figure 2.6). In contrast, tumor onset in the liver was detected much earlier in *Eμ-Myc;Mdm2*$^{m/m}$, *Eμ-Myc;p19Arf*$^{-/-}$ and *Eμ-Myc;Mdm2*$^{m/m}$*;p19Arf*$^{-/-}$ mice, with progressively shorter time of onset at 13, 11 and 9 weeks, respectively (Figure 2.6). These results demonstrate that individually the *Mdm2*^{C305F} mutation and *p19Arf* deletion promote local invasion and distant metastasis of *Eμ-Myc*-induced lymphomas, with *p19Arf* deletion having a stronger effect than *Mdm2*^{C305F} mutation, which is consistent with the shorter lifespan of the *Eμ-Myc;p19Arf*$^{-/-}$ mice compared to the *Eμ-Myc;Mdm2*$^{m/m}$ mice (Figure 2.3a). Concurrent *Mdm2*^{C305F} mutation and *p19Arf* deletion further accelerates the aggressiveness of the lymphoma, resulting in an even shorter lifespan, consistent with the notion that the p19ARF-MDM2-p53 and the RP-MDM2-p53 represent two non-redundant, independent pathways for tumor suppression.

<u>The p19ARF-MDM2-p53 and the RP-MDM2-p53 pathways function independently in oncogenic c-MYC-induced p53 activation</u>

Oncogene c-MYC induces p53 to promote apoptosis, functioning as part of a major tumor suppression network. Because *Eμ-Myc*-induced lymphomagenesis in mice can be further accelerated by concurrent disruption of the p19ARF-MDM2-p53 and the RP-MDM2-p53 pathways compared to disruption of either pathway alone, we reasoned that the two pathways could each individually be required for oncogenic c-MYC-induced p53 activation. To test this

hypothesis, spleen extracts from 4 week old, non-tumor-bearing *Eμ-Myc;WT*, *Eμ-Myc;Mdm2*$^{m/m}$, *Eμ-Myc;p19Arf*$^{-/-}$ and *Eμ-Myc;Mdm2*$^{m/m}$*;p19Arf*$^{-/-}$ transgenic mice, as well as from their non-transgenic counterparts, were analyzed for p53 expression. At this age the spleens harboring the *Eμ-Myc* transgene are moderately hyperplastic, but still comparable in size and morphology to the spleens of non-transgenic mice (data not shown). The *Eμ-Myc* transgene markedly induced p53 protein expression in WT mouse spleens (Figure 2.7a, lane 2), which is accompanied by increased expression of p19ARF, RPL5 and RPL11, all of which are known transcriptional targets of c-MYC (van Riggelen et al., 2010; Zindy et al., 1998). The *Eμ-Myc* transgene also induced p53 expression in *Eμ-Myc;Mdm2*$^{m/m}$ and *Eμ-Myc;p19Arf*$^{-/-}$ spleens to a similar level, although slightly lower than what is detected in *Eμ-Myc;WT* spleens (Figure 2.7a, compare lanes 2, 4 and 6). Remarkably, p53 induction was not observed *Eμ-Myc;Mdm2*$^{m/m}$*;p19Arf*$^{-/-}$ compound mouse spleens (Figure 2.7a, lane 8). These data demonstrate that individual disruption of the p19ARF-MDM2-p53 pathway by *p19Arf* deletion or the RP-MDM2-p53 pathway by *Mdm2*^{C305F} mutation does not block c-MYC induction of p53, while simultaneous disruption of both pathways blocks c-MYC-induced p53 expression. To ascertain whether these observations are *Eμ-Myc* transgene specific, we infected early passage *WT*, *Mdm2*$^{m/m}$, *p19Arf*$^{-/-}$ and *Mdm2*$^{m/m}$*;p19Arf*$^{-/-}$ MEF cells with retrovirus expressing pBabe-c-MYC to determine if transient expression of c-MYC gives rise to similar results. Consistent with observations made in mouse spleens, transient expression of pBabe-c-MYC resulted in p53 induction in *WT*, *Mdm2*$^{m/m}$ and *p19Arf*$^{-/-}$ MEFs, but not in *Mdm2*$^{m/m}$*;p19Arf*$^{-/-}$ MEFs (Figure 2.7b). Furthermore, the increased protein level of p53 was directly correlated with its transcriptional activity, indicated by S-18 phosphorylation of p53 in the spleens (p21 was undetectable in spleens; Figure 2.7a), and increased p21 protein level in pBabe-c-MYC infected MEFs (Figure 2.7b).

To corroborate the protein analysis, we carried out quantitative PCR (qPCR) to further examine p53 activity in 4 week old, non-tumor-bearing *Eμ-Myc;WT*, *Eμ-Myc;Mdm2*$^{m/m}$, *Eμ-*

Myc;p19Arf$^{-/-}$ and *Eμ-Myc;Mdm2*$^{m/m}$*;p19Arf*$^{-/-}$ mouse spleens and in spleens from their non-transgenic counterparts. We chose p53 targets involved in cell cycle regulation (*p21*), apoptosis induction (*bax* and *apaf1*) and metabolic regulation (*tigar*) to determine whether p53 is activated universally for its target genes. Induction of each of these p53 target genes was evident in *Eμ-Myc;WT*, *Eμ-Myc;Mdm2*$^{m/m}$ and *Eμ-Myc;p19Arf*$^{-/-}$ mouse spleens, but not in *Eμ-Myc;Mdm2*$^{m/m}$*;p19Arf*$^{-/-}$ mouse spleens (Figure 2.8), consistent with protein analysis. Together, our data indicate that not only can the p19ARF-MDM2-p53 and the RP-MDM2-p53 pathways be independently responsible for oncogenic c-MYC induction of p53, but also that the two pathways together contribute to most if not all p53 tumor suppressor response to c-MYC activation. Disabling both pathways results in undetectable p53 activation by oncogenic c-MYC overexpression.

DISCUSSION

The importance of p19ARF-MDM2-p53 and RP-MDM2-p53 signaling pathways in defending against oncogenic c-MYC induced tumorigenesis is well established, and studies have shown that disruption of each of the two pathways by deletion or mutation accelerates the progression of malignancy in c-MYC expressing mice (Eischen et al., 1999; Macias et al., 2010). In this study, we generated and analyzed mice with concurrent disruption of these two pathways and compared p53 activity and tumorigenesis to mice with disruption of each pathway alone. The significance and implications of these findings are discussed below.

The p19ARF-MDM2-p53 and the RP-MDM2-p53 signaling pathways act independently in oncogenic c-MYC-induced p53 activation

The generation of *Mdm2*$^{m/m}$ mice has allowed for a detailed *in vivo* characterization of the role of RP-MDM2 binding in p53 activation and tumor suppression. Unlike the disruption of the p19ARF-MDM2-p53 pathway by *p19Arf* deletion, which results in spontaneous tumor

development (Kamijo et al., 1997), disruption of the RP-MDM2-p53 pathway by *Mdm2*^{C305F} mutation does not result in spontaneous tumor development (Macias et al., 2010). The different tumorigenic potential between the two mouse models could be a result of the nature of the two pathways in each of the mouse models. In *p19Arf*$^{-/-}$ mice the entire *p19Arf* gene is deleted, disrupting p19ARF-MDM2 binding as well as all other p19ARF-related functions; in *Mdm2*$^{m/m}$ mice, however, the single-point mutation in *mdm2* is less disruptive, and while MDM2^{C305F} mutant protein cannot properly bind to RPL5/RPL11, it retains binding to other RPs like RPL23 (Lindström et al., 2007), thus only reducing but not eliminating the functions of this pathway. Alternatively, it is conceivable that the p19ARF-MDM2-p53 pathway primarily responds to deregulated oncogenes, which inflict a great risk of tumor formation if left unchecked, whereas the RP-MDM2-p53 pathway may primarily respond to deregulated ribosome biosynthesis, which may play a lesser role in promoting cancerous growth.

In addition, it has been shown that p19ARF binds to and inhibits the ability of c-MYC to induce hyperproliferation and transformation (Qi et al., 2004; Zhang et al., 2013b) indicating that loss of p19ARF could contribute to c-MYC-induced tumorigenesis by at least two mechanisms. Similarly, it has been shown that RPL11 binds to c-MYC and inhibits its transcriptional activity (Dai et al., 2007) and that RPL5, cooperatively with RPL11, guides the RNA-induced silencing complex to c-MYC mRNA and mediates the degradation of c-MYC mRNA (Liao et al., 2014). These studies in combination with our results point to the importance of both p19ARF and RP signaling in c-MYC-induced lymphomagenesis. Our results agree with the notion that *Eμ-Myc*-induced lymphomagenesis can be accelerated by disruption of negative regulators of c-MYC in each pathway in addition to disruption of p53 activation.

Our study also addresses the degree of cooperation between the p19ARF-MDM2-p53 and RP-MDM2-p53 pathways in p53 response to oncogenic c-MYC overexpression. When *Mdm2*^{C305F} mutation or *p19Arf* deletion occur individually, c-MYC overexpression still elicits sufficient p53 response; however, when *Mdm2*^{C305F} mutation and *p19Arf* deletion occur

concurrently, c-MYC overexpression does not elicit p53 activation. Given the role of oncogenic c-MYC in promoting aberrant ribosomal biogenesis, the p19ARF-independent, c-MYC-mediated induction of p53 in *p19Arf*$^{-/-}$ cells is conceivably dependent on c-MYC-induced overexpression of RPs, which activate p53 through interaction with MDM2 (Macias et al., 2010). Conversely, activation of p53 by c-MYC in *Mdm2*$^{m/m}$ mice is p19ARF dependent, as the p19ARF-MDM2-p53 pathway remains intact in mice and c-MYC can induce p19ARF expression (Figures 2.7-8). Our data suggest that p53 responds to c-MYC overexpression via two independent signaling pathways: p19ARF-MDM2-p53 and RP-MDM2-p53. Each pathway conveys a share of c-MYC signaling to p53, and disruption of either one reduces, but not eliminates, p53 response to c-MYC overexpression. Consequently, disrupting either pathway will accelerate c-MYC-induced tumor formation, as illustrated by shortened survival times of *Eμ-Myc;Mdm2*$^{m/m}$ and *Eμ-Myc;p19Arf*$^{-/-}$ mice compared to *Eμ-Myc;WT* mice. Disrupting both pathways further accelerates c-MYC-induced tumorigenesis, as illustrated by the comparatively shorter tumor-free lifespan of *Eμ-Myc;Mdm2*$^{m/m}$*;p19Arf*$^{-/-}$ compound mice. Our data support a model in which the RP-MDM2-p53 and p19ARF-MDM2-p53 pathways represent two non-redundant, parallel mechanisms for p53 induction (Figure 2.9). Intriguingly, the lack of detectable p53 activation in the *Eμ-Myc;Mdm2*$^{m/m}$*;p19Arf*$^{-/-}$ compound mice implies that other active mechanisms transmitting oncogenic c-MYC signal to p53 either may not exist or be insufficient to raise p53 to a detectable level.

The p19ARF-MDM2 connection mediates a p53-dependent checkpoint in response to a broad range of oncogenic insults, including elevated expression of c-MYC, E2F1, RAS, E1A and BCR-ABL. However, the RP-MDM2 connection provides evidence for a prevailing *in vivo* checkpoint for the integrity of ribosome biogenesis to invoke p53 response if the process goes awry. Given that overexpression of many oncogenes promotes fast growth and proliferation, which inevitably requires accelerated ribosomal biogenesis it is reasonable to speculate that the RP-MDM2-p53 signaling pathway, in addition to responding to c-MYC overexpression, may also

respond to other deregulated oncogenes that cause superfluous ribosomal biogenesis. The *Mdm2*$^{m/m}$ mouse model provides a convenient tool to investigate whether the RP-MDM2-p53 pathway, as in the case of the p19ARF-MDM2-p53 pathway, functions generally in oncogenic signaling surveillance, capable of responding to a broad range of deregulated oncogenes, or is only specific to oncogenic c-MYC.

EXPERIMENTAL PROCEDURES

Cell culture

Primary MEFs were isolated on embryonic (E) day 13.5 and grown in a 37°C incubator with 5% CO_2 in Dulbecco's modified Eagle's medium supplied with 10% fetal bovine serum and penicillin-streptomycin. For retroviral infections, *WT*, *Mdm2*$^{m/m}$, *p19Arf*$^{-/-}$ and *Mdm2*$^{m/m}$*;p19Arf*$^{-/-}$ MEFs were infected with retroviruses expressing c-MYC or pBabe control vector, and selected with puromycin (2.5 μg/ml) for 3 days. Infected MEFs were then allowed to recover for 48 h and harvested for analysis. MEFs at passage 4 were used for growth curves, western blotting (WB) and other analyses.

Mouse experiments

Mice were bred and maintained strictly under protocol (13-044) approved by the Institutional Animal Care and Use Committee in the University of North Carolina Animal Care Facility. *Mdm2*$^{m/m}$ females were bred with *p19Arf*$^{-/-}$ males to obtain *Mdm2*$^{+/m}$*;p19Arf*$^{+/-}$ offspring, which were then crossed with *Mdm2*$^{+/m}$*;p19Arf*$^{+/-}$ mice to obtain *Mdm2*$^{m/m}$*;p19Arf*$^{-/-}$ compound mice. For c-MYC-mediated tumorigenesis studies, *Mdm2*$^{m/m}$*;p19Arf*$^{-/-}$ females were bred with *Eμ-Myc* transgenic males to obtain *Eμ-Myc;Mdm2*$^{+/m}$*;p19Arf*$^{+/-}$ offspring, which were then crossed with *Mdm2*$^{+/m}$*;p19Arf*$^{+/-}$ mice to obtain *Eμ-Myc;Mdm2*$^{m/m}$*;p19Arf*$^{-/-}$ compound mice. *Eμ-Myc* mice were purchased from Jackson Laboratory (002728). For survival studies, mice were palpated regularly for early signs of inguinal lymph node enlargement and monitored for tumor

progression and signs of morbidity. Moribund mice were humanely euthanized. Mouse tumors and organs were fixed in formalin for histopathology and snap frozen for protein and RNA extraction.

Protein analysis

For western blots, MEFs were lysed with 0.5% (Tergitol, Sigma, St Louis, MO, USA) NP-40 lysis buffer. For mouse tissue protein extraction, tissue from the spleen, thymus and lymphomas was ground by mortar and pestle with liquid N_2, and protein was extracted with 0.5% NP-40 lysis buffer. Mouse monoclonal anti-MDM2 (2A10, Calbiochem, Billerica, MA, USA), mouse monoclonal anti-p53 (NCL-505, Novocastra, Buffalo Grove, IL, USA), mouse monoclonal anti-Actin (MAB1501, Chemicon International, Billerica, MA, USA), goat polyclonal anti-p53 (FL-393, Santa Cruz Biotechnology, Dallas, TX, USA) and rat monoclonal anti-p19ARF (5-C3-1, Santa Cruz Biotechnology) antibodies were purchased commercially. Rabbit polyclonal antibodies to p21 were gifts from Dr. Yue Xiong (UNC-Chapel Hill). Rabbit polyclonal antibodies to RPL5 and RPL11 were made in house as previously described (Lindström et al., 2007).

Measurement of mouse tissue

Spleens, kidneys and livers from 9 week old mice were excised, photographed and weighed. All procedures involving mice were carried out according to protocol 13-044, approved by the University of North Carolina Institutional Animal Care and Use Committee.

Histopathology

Animals were autopsied and all tissues were examined regardless of their pathological status. Spleen, kidney and liver tissue from *Eμ-Myc;WT*, *Myc;Mdm2*$^{m/m}$, *Eμ-Myc;p19Arf*$^{-/-}$ and *Eμ-Myc;Mdm2*$^{m/m}$*;p19Arf*$^{-/-}$ transgenic mice, as well as tissue from non-transgenic counterparts were fixed overnight in 10% phosphate-buffered formalin and then transferred to 70% ethanol.

Samples were sent to the UNC Histology Core Facility for paraffin embedding. Paraffin blocks were sectioned at 5-mm intervals for successive layers and stained with H&E for histopathology examination.

Proliferation analysis

Ki-67 IHC staining of mouse spleen samples was used to detect proliferating cells. Antigen retrieval for antibody on formalin-fixed paraffin sections was carried out by boiling paraffin samples in citrate buffer (pH 6.0) for 15 min. Endogenous peroxidase activity was quenched by incubation in 3% H_2O_2 in methanol for 10 min. Antibody detection was carried out with purified mouse anti Ki-67 primary antibody (BD Pharmingen, San Diego, CA, USA) and biotin-conjugated anti-mouse secondary antibody (Vector Laboratories, Burlingame, CA, USA). Ki-67-expressed cells were stained brown color by biotin-peroxidase kit (VECTASTAIN Elite, Vector Laboratories). The ratio of positively stained cells to total cells was calculated. Student's t-test ($P<0.05$ was considered significant) was used to compare the differences in proliferation levels between the different mouse genotypes.

Apoptosis analysis

Levels of apoptosis in mouse spleen sections were assessed by the TUNEL assay according to instructions (ApopTag Peroxidase in situ kit, S7100, Millipore, Temecula, CA, USA).

Quantitative real-time PCR

Total RNA was isolated using an RNeasy kit (74104, Qiagen, Hilden, Germany) and cDNA was synthesized using SuperScript III (18080400, Life Technologies, Waltham, MA, USA). qPCR was performed with SYBR green master mix using the 7900HT fast real-time PCR system (Applied Biosystems, Waltham, MA, USA) according to manufacturers' instructions.

Data were collected and exported with SDS 2.2.2 software (Applied Biosystems). Relative expression was calculated using *actin* as an internal control as indicated. Primers used were as follows: *p21*, 5′-CCTGGTGATGTCCGACCTG-3′ and 5′-CCATGAGCGCATCGCAATC-3′; *bax*, 5′-GGACAGCAATATGGAGCTGCAGAGG-3′ and 5′-GGAGGAAGTCCAGTGTCCAGCC-3′; *apaf1*, 5′-CGGTGAAGGTGTGGAATGTCATTACCG-3′ and 5′-GGATTTCTCCATTGTCATCTCCAGTTGC-3′; *tigar*, 5′-CGATCTCACGAGGACTAAGCAGACC-3′ and 5′-GCCAAAGAGCTTTCCAAACCGCTGC-3′; and *actin*, 5′-CCACAGCTGAGAGGGAAATCGTGC-3′ and 5′CCAGAGCAGTAATCTCCTTCTGCATCC-3′.

Statistical analysis

Statistical analysis was carried out using GraphPad Prism 5 Software (Graph-Pad Software, San Diego, CA, USA). Kaplan-Meier survival analysis was carried out to assess lifespan.

Ethics statement

Investigation has been conducted in agreement with the ethical standards according to the Declaration of Helsinki, national and international guidelines, and has been approved by the authors' institutional review board.

A

Genotype	Ratio	Expected	Actual	Male	Female
WT	1/9	20.67	21	11	10
Mdm2$^{+/m}$;*ARF*$^{+/-}$	1/9	20.67	23	9	14
Mdm2$^{m/m}$;*ARF*$^{-/-}$	1/9	20.67	20	12	8

B

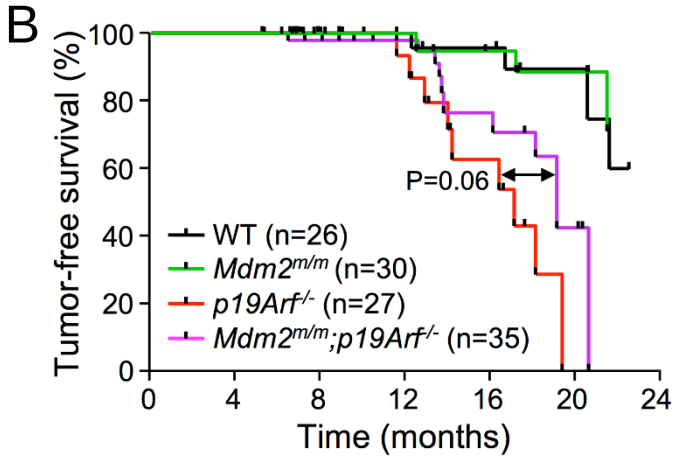

Figure 2.1 Disruption of the p19ARF-MDM2-p53 pathway, but not the RP-MDM2-p53 pathway, results in spontaneous tumor development.

A. The image shown are expected and observed birth ratios from a total of 186 mice obtained from *Mdm2*$^{+/m}$;*p19Arf*$^{+/-}$ mice intercrosses (shown only three genotypes for simplicity).

B. Kaplan-Meier survival curves for *WT*, *Mdm2*$^{m/m}$, *p19Arf*$^{-/-}$ and *Mdm2*$^{m/m}$;*p19Arf*$^{-/-}$ mice are shown. Two to five mice of the same gender were housed in each cage, and the mice were observed over a 24 month period. Median survival time of *p19Arf*$^{-/-}$ and *Mdm2*$^{m/m}$;*p19Arf*$^{-/-}$ mice was 16 and 19 months, respectively. There was no significant difference between survival of *p19Arf*$^{-/-}$ and *Mdm2*$^{m/m}$;*p19Arf*$^{-/-}$ mice (analyzed by log-rank test, P=0.06).

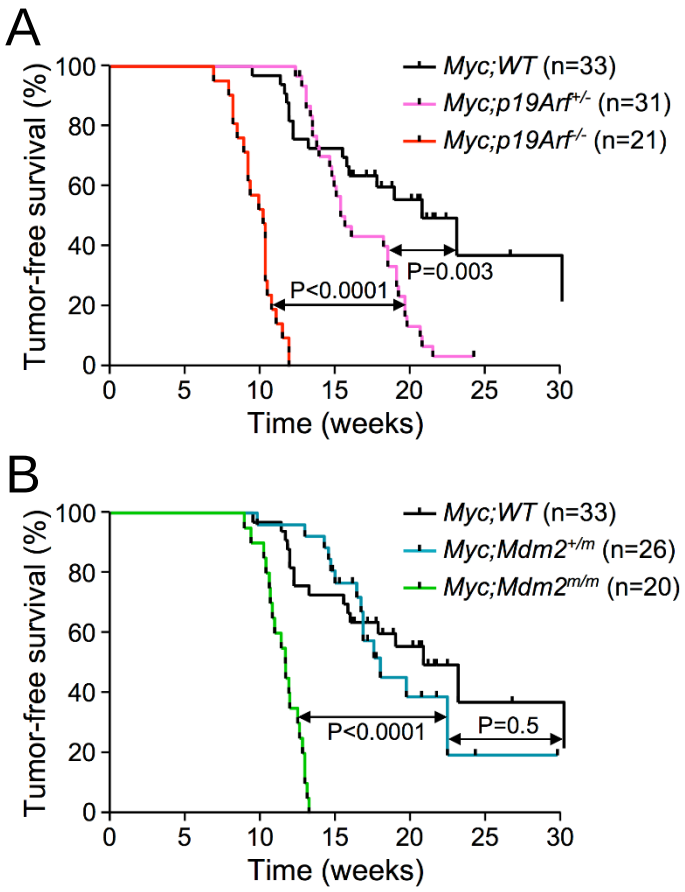

Figure 2.2 c-MYC-induced lymphomagenesis is accelerated by *Mdm2$^{m/m}$* or *p19Arf$^{-/-}$* alterations.

A. Survival of *Eμ-Myc* transgenic *p19Arf* deletion mice. The median survival time for each genotype was as follows: *Eμ-Myc;WT* (20.7 weeks), *Eμ-Myc;p19Arf$^{+/-}$* (15.6 weeks) and *Eμ-Myc;p19Arf$^{-/-}$* (10.1 weeks). Log-rank test, P=0.003 between *Eμ-Myc;WT* and *Eμ-Myc;p19Arf$^{+/-}$* mice; P<0.0001 between *Eμ-Myc;p19Arf$^{+/-}$* and *Eμ-Myc;p19Arf$^{-/-}$* mice.

B. Survival of *Eμ-Myc* transgenic Mdm2^{C305F} mutation mice. The median survival times were as follows: *Eμ-Myc;WT* (20.7 weeks), *Eμ-Myc;Mdm2$^{+/m}$* (17.9 weeks) and *Eμ-Myc;Mdm2$^{m/m}$* (11.6 weeks). Log-rank test, P=0.5 between *Eμ-Myc;WT* and *Eμ-Myc;Mdm2$^{+/m}$* mice; P<0.0001 between *Eμ-Myc;Mdm2$^{+/m}$* and *Eμ-Myc;Mdm2$^{m/m}$* mice.

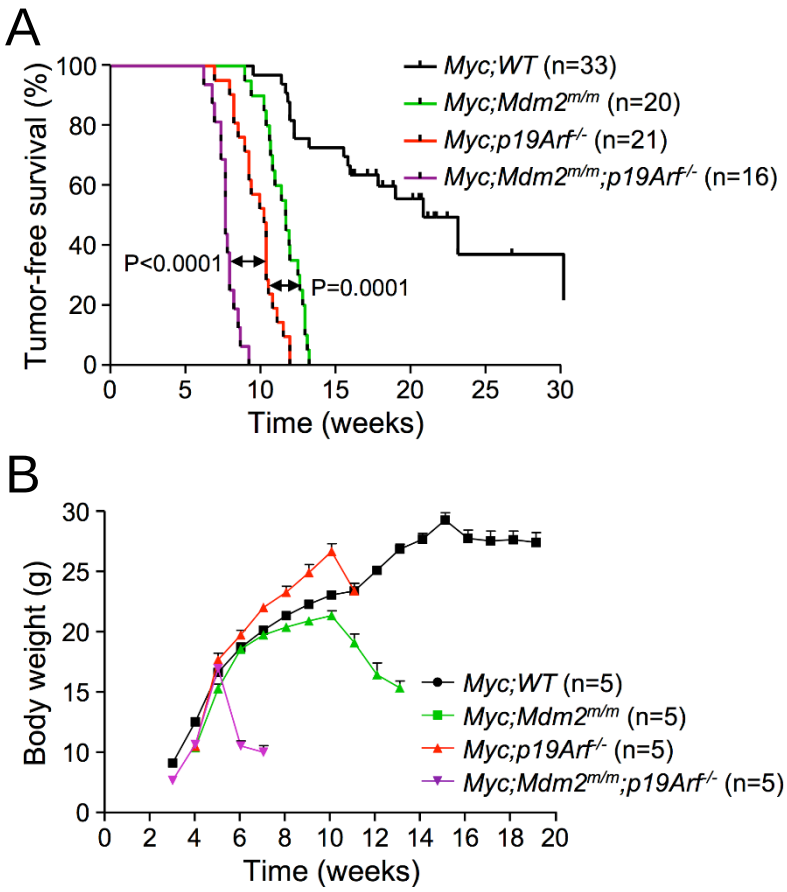

Figure 2.3 c-MYC-induced lymphomagenesis is further accelerated by concurrent *Mdm2$^{m/m}$;p19Arf$^{-/-}$* alterations.

A. Survival of *Eμ-Myc;WT* (20.7 weeks), *Eμ-Myc;Mdm2$^{m/m}$* (11.6 weeks), *Eμ-Myc;p19Arf$^{-/-}$* (10.1 weeks) and *Eμ-Myc;Mdm2$^{m/m}$;p19Arf$^{-/-}$* (7.6 weeks) mice. Log-rank test, P=0.0001 between *Eμ-Myc;Mdm2$^{m/m}$* and *Eμ-Myc;p19Arf$^{-/-}$* mice; P<0.0001 between *Eμ-Myc;p19Arf$^{-/-}$* and *Eμ-Myc;Mdm2$^{m/m}$;p19Arf$^{-/-}$* mice.

B. Body weight of mice expressing *Eμ-Myc*.

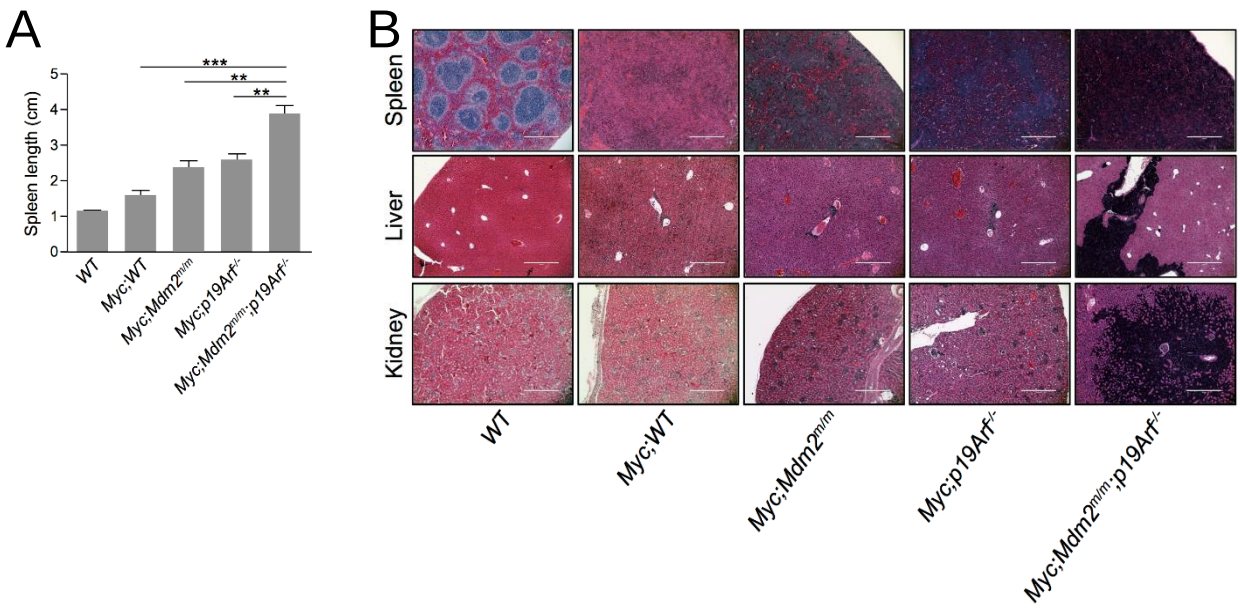

Figure 2.4 *Mdm2$^{m/m}$;p19Arf$^{-/-}$* compound mice demonstrate accelerated lymphoma formation.

A. Length of 9 week old (±3 days) mouse spleens of *WT* (n=5), *Eμ-Myc;WT* (n=5), *Eμ-Myc;Mdm2$^{m/m}$* (n =5), *Eμ-Myc;p19Arf$^{-/-}$* (n=5) and *Eμ-Myc;Mdm2$^{m/m}$;p19Arf$^{-/-}$* (n=5) mice. Spleen length was measured and the median lengths were as follows: *WT* (1.14 cm), *Eμ-Myc;WT* (1.56 cm), *Eμ-Myc;Mdm2$^{m/m}$* (2.36 cm), *Eμ-Myc;p19Arf$^{-/-}$* (2.54 cm) and *Eμ-Myc;Mdm2$^{m/m}$;p19Arf$^{-/-}$* (3.82 cm). Data are represented as mean ±SEM and were analyzed by Student's t-test. ***P<0.001; **P<0.01.

B. H&E staining of spleen, liver and kidney tissues. *WT* mouse spleen serves as a positive control for normal spleen structure. Structure of spleens from *Eμ-Myc* transgenic mice was destroyed by lymphocyte infiltration. Lymphocyte infiltration was observed as dark blue staining. The malignant cells are dispersed and the nuclei are larger than normal lymphocytes. Aggregates of small lymphocytes are observed in the livers and kidneys of *Eμ-Myc* transgenic mice. Scale bar, 400 μm.

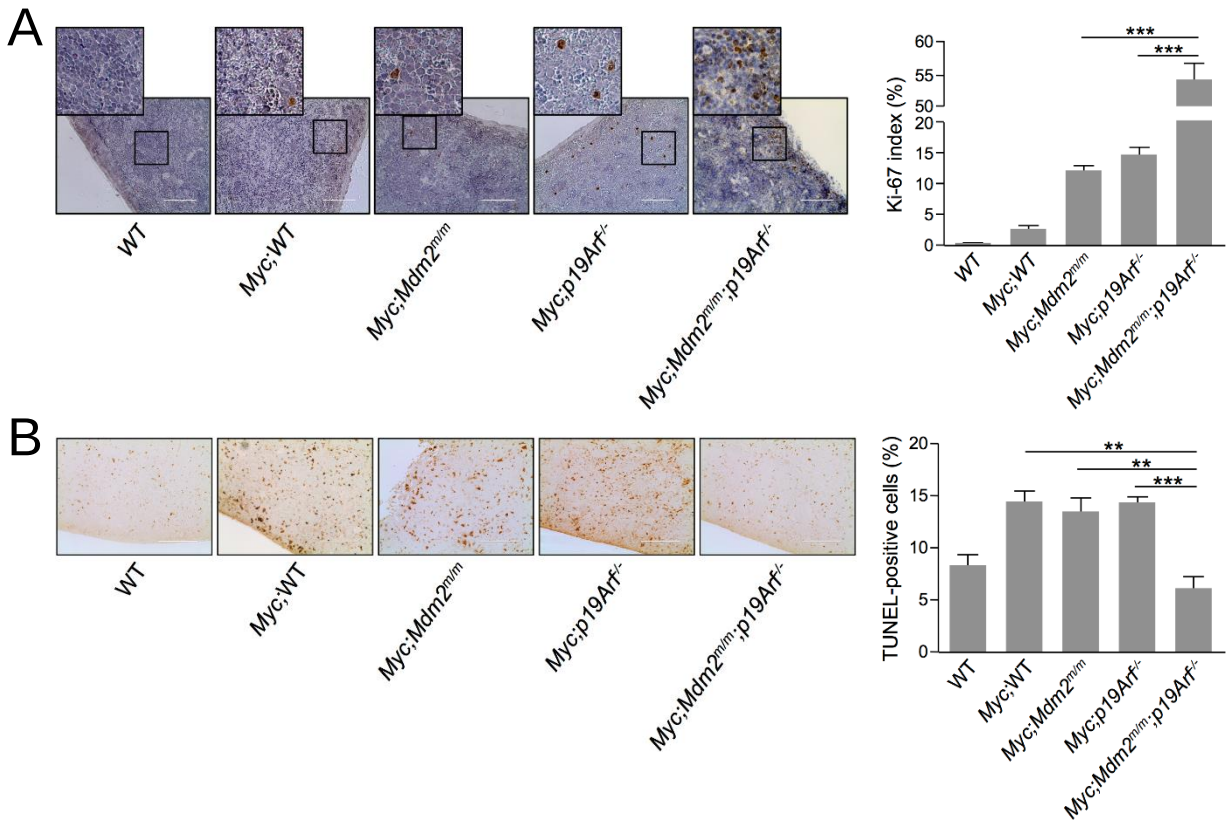

Figure 2.5 *Mdm2$^{m/m}$;p19Arf$^{-/-}$* compound mice exhibit accelerated c-MYC-induced tumor progression.

A. Representative Ki-67 staining of spleens from different genotypes of 9 week old mice, as indicated. Brown staining indicates Ki-67-positive proliferating cells. Scale bar, 100 μm. The Ki-67 index (calculated as the percentage of Ki-67-positive tumor cells vs total cells in the view field from at least five randomly chosen fields along the edge of spleens) for the genotypes assayed are indicated in parentheses: WT (0.4), Eμ-Myc;WT (2.8), Eμ-Myc;Mdm2$^{m/m}$ (12.2), *Eμ-Myc;p19Arf$^{-/-}$* (14.6) and *Eμ-Myc;Mdm2$^{m/m}$;p19Arf$^{-/-}$* (53.9) mice. Data are represented as mean ±SEM. ***P<0.001.

B. Representative TUNEL staining of spleens from different genotypes of 9 week old mice. The percentage of TUNEL-positive cells in the view field was calculated from at least five randomly chosen fields along the edge of spleens and is indicated in parentheses: *WT* (8.4%), *Eμ-Myc;WT* (14.6%), *Eμ-Myc;Mdm2$^{m/m}$* (13.6%), *Eμ-Myc;p19Arf$^{-/-}$* (14.4%) and *Eμ-Myc;Mdm2$^{m/m}$;p19Arf$^{-/-}$* (6.2%). Data are represented as mean±SEM. ***P<0.001; **P<0.01. Scale bar, 200 μm.

Figure 2.6 *Mdm2$^{m/m}$;p19Arf$^{-/-}$* compound mice exhibit accelerated liver metastasis.

H&E staining of livers from different genotypes of similar metastasis stage. Mouse livers were collected at the time of death. Time of metastasis is indicated in parentheses: *Eμ-Myc;WT* (22 weeks), *Eμ-Myc;Mdm2$^{m/m}$* (12.5 weeks), *Eμ-Myc;p19Arf$^{-/-}$* (11 weeks) and *Eμ-Myc;Mdm2$^{m/m}$;p19Arf$^{-/-}$* (9 weeks). Scale bar, 400 μm.

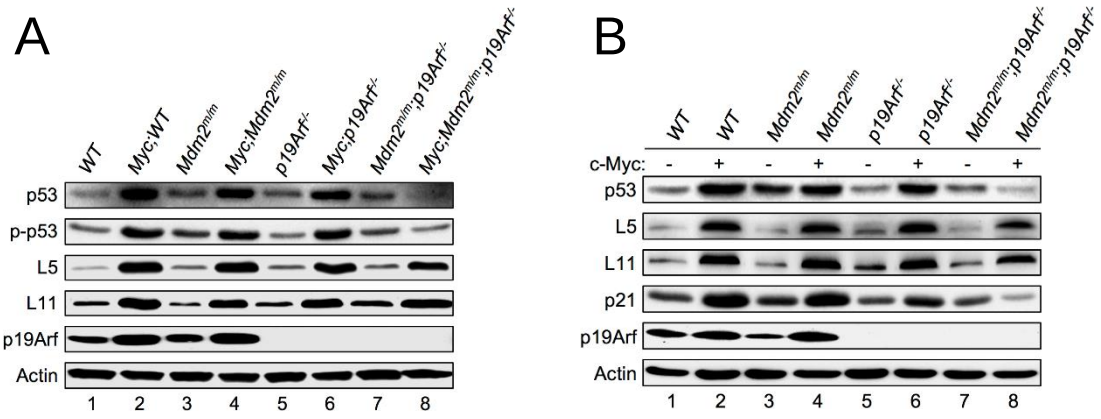

Figure 2.7 The RP-MDM2-p53 and p19ARF-MDM2-p53 signaling pathways function independently in oncogenic c-MYC-induced p53 stabilization.

A. Extracts from spleens of 4 week old, non-tumor-bearing *Eμ-Myc;WT*, *Eμ-Myc;Mdm2*$^{m/m}$, *Eμ-Myc;p19Arf*$^{-/-}$ and *Eμ-Myc;Mdm2*$^{m/m}$*;p19Arf*$^{-/-}$ transgenic mice and spleens from their non-transgenic counterparts were analyzed by western blot.

B. Early passage *WT*, *Mdm2*$^{m/m}$, *p19Arf*$^{-/-}$ and *Mdm2*$^{m/m}$*;p19Arf*$^{-/-}$ MEFs were infected with retrovirus expressing either pBabe vector (-) or pBabe-c-MYC (+), selected by puromycin for 3 days, then allowed to recover for 48 h before harvesting for western blot analysis.

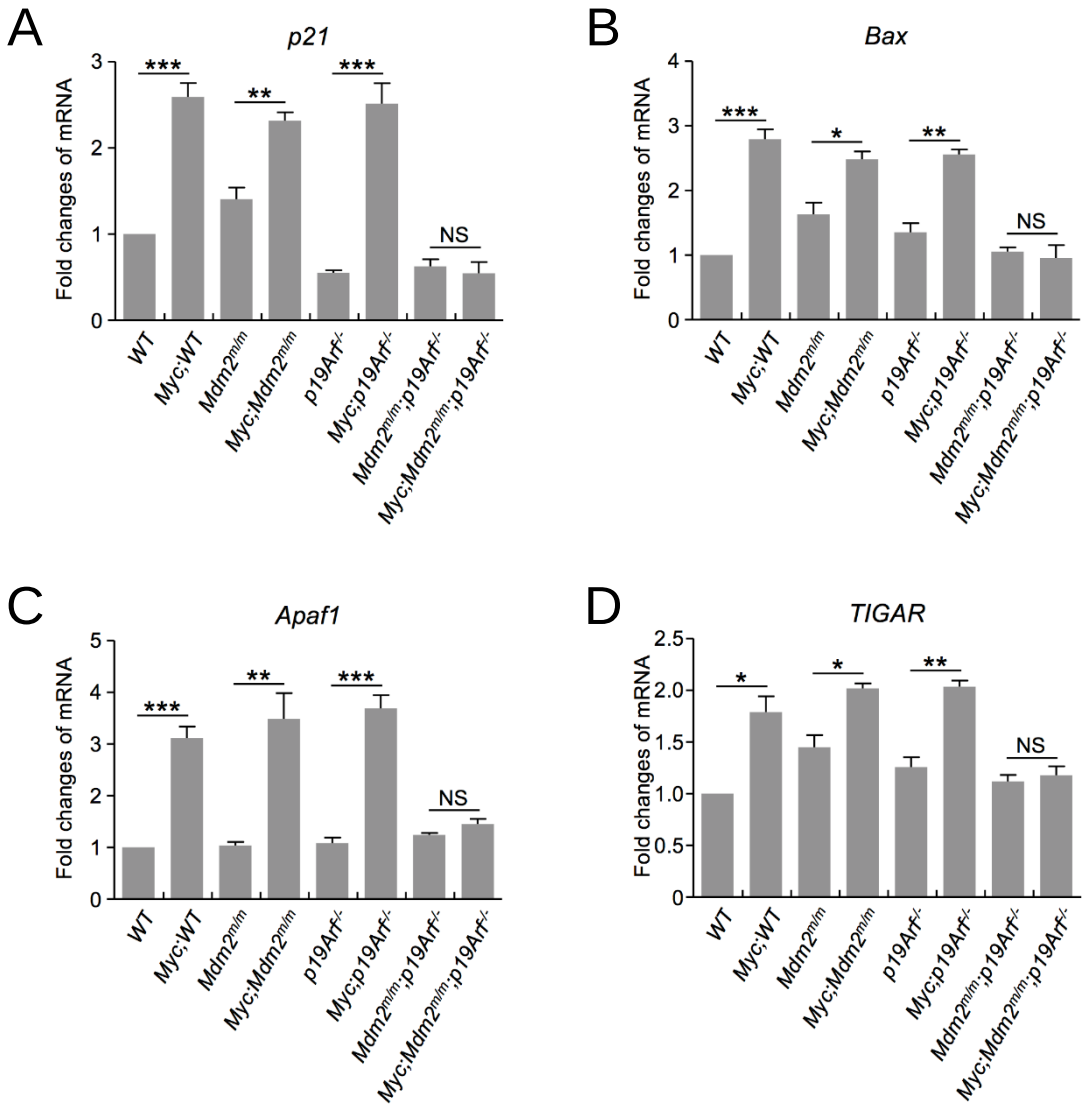

Figure 2.8 The RP-MDM2-p53 and p19ARF-MDM2-p53 signaling pathways function independently in oncogenic c-MYC-induced p53 activation.

(A-D) mRNA levels of *p21* (A), *bax* (B), *apaf1* (C) and *tigar* (D) in spleens of 4 week old, non-tumor-bearing *Eμ-Myc;WT*, *Eμ-Myc;Mdm2*$^{m/m}$, Eμ-Myc;p19Arf$^{-/-}$ and *Eμ-Myc;Mdm2*$^{m/m}$*;p19Arf*$^{-/-}$ transgenic mice, and in spleens of their non-transgenic counterparts, analyzed by qPCR. All samples were analyzed in triplicate. Data are calculated from three independent experiments and normalized to actin. Data are represented as mean ±SEM, and were analyzed by Student's t-test. *P<0.1; **P<0.01; ***P<0.001; and NS indicates no significant difference.

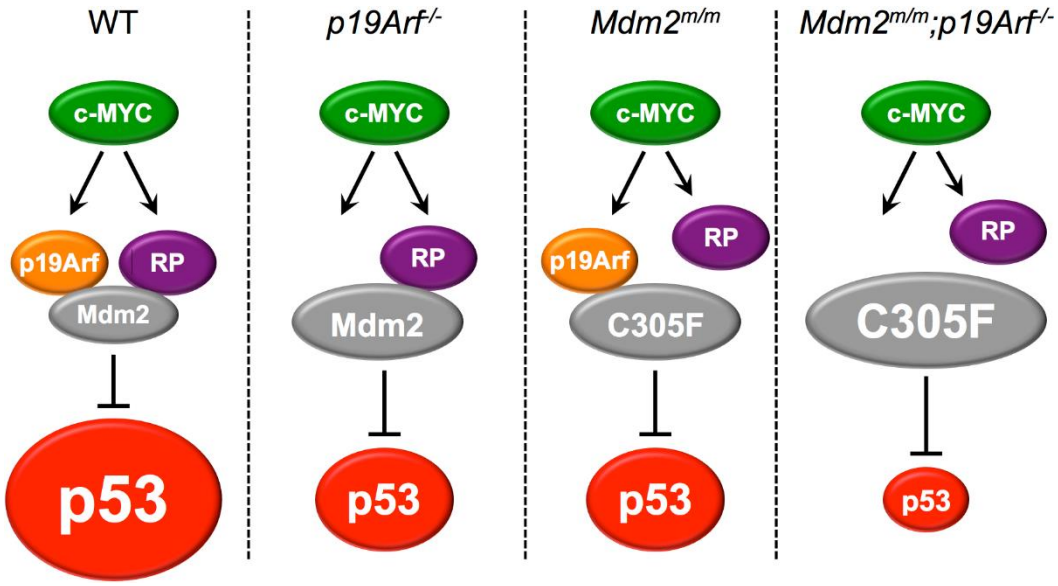

Figure 2.9 A model depicting non-overlapping functions of the p19ARF-MDM2-p53 and the RP-MDM2-p53 pathways in oncogenic c-MYC-induced p53 activation.

In *WT* cells, oncogenic c-MYC signal engages with both p19ARF-MDM2-p53 and RP-MDM2-p53 pathways, resulting in maximum MDM2 inhibition and p53 stabilization and activation (first panel). In cells with *p19Arf* deletion (second panel) or $MDM2^{C305F}$ mutation (third panel), c-MYC signal engages with one of the remaining pathways to induce p53, but to a lesser degree. In cells with concurrent *p19Arf* deletion and $MDM2^{C305F}$ mutation, c-MYC overexpression cannot induce p53 to detectable levels (fourth panel).

CHAPTER 3: RPL23 LINKS ONCOGENIC RAS SIGNALING TO P53-MEDIATED TUMOR SUPPRESSION[3]

INTRODUCTION

The tumor suppressor gene *TP53* is mutated in about 50% of all human cancers (Lane, 1992). As a transcription factor, p53 triggers cell cycle arrest, differentiation, apoptosis, and senescence in response to a variety of stresses. MDM2 is the primary negative regulator of p53, and it accomplishes this by both binding to and inhibiting the transactivation domain of p53 (Momand et al., 2011), as well as serving as an E3 ubiquitin ligase for p53 degradation (Geyer et al., 2000; Honda et al., 1997). Meanwhile, p53 enhances *mdm2* transcription, forming an autoregulatory feedback loop (Wu et al., 1993).

It has been demonstrated that several ribosomal proteins (RPs), such as RPL5, RPL11, and RPL23, interact with MDM2 to inhibit its E3 ligase function, thereby stabilizing and activating p53, suggesting an RP-MDM2-p53 signaling pathway (Zhang and Lu, 2009). Ribosomal biogenesis is one of the most energetically demanding and tightly regulated processes during cell growth and proliferation. Because cancer cells undergo uncontrolled growth and proliferation, they require accelerated ribosomal biogenesis, mandating increased RP production. Using knockin mice bearing an $MDM2^{C305F}$ point mutation, which prevents

---

[3] This chapter is adapted from a research article originally published in Cancer Research. Xuan Meng, Adrienne Cox, Yanping Zhang and I contributed to the design of the study. Xuan Meng completed all mouse breeding/dissection and qPCR experiments. Xuan Meng, Conying Wu, Jing Yang and I completed RAS retroviral overexpression in MEFs and WB analyses of MEFs and tissue. Xuan Meng, Shijie Liu, and I completed the IHC and histopathological staining. Xuan Meng, Adrienne Cox, Yanping Zhang and I analyzed the data. I wrote and edited the manuscript with Xuan Meng, Adrienne Cox, and Yanping Zhang. Jiahong Dong and Yanping Zhang finalized the manuscript. Xuan Meng and I are co-first authors on the study. The original citation is as follows: Meng, X., Tackmann, N.R., Liu, S., Yang, J., Dong, J., Wu, C., Cox, A.D., and Zhang, Y. (2016). RPL23 links oncogenic RAS signaling to p53-mediated tumor suppression. Cancer Research *76*, 5030-5039.

binding of RPL5 and RPL11 to MDM2 (Lindström et al., 2007), previous studies have established the physiologic significance of the RP-MDM2 interaction in responding to ribosomal stress and demonstrated that the RP-MDM2-p53 pathway is critical in preventing oncogenic c-MYC-induced lymphomagenesis in mice (Macias et al., 2010).

The tumor suppressor p19ARF (p14ARF in human) is uniquely transcribed from an alternative reading frame of the INK4a/ARF gene locus. Similar to RPL11 and RPL5, p19ARF can inhibit MDM2 E3 ligase activity by directly binding to MDM2, stabilizing and activating p53, instituting a p19ARF-MDM2-p53 signaling pathway (Sherr, 2006). Previous studies have shown that mice with homozygous deletion of p19ARF (*p19Arf*$^{-/-}$) are predisposed to spontaneous tumor development (Kamijo et al., 1999). In addition, oncogenic proteins, such as c-MYC and RAS, can drive tumors by selectively inactivating the p19ARF-MDM2-p53 pathway. Accelerated cancer progression is observed in *Eμ-Myc;p19Arf*$^{-/-}$ transgenic mice, which die of lymphoma within a few weeks of birth (Eischen et al., 1999), and in *Hras*^{G12V}*;p19Arf*$^{-/-}$ transgenic mice, which die of melanoma within a few months of birth (Chin et al., 1997), demonstrating the importance of p19ARF in tumor suppression.

Overexpression of oncogenic RAS induces cell-cycle arrest in WT murine keratinocytes, which is mediated by increased expression of p19ARF (Lin and Lowe, 2001). Conversely, oncogenic RAS transforms *p19Arf*$^{-/-}$ MEFs by bypassing p53-mediated checkpoint control (Kamijo et al., 1997). The RP-MDM2-p53 signaling pathway responds to deregulated ribosomal biogenesis caused by c-MYC overexpression to activate p53 and prevent tumorigenesis (Macias et al., 2010). Given that overexpression of RAS promotes growth and proliferation, which like c-MYC overexpression involves enhanced ribosomal biogenesis, we sought to determine whether the RP-MDM2-p53 signaling pathway might also respond to oncogenic RAS overexpression and play a role in tumor suppression.

RESULTS

MDM2^{C305F} mutation partially rescues oncogenic H-RAS-induced tumorigenesis

We crossed *Mdm2*$^{m/m}$ mice with mice expressing an activated melanocyte-specific *Hras*^{G12} transgene and examined melanomagenesis in the *Hras*^{G12V}*;Mdm2*$^{m/m}$ transgenic mice. Consistent with previous studies (Chin et al., 1997), *Hras*^{G12V}*;p19Arf*$^{-/-}$ mice developed spontaneous melanomas, and the median survival of the transgenic mice was about 6 months (Figure 3.1, red line). Unexpectedly, however, the median survival for *Hras*^{G12V}*;Mdm2*$^{m/m}$*;p19Arf*$^{-/-}$ compound mice was significantly longer than that of *Hras;p19Arf*$^{-/-}$ mice at more than 12 months (Figure 3.1, purple line, P=0.0007). This result indicates that, in contrast to accelerating oncogenic c-MYC-induced tumorigenesis (Macias et al., 2010), the MDM2^{C305F} mutation partially rescues oncogenic RAS-induced tumorigenesis. Tumors from *Hras*^{G12V}*;Mdm2*$^{m/m}$*;p19Arf*$^{-/-}$ mice were indistinguishable to those from *Hras*^{G12V}*; p19Arf*$^{-/-}$ mice (Figures 3.2-3). Although the latency of tumors differed depending on the presence or absence of MDM2^{C305F} mutation, the histologic characteristics of established tumors were equivalent between tumors from *Hras*^{G12V}*;Mdm2*$^{m/m}$*;p19Arf*$^{-/-}$ mice and those from *Hras*^{G12V}*;p19Arf*$^{-/-}$ mice, indicating that the MDM2^{C305F} mutation does not ultimately affect the pathophysiologic nature of tumors induced upon p19ARF deletion and oncogenic RAS overexpression.

We next determined the proliferative capacities of melanomas from the *Hras*^{G12V}*;p19Arf*$^{-/-}$ and *Hras*^{G12V}*;Mdm2*$^{m/m}$*;p19Arf*$^{-/-}$ mice. As shown in Figure 3.4a, tumors from *Hras*^{G12V}*;p19Arf*$^{-/-}$ mice displayed a higher percentage of Ki-67-positive cells (Ki-67 index 51.8) than tumors from *Hras*^{G12V}*;Mdm2*$^{m/m}$*;p19Arf*$^{-/-}$ mice (Ki-67 index 11.8). TUNEL (terminal deoxynucleotidyl transferase mediated dUTP-biotin nick end labeling) immunohistochemical analysis was performed to measure levels of apoptosis. Tumors isolated from *Hras*^{G12V}*;Mdm2*$^{m/m}$*;p19Arf*$^{-/-}$ mice displayed a significantly higher percentage of TUNEL-positive cells (13.6%) than those of *Hras*^{G12V}*;p19Arf*$^{-/-}$ tumors (3.2%; Figure 3.4b). These data suggest that the MDM2^{C305F} mutation

decelerates oncogenic RAS-induced tumorigenesis by inhibiting proliferation and inducing apoptosis.

The deceleration of RAS-induced tumorigenesis by MDM2^{C305F} mutation was unexpected. Because p53 is the primary target of MDM2, we therefore compared basal levels of p53 in *Hras*^{G12V}*;p19Arf*$^{-/-}$ and *Hras*^{G12V}*;Mdm2*$^{m/m}$*;p19Arf*$^{-/-}$ tumors. As shown in Figure 3.5a, *Hras*^{G12V}*;Mdm2*$^{m/m}$*;p19Arf*$^{-/-}$ tumors expressed higher levels of p53. To determine whether p53 activity also correlated with expression in these tumors, we analyzed p21 and found that there was greater p21 staining in *Hras*^{G12V}*;Mdm2*$^{m/m}$*;p19Arf*$^{-/-}$ tumors compared with *Hras*^{G12V}*;p19Arf*$^{-/-}$ tumors (Figure 3.5b). We then used a tumor-free system to compare whether the MDM2^{C305F} mutation had any effect on basal p53 accumulation. We analyzed p53 levels in *WT*, *Mdm2*$^{m/m}$, *p19Arf*$^{-/-}$, and *Mdm2*$^{m/m}$*;p19Arf*$^{-/-}$ MEFs. *Mdm2*$^{m/m}$ MEFs expressed higher levels of p53 than did *WT* MEFs (Figure 3.5c). Likewise, *Mdm2*$^{m/m}$*;p19Arf*$^{-/-}$ MEFs expressed higher levels of p53 than did *p19Arf*$^{-/-}$ MEFs. Thus, the deceleration of RAS-induced tumorigenesis by MDM2^{C305F} mutation correlates with higher levels of p53 expression and activity.

RAS induces RPL23 expression via MEK/PI3K and mTOR pathways

Previous studies have shown that MDM2^{C305F} mutation accelerates oncogenic c-MYC-induced tumorigenesis in mice due to loss of RPL11-MDM2 interaction (Macias et al., 2010). However, the MDM2^{C305F} mutation does not affect MDM2 binding to RPL23 (Lindström et al., 2007; Macias et al., 2010); and like RPL11, RPL23 interacts with MDM2 and activates p53 (Dai et al., 2004; Jin et al., 2004). To provide further insight for the deceleration of RAS-induced tumorigenesis by the MDM2^{C305F} mutation, we sought to determine whether RAS, like c-MYC (Guo et al., 2000; Kim et al., 2000), could also upregulate RP expression. We assessed the levels of RPL11 and RPL23 in RAS overexpressing mice. Interestingly, the protein levels of RPL23, but not RPL11, were elevated in pretumor mouse melanocytes expressing the *Hras*^{G12V} transgene (Figures 3.6a-b, compare lane 1 with lane 3, and lane 2 with lane 4).

Furthermore, we infected MEFs with retrovirus-expressing pBabe-HRAS^{G12V} and found that the expression of RPL23 was induced by ectopic HRAS^{G12V} (Figure 3.6c, compare lane 1 with lane 3, and lane 2 with lane 4). Conversely, the expression of RPL11 was unaffected by either endogenous or ectopic HRAS^{G12V} (Figure 3.6). We also observed elevated levels of *rpl23* mRNA in HRAS^{G12V} retrovirus-infected *WT*, *Mdm2*$^{m/m}$, *p19Arf*$^{-/-}$, and *Mdm2*$^{m/m}$*;p19Arf*$^{-/-}$ MEFs (Figure 3.7). On the other hand, *rpl11* mRNA levels remained unchanged in these cells (Figure 3.8). The induction of RPL23 by oncogenic RAS also appears to be p53 independent, because infection of pBabe-HRAS^{G12V} retrovirus resulted in RPL23 overexpression to similar levels in both *WT* and p53-null MEFs (Figure 3.9a).

We noticed that the levels of RPL23 were higher in *Mdm2*$^{m/m}$ mouse skin tissue and *Mdm2*$^{m/m}$ MEFs compared with their counterparts expressing WT MDM2 (Figure 3.6a, compare lane 1 with lane 2; Figure 3.6b, compare lane 1 with lane 2). To analyze this phenomenon, we examined RPL23 expression in multiple tissues, including MEFs, spleen, liver, and skin. We found that RPL23 levels were indeed higher in tissues of *Mdm2*$^{m/m}$ mice than in those of *WT* mice (Figure 3.9b). Furthermore, tumors from *Hras*^{G12V}*;Mdm2*$^{m/m}$*;p19Arf*$^{-/-}$ mice showed stronger RPL23 staining than those from *Hras*^{G12V}*;p19Arf*$^{-/-}$ mice (Figure 3.9c). To further investigate the MDM2^{C305F} mutation-mediated increase of RPL23 protein levels, we analyzed *rpl23* mRNA in *WT* and *Mdm2*$^{m/m}$ MEFs and observed elevated levels in *Mdm2*$^{m/m}$ MEFs (Figure 3.9d). To test whether the elevated levels of RPL23 can also be explained by increased protein stability, we performed a protein half-life assay using early passage MEFs. A normal rate of protein degradation was observed for RPL23 in *Mdm2*$^{m/m}$ MEFs (Figure 3.10a), indicating that the stability of RPL23 is not altered by MDM2^{C205F} mutation. An unaltered rate of protein degradation was also observed for RPL11 in *Mdm2*$^{m/m}$ MEFs (Figure 3.10b-d).

We examined RPL23 subcellular localization by immunofluorescence staining, and no difference was observed between *WT* and *Mdm2*$^{m/m}$ cells (Figure 3.11a). Elevated RPL23 expression was also observed in *Mdm2*$^{m/m}$ cells under a p53-null background (Figure 3.11b),

indicating that it is a p53-independent event. These data indicate that the MDM2^{C305F} mutation increases *rpl23* mRNA levels and RPL23 protein production. We have yet to explain the mechanism for the increase of *rpl23* mRNA expression in cells with the MDM2^{C305F} mutation, but we believe that the increased *rpl23* mRNA and protein levels are likely a cause for the increased p53 expression (Figure 3.5c) and the deceleration of RAS-induced tumorigenesis observed in *Hras*^{G12V}*;Mdm2*$^{m/m}$*;p19Arf*$^{-/-}$ mice (Figure 3.1).

It has been previously shown that regulation of RPL23 can occur at the translational level through mRNA cap binding of eukaryotic translation initiation factor 4E (eIF4e) (Mamane et al., 2007), a well-characterized downstream target of the mTOR pathway. We therefore investigated the mechanism of RAS-induced RPL23 expression at translational control. Because mTOR is a known downstream target of RAS signaling, we hypothesized that RAS induction of RPL23 could be mediated by the mTOR signaling pathway. To test this idea, we infected *WT* MEFs with pBabe-HRAS^{G12V} retrovirus and followed with rapamycin treatment to inhibit mTOR activity. Expression of RPL23, but not RPL11, was induced by RAS overexpression in MEF cells; however, upon treatment with rapamycin RAS-induced RPL23 expression was inhibited (Figure 3.12a). Consistent with observations made in MEFs, RPL23 expression was elevated in human embryonic kidney (HEK-293T) cells infected with pBabe-HRAS^{G12V} retrovirus, and the expression was inhibited by rapamycin (Figure 3.12b). These data indicate that RAS regulates RPL23 translation through an mTOR-dependent mechanism.

RAS signaling to mTOR can occur through PI3K and mitogen activated protein kinase (MEK) pathways. To further investigate the signaling pathways through which RAS induces RPL23 expression, we infected WT MEFs and HEK-293T cells with pBabe-HRAS^{G12V} retrovirus and treated the cells with small-molecule inhibitors of RAS signaling. RPL23 induction by RAS was partially inhibited by treatment with either the MEK inhibitor trametinib or the PI3K inhibitor LY294002, respectively (Figure 3.13). Together, these data suggest that RAS mediated

induction of RPL23 translation is mTOR dependent and mediated by both PI3K and MEK signaling pathways.

RAS induces p53 expression in the absence of p19ARF

Oncogenic RAS induces p19ARF-dependent activation of p53 (Serrano et al., 1997). To determine whether p19ARF is required for RAS-induced p53 expression in our system, we analyzed pretumor skin extracts from *p19Arf*$^{-/-}$ and *Mdm2*$^{m/m}$*;p19Arf*$^{-/-}$ mice expressing *Hras*^{G12V} transgene for p53 expression. Interestingly, in the absence of p19ARF, the *Hras*^{G12V} transgene still induced p53 expression (Figure 3.14a, compare lane 1 with lane 3), and the induction was further augmented by MDM2^{C305F} mutation (Figure 3.14a, compare lane 3 with lane 4). A similar conclusion was reached using MEFs infected with pBabe-HRAS^{G12V} retrovirus, which resulted in p53 accumulation in p19ARF-null MEFs (Figure 3.14b, compare lane 1 with lane 3), and this HRAS^{G12V}-induced p53 expression was further increased in *Mdm2*$^{m/m}$*;p19Arf*$^{-/-}$ MEFs compared with *p19Arf-/-* MEFs (Figure 3.14b, compare lane 3 with lane 4). These results indicate that oncogenic RAS can induce p53 in a p19ARF-independent manner. This is consistent with the observation that HRAS^{G12V}-induced RPL23 expression in p19ARF-null mice and cells (Figures 3.6b, 3.7c-d).

We noticed that even though oncogenic RAS can induce p53 accumulation in the absence of p19ARF, the levels of the induction were notably reduced compared with those in the presence of p19ARF. In the presence of p19ARF the *Hras*^{G12V} transgene induced an approximately 2.5-fold increase of p53 in mouse melanocytes (Figure 3.14c, compare lane 1 with lane 3), whereas in the absence of p19ARF the *Hras*^{G12V} transgene induced an approximately 1.5-fold increase of p53 (Figure 3.14a, compare lane 1 with lane 3). Similarly, ectopic expression of pBabe-HRAS^{G12V} induced an approximately 3-fold increase of p53 in *WT* MEFs (Figure 3.14d, compare lane 1 with lane 3), whereas the same virus induced an only 1.6-fold increase of p53 in *p19Arf*$^{-/-}$ MEFs (Figure 3.14b, compare lane 1 with lane 3). This evidence

supports the notion that there exists a p19ARF-independent signaling pathway engaged by oncogenic RAS to induce p53 accumulation.

RPL23 is required for RAS induction of p53 in the absence of p19ARF

Given that oncogenic RAS induces expression of RPL23, and that ectopic expression of RPL23 can stabilize p53 by inhibiting MDM2-mediated p53 ubiquitination and degradation (Dai et al., 2004; Jin et al., 2004), we wanted to investigate whether RPL23 is necessary for oncogenic RAS-mediated accumulation of p53 in the absence of p19ARF. We knocked down RPL23 by siRNA in *p19Arf*$^{-/-}$ MEFs, infected the cells with pBabe-HRAS^{G12V} retrovirus, and examined p53 levels. Downregulation of RPL23 significantly attenuated RAS-induced p53 expression in *p19Arf*$^{-/-}$ MEFs (Figure 3.15a) as well as in *Mdm2*$^{m/m}$*;p19Arf*$^{-/-}$ compound MEFs (Figure 3.15b), suggesting that in the absence of p19ARF, RPL23 is a major mediator of p53 expression induced by oncogenic RAS. On the other hand, in the presence of p19ARF downregulation of RPL23 did not affect RAS induction of p53 (Figure 3.15c-d). This suggests that p19ARF is the primary responder to oncogenic RAS expression whereas the RPL23-mediated response might be a fail-safe mechanism that comes into play upon loss of p19ARF.

DISCUSSION

Both RPL23 and p19ARF induce p53 expression in response to oncogenic RAS insult

We have provided evidence that the induction of p53 by oncogenic RAS does not occur solely through p19ARF (Figure 3.14), and that another pathway to p53 induction exists through RPL23 (Figure 3.15). There are several possible reasons for this redundancy. First, p19ARF and RPL23 could work together to produce a more rapid and robust p53 response to oncogenic RAS expression than either one alone. We have shown that in the absence of p19ARF, p53 can still be induced by RAS through RPL23, but that this happens to a lesser degree than when p19ARF is present (Figure 3.14), suggesting that the two pathways could act concurrently

(Figure 3.16a). However, we believe it is more likely that p19ARF, as a canonical tumor suppressor, is the primary responder to RAS overexpression and that RPL23 acts as a backup response to induce p53 activation, particularly when the function of p19ARF is lost. This notion is supported by the observation that knockdown of RPL23 by siRNA does not significantly attenuate p53 activation by RAS when p19ARF is present (Figures 3.15c-d), but it does so when p19ARF is absent (Figures 3.15a-b).

The loss of p19ARF in the presence of RAS overexpression can drive tumor progression through inactivation of the p19ARF-MDM2-p53 pathway (Chin et al., 1997), so the presence of a backup mechanism for p53 activation would be advantageous for tumor prevention. In support of this idea, *Mdm2*$^{m/m}$ mice which demonstrate increased levels of RPL23 (Figures 3.6 and 3.9) and higher levels of p53 (Figure 3.14) under a p19ARF deletion background, are more resistant to RAS overexpression-induced tumors as compared with mice with p19ARF deletion alone (Figure 3.1). Different RPs respond to specific oncogenic stresses to stabilize p53. In general, deregulated oncogenes drive cell growth and proliferation, which requires accelerated ribosomal biogenesis.

This current study and studies by others have demonstrated that RAS and c-MYC can drive expression of RPs. Although RP upregulation is generally associated with oncogenic growth, it appears that RPs can also serve as tumor-suppressive signaling molecules. It is presently unclear why multiple RPs interact with MDM2 and appear to have similar functions in p53 stabilization. We propose that the RP-MDM2 interaction represents a system of checkpoints for cell growth, and here we have provided evidence to suggest that the different RPs may respond to distinct oncogenic stimuli to engage the MDM2-p53 pathway. For example, RPL23, but not RPL11, is specifically induced by RAS overexpression (Figures 3.6-8), whereas previous studies have shown that RPL11 responds to oncogenic c-MYC overexpression (Macias et al., 2010). The MDM2^{C305F} mutation specifically disrupts interaction of RPL11 but not RPL23 with MDM2. Creation of the *Mdm2*$^{m/m}$ mice thus allowed us to dissect the distinct contributions of

RPL11 and RPL23 to p53 induction by oncogenic c-MYC and oncogenic RAS overexpression, respectively. To date, at least 16 RPs have been shown to bind directly to MDM2 and modulate p53 in a similar fashion (Kim et al., 2014), but the specific signals that these RPs transduce have yet to be elucidated. We postulate that a possible reason that so many RPs bind MDM2 is to confer insult-specific modulation of p53. In this study, we demonstrate that RPL23 can respond to RAS to induce p53. However, although our data demonstrate that RPL23 is essential for RAS-induced p53 expression in the absence of p19ARF, we cannot conclude whether other RPs may have a role in the pathway, given that there are 16 RPs have been shown to bind to MDM2 and affect p53. Significant investigation will be required to parse out whether other RPs respond to specific stress signals to induce p53 activation and which signals are responsible for each potential RP-MDM2 interaction and subsequent p53 activation.

RPL23 expression via the MEK-PI3K and mTOR pathways

We have shown that the increased latency to tumor formation in *Hras*^{G12V}*;Mdm2*$^{m/m}$*;p19Arf*$^{-/-}$ mice compared with *Hras*^{G12V}*;p19Arf*$^{-/-}$ mice is possibly due to oncogenic HRAS^{G12V} overexpression combined with MDM2^{C305F} mutation-induced RPL23 expression, leading to increased p53 accumulation and activation. RAS induces *rpl23* mRNA expression (Figure 3.7) and protein production through both MEK and PI3K signaling pathways (Figure 3.13), which are dependent on mTOR but independent of p53 (Figure 3.9a). It is likely that RAS induction of RPL23 is mediated through both an increase in transcription, as well as an increase in mTOR-dependent translation (Figure 3.12). Although our results suggest that RAS can induce p53 through increased inhibition of MDM2 by RPL23, we cannot rule out the possibility that RPL23 induction by RAS can induce p53 through an MDM2-independent mechanism. Previous studies have shown that mTOR can upregulate p53 translation (Astle et al., 2012), and because mTOR is a downstream target of RAS, it is also possible that upregulation of RPL23 could aid in mTOR-dependent increases in p53 translation.

MDM2^{C305F} mutation facilitates an increase in *rpl23* mRNA expression, and we have shown that MDM2^{C305F} mutation does not affect RPL23 protein stability or subcellular localization. Although how MDM2^{C305F} mutation increases *rpl23* mRNA transcription is presently unclear, several possibilities can be envisioned. First, RP-MDM2 interactions are thought to occur in response to perturbations of ribosomal biogenesis (Zhang and Lu, 2009). We speculate that there is some low level of basal RP-MDM2 interaction, mildly inhibiting MDM2, to allow for normal physiologic levels of p53 expression. It is possible that upon loss of RPL11-MDM2 binding due to MDM2^{C305F} mutation, the basal level of MDM2 inhibition is decreased and RPL23 could be upregulated as a compensatory mechanism to counteract the decrease in MDM2 inhibition.

Second, ribosomal biogenesis and RP expression is a highly-coordinated process, with imbalances in RP ratios often causing p53-dependent cell-cycle arrest. In the case of MDM2^{C305F} mutation, the loss of RPL11-MDM2 binding could liberate RPL11, leading to an increase in the relative levels of RPL11 in the RP pool and creating imbalances in otherwise tightly regulated RP ratios. To combat this imbalance, the cell may increase expression of other RPs, including, in this case, RPL23.

Finally, a possibility formally remains, for reasons yet unknown, that MDM2^{C305F} mutation could facilitate low but constitutive overexpression of RAS and RAS target genes. The *Mdm2*$^{m/m}$ mouse, with its elevated expression of endogenous RPL23, serves as a useful *in vivo* tool for investigating the function and mechanism of a RAS-RPL23-MDM2-p53 pathway, without the effects of RPL11-MDM2 binding, and sets the stage for further investigations of RP-MDM2-p53 pathway activation.

EXPERIMENTAL PROCEDURES

Immunoblotting and immunoprecipitation

For Western blotting, MEFs were lysed with 0.5% NP-40 lysis buffer. For mouse tissue protein extraction, tissue from the skin and lymphomas was ground by pestle and mortar with liquid N2, and protein was extracted with 0.5% NP-40 lysis buffer. To assess the half-life of RPL11 and RPL23, low passage MEF cells were treated with cycloheximide (50 mg/mL), chased for the indicated time points, and harvested with SDS lysis buffer (2% SDS, 10% glycerol, 50 mmol/L Tris). Mouse monoclonal anti-MDM2 (2A10; Calbiochem), mouse monoclonal anti-p53 (NCL-505; Novocastra), goat polyclonal anti-p53 (FL-393, Santa Cruz Biotechnology), mouse monoclonal anti-ACTIN (MAB1501; Chemicon International), rabbit monoclonal anti-β-TUBULIN (ab179513; Abcam), rabbit monoclonal anti-RAS (ab52939; Abcam), mouse monoclonal anti-RAS (BD610001; BD Biosciences), rat polyclonal anti-p19ARF (Santa Cruz Biotechnology), rabbit polyclonal anti-phospho (Ser473)-AKT (9271S; Cell Signaling Technology), mouse monoclonal antiphospho-p44/42 (Thr202/204) ERK1/2 (9107S; Cell Signaling Biotechnology), rabbit monoclonal anti-phospho (Ser473)-AKT(4060S; Cell Signaling Technology), rabbit polyclonal anti-AKT (9272S; Cell Signaling Technology), rabbitmonoclonal anti-phospho-p44/42 (Thr201/Tyr204) ERK1/2 (4370S;Cell Signaling Technology), rabbit polyclonal anti-ERK1/2 (9102S; Cell Signaling Technology) and anti-GAPDH (RM2002; Ray Antibody Biotechnology) antibodies were purchased commercially. Rabbit polyclonal antibodies to p21 were gifts from Dr. Yue Xiong (University of North Carolina at Chapel Hill, Chapel Hill, NC). Rabbit polyclonal antibodies to RPL11 and RPL23 were made in house as described previously (Lindström et al., 2007). Procedures and conditions for immunoprecipitation were performed as described previously (Itahana et al., 2003).

Immunohistochemical analysis

Antigen retrieval for antibody on formalin-fixed paraffin sections was done by boiling paraffin samples in citrate buffer (pH 6.0) for 15 min. Endogenous peroxidase activity was quenched by incubation in 3% H_2O_2 in methanol for 10 min. Ki-67 IHC staining of mouse spleen samples was used to detect proliferating cells. Antibody detection was performed with purified mouse anti-Ki-67 primary antibody (BD Pharmingen) and biotin-conjugated anti-mouse secondary antibody (Vector Laboratories). Ki-67-expressing cells were stained brown using a biotin-peroxidase kit (Vectastain Elite, Vector Laboratories). The ratio of positively stained cells to total cells was calculated. Student t test ($P < 0.05$ was considered significant) was used to compare the differences in proliferation levels between the different mouse genotypes. Antibodies to p53 (CM5; Leica Biosystems), BAX (#554104; BD Biosciences), and p21 (DCS 60.2; Thermo Scientific) were purchased commercially, whereas antibodies to RPL23 were made in-house as described previously (Lindström et al., 2007).

Mouse experiments

Mice were bred and maintained strictly under protocol (13-044) approved by the Institutional Animal Care and Use Committee in the University of North Carolina Animal Care Facility. *Mdm2*$^{m/m}$ females were bred with *p19Arf*$^{-/-}$ males to obtain *Mdm2*$^{+/m}$*;p19Arf*$^{+/-}$ offspring, which were then crossed with *Mdm2*$^{+/m}$*;p19Arf*$^{+/-}$ mice to obtain *Mdm2*$^{m/m}$*;p19Arf*$^{-/-}$ compound mice. For RAS-mediated tumorigenesis studies, *Mdm2*$^{m/m}$*;p19Arf*$^{-/-}$ females were bred with *Hras*^{G12V} transgenic males to obtain *Hras*^{G12V}*;Mdm2*$^{+/m}$*;p19Arf*$^{+/-}$ offspring, which were then crossed with *Mdm2*$^{+/m}$*;p19Arf*$^{+/-}$ mice to obtain *Hras*^{G12V}*;Mdm2*$^{m/m}$*;p19Arf*$^{-/-}$ compound mice. *Hras*^{G12V} transgenic mice were generously provided by Norman Sharpless (University of North Carolina at Chapel Hill). For survival studies, mice were palpated regularly for early signs of skin tumors and monitored for tumor progression and signs of morbidity. Moribund mice were

humanely euthanized. Mouse tumors and organs were fixed in formalin for histopathology and snap frozen for protein and RNA extraction.

Statistical analysis

Statistical analysis was carried out using GraphPad Prism 5 Software (GraphPad Software). Kaplan-Meier survival curves were generated to assess lifespan. Quantitative PCR data are represented as mean ±SEM, and were analyzed by the Student's *t* test.

Apoptosis analysis

Apoptosis levels of mouse tumor sections were assessed by the terminal deoxynucleotidyl transferase-mediated dUTP-biotin nick end labeling (TUNEL) assay (ApopTaq Peroxidase in situ Kit, S7100, Millipore, Temecula, CA).

Histopathology

Animals were autopsied and all tissues were examined regardless of their pathological status. Skin, tail and tumor tissue from *Hras*^{G12V}*;WT*, *Hras*^{G12V}*;Mdm2*$^{m/m}$, *Hras*^{G12V}*;p19Arf*$^{-/-}$ and *Hras*^{G12V}*;Mdm2*$^{m/m}$*;p19Arf*$^{-/-}$ transgenics, as well as tissue from nontransgenic counterparts were fixed overnight in 10% phosphate-buffered formalin and then transferred to 70% ethanol. Samples were sent to the UNC Histology Core Facility for paraffin embedding. Paraffin blocks were sectioned at 5-mm intervals for successive layers and stained with Hematoxylin and Eosin for histopathological examination.

Cell culture

Primary MEFs were isolated on embryonic day 13.5 and grown in a 37°C incubator with 5% CO_2 in Dulbecco's Modified Eagle's medium supplied with 10% fetal bovine serum and penicillin-streptomycin. For viral infections, *WT*, *Mdm2*$^{m/m}$, *p19Arf*$^{-/-}$ and *Mdm2*$^{m/m}$*;p19Arf*$^{-/-}$ MEFs

were infected with retroviruses expressing $HRAS^{G12V}$ or pBabe control vector and selected with puromycin (2.5 μg/mL) for 3 days. Retrovirus-infected MEFs were then allowed to recover for 48 h and harvested for analysis. For rapamycin treatments, retrovirus-infected cells were allowed to recover for 24 h before treatment with rapamycin (200 nM) for 18 h. For RAS inhibitor treatments, cells were infected with retroviruses expressing $H\text{-}RAS^{G12V}$ or pBabe control vector and selected with puromycin (2.5 μg/mL) for two days. Retrovirus-infected cells were then allowed to recover for 24 h before treatment with trametinib or LY294002 for 8 h (HEK-293T) or 48 h (MEFs) and harvested for analyses. MEFs at passage 1 to 4 were used for growth curves, western blotting and other analyses.

siRNA interference

Purified and annealed duplex small interfering RNA (siRNA) oligonucleotides targeting nucleotides relative to the translation initiation codon of mouse RPL23 (sequence: AATTCCGGATTTCCTTGGGTC) and control scrambled siRNA oligonucleotides were synthesized at Dharmacon (Lafayette, Colo.). Transfection was performed by using Lipofectamine and Plus reagents (Invitrogen) according to the manufacturer's instructions.

Quantitative PCR

Total RNA was isolated using an RNeasy kit (74104, Qiagen, Hilden, Germany) and cDNA was synthesized using SuperScript III (18080400, Life Technologies, Waltham, MA, USA). qPCR was performed with SYBR Green master mix using the 7900HT Fast Real-time PCR system (Applied Biosystems, Waltham, MA, USA) according to the manufacturer's instructions. Data were collected and exported with SDS 2.2.2 software (Applied Biosystems). Relative expression was calculated using *β-GAPDH* as an internal control as indicated. Primers used were as follows: *rpl23*, 5'-GGACATGGTGATGGCCACAGTTAAG-3' and 5'-ACACTCCTTTGCCACTGGACCTG-3'; *rpl11*, 5'-CCTTTGGCATCCGGAGAAATGAGAAG-3'

and 5’-GATCCCAATGCTTGGGTCGTATTTGATG3-’; and *β-GAPDH*, 5′-AGGTCGGTGTGAACGGATTTG-3′ and 5′-TGTAGACCATGTAGTTGAGGTCA-3′.

Immunofluorescence and confocal imaging

Cells were fixed in 4% paraformaldehyde for 10 min at room temperature and permeabilized in 0.2% Triton X-100 for 5 min at 4°C. Permeabilized cells were blocked for 30 min in 0.5% bovine serum albumin (BSA) in PBS, incubated in rabbit anti-RPL23 and mouse anti-B23/NPM (32-5200, Invitrogen) antibodies overnight at 4°C with rocking, and incubated with Alexa Fluor® secondary antibodies (488 donkey anti-rabbit and 594 donkey anti-mouse, Jackson ImmunoResearch) for 30 min at room temperature. Cells were mounted in fluorescence mounting medium (Dako, Carpenteria, CA, USA) and analyzed using an Olympus IX81 inverted microscope with SPOT™ digital microscope camera and imaging software (SPOT™ Imaging Solutions, Sterling Heights, MI, USA).

Ethics statement

This investigation has been conducted in accordance with ethical standards, the Declaration of Helsinki, national and international guidelines, and has been approved by the authors' Institutional Review Board.

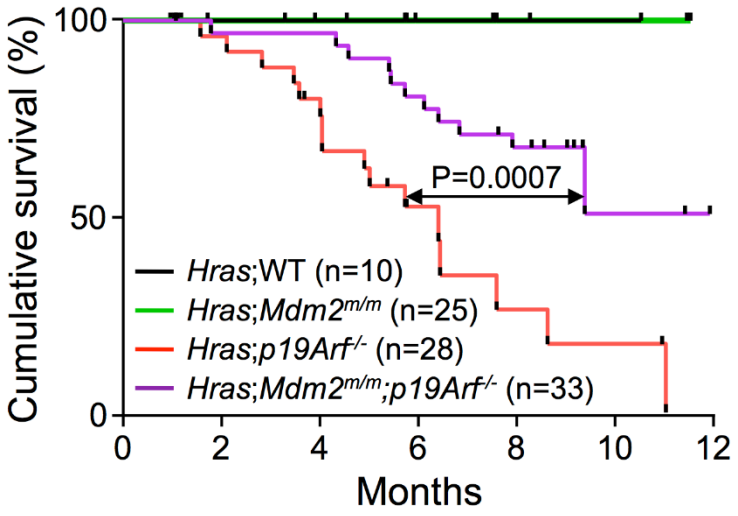

Figure 3.1 MDM2^{C305F} mutation partially rescues HRAS-induced tumorigenesis.

Kaplan-Meier survival curves for *Hras*^{G12V}*;WT*, *Hras*^{G12V}*;Mdm2*$^{m/m}$, *Hras*^{G12V}*;p19Arf*$^{-/-}$, and *Hras*^{G12V}*;Mdm2*$^{m/m}$*;p19Arf*$^{-/-}$ are shown. Median survival time for *Hras*^{G12V}*;p19Arf*$^{-/-}$ mice was 6.4 months. There was a significant difference between survival curves for *Hras*^{G12V}*;p19Arf*$^{-/-}$ and *Hras*^{G12V}*;Mdm2*$^{m/m}$*;p19Arf*$^{-/-}$ mice (analyzed by log-rank test; P=0.0007).

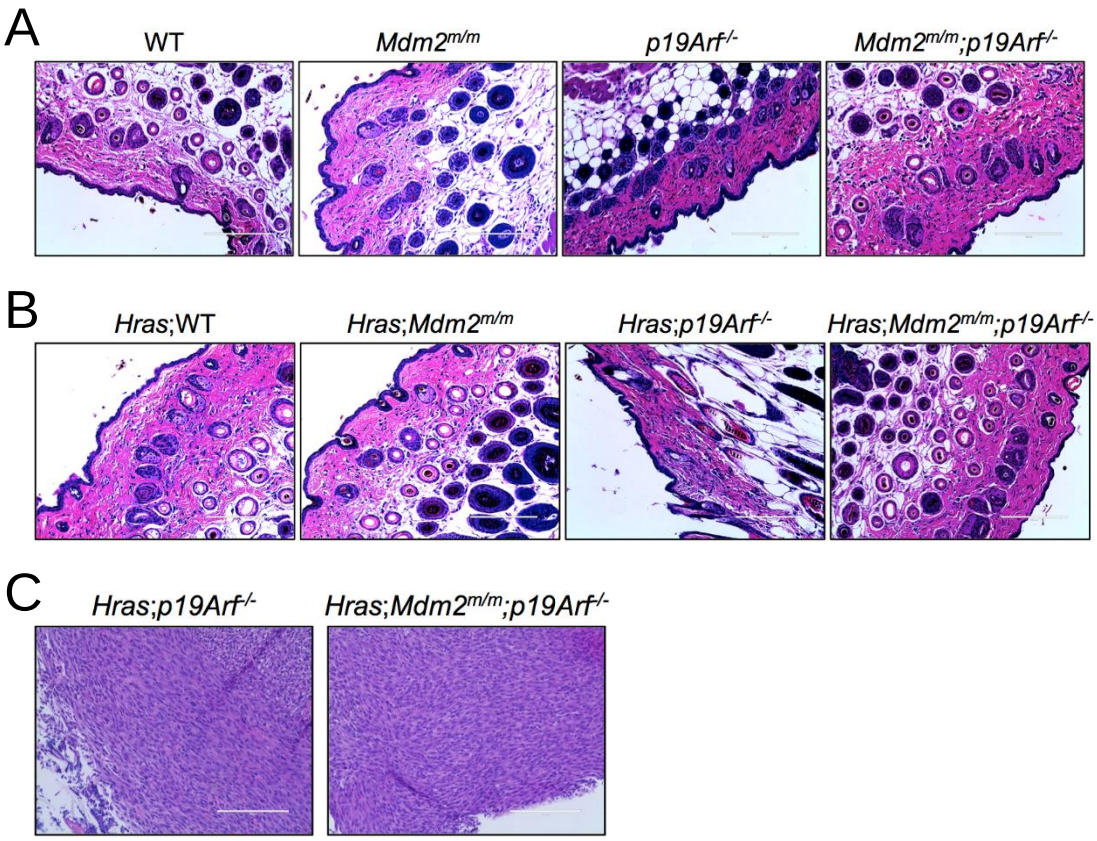

Figure 3.2 MDM2^{C305F} mutation does not affect the pathophysiology of p19ARF deletion and oncogenic RAS overexpression in tumor free skin tissue.

A. H&E staining of the tumor-free skin areas of 16 week old *WT*, *Mdm2$^{m/m}$*, *p19Arf$^{-/-}$* and *Mdm2$^{m/m}$;p19Arf$^{-/-}$* mice. Scale bar, 200 µm.

B. H&E staining of the tumor-free skin areas of 16 week old *Hras^{G12V};WT*, *Hras^{G12V};Mdm2$^{m/m}$*, *Hras^{G12V};p19Arf$^{-/-}$*, and *Hras^{G12V};Mdm2$^{m/m}$;p19Arf$^{-/-}$* mice. Scale bar, 200 µm.

C. H&E staining of the skin tumors of *Hras^{G12V};p19Arf$^{-/-}$* and *Hras^{G12V};Mdm2$^{m/m}$;p19Arf$^{-/-}$* mice. Skin tumors were collected at the time of death. Scale bar, 200 µm.

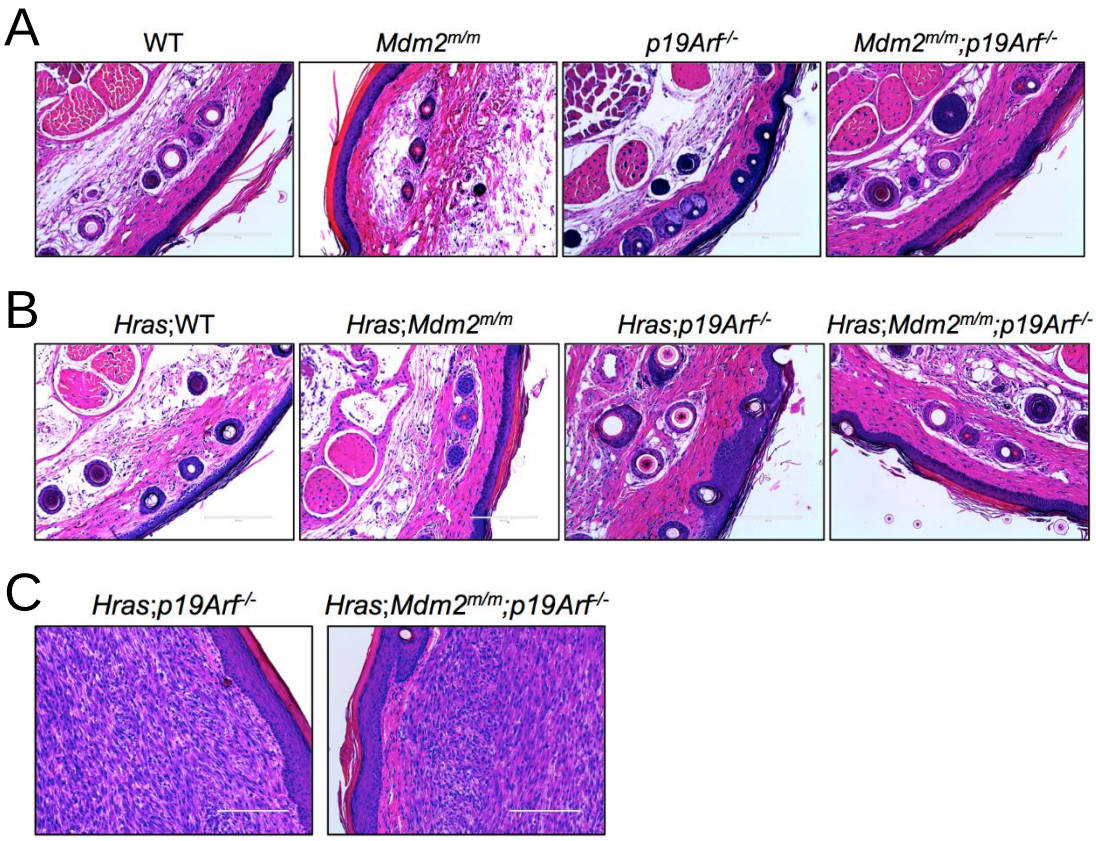

Figure 3.3 MDM2^{C305F} mutation does not affect normal skin tissue.

A. H&E staining of the tumor-free tails of 16 week old *WT*, *Mdm2*$^{m/m}$, *p19Arf*$^{-/-}$, and *Mdm2*$^{m/m}$*;p19Arf*$^{-/-}$ mice. Scale bar, 200 µm.

B. H&E staining of the tumor-free tails of 16 week old *Hras*^{G12V}*;WT*, *Hras*^{G12V}*;Mdm2*$^{m/m}$, *Hras*^{G12V}*;p19Arf*$^{-/-}$, and *Hras*^{G12V}*;Mdm2*$^{m/m}$*;p19Arf*$^{-/-}$ mice. Scale bar, 200 µm.

C. H&E staining of the tail tumors of *Hras*^{G12V}*;p19Arf*$^{-/-}$ and *Hras*^{G12V}*;Mdm2*$^{m/m}$*;p19Arf*$^{-/-}$ mice. Tumors were collected at the time of death. Scale bar, 200 µm.

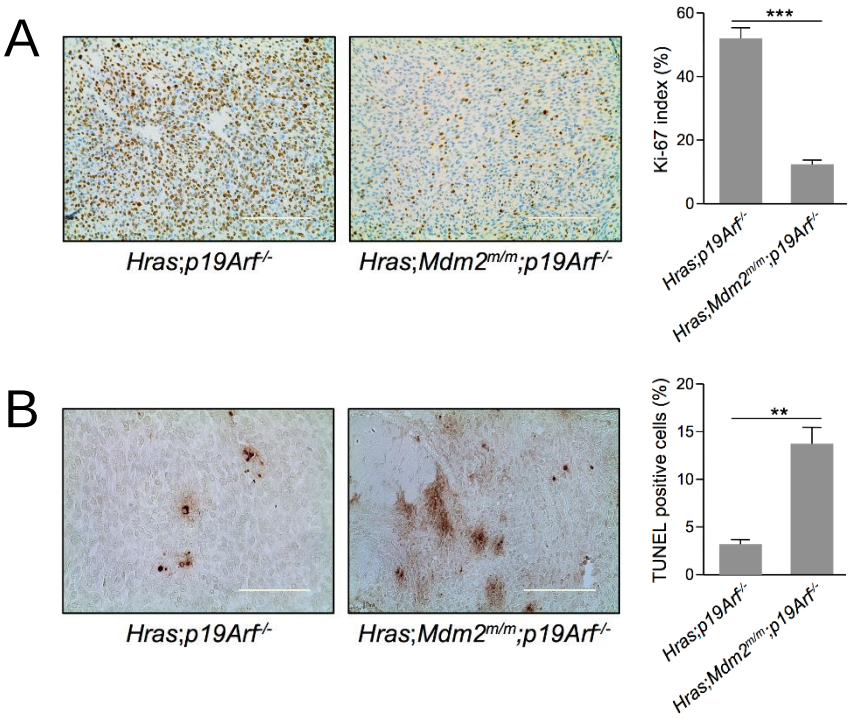

Figure 3.4 MDM2^{C305F} mutation partially rescues HRAS-induced tumorigenesis.

A. Representative Ki-67 staining of skin tumors from 16 week old mice. Brown staining, Ki-67-positive proliferating cells; scale bar, 200 μm. The Ki-67 index (calculated as the percentage of Ki-67-positive tumor cells vs total cells in the view field from at least five randomly chosen fields along the edge of tumors) for the genotypes assayed is indicated in parentheses: *Hras^{G12V};p19Arf$^{-/-}$* mice (51.8) and *Hras^{G12V};Mdm2$^{m/m}$;p19Arf$^{-/-}$* mice (11.8). Data are represented as mean ±SEM; ***, P < 0.001.

B. Representative TUNEL staining of skin tumors from different genotypes of 16 week old mice; scale bar, 200 μm. The percentage of TUNEL-positive cells in the view field was calculated from at least five randomly chosen fields along the edge of tumors and is indicated in parentheses: *Hras^{G12V};p19Arf$^{-/-}$* mice (3.2%) and *Hras^{G12V};Mdm2$^{m/m}$;p19Arf$^{-/-}$* mice (13.6%). Data are represented as mean ±SEM; **, P < 0.01.

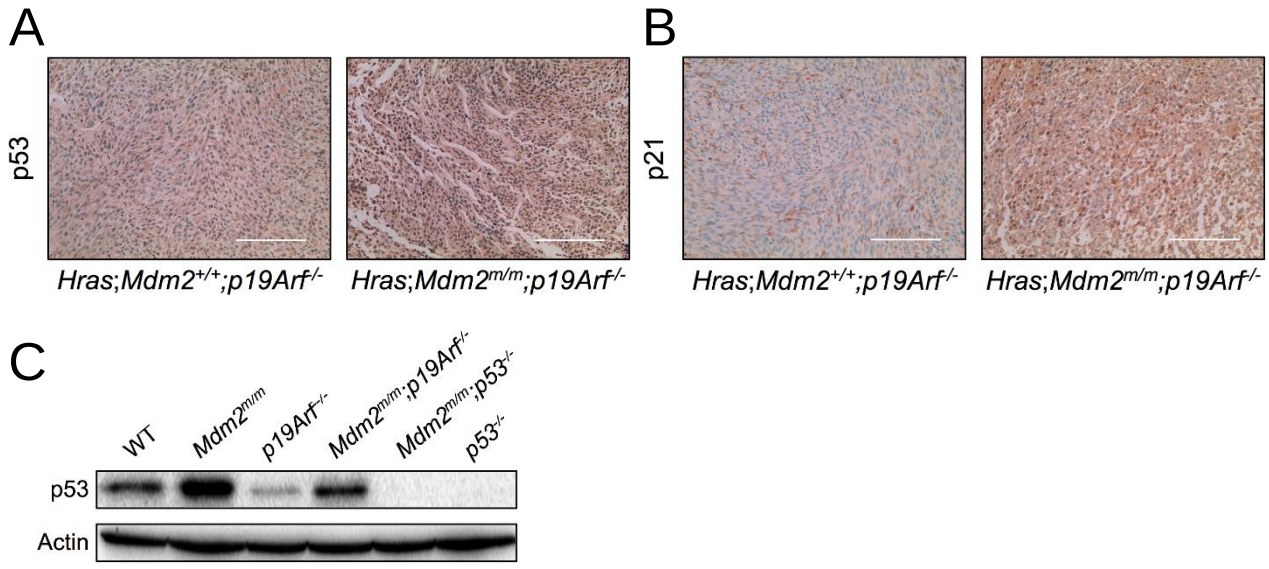

Figure 3.5 MDM2^{C305F} mutation correlates with increased p53 activity in HRAS-induced tumors.

A. Representative p53 IHC staining of skin tumors from 16 week old *Hras^{G12V};p19Arf$^{-/-}$* and *Hras^{G12V};Mdm2$^{m/m}$;p19Arf$^{-/-}$* mice; scale bar, 200 μm.

B. Representative p21 IHC staining of skin tumors from 16 week old *Hras^{G12V};p19Arf$^{-/-}$* and *Hras^{G12V};Mdm2$^{m/m}$;p19Arf$^{-/-}$* mice; scale bar, 200 μm.

C. Early passage *WT*, *Mdm2$^{m/m}$*, *p19Arf$^{-/-}$*, *Mdm2$^{m/m}$;p19Arf$^{-/-}$*, *Mdm2$^{m/m}$;p53$^{-/-}$*, and *p53$^{-/-}$* MEFs were harvested for Western blot analysis for p53 expression.

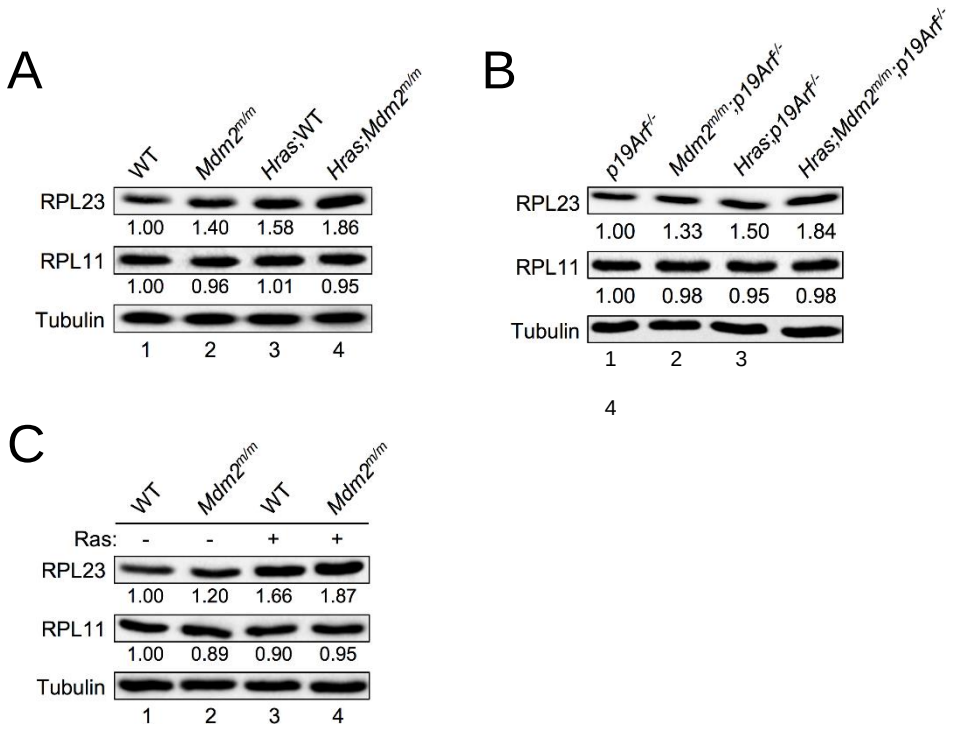

Figure 3.6 RAS induces RPL23 expression.

A. Extracts from skin tissue of nontumor-bearing *WT* and *Mdm2*$^{m/m}$ mice and from their *Hras* transgenic counterparts were analyzed by Western blot. The relative expression of RPL23 and RPL11 is shown under the blot.

B. Extracts from skin tissue of non-tumor-bearing *p19Arf*$^{-/-}$ and *Mdm2*$^{m/m}$*;p19Arf*$^{-/-}$ mice and from their *Hras* transgenic counterparts were analyzed by Western blot. The relative expression of RPL23 and RPL11 is shown under the blot.

C. Early passage *WT* and *Mdm2*$^{m/m}$ MEFs were infected with retrovirus expressing either pBabe vector (-) or pBabe-HRAS^{G12V} (+), selected with puromycin for 3 days, then allowed to recover for 48 hours before harvesting for Western blot analysis.

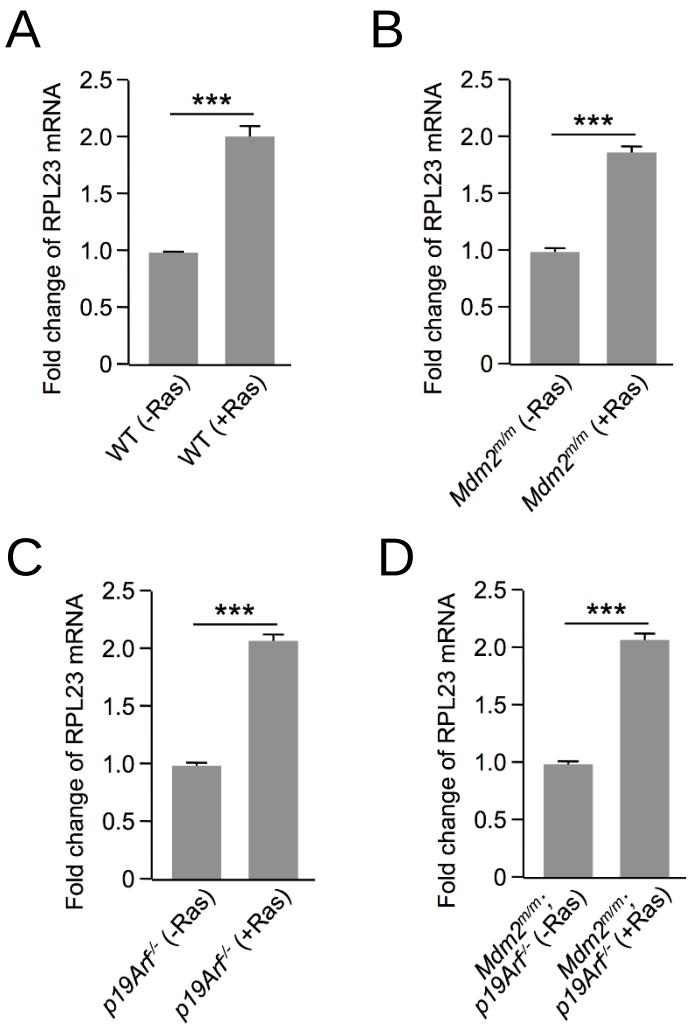

Figure 3.7 HRAS overexpression induces increased *rpl23* transcription.

A. *WT* MEFs were infected with retrovirus expressing either pBabe vector (-Ras) or pBabe-HRAS^{G12V} (+Ras) and harvested for qPCR mRNA analysis. Relative *rpl23* mRNA expression was calculated using β-GAPDH as an internal control. Data are represented as mean ±SEM, and were analyzed by Student's *t* test; ***, P <0.001.

B. *Mdm2$^{m/m}$* MEFs were infected with retrovirus expressing either pBabe vector (-Ras) or pBabe-HRAS^{G12V} (+Ras) and harvested for qPCR mRNA analysis. Relative *rpl23* mRNA expression was calculated as in (A).

C. *p19Arf$^{-/-}$* MEFs were infected with retrovirus expressing either pBabe vector (-Ras) or pBabe-HRAS^{G12V} (+Ras) and harvested for qPCR mRNA analysis. Relative *rpl23* mRNA expression was calculated as in (A).

D. *Mdm2$^{m/m}$;p19Arf$^{-/-}$* MEFs were infected with retrovirus expressing either pBabe vector (-Ras) or pBabe-HRAS^{G12V} (+Ras) and harvested for qPCR mRNA analysis. Relative *rpl23* mRNA expression was calculated as in (A).

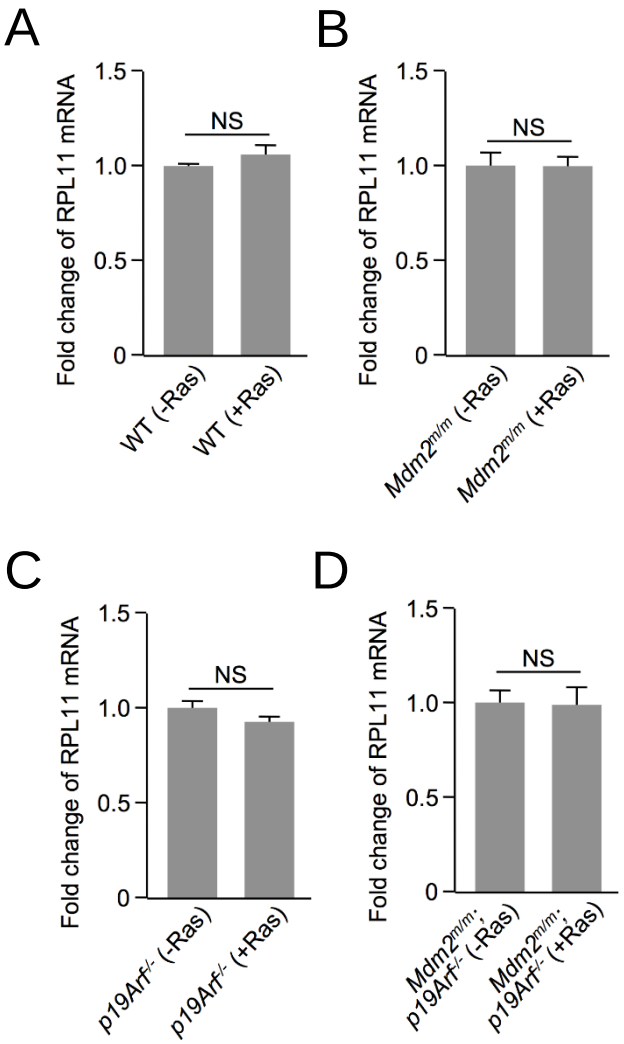

Figure 3.8 HRAS overexpression does not induce increased *rpl11* transcription.

A. *WT* MEFs were infected with retrovirus expressing either pBabe vector (-Ras) or pBabe-HRASG12V (+Ras) and harvested for qPCR mRNA analysis. Relative *rpl11* mRNA expression was calculated using β-GAPDH as an internal control. Data are represented as mean ±SEM, and were analyzed by Student's *t* test; NS, no statistically significant difference between samples.

B. *Mdm2*$^{m/m}$ MEFs were infected with retrovirus expressing either pBabe vector (-Ras) or pBabe-HRAS^{G12V} (+Ras) and harvested for qPCR mRNA analysis. Relative *rpl11* mRNA expression was calculated as in (A).

C. *p19Arf*$^{-/-}$ MEFs were infected with retrovirus expressing either pBabe vector (-Ras) or pBabe-HRAS^{G12V} (+Ras) and harvested for qPCR mRNA analysis. Relative *rpl11* mRNA expression was calculated as in (A).

D. *Mdm2*$^{m/m}$*;p19Arf*$^{-/-}$ MEFs were infected with retrovirus expressing either pBabe vector (-Ras) or pBabe-HRAS^{G12V} (+Ras) and harvested for qPCR mRNA analysis. Relative *rpl11* mRNA expression was calculated as in (A).

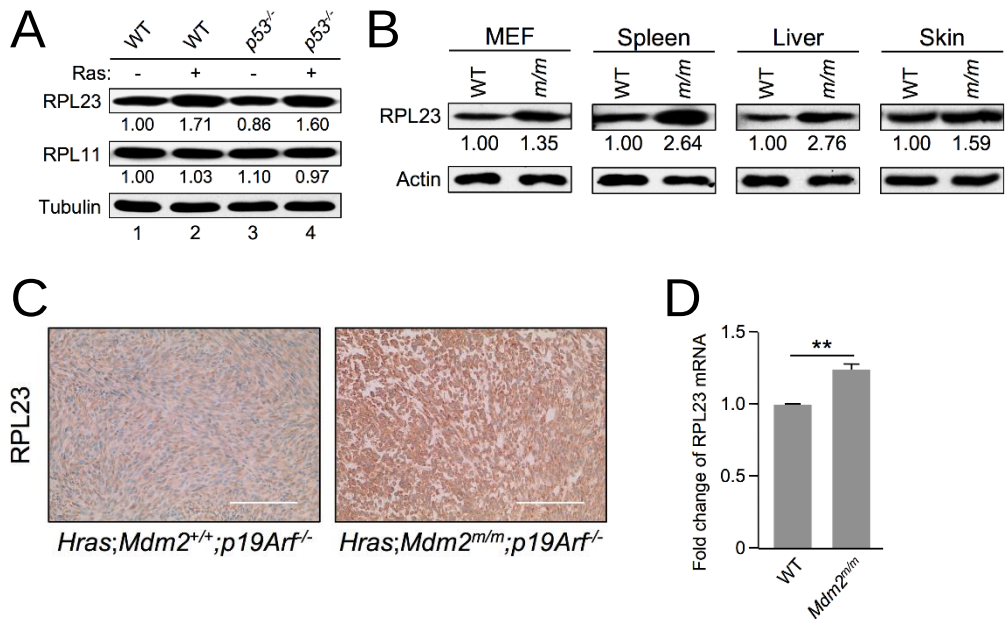

Figure 3.9 MDM2^{C305F} mutation may increase relative RPL23 levels independent of p53.

A. Early passage *WT* and *p53*$^{-/-}$ MEFs were infected with retrovirus expressing either pBabe vector (-) or pBabe-HRAS^{G12V} (+), selected with puromycin for 3 days, then allowed to recover for 48 hours before harvesting for Western blot analysis. The relative expression of RPL23 and RPL11 is shown under the blot.

B. Extracts from *WT* and *Mdm2*$^{m/m}$ MEFs and from tissues of 30 week old *WT* and *Mdm2*$^{m/m}$ mice were analyzed by Western blot. The relative expression of RPL23 is shown under the blot.

C. Representative RPL23 IHC staining of skin tumors from 16 week old *Hras*^{G12V}*;p19Arf*$^{-/-}$ and *Hras*^{G12V}*;Mdm2*$^{m/m}$*;p19Arf*$^{-/-}$ mice. Scale bar, 200 μm.

D. Early passage *WT* and *Mdm2*$^{m/m}$ MEFs were harvested for qPCR mRNA analysis. Relative *rpl23* mRNA expression was calculated using β-GAPDH as an internal control. Data are represented as mean ±SEM, and were analyzed by Student's *t* test; **, P <0.01.

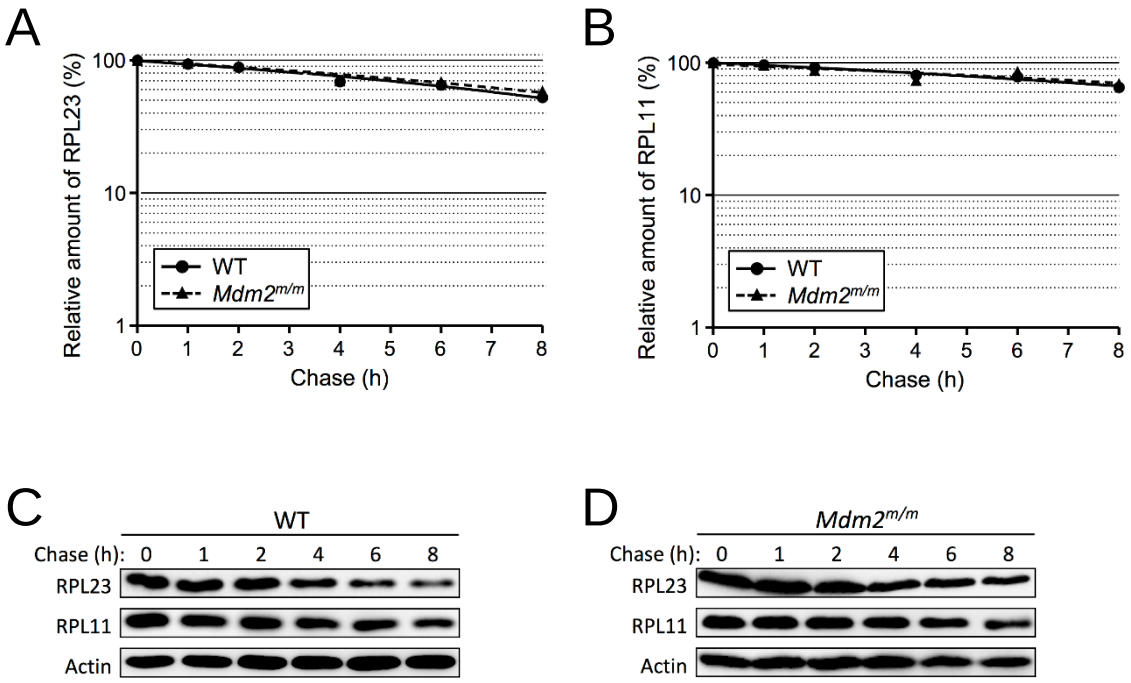

Figure 3.10 MDM2^{C305F} mutation does not alter RPL23 or RPL11 half-life.

A. RPL23 half-life was determined in early passage WT and Mdm2$^{m/m}$ MEFs, which were treated with cycloheximide (50 mg/mL) and harvested with SDS lysis buffer at the indicated time points. The amount of RPL23 was quantified by densitometry, normalized to the level of actin, and plotted. Representative Western blots are shown in (C) and (D).

B. Half-life of RPL11 in WT and *Mdm2*$^{m/m}$ MEFs as in (A). Representative Western blots are shown in (C) and (D).

C. Representative Western blot of the half-life assay shown in (A) and (B) using early passage WT MEFs treated with Cycloheximide (50 μg/mL) and harvested with SDS lysis buffer at the indicated time points.

D. Representative Western blot of the half-life assay shown in (A) and (B) using early passage *Mdm2*$^{m/m}$ MEFs treated with cycloheximide (50 μg/mL) and harvested with SDS lysis buffer at the indicated time points.

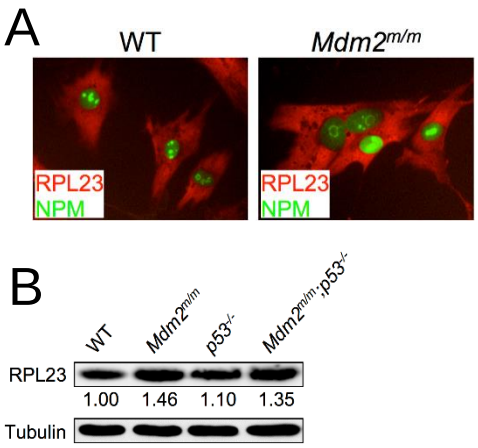

Figure 3.11 MDM2^{C305F} mutation does not alter RPL23 localization but induces p53-independent RPL23 upregulation.

A. Early passage *WT* and *Mdm2*$^{m/m}$ MEFs were fixed and stained with rabbit anti-RPL23 antibody followed by fluorescein isothiocyanate-conjugated anti-rabbit secondary antibody (red), and mouse anti-B23/NPM antibody followed by fluorescein isothiocyanate-conjugated anti-mouse secondary antibody (green). Fluorescence images were captured with a cooled charge-coupled device color digital camera (Model 2.2.0, Diagnostic) on an Olympus IX81 inverted microscope equipped with the appropriate fluorescence filters.

B. Extracts from *WT*, *Mdm2*$^{m/m}$, *p53*$^{-/-}$, and *Mdm2*$^{m/m}$;*p53*$^{-/-}$ MEFs were analyzed by Western blot. The relative expression of RPL23 is shown below the blot.

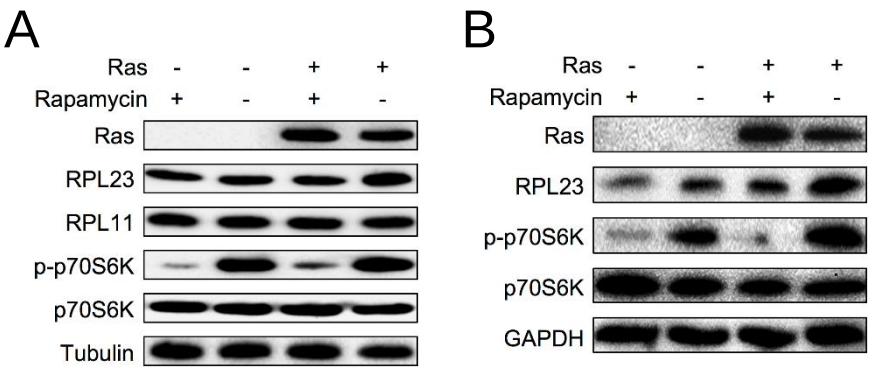

Figure 3.12 HRAS induces RPL23 protein increase through mTOR signaling.

A. Early passage *Mdm2*$^{m/m}$ MEFs were infected with retrovirus expressing either pBabe vector (-) or pBabe-HRAS^{G12V} (+), treated with 200 nM rapamycin, and then harvested for Western blot analysis.

B. HEK 293T cells were infected with retrovirus expressing either pBabe vector (-) or pBabe-HRAS^{G12V} (+), treated with 200 nM rapamycin, and then harvested for Western blot analysis.

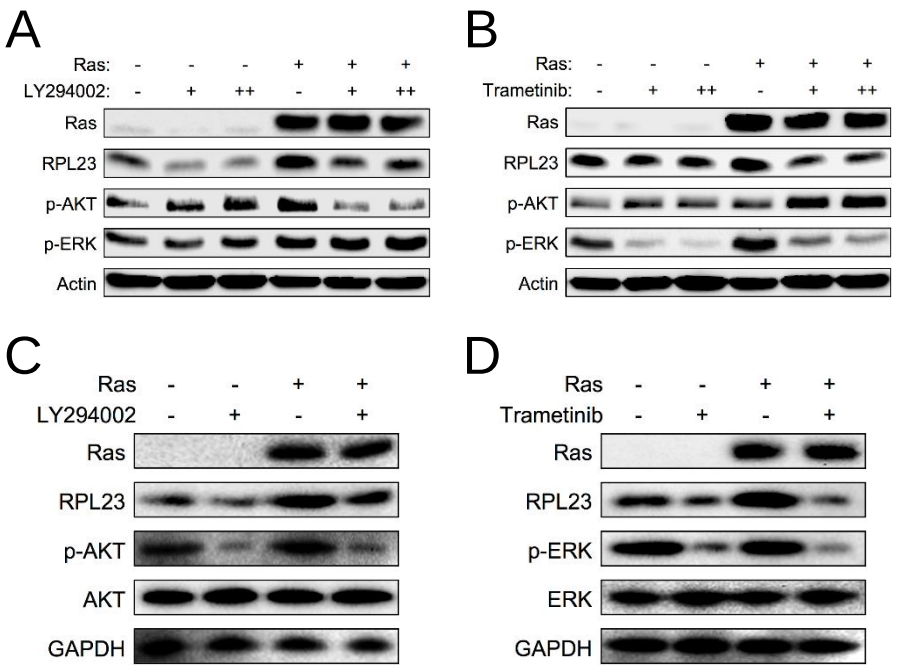

Figure 3.13 HRAS induces RPL23 protein increase through PI3K/MEK signaling.

A. Early passage WT MEFs infected with retrovirus expressing either pBabe vector (-) or pBabe-HRAS^{G12V} (+) were treated with PI3K inhibitor LY294002 [1 nM (+) or 5 nM (++)] and then harvested for Western blot analysis.

B. Early passage WT MEFs infected with retrovirus expressing either pBabe vector (-) or pBabe-HRAS^{G12V} (+) were treated with MEK inhibitor trametinib [1 nM (+) or 2.5 nM (++)] and then harvested for Western blot analysis.

C. HEK 293T cells infected with retrovirus expressing either pBabe vector (-) or pBabe-HRAS^{G12V} (+) were treated with (+) or without (-) PI3K inhibitor LY29004 (10 nM) before harvesting for Western blot analysis.

D. HEK 293T cells infected with retrovirus expressing either pBabe vector (-) or pBabe-HRAS^{G12V} (+) were treated with (+) or without (-) MEK inhibitor trametinib (10 nM) before harvesting for Western blot analysis.

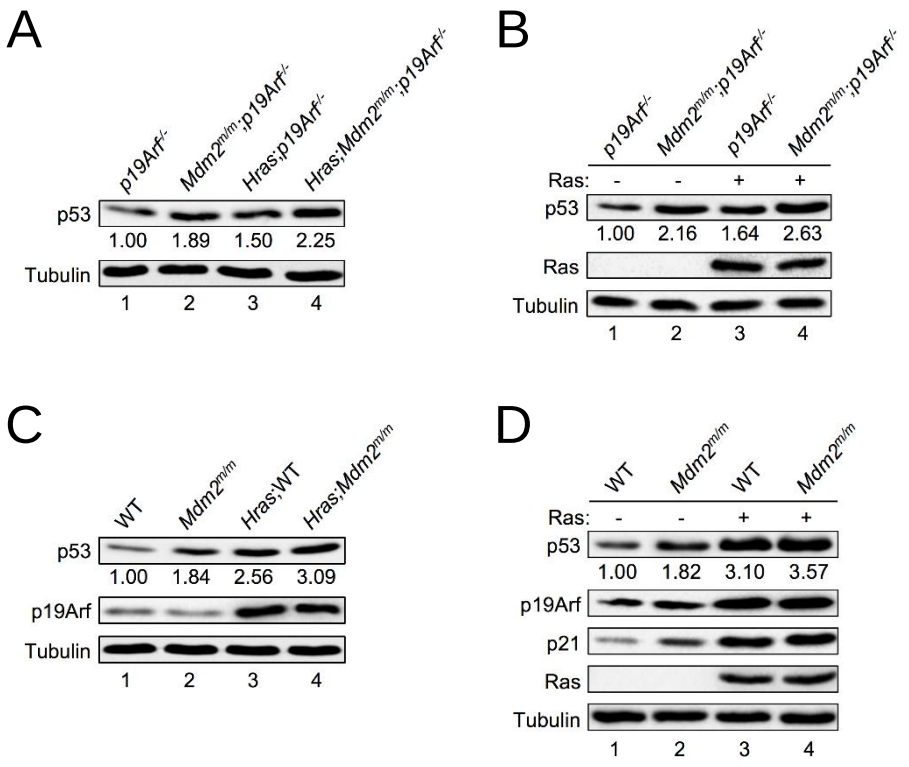

Figure 3.14 HRAS induces p53 expression in the absence of p19ARF.

A. Extracts from skin tissues of non-tumor-bearing *p19Arf*$^{-/-}$ and *Mdm2*$^{m/m}$*;p19Arf*$^{-/-}$ mice and their non-tumor-bearing *Hras* transgenic counterparts were analyzed by Western blot. The relative expression of p53 is shown under the blot.

B. Early passage *p19Arf*$^{-/-}$ and *Mdm2*$^{m/m}$*;p19Arf*$^{-/-}$ MEFs were infected with retrovirus expressing either pBabe vector (-) or pBabe-HRAS^{G12V} (+) before harvesting for Western blot analysis. The relative expression of p53 is shown under the blot.

C. Extracts from skin tissues of *WT* and *Mdm2*$^{m/m}$ mice and their non-tumor-bearing *Hras* transgenic counterparts were analyzed by Western blot. The relative expression of p53 is shown underneath the blot.

D. Early passage *WT* and *Mdm2*$^{m/m}$ MEFs were infected with retrovirus expressing either pBabe vector (-) or pBabe-HRAS^{G12V} (+) before harvesting for Western blot analysis. The relative expression of p53 is shown under the blot.

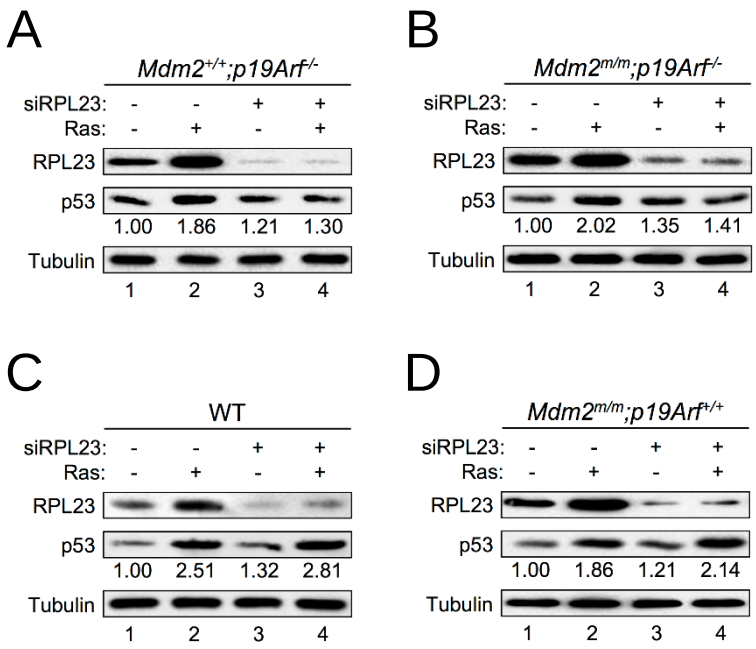

Figure 3.15 RPL23 is required for RAS-mediated p53 induction in the absence of p19ARF.

A. *p19Arf*$^{-/-}$ MEFs infected with retrovirus expressing either pBabe vector (-) or pBabe-HRAS^{G12V} (+) were transfected with a control scrambled RNA duplex (-) or RPL23 siRNA (+) for 2 days. Cell extracts were collected and analyzed by Western blot with the indicated antibodies. The relative expression of p53 is shown under the blot.

B. *Mdm2*$^{m/m}$*;p19Arf*$^{-/-}$ MEFs were treated and analyzed as in (A).

C. *WT* MEFs were treated and analyzed as in (A).

D. *Mdm2*$^{m/m}$ MEFs were treated and analyzed as in (A).

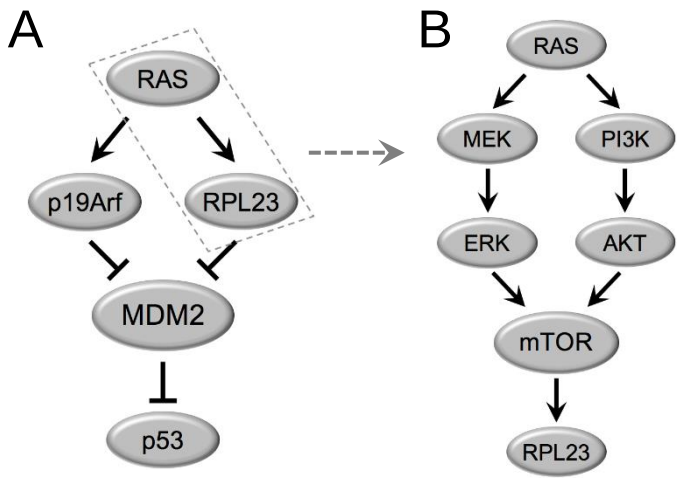

Figure 3.16 A model depicting a RAS-RPL23-MDM2-p53 pathway.

A. Oncogenic RAS induces expression of both RPL23 and p19ARF independently. RPL23 and p19ARF both bind and inhibit MDM2 to stabilize p53.

B. The RAS-MAPK-ERK and RAS-PI3K-AKT signaling cascades induce mTOR-dependent expression of RPL23.

CHAPTER 4: DISRUPTION OF THE RP-MDM2-P53 PATHWAYS ACCELERATES APC LOSS-INDUCED COLORECTAL TUMORIGENESIS[4]

INTRODUCTION

Colorectal cancer is the third most common cancer and the third leading cause of cancer-associated death worldwide (Jemal et al., 2009; Kamangar et al., 2006). Adenomatous polyposis coli (APC) loss or inactivation is sufficient to induce colorectal tumorigenesis, and inactivation of APC through mutation occurs in an estimated 80% of adenomatous polyposis (Groden et al., 1991; Kinzler et al., 1991; Kinzler and Vogelstein, 1996; Network, 2012; Nishisho et al., 1991). APC loss is also the cause of familial adenomatous polyposis (Groden et al., 1991). This striking importance of APC in colorectal cancer has led APC to be named the 'gatekeeper' of colonic carcinogenesis (Kinzler and Vogelstein, 1996).

It has been established that a major function of APC is to degrade cytosolic β-catenin, thus preventing the formation of the nuclear β-catenin/T-cell factor-4 transcriptional complex and switching off Wnt signaling pathway transduction (Morin et al., 1997). The proto-oncogene c-MYC has been identified as a target of the Wnt signaling pathway (He et al., 1998; Sansom et al., 2004; Van De Wetering et al., 2002). In addition, Sansom et al. discovered that deletion of c-MYC diminishes the tumorigenic capacity of APC deficiency in the small intestine, establishing c-MYC as a critical mediator of intestinal neoplasia following APC loss (Sansom et al., 2007). As a transcription factor, the pro-tumorigenic functions of c-MYC have been attributed to its ability

[4] This chapter is adapted from a research article originally published in Oncogene. Shijie Liu, Yanping Zhang and I contributed to the design of the study. Shijie Liu and Jing Yang performed all of the experiments. Shijie Liu, Yanping Zhang, and I analyzed the data. I wrote the manuscript. Yanping Zhang, Shijie Liu and I edited the manuscript. Yanping Zhang finalized the manuscript. The original citation is as follows: Liu, S., Tackmann, N., Yang, J., and Zhang, Y. (2016a). Disruption of the RP-MDM2-p53 pathway accelerates APC loss-induced colorectal tumorigenesis. Oncogene. *36*, 1374-1383.

to regulate a wide spectrum of gene expression programs (Dang et al., 2006; Eilers and Eisenman, 2008; Sabò and Amati, 2014). c-MYC target genes are believed to promote cell proliferation, tumorigenesis and cell transformation (Dang et al., 2006; Ji et al., 2011; Kim et al., 2006; Schlosser et al., 2005; Schuhmacher et al., 2001; Zeller et al., 2003). Notably, elevated expression of c-MYC can also induce apoptosis (Hoffman and Liebermann, 2008). The biological meaning of this function is not yet fully understood, but is thought to result from a protective mechanism to counteract the effects of oncogenic activation and avoid propagation of transformed cells.

Mutations in p53, known as a 'the guardian of the genome' and an overarching tumor suppressor, are the second most common genomic alteration in colorectal cancers (Network, 2012). Loss of p53 activation has been shown to be important in the progression of c-MYC-driven cancers. One recent study showed that p53-inactivating mutations are a leading cause of the relapse of MYC-driven medulloblastoma, and restoration of p53 activity reduces tumor growth and prolongs survival (Hill et al., 2015). On its own, c-MYC overexpression in B cells induces lymphomagenesis (Adams et al., 1985), and in c-MYC-driven lymphomas, p53 deletion significantly accelerates tumor growth (Schmitt et al., 1999). The role of p53 in APC loss-driven cancers is less clear, but some reports have shown that p53 loss can enhance the incidence and invasiveness of tumors in *Apc*$^{Min/+}$ mice (Halberg et al., 2000). Nevertheless, the intricate interactions between c-MYC and p53 have yet to be clarified in the context of APC loss-driven tumor environments.

The regulation of p53 is complex, but it is well established that MDM2 is the primary negative regulator of p53. MDM2 regulates p53 both by binding and inhibiting the transactivation domain of p53 and also serving as an E3 ubiquitin ligase for p53, causing its proteasomal degradation (Honda et al., 1997; Oliner et al., 1993). Upon various cellular stresses, transducer proteins bind and inhibit MDM2, thereby stabilizing p53.

c-MYC expression causes p53 stabilization and activation through two primary pathways. c-MYC induces the expression of p19ARF, which binds and inhibits MDM2 (Chen et al., 2013; Zhang et al., 1998; Zindy et al., 1998). In addition, c-MYC serves as a regulator of ribosomal biogenesis. When active, c-MYC induces the transcription of ribosomal proteins (RPs), which also bind and inhibit MDM2 (Kim et al., 2014; Lohrum et al., 2003; Macias et al., 2010). This results in dual p19ARF-MDM2-p53 and RP-MDM2-p53 signaling pathways responsive to c-MYC overexpression. Deletion of p19ARF or disruption of the RP-MDM2-p53 pathway by $MDM2^{C305F}$ mutation causes significant acceleration of c-MYC-driven lymphomas (Eischen et al., 1999; Macias et al., 2010). In the *Eμ-Myc* mouse model system these pathways are non-redundant, as concomitant disruption of both further accelerates c-MYC-driven lymphoma progression (Meng et al., 2015b).

Although the deletion of c-MYC diminishes APC loss-driven intestinal tumorigenicity (Sansom et al., 2007), the elimination of p19ARF does not increase intestinal tumor formation in $Apc^{Min/+}$ mice (Gibson et al., 2005), indicating that p19ARF signaling is not essential in this situation. Whether or not the RP-MDM2-p53 response pathway is important in preventing APC loss-induced tumor formation has not been explored. In this work, we sought to determine whether the RP-MDM2-p53 pathway could respond to APC loss-induced c-MYC upregulation to induce p53. To test the importance of this pathway, we crossed $Apc^{Min/+}$ mice with mice bearing an $MDM2^{C305F}$ mutation, which disrupts the binding of RPL11 and RPL5 to MDM2, and analyzed intestinal tumorigenesis.

RESULTS

$MDM2^{C305F}$ mutation has no discernable effect on APC loss-induced small intestinal tumors

As the loss of APC induces c-MYC expression through the Wnt signaling pathway (He et al., 1998), and the RP-MDM2-p53 pathway has been shown to be important in preventing c-MYC-induced lymphomagenesis (Macias et al., 2010), we sought to determine whether this

pathway could also contribute to APC loss-induced tumor prevention. To this end, we crossed *Apc*$^{Min/+}$ mice, which are prone to developing intestinal tumors, with *Mdm2*$^{m/m}$ mice, thus disrupting the RP-MDM2-p53 pathway.

As *Mdm2*$^{m/m}$ mice have been shown to have a normal lifespan (Macias et al., 2010), we wanted to first examine normal intestinal tissues from *W*) and *Mdm2*$^{m/m}$ mice to ascertain whether the MDM2^{C305F} mutation affects normal intestinal homeostasis. We harvested small intestine and colon tissue from 8 month old mice and performed both H&E staining and IHC staining to detect Ki-67 and cleaved caspase-3 (CC-3). *Mdm2*$^{m/m}$ mice have a normal intestinal epithelium compared with *WT* mice, with normal appearance of villi and crypts (Figure 4.1a). In addition, the Ki-67 and CC-3 staining of the intestinal epithelium did not differ between *WT* and *Mdm2*$^{m/m}$ mice (Figures 4.1b-c), indicating a similar intestinal proliferative and apoptotic rate between the two genotypes. Furthermore, we examined the expression of several intestinal cell markers, including an intestinal stem cell marker (*lgr5*), Paneth cell marker (*lyz1*), Goblet cell marker (*muc2*) and enteroendocrine cell marker (*chga*) by qPCR (Sato et al., 2009). No significant differences in the expression of any of these markers were detected between *WT* and *Mdm2*$^{m/m}$ mice in either the small intestine or the colon (Figure 4.1d).

We next compared APC loss-induced tumor initiation in these mice by analyzing small intestinal polyp development in 15 week old *Apc*$^{Min/+}$*;Mdm2*$^{+/+}$ and *Apc*$^{Min/+}$*;Mdm2*$^{m/m}$ littermates. Upon gross examination of the small intestine, we did not observe a difference in the incidence of small intestinal polyps in the presence of the MDM2^{C305F} mutation (Figure 4.2a). We performed histological analysis of the small intestinal tumor tissue and found that the average size of the tumors also did not differ between *Apc*$^{Min/+}$*;Mdm2*$^{+/+}$ and *Apc*$^{Min/+}$*;Mdm2*$^{m/m}$ mice (Figure 4.2b). In agreement with this observation, between the two genotypes there was no significant difference in overall lifespan (Figure 4.2c). Hence, the MDM2^{C305F} mutation does not affect APC loss-induced small intestinal tumorigenesis, which is a major contributor to mortality in *Apc*$^{Min/+}$ mice.

MDM2^{C305F} mutation accelerates APC loss-induced colorectal cancer

Although the overall survival and small intestinal tumor formation of *Apc*$^{Min/+}$;*Mdm2*$^{+/+}$ and *Apc*$^{Min/+}$;*Mdm2*$^{m/m}$ mice did not differ significantly, we noticed an increased frequency of rectal prolapse and bleeding in the *Apc*$^{Min/+}$;*Mdm2*$^{m/m}$ mice. More than 30% of *Apc*$^{Min/+}$;*Mdm2*$^{m/m}$ mice presented with rectal prolapse and bleeding compared with <10% of *Apc*$^{Min/+}$;*Mdm2*$^{+/+}$ mice. Rectal prolapse and bleeding are indicative of increased colonic tumor formation, so we examined colonic polyps in *Apc*$^{Min/+}$;*Mdm2*$^{+/+}$ and *Apc*$^{Min/+}$;*Mdm2*$^{m/m}$ mice. We observed significantly more polyps in the colon of *Apc*$^{Min/+}$;*Mdm2*$^{m/m}$ mice than in their *Apc*$^{Min/+}$;*Mdm2*$^{+/+}$ counterparts (on average 0.66 polyps per mouse in *Apc*$^{Min/+}$;*Mdm2*$^{+/+}$ vs 1.75 per mouse in *Apc*$^{Min/+}$;*Mdm2*$^{m/m}$) (Figure 4.3a), further suggesting increased colon tumor initiation. After histopathological examination, we determined that the average size of these polyps was significantly larger in *Apc*$^{Min/+}$;*Mdm2*$^{m/m}$ mice (2.00 mm in *Apc*$^{Min/+}$;*Mdm2*$^{+/+}$ vs 2.95 mm in *Apc*$^{Min/+}$;*Mdm2*$^{m/m}$) (Figure 4.3b). Furthermore, the average size of the adenomas found in the tumor-bearing colons was also larger in *Apc*$^{Min/+}$;*Mdm2*$^{m/m}$ mice (Figure 4.3c). Although both *Apc*$^{Min/+}$;*Mdm2*$^{+/+}$ and *Apc*$^{Min/+}$;*Mdm2*$^{m/m}$ mice developed small intestinal tumors with almost 100% penetrance, on average only 40% of *Apc*$^{Min/+}$;*Mdm2*$^{+/+}$ mice developed colon adenocarcinomas, compared with almost 75% of *Apc*$^{Min/+}$;*Mdm2*$^{m/m}$ mice (Figure 4.3d). The sizes of colon polyps in *Apc*$^{Min/+}$;*Mdm2*$^{m/m}$ mice were variable, but there were many more large polyps (>4 mm) than in *Apc*$^{Min/+}$;*Mdm2*$^{+/+}$ mice (Figure 4.4a). Although the architecture of the normal colonic epithelium in *Apc*$^{Min/+}$;*Mdm2*$^{m/m}$ mice was similar to that of *Apc*$^{Min/+}$;*Mdm2*$^{+/+}$ mice, the architecture of the colon adenocarcinomas in the *Apc*$^{Min/+}$;*Mdm2*$^{m/m}$ mice showed higher grade complex glandular structures than the colon adenocarcinomas from *Apc*$^{Min/+}$;*Mdm2*$^{+/+}$ mice of same age (Figure 4.4b). Taken together, these evidences suggest that the disruption of the RP-MDM2-p53 pathway by MDM2^{C305F} mutation accelerates APC loss-driven colonic tumor initiation and growth.

MDM2^{C305F} mutation promotes proliferation and inhibits apoptosis in APC loss-induced colon cancers

We sought to further characterize the colon tumors. To this end, we first performed Ki-67 staining in normal and tumor samples (Figures 4.5a-b). We observed significantly more cells with positive Ki-67 staining in *Apc$^{Min/+}$;Mdm2$^{m/m}$* tumors compared with their *WT* MDM2 counterparts (46% in *Apc$^{Min/+}$;Mdm2$^{+/+}$* vs 60% in *Apc$^{Min/+}$;Mdm2$^{m/m}$*), indicating increased proliferation upon MDM2^{C305F} mutation. We also performed IHC staining to detect CC-3 in colon and tumor tissues (Figures 4.5c-d). We observed a significantly lower percentage of cells with CC-3 staining in *Apc$^{Min/+}$;Mdm2$^{m/m}$* tumors as compared with *Apc$^{Min/+}$;Mdm2$^{+/+}$* tumors (2.7% of cells in *Apc$^{Min/+}$;Mdm2$^{+/+}$* vs 1.1% in *Apc$^{Min/+}$;Mdm2$^{m/m}$*), indicating a decreased percentage of cells undergoing apoptosis. Next, we detected average overall CC-3 levels in these tissues by western blot (Figure 4.6a), and observed a similarly muted CC-3 signal in *Apc$^{Min/+}$;Mdm2$^{m/m}$* tumors. As a result of the difference in average Actin levels between normal colon and tumor tissues, we included Ponceau S staining as an additional loading control. To confirm the CC-3 results, we performed additional TUNEL assays (Figures 4.6b-c) and observed a significantly decreased TUNEL signal in *Apc$^{Min/+}$;Mdm2$^{m/m}$* tumors (5.3% of cells in *Apc$^{Min/+}$;Mdm2$^{+/+}$* vs 2.4% in *Apc$^{Min/+}$;Mdm2$^{m/m}$*). This result is consistent with decreased levels of apoptosis in these cells. Together, these results indicate that the MDM2^{C305F} mutation promotes proliferation and inhibits apoptosis in colon cancers induced by APC loss.

APC loss-induced colon cancers express high levels of c-MYC and RPL11

As the MDM2^{C305F} mutation disrupts the binding of RPL11 and RPL5 to MDM2 (Lindström et al., 2007; Macias et al., 2010), and RPL11 and RPL5 are transcriptional targets of c-MYC (Coller et al., 2000; Menssen and Hermeking, 2002) we analyzed c-MYC, RPL11 and RPL5 levels to determine if the MDM2^{C305F} mutation affects APC loss-induced c-MYC signaling.

First, we performed IHC staining for c-MYC in normal and tumor tissues (Figure 4.7a). As expected, there was an increase in c-MYC detected in tumor tissue compared with normal tissue and there was no difference in c-MYC levels between the two genotypes. This pattern was also observed in IHC staining for RPL11, a downstream target of c-MYC (Figure 4.7b). In order to evaluate the expression of c-MYC, RPL11 and RPL5 more precisely, we performed qPCR and western blotting using samples from normal colon or colonic adenomas. Consistent with IHC staining, we observed an approximately 2.5-fold increase in *c-myc*, *rpl11* and *rpl5* mRNAs in tumor samples of either genotype (Figures 4.7c-e).

By western blot, we were able to confirm the loss of APC in tumor tissue of both $Apc^{Min/+};Mdm2^{+/+}$ and $Apc^{Min/+};Mdm2^{m/m}$ mice, as well as observe a comparable increase in c-MYC, RPL11 and RPL5 abundance (Figure 4.8a). These results indicate that the $MDM2^{C305F}$ mutation does not ultimately affect the expression of upstream c-MYC, RPL11 and RPL5 signaling in colon cancers and that APC loss still induces relatively high levels of these proteins independent of MDM2 mutational status.

To investigate the apparent discrepancy in tumor formation after $MDM2^{C305F}$ mutation between small intestine (Figure 4.2) and colon (Figure 4.3), we also analyzed c-MYC and RPL11 levels in normal small intestine and small intestinal adenoma tissues (Figure 4.8b). Although we were unable to detect c-MYC in these tissues, we found that RPL11 levels were unchanged after small intestinal tumor formation, in contrast to what we observed in colon tumors. This provides a potential explanation for the disparity of tumor formation rates in colon and small intestine of $Apc^{Min/+};Mdm2^{m/m}$ mice compared with $Apc^{Min/+};Mdm2^{+/+}$ mice, as there is likely to be little RP-MDM2-p53 signaling action in small intestinal tissues. Although c-MYC has been shown to be an oncogene critical in mediating colorectal tumorigenesis following APC deletion, in our hands the role of RPL11 in mediating c-MYC-induced tumorigenesis appears to be colon tissue specific.

MDM2^{C305F} mutation attenuates p53 activation in colon tumors

As the MDM2^{C305F} mutation disrupts the binding of RPL11 and RPL5 to MDM2, thus abrogating ribosomal stress-mediated p53 induction, we wanted to analyze p53 levels and activity in *Apc*$^{Min/+}$*;Mdm2*$^{+/+}$ and *Apc*$^{Min/+}$*;Mdm2*$^{m/m}$ mouse colon tumors to determine whether p53 induction correlated with the observed increase in proliferation and decrease in apoptosis in *Apc*$^{Min/+}$*;Mdm2*$^{m/m}$ tumors. We found that in *Apc*$^{Min/+}$*;Mdm2*$^{m/m}$ mouse colon tumors, p53 protein levels were notably lower than in tumors from *Apc*$^{Min/+}$*;Mdm2*$^{+/+}$ mice (Figure 4.9a). The protein levels of BAX, a p53 target important for induction of apoptosis (Toshiyuki and Reed, 1995), and of MDM2, also a p53 target, followed the same trend. We also compared p53 transcriptional activation in these tissues. In normal tissues, we observed no significant difference between the relative levels of *mdm2* and *bax* mRNA; however, in tumor tissues, there was significantly less transcription of *mdm2* and *bax* (Figures 4.9b-c) in *Apc*$^{Min/+}$*;Mdm2*$^{m/m}$ mice compared with *Apc*$^{Min/+}$*;Mdm2*$^{+/+}$, indicating attenuated p53 induction upon MDM2^{C305F} mutation.

To more precisely determine whether APC loss will increase signaling to the RP-MDM2-p53 pathway, we knocked down *Apc* expression in the colonic tumor cell line HCT116, which has WT p53. We infected HCT116 cells with a lentivirus containing short hairpin RNA (shRNA) targeting *Apc*, and after puromycin selection we confirmed a decrease in *Apc* expression by qPCR (Figure 4.10a). As expected, knockdown of *Apc* induced the expression of c-MYC, RPL11 and RPL5 (Figure 4.10b). In addition, p53 was stabilized. We next performed immunoprecipitation of MDM2 and probed for RPL11 and RPL5 binding. After *Apc* knockdown, there was a clear increase in both RPL11-MDM2 and RPL5-MDM2 binding, suggesting that APC loss triggers RP-MDM2 interaction to activate p53 in colon tumors (Figure 4.10b). Taken together, these results collectively suggest that the RP-MDM2-p53 pathway is important for the prevention of APC loss-induced colonic tumors.

DISCUSSION

The roles of APC deletion and p53 inactivation in intestinal tumorigenesis are not completely understood. Although p53 is widely known as an overarching tumor-suppressor protein, APC has been established as the most important intestinal tumor suppressor. Large-scale sequencing of intestinal tumors has indicated that *Apc* and *p53* are the most frequently mutated genes at 81% and 60% of these tumors, respectively (Network, 2012).

In addition, several mouse models have established that upon Wnt signaling pathway activation, the major consequence of APC loss, p53 has critical tumor-suppressive functions (Elyada et al., 2011; Schwitalla et al., 2013). It is possible that activation of the Wnt signaling target c-MYC drives growth and proliferation, stimulating p53 to perform its tumor-suppressive functions but at the same time pressuring its inactivation, allowing for tumor maintenance. Here, we confirm that p53 is indeed induced by APC deletion (Figure 4.9). Although inactivating mutations of APC are considered to be a first step for colonic carcinogenesis, p53 is thought to act as a final barrier to carcinoma formation (Kinzler and Vogelstein, 1996). Our results are consistent with this notion.

We also demonstrate that inactivation of the c-MYC responsive RP-MDM2-p53 pathway through $MDM2^{C305F}$ mutation allows for increased APC loss-driven colon tumorigenesis. $Apc^{Min/+};Mdm2^{m/m}$ mice display increased tumor size and incidence compared with their $Apc^{Min/+};Mdm2^{+/+}$ counterparts (Figure 4.3), which correlates with decreased p53 protein abundance and activation (Figure 4.9).

The importance of p19ARF- and RP-dependent p53 activation is tissue specific

Along with others, this work also clarifies that there are distinct and tissue-specific roles for the RP-MDM2-p53 and p19ARF-MDM2-p53 pathways in tumorigenesis. Although each of these pathways have been shown to be independently critical for the prevention of c-MYC-driven lymphoma (Meng et al., 2015b), the role of these pathways in APC loss driven, c-MYC-

dependent tumorigenesis is more ambiguous. It has been previously established that p19ARF loss does not accelerate or promote intestinal tumors upon APC loss (Gibson et al., 2005), but our work indicates that loss of RP-MDM2 interaction can sensitize mice to APC loss-driven colonic tumorigenesis (Figure 4.3). In this study, we observed no difference in survival between *Apc*$^{Min/+}$*;Mdm2*$^{+/+}$ and *Apc*$^{Min/+}$*;Mdm2*$^{m/m}$ mice; however, in both genotypes there were many more tumors in the small intestine than colon, which is consistent with previous reports (Moser et al., 1992; Moser et al., 1990). Observed differences in colon tumor formation depending on MDM2 mutational status may not have an effect on survival because of the relatively higher tumor burden in the small intestine compared with the colon. In future studies, it would be informative to cross MDM2^{C305F} mice with mice expressing a colon tissue-specific *Apc* deletion, such as the *CDX2P-CreERT2 Apc*$^{flox/flox}$ model (Feng et al., 2013), to determine whether differential RP-MDM2-p53 pathway activation could contribute to a difference in tumor burden and overall lifespan.

As RPL11 is a primary RP responder from c-MYC to p53 (Fumagalli et al., 2009a; Fumagalli et al., 2012), disruption of RPL11-MDM2 binding by MDM2^{C305F} mutation is likely to have little effect on p53 activation if RPL11 protein abundance does not change. It appears from our data that c-MYC signaling to RPL11 is much more prominent in colon tissue than in small intestine (Figure 4.8), but the reason for this is presently unclear. Although this study demonstrates that there are tissue-specific roles for each of the RP-MDM2-p53 and p19ARF-MDM2-p53 signaling pathways, it also raises questions about why p19ARF signaling is less important in APC loss-driven c-MYC activation.

One possible reason for the difference in activation of these two pathways during colonic tumorigenesis could be due to a difference in threshold of c-MYC response. As a global transcriptional amplifier (Littlewood et al., 2012), c-MYC can trigger different programs depending on certain levels of expression. Both *in vitro* and *in vivo* studies have demonstrated that p19ARF induction requires a high level of c-MYC expression (Chen et al., 2013; Murphy et

al., 2008). On the other hand, c-MYC serves as a direct regulator of ribosomal biogenesis via the transcriptional control of RNA and protein components of ribosomes, the gene products required for the processing of ribosomal RNA, the nuclear export of ribosomal subunits and the initiation of mRNA translation (van Riggelen et al., 2010). It is possible that RP-MDM2-p53 activation requires a lower level of c-MYC activation than that of the p19ARF-MDM2-p53 pathway. In mouse model systems, where c-MYC is directly overexpressed (for example, *Eμ-Myc*), rather than upregulated by a change in upstream signaling (for example, $Apc^{Min/+}$), p19ARF is critical in prevention of tumorigenesis (Eischen et al., 1999). The presence of the RP-MDM2-p53 pathway could explain why deletion of p19ARF does not sensitize mice to APC loss-induced intestinal tumorigenesis.

In this study, we demonstrated that RPL11 and RPL5 are upregulated by the APC-MYC axis, correlating with p53 induction and apoptosis. We postulate that the RP-MDM2-p53 pathway is a fail-safe mechanism for c-MYC-dependent tumorigenesis because it can be executed directly after c-MYC activation. It is clear from the $Apc^{Min/+}$ mouse model and others that the interplay of these pathways is tissue specific, and more work will need to be done to establish the biological and contextual significance for these tumor-suppressive pathways.

EXPERIMENTAL PROCEDURES

Mouse experiments

All mice were bred and maintained on a 12-h light and dark cycle. $Mdm2^{C305F}$ mutant mice were generated as previously described (Macias et al., 2010). $Apc^{Min/+}$ mice on C57BL/6 J background were purchased from The Jackson Laboratory (Bar Harbor, ME, USA) (stock number J002020). All mice were handled in strict accordance with protocol (10-045) approved by the Institutional Animal Care and Use Committee at The University of North Carolina at Chapel Hill.

Histological analysis

Intestines were dissected and flushed gently with cold phosphate-buffered saline and rolled into a compact circle. They were then fixed in 10% formalin overnight, dehydrated in 50% ethanol and stored in 70% ethanol until they were transferred to the Histology Research Core Facility at the University of North Carolina at Chapel Hill (UNC) for paraffin embedding. Sections (4 μm) were cut and then processed for H&E staining or for IHC staining. For IHC staining, sections were deparaffinized in SafeClear II (Fisher Scientific, Waltham, MA, USA) and rehydrated in gradient alcohols (100%, 95%, 85%, 70%, H_2O). Antigen retrieval was performed by boiling slides in 10 mM sodium citrate buffer, pH 6.0. Endogenous peroxidase activity was quenched with 3% H_2O_2 in methanol for 15 min. To develop the staining, we used the VECTASTAIN Elite ABC kit (PK6100, Vector Laboratories) following the manufacturer's instructions. Slides were counterstained with Harris' hematoxylin (Sigma, St Louis, MO, USA) and then dehydrated and mounted in Permount (Fisher Scientific). The following primary antibodies were used: rabbit monoclonal anti-Ki-67 (NeoMarkers, Fremont, CA, USA, #RM-9106), rabbit polyclonal anti-CC-3 (Cell Signaling, Beverly, MA, USA, #9661), rabbit polyclonal anti-c-MYC (Santa Cruz, Dallas, TX, USA, N262) and rabbit polyclonal anti-RPL11 (homemade). All primary antibodies were incubated overnight. For TUNEL assays, sections were deparaffinized following the IHC protocol, and then stained with the Apoptosis Detection Kit (S7100, Millipore, Billerca, MA, USA) following the manufacturer's instructions.

Quantitative PCR

Total RNA was prepared from mouse tissues using Trizol Reagent (Invitrogen, Carlsbad, CA, USA, #15596-026). RNA concentration was determined using a NanoDrop spectrophotometer (Thermo Scientific, Waltham, MA, USA, NanoDrop 2000c) and quality was assessed by agarose gel electrophoresis. Complementary DNA was synthesized using Superscript III reverse transcriptase (Invitrogen, 18080-051). qPCR was performed with SYBR

Green probes using the Applied Biosystems (Carlsbad, CA, USA) 7900HT Fast Real-Time PCR system. Thermal cycling conditions were 50 °C for 2 min, 95 °C for 5 min, followed by 40 cycles of 95 °C for 15 s and 60 °C for 1 min. Target gene transcript levels were normalized to *β-actin* transcript levels obtained in each sample via the subtraction of the Ct value of *β-actin* from the Ct value for each target gene. Results were expressed as the fold-change in transcript levels. Primers used for qPCR were as follows: *β-actin*, 5′-GGCTGTATTCCCCTCCATCG-3′ and 5′-CCAGTTGGTAACAATGCCATGT-3′; *c-myc*, 5′-TGAGCCCCTAGTGCTGCAT-3′ and 5′-AGCCCGACTCCGACCTCTT-3′; *rpl11*, 5′-CAATATCTGCGTCGGGGAGA-3′ and 5′-TTCCGCAACTCATACTCCCG-3′; *rpl5*, 5′-AGCATTGACGGTCAGCCTGGTG-3′ and 5′-CTGACCCATGATGTGCTTCCGATG-3′; *bax*, 5′-GGACAGCAATATGGAGCTGCAGAGG-3′ and 5′-GGAGGAAGTCCAGTGTCCAGCC-3′; *mdm2*, 5′-TGTGTGAGCTGAGGGAGATG-3′ and 5′-CACTTACGCCATCGTCAAGA-3′; *lgr5*, 5′-CAAGCCATGACCTTGGCCCTG-3′ and 5′-TTTCCCAGGGAGTGGATTCTATT-3′; *lyz1*, 5′-GGAATGGATGGCTACCGTGG-3′ and 5′-CATGCCACCCATGCTCGAAT-3′; *muc2*, 5′-CGGTTCCAGAACCATACCTG-3′ and 5′-GGTCAGCAGCCTCTCACATT-3′; *chga*, 5′-CACAGCAGCTTTGAGGATGA-3′ and 5′-ATGGGGGACTCTTGGTTAGG-3′.

Protein analysis

For western blotting, proteins were extracted from tissues as previously described (Macias et al., 2010). Briefly, mouse tissue was homogenized and lysed in 0.5% NP-40 lysis buffer. Proteins were detected by using either Pico or Dura enhanced chemiluminescence systems (Thermo Scientific, SuperSignal West Dura Substrate). The following primary antibodies were used: rabbit polyclonal anti-c-MYC (N262; Santa Cruz), mouse monoclonal anti-p53 (NCL-505; Novocastra, Buffalo Grove, IL, USA), mouse monoclonal anti-MDM2 (2A10, homemade), rabbit polyclonal anti-CC-3 (#9661; Cell Signaling), rabbit polyclonal anti-APC (NBP2-15422; Novus Biologicals, Littleton, CO, USA), rabbit polyclonal anti-BAX (554104, BD

Biosciences, San Jose, CA, USA), rabbit polyclonal anti-RPL11 and RPL5 (made in house as previously described) (Macias et al., 2010). For protein analysis of HCT116 cells (purchased and authenticated from the UNC Tissue Culture Facility, Chapel Hill, NC, USA), we homogenized and lysed cells in 0.1% NP-40 lysis buffer. For each sample, 2.5 mg of protein extract was incubated with antibodies against MDM2 (4B11) overnight at 4 °C before incubation with protein A beads for 60 min. Immunoprecipitates were washed three times in ice-cold lysis buffer, resuspended in sodium dodecyl sulfate loading buffer and subjected to western blot analysis.

Lentiviral vector and infection

For shRNA transduction, a pLKO.1-puro vector (Addgene, Cambridge, MA, USA) containing shRNA targeting human *Apc* (5′-GAAAGTGGAGGTGGGATATTA-3′) and a scrambled control (5′-CAACAAGATGAAGAGCACCAA-3′) were used. We made the viral particles in HEK-293 T cells using pspAX2 and pMD2.G plasmids. Twenty-four hours after infection, positively infected HCT116 cells were selected with puromycin. Stable shRNA knockdown cell lines were used for further analysis.

Statistical analysis

Results are represented as mean ±SEM. Differences in tumor size measurements and tumor numbers were evaluated for significance using the unpaired t-test. Quantitative PCR data and IHC quantification differences were also evaluated for significance using the unpaired t-test. Variances were not significantly different within treatment groups. A P-value <0.05 was considered significant for all analyses. Significant differences between experimental groups were: *$P<0.05$, **$P<0.01$ or ***$P<0.001$. Each experiment was performed at least two times. At least three mice per group were used for every experiment. No blinding or randomization were used. Calculations were performed using the GraphPad Prism 5 software (La Jolla, CA, USA).

Ethics statement

This investigation has been conducted in accordance with ethical standards, the Declaration of Helsinki, national and international guidelines, and has been approved by the authors' institutional review board.

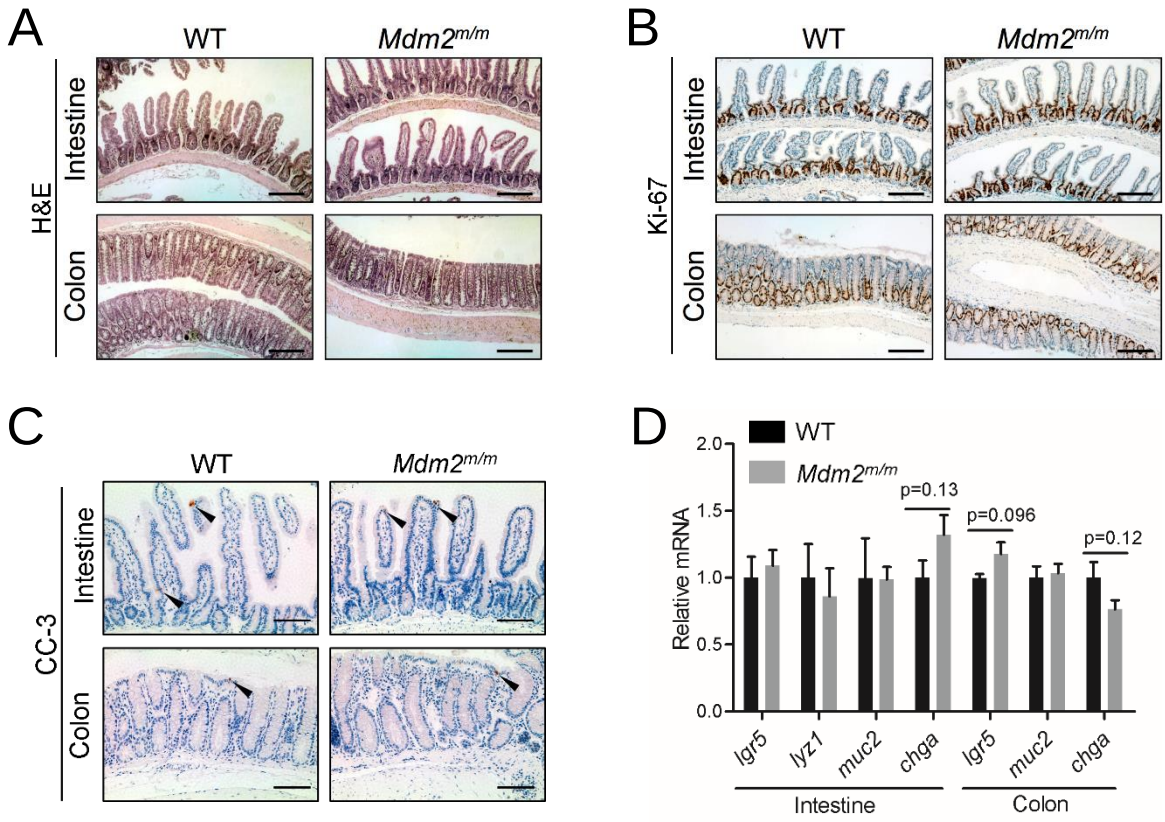

Figure 4.1 MDM2^{C305F} mutation has no discernable effect on intestinal homeostasis.

A. H&E staining of small intestine and colon isolated from 8 month old *WT* and *Mdm2*$^{m/m}$ mice. Scale bar, 200 μm.

B. Ki-67 IHC staining of proliferating cells in small intestine and colon isolated from 8 month old mice. Proliferating cells are located at the bottom of crypts in both the small intestine and colon. Scale bar, 200 μm.

C. IHC staining of CC-3 to probe for apoptotic cells (indicated by arrows) in small intestine and colon tissue isolated from 8 month old mice. Scale bar, 100 μm.

D. mRNA expression of *lgr5*, *lyz1*, *muc2* and *chga* in small intestine or colon from 8 month old *WT* or *Mdm2*$^{m/m}$ mice was analyzed by qPCR. n=3 for each genotype. Error bars, ±SEM.

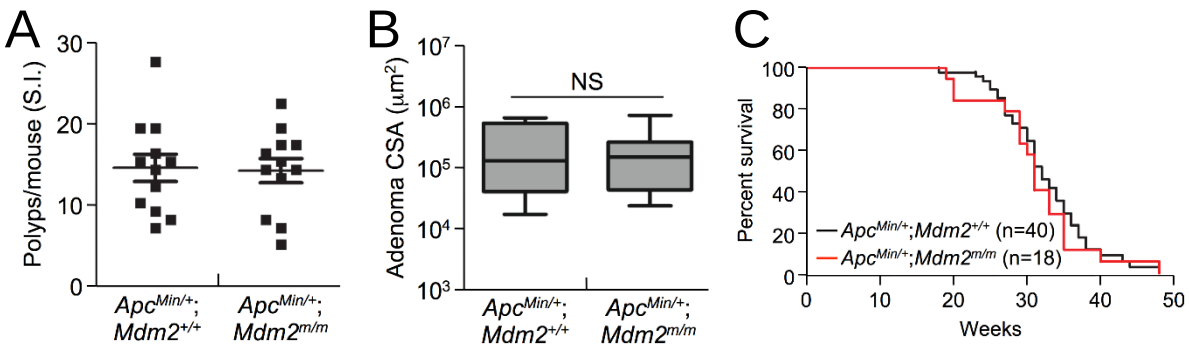

Figure 4.2 MDM2^{C305F} mutation has no discernable effect on APC loss-induced small intestinal tumors.

A. Small intestines were isolated from 15 week old mice, and polyp numbers per mouse were counted under a dissection microscope (n=12 for each genotype).

B. The average cross sectional areas (CSAs) of H&E-stained small intestinal adenomas were determined quantitatively using publicly available ImageJ software.

C. Kaplan-Meier survival curves for *Apc$^{Min/+}$;Mdm2$^{+/+}$* (n=40) and *Apc$^{Min/+}$;Mdm2$^{m/m}$* (n=18) mice are shown. The median survival times did not differ significantly between the two genotypes.

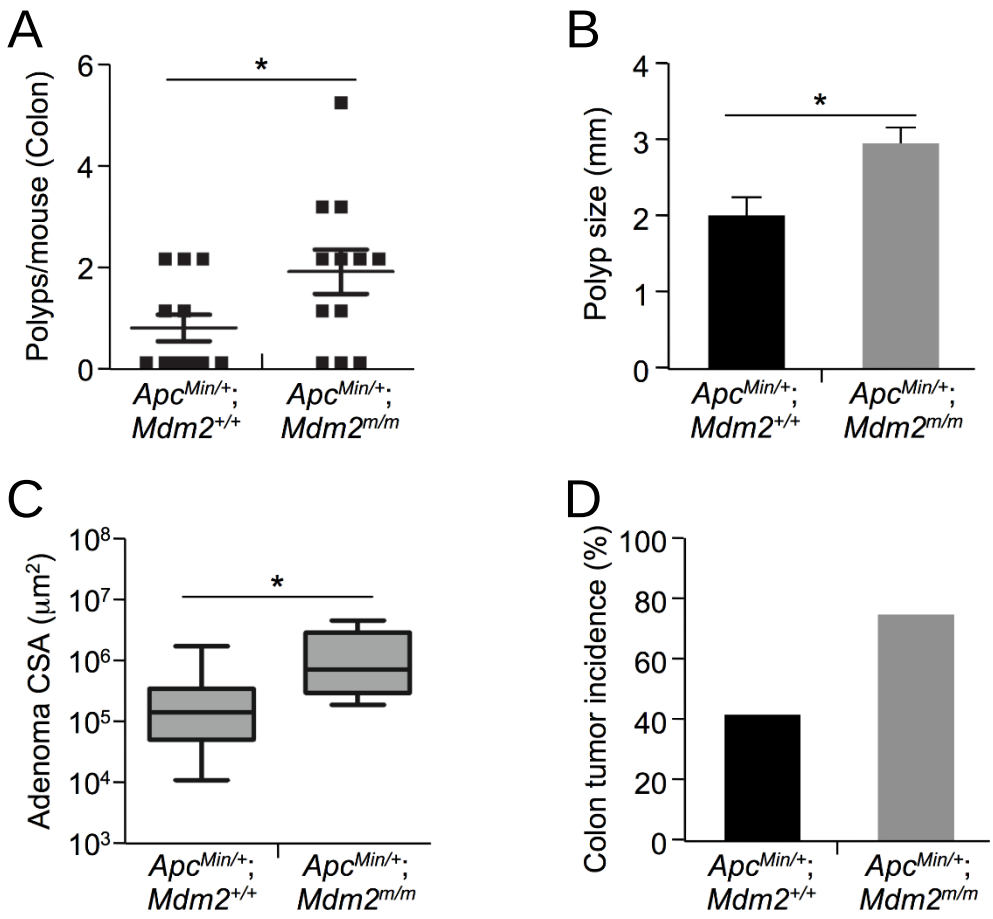

Figure 4.3 MDM2^{C305F} mutation increases prevalence of APC loss-induced colon cancer.

A. Colon tissue was isolated from 15 week old mice, and polyp numbers per mouse were counted under a dissection microscope. Error bars, ±SEM.; *P<0.05.

B. The average size of colonic polyps in each genotype (n=12 mice). *Apc$^{Min/+}$;Mdm2$^{m/m}$* mice had significantly more large (44 mm) polyps. Error bars, ±SEM; *P<0.05.

C. The average cross sectional areas (CSA) of H&E stained colon adenomas were determined quantitatively using ImageJ. Error bars, ±SEM;*P<0.05.

D. The incidence of colon tumors in each genotype (n =12), measured by percentage of mice with observed colon tumors.

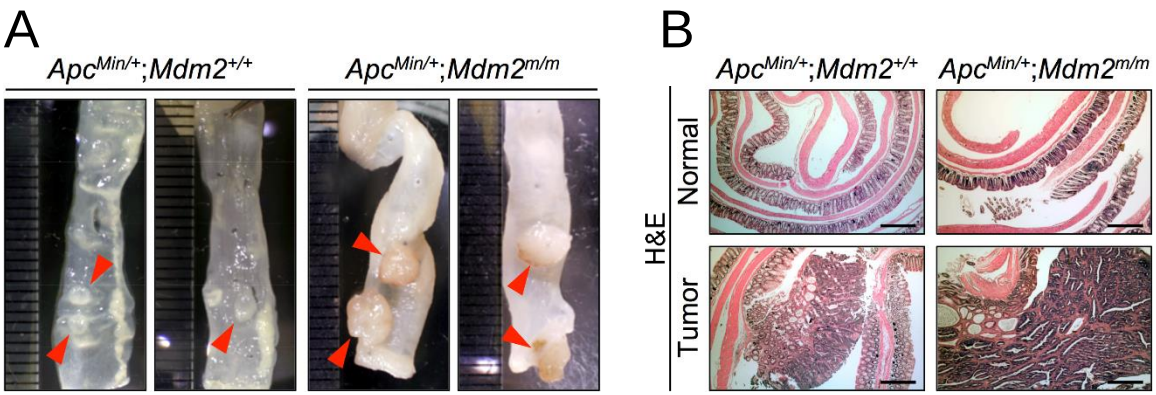

Figure 4.4 MDM2^{C305F} mutation changes the pathophysiology of APC loss-induced colon cancer.

A. Pictures depicting the colonic polyps from *Apc*$^{Min/+}$;*Mdm2*$^{+/+}$ or *Apc*$^{Min/+}$;*Mdm2*$^{m/m}$ mice under a dissection microscope. Adenomas from *Apc*$^{Min/+}$;*Mdm2*$^{m/m}$ mice appeared significantly larger.

B. Representative H&E-stained sections from *Apc*$^{Min/+}$;*Mdm2*$^{+/+}$ or *Apc*$^{Min/+}$;*Mdm2*$^{m/m}$ mouse colon (normal) and colon adenoma (tumor) tissue. Scale bar, 500 μm.

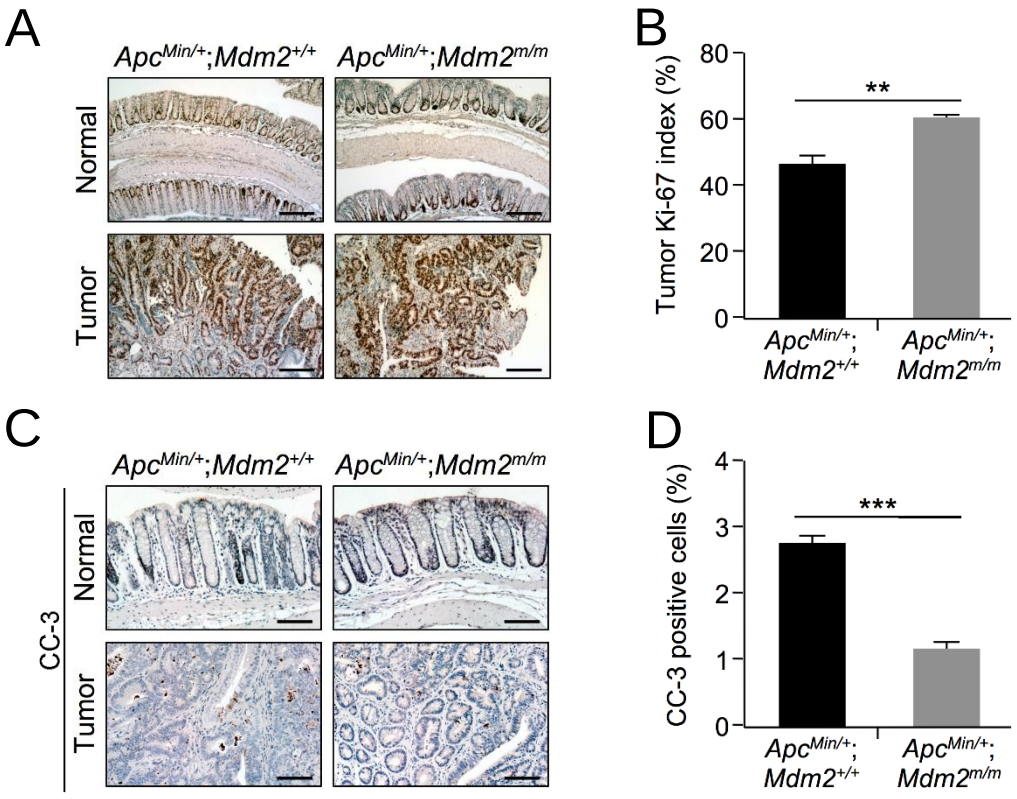

Figure 4.5 APC loss-induced colon cancers containing MDM2^{C305F} mutation grow quickly.

A. Ki-67 IHC staining of proliferating cells in colon (normal) and colonic adenoma (tumor) tissue isolated from 15 week old mice. In normal colon, the proliferating cells are located at the bottom of crypts, whereas tumor cells are highly proliferative. Scale bar, 200 μm.

B. Percentage of Ki-67-positive cells in colonic adenomas was calculated quantitatively from five images using ImageJ. Error bars, ±SEM; **P<0.01.

C. Apoptosis was measured by IHC staining of CC-3 in colon (normal) and colonic adenoma (tumor) tissue. Scale bar, 100 μm.

D. Percentage of CC-3 positive cells in colonic adenomas was calculated quantitatively from five images using ImageJ. Error bars, ±SEM; ***P<0.001.

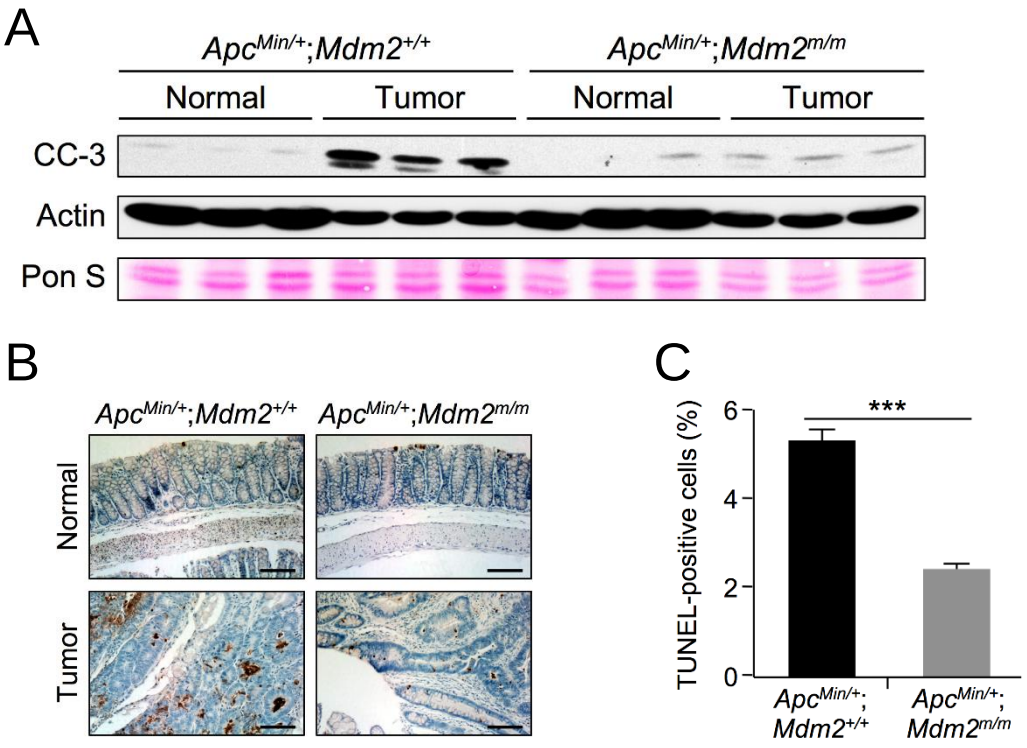

Figure 4.6 MDM2^{C305F} mutation inhibits apoptosis in APC loss-induced colon cancers.

A. Western blotting was performed with protein lysates isolated from colonic polyps (tumor) or adjacent normal colon tissues (normal). n =3 for each group. Pon S, Ponceau S staining.

B. Apoptosis was measured by TUNEL staining in colon (normal) and colonic adenoma (tumor) tissue. In normal colon, apoptotic cells are located at the tips of the villi. Scale bar, 125 μm.

C. Percentage of TUNEL-positive cells from colonic adenomas was calculated quantitatively from five images using ImageJ. Error bars, ±SEM; ***P<0.001.

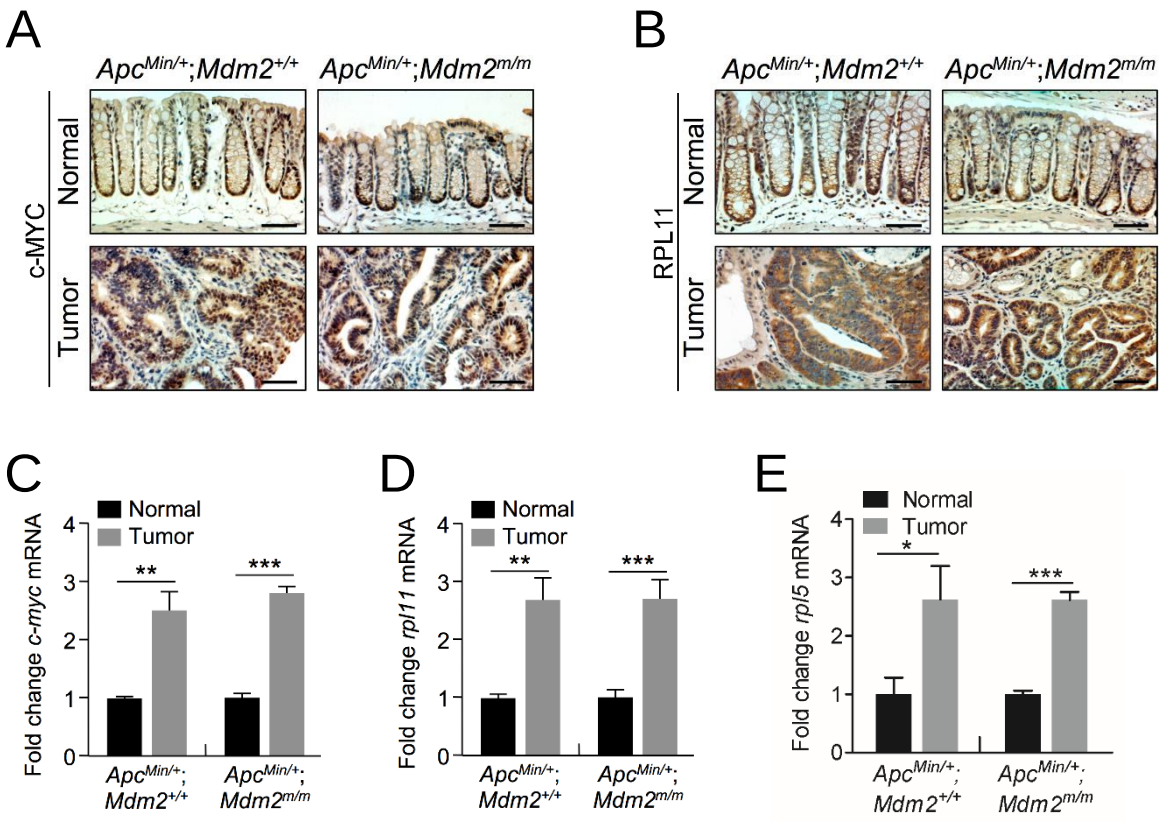

Figure 4.7 APC loss-induced colon cancers express increased levels of c-MYC and RPL11.

A. IHC staining was performed in colon (normal) and colonic adenomas (tumor) to detect the expression of c-MYC. Scale bar, 75 μm.

B. IHC staining was performed in colon (normal) and colonic adenomas (tumor) to detect the expression of RPL11. Scale bar, 75 μm.

C. qPCR analysis of mRNA expression of *c-myc* in colon (normal) or colonic adenomas (tumor) from *Apc*$^{Min/+}$*;Mdm2*$^{+/+}$ and *Apc*$^{Min/+}$*;Mdm2*$^{m/m}$ mice. n=3 for each genotype. Error bars, ±SEM; **P<0.01, ***P<0.001.

D. qPCR analysis of mRNA expression of *rpl11* in colon (normal) or colonic adenomas (tumor) from *Apc*$^{Min/+}$*;Mdm2*$^{+/+}$ and *Apc*$^{Min/+}$*;Mdm2*$^{m/m}$ mice. n=3 for each genotype. Error bars, ±SEM; **P<0.01, ***P<0.001.

E. qPCR analysis of mRNA expression of *rpl5* in colon (normal) or colonic adenomas (tumor) from *Apc*$^{Min/+}$*;Mdm2*$^{+/+}$ and *Apc*$^{Min/+}$*;Mdm2*$^{m/m}$ mice. n=3 for each genotype. Error bars, ±SEM; *P<0.05, ***P<0.001.

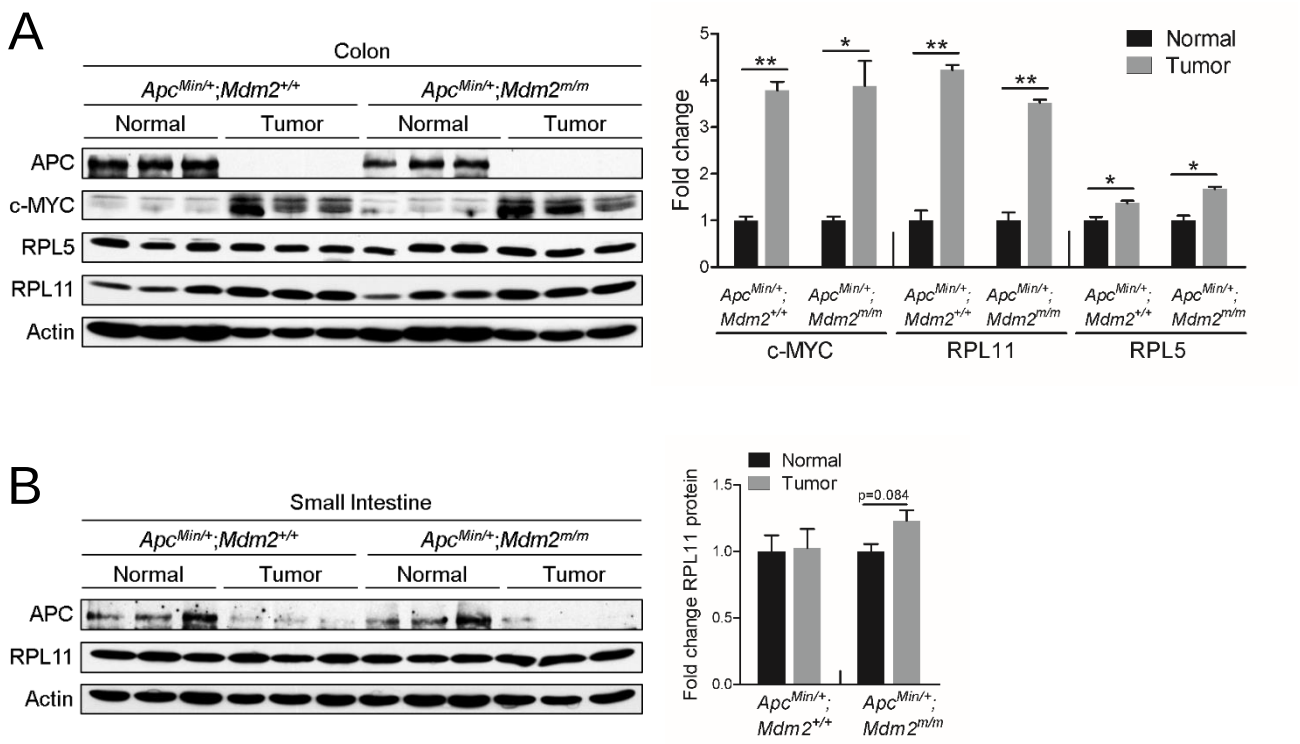

Figure 4.8 APC loss-induced colon tumors, but not small intestine tumors, express increased levels RPL11.

A. Western blotting analysis of protein lysates isolated from colon (normal) or adjacent colonic adenomas (tumor) with three mice per genotype. APC expression was undetectable in colonic adenomas, implying the loss of both WT alleles. The bar graph illustrates the quantification of the western blot. Error bars, ±SEM; *P<0.05, **P<0.01.

B. Western blotting analysis of protein lysates isolated from small intestine (normal) or adjacent adenomas (tumor) with three mice per genotype. c-MYC expression was undetectable in small intestinal tissue. The bar graph illustrates the quantification of the western blot. Error bars, ±SEM.

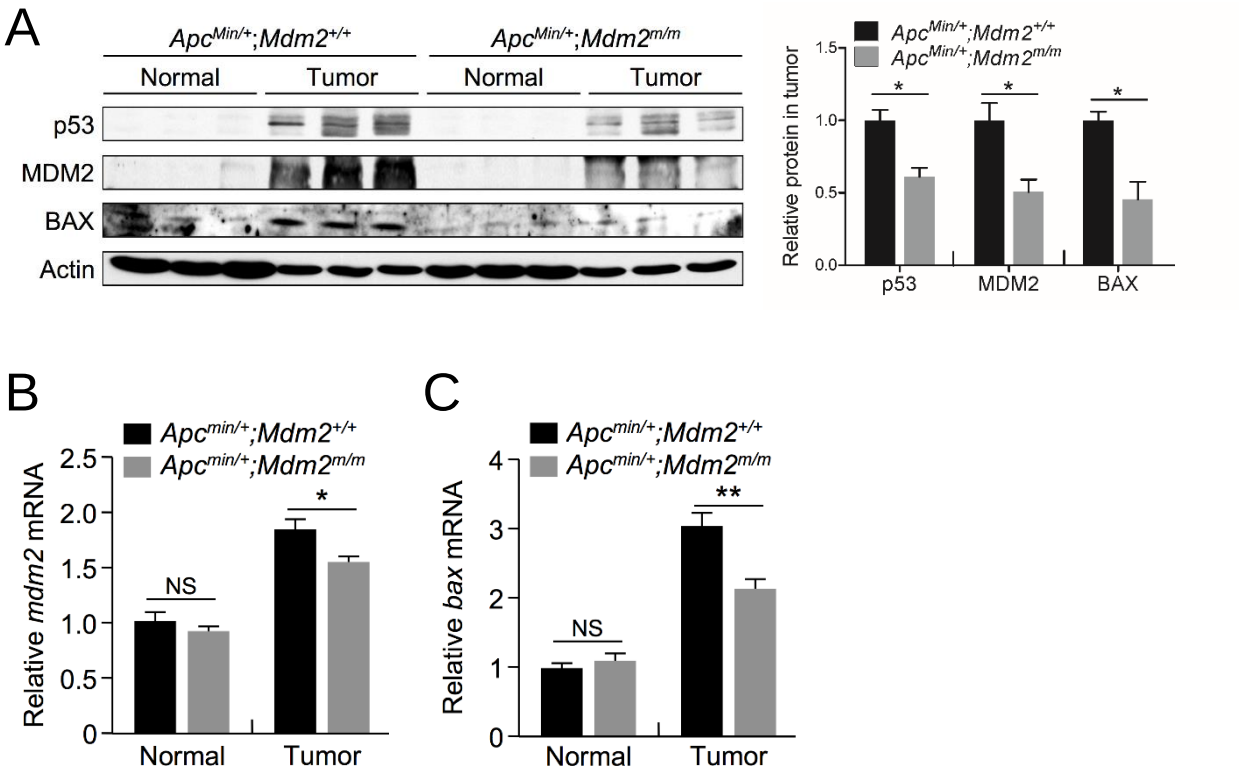

Figure 4.9 MDM2^{C305F} mutation attenuates p53 activation in APC loss-induced colon cancers.

A. Western blotting analysis of protein lysates isolated from colon (normal) or adjacent colonic adenomas (tumor) with three mice per genotype. p53 and MDM2 were undetectable in normal colon. The bar graph illustrates the relative protein levels in tumor samples from *Apc*$^{Min/+}$;*Mdm2*$^{+/+}$ and *Apc*$^{Min/+}$;*Mdm2*$^{m/m}$ mice. Error bars, ±SEM; *P<0.05.

B. qPCR analysis of relative mRNA expression of *mdm2* in colon (normal) or colonic adenomas (tumor) from *Apc*$^{Min/+}$;*Mdm2*$^{+/+}$ and *Apc*$^{Min/+}$;*Mdm2*$^{m/m}$ mice. n=3 for each genotype. Error bars, ±s.e.m.; NS, not significant, *P<0.05.

C. qPCR analysis of relative mRNA expression of *bax* in colon (normal) or colonic adenomas (tumor) from *Apc*$^{Min/+}$;*Mdm2*$^{+/+}$ and *Apc*$^{Min/+}$;*Mdm2*$^{m/m}$ mice. n =3 for each genotype. Error bars, ±SEM, **P<0.01.

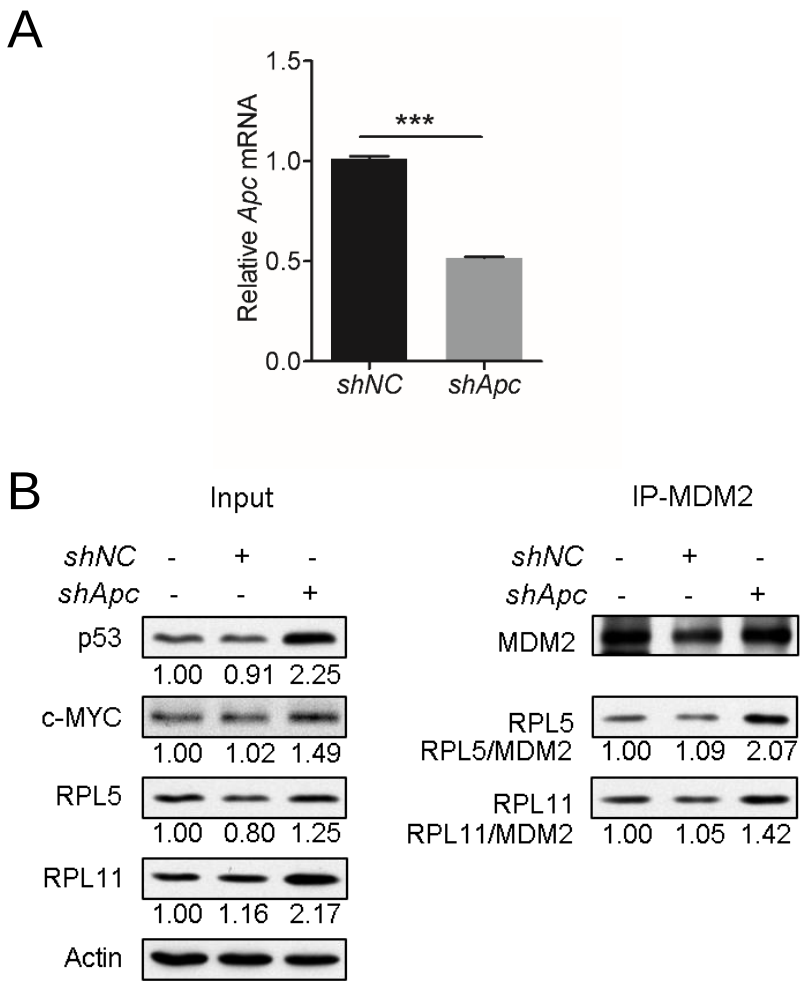

Figure 4.10 MDM2^{C305F} mutation attenuates RP-mediated p53 activation in APC loss-induced colon cancers.

A. qPCR analysis of relative mRNA expression of *Apc* in HCT116 cells infected with lentivirus containing either a negative control scrambled shRNA (*shNC*) or *Apc* shRNA (*shApc*). Error bars, ±SEM; ***P<0.001.

B. HCT116 cells were infected with lentivirus containing shRNA targeting either *Apc* (*shApc*) or a scrambled control (*shNC*). Following selection with puromycin, immunoprecipitation (IP) of MDM2 was performed, followed by western blotting with the indicated antibodies. Quantification of protein expression was performed using ImageJ, and the relative protein expression is indicated under the blots. The amount of RPL11 or RPL5 immunoprecipitated (relative to MDM2 IP protein levels) is also indicated under each IP blot.

CHAPTER 5: DISRUPTING MDM2 E3 LIGASE ACTIVITY PROLONGS SURVIVAL IN MYC-INDUCED LYMPHOMA[5]

INTRODUCTION

p53, also known as “the guardian of the genome,” is an important transcription factor that is capable of tumor suppression through promoting or repressing the transcription of genes involved in cell cycle arrest, senescence, apoptosis, and metabolic regulation (Lane, 1992). The regulation of p53 is thought to be primarily mediated by MDM2 and MDMX, which form a heterodimer through their RING domains (Wade et al., 2010). Together, MDM2 and MDMX regulate p53 both by binding to p53 and inhibiting its gene transactivation activity, as well as promoting p53 ubiquitination, nuclear export, and proteasomal degradation. MDM2 harbors E3 ubiquitin ligase activity, while MDMX does not (Shvarts et al., 1996), but it is hypothesized that the MDM2/MDMX heterodimer is able to promote more efficient p53 inhibition than MDM2 alone (Linares et al., 2003).

p53 is continuously transcribed and translated, but upon the induction of a stress, such as DNA damage or oncogene activation, MDM2 and MDMX inhibitory functions are repressed by various upstream factors, promoting the stabilization and activation of p53. After resolving the stress, the cell must return p53 protein and activity to basal levels or risk the consequences of prolonged apoptosis, cell cycle arrest, or senescence signals. Interestingly, mice lacking *mdm2* or *mdmx* exhibit p53 dependent embryonic lethality, demonstrating the importance of each protein to proper p53 regulation (de Oca Luna et al., 1995; Jones et al., 1995; Parant et al., 2001). Further targeted knockin mouse models have explored the contributions of individual

[5] This chapter represents preliminary data from ongoing research. I have performed all experiments under the direction of Yanping Zhang.

MDM2 and MDMX functions towards *in vivo* p53 regulation. For instance, MDM2- or MDMX-p53 binding in the absence of MDM2-MDMX heterodimer formation or MDM2 E3 ligase activity is insufficient to control p53 during embryogenesis (Itahana et al., 2007). In this *in vivo* study, a mutation in the RING domain of MDM2 ($MDM2^{C462A}$) prevents its ability to ubiquitinate p53 and interact with MDMX. Mice homozygous for this mutation demonstrated p53-dependent embryonic lethality. Similarly, it has been shown that MDM2/MDMX heterodimer formation is critical for controlling p53 activation during embryonic development (Huang et al., 2011; Pant et al., 2011).

On the other hand, mice containing a mutation in the C-terminal domain of MDM2 ($MDM2^{Y487A}$), which disrupts MDM2 E3 ligase activity while maintaining MDM2-MDMX interaction, survive to adulthood and exhibit normal lifespans even though p53 degradation is absent (Tollini et al., 2014). However, these mice are abnormally susceptible to sub lethal doses of ionizing radiation (IR), succumbing to hematopoietic failure an average of 22 days after treatment. This suggests that, though MDM2 E3 ligase function is dispensable for basal p53 regulation, it is especially important for regulating p53 in response to stress. This study underscored the situation-specific importance of individual MDM2/MDMX functions towards p53 regulation. To fully understand p53 regulation, it is important to determine under which contexts various MDM2/MDMX functions are required.

Although it has been demonstrated that MDM2 E3 ligase activity is important for reducing p53 levels and activity following acute DNA damage stress, it is unknown whether other stresses require such careful intervention. In this study, $MDM2^{Y487A}$ mice were crossed with *Eμ-Myc* mice to determine whether there is a difference in the necessity of MDM2 E3 ligase activity-mediated p53 regulation *in vivo* between an acute DNA-damaging stress versus chronic oncogenic c-MYC overexpression.

Eμ-Myc mice overexpress c-MYC in B-lymphoid cells due to the integration of *c-myc* under the control of the IgG heavy chain enhancer element (Harris et al., 1988). This

overexpression leads to hyperproliferation of B cells and development of lymphoma within about 3 months of birth. *Eμ-Myc* mice lacking p53 demonstrate even faster tumor development and death (Hsu et al., 1995). c-MYC induces p53 activation through several pathways. For example, c-MYC induces transcriptional upregulation of the p19ARF tumor suppressor, which can bind to MDM2 and promote its degradation as well as sequester MDM2 in the nucleolus and prevent its interaction with p53 (Kamijo et al., 1998; Weber et al., 1999; Zhang et al., 1998). c-MYC also plays a large role in regulating ribosome biogenesis, in part through increasing the transcription of ribosomal proteins (RPs), which also bind to MDM2 and inhibit its ability to regulate p53 (Dang, 2013; van Riggelen et al., 2010; Zhang and Lu, 2009).

Here I present preliminary data suggesting that c-MYC activation does not mandate p53 regulation through MDM2 E3 ligase activity. This data also suggests that hampering p53 degradation mediates prolonged animal survival during oncogenic stress.

RESULTS

Loss of MDM2 E3 ligase function prolongs survival during MYC-induced lymphoma

Previous work has demonstrated that mice bearing a tyrosine to alanine substitution in the C-terminal tail region of MDM2 ($MDM2^{Y487A}$) are viable, phenotypically normal, and born at expected Mendelian ratios (Tollini et al., 2014). In this study, *Eμ-Myc* mice were crossed with $Mdm2^{Y487A/Y487A}$ mice to obtain *Eμ-Myc;*$Mdm2^{Y487A/Y487A}$ mice. Similar to $Mdm2^{Y487A/Y487A}$ mice, *Eμ-Myc;*$Mdm2^{Y487A/Y487A}$ mice were born at expected ratios (data not shown). It has been observed that $Mdm2^{Y487A/Y487A}$ mice present with slightly lower body weight than *WT* mice. In the presence of the *Eμ-Myc* transgene, both male and female *Eμ-Myc;*$Mdm2^{Y487A/Y487A}$ mice also weigh slightly less than their WT counterparts (Figure 5.1).

Previous work has shown that acute DNA damage stress that is sub lethal in WT mice induces lethality in $Mdm2^{Y487A/Y487A}$ mice. Although $Mdm2^{Y487A/Y487A}$ mice live normal lifespans compared to *WT* mice, in the presence of the *Eμ-Myc* transgene, it appears that the $MDM2^{Y487A}$

mutation significantly increased average survival compared to mice with WT MDM2 (Figure 5.2). Interestingly, although *Eμ-Myc;Mdm2*$^{Y487A/Y487A}$ mice develop lymphomas with 100% penetrance, the survival extension does not appear to have a high penetrance, as about half of *Eμ-Myc;Mdm2*$^{Y487A/Y487A}$ mice appear to succumb to lymphoma at the same rate as WT mice. As a result, there is not a large difference in the median survival time between the two genotypes (98.5 days for *Eμ-Myc;Mdm2*$^{+/+}$ mice versus 107.0 days for *Eμ-Myc;Mdm2*$^{Y487A/Y487A}$ mice), but intriguingly ~50% of *Eμ-Myc;Mdm2*$^{Y487A/Y487A}$ mice display significant lifespan extension compared to *Eμ-Myc;Mdm2*$^{+/+}$ mice (Figure 5.2).

MDM2^{Y487A} mice demonstrate increased basal p53 stability along with increased p53 stability and activity in response to stress (Tollini et al., 2014). In order to explore the reason for the differences in lifespan before and after the median survival times of *Eμ-Myc;Mdm2*$^{+/+}$ and *Eμ-Myc;Mdm2*$^{Y487A/Y487A}$ mice, p53 levels and activity were examined in various tissues isolated from the mice both before and after the onset of lymphoma symptoms.

First, spleens from 8 week old mice of each genotype were harvested. Splenomegaly is a common feature in *Eμ-Myc* mice and is indicative of increased B-cell lymphoma infiltration. Prior to the onset of lymphoma symptoms, there appears to be no difference in spleen size between *Eμ-Myc;Mdm2*$^{+/+}$ and *Eμ-Myc;Mdm2*$^{Y487A/Y487A}$ mice (Figure 5.3a). In addition, there appears to be little difference in p53 protein levels at this age (Figure 5.3b). However, there appears to be a slight increase in p21 expression (indicative of increased p53 activity) in *Eμ-Myc;Mdm2*$^{Y487A/Y487A}$ mice compared to their *Eμ-Myc;Mdm2*$^{+/+}$ counterparts.

Next, thymus and lymph node tissue from these mice were examined. At 8 weeks of age, there did not appear to be any gross morphological differences between the two genotypes. Unexpectedly, average p53 protein levels appeared to be greater in in both tissues examined from *Eμ-Myc;Mdm2*$^{+/+}$ compared to *Eμ-Myc;Mdm2*$^{Y487A/Y487A}$ mice (Figure 5.4). On the other hand, p21 levels appeared to be increased in *Eμ-Myc;Mdm2*$^{Y487A/Y487A}$ mice compared to *Eμ-Myc;Mdm2*$^{+/+}$ mice, possibly indicating that the increased p53 protein levels observed in

select *Eμ-Myc;Mdm2*$^{+/+}$ mice could be due to p53 mutation, which has been shown to be stabilized in cancerous cells (Lang et al., 2004; Olive et al., 2004). At the same time, thymic tissue isolated from *Eμ-Myc;Mdm2*$^{Y487A/Y487A}$ mice appeared to have greater cleaved caspase-3 (CC-3) staining than *Eμ-Myc;Mdm2*$^{+/+}$ mice, indicating increased levels of apoptosis, which is often correlated with p53 activity. On the other hand, the opposite trend was present in lymph tissue, with *Eμ-Myc;Mdm2*$^{+/+}$ tissue displaying higher CC-3 levels (Figure 5.4). The reason for this discrepancy is currently unclear.

Loss of MDM2 E3 ligase function allows for increased c-MYC-induced p53 stabilization

To determine whether loss of MDM2 E3 ligase function could allow for increased p53 stabilization and activation in a cell-based system, *WT* and *Mdm2*$^{Y487A/Y487A}$ MEFs were infected with retrovirus expressing c-MYC or a pBABE vector (Figure 5.5). As expected, c-MYC overexpression promoted p19ARF expression and p53 stabilization in WT MEFs. Despite the inability of MDM2^{Y487A} to degrade p53, further stabilization of p53 was also observed upon c-MYC overexpression in *Mdm2*$^{Y487A/Y487A}$ MEFs. It has been previously shown that prolonged DNA damage further increases the stabilization of p53 in *Mdm2*$^{Y487A/Y487A}$ MEFs, likely due to a combination of the inability of MDM2^{Y487A} to degrade p53 and stress-induced increased p53 transcription and translation (Tollini et al., 2014). Compared to *WT* MEFs, *Mdm2*$^{Y487A/Y487A}$ MEFs demonstrate elevated p53 levels basally and upon c-MYC overexpression. However, the ratio of p53 protein level increase between basal and after c-MYC expression appears to be similar between the two genotypes (3.40 fold vs 3.98 fold). It is possible that with prolonged exposure to c-MYC, p53 levels in *Mdm2*$^{Y487A/Y487A}$ MEFs could continue to rise beyond that of *WT* MEFs, as has been shown to occur in the presence of DNA damage. Although it has been previously shown that *Mdm2*$^{Y487A/Y487A}$ MEFs express increased basal p53 protein levels compared to *WT* MEFs, upon the introduction of c-MYC, p53 activity does not appear to be different between the two genotypes, as indicated by similar MDM2 expression.

Following the onset of lymphoma symptoms, including enlarged lymph nodes, hunched posture, slow movement, and irregular breathing (Harris et al., 1988), tissues were harvested from age-matched mice to assess p53 stability and activity by Western blot. In spleen tissue, average p53 protein levels and activity were slightly higher in *Eμ-Myc;Mdm2*$^{Y487A/Y487A}$ mice (Figure 5.6), while in lymph nodes p53 protein levels are more clearly elevated in *Eμ-Myc;Mdm2*$^{Y487A/Y487A}$ mice compared to *Eμ-Myc;Mdm2*$^{+/+}$ mice (Figure 5.7). In addition, elevated MDM2 protein levels indicate increased p53 activity in lymph tissue (Figure 5.7). Thymic tissue demonstrated a similar phenotype, as average p53 and MDM2 levels appeared to be increased in *Eμ-Myc;Mdm2*$^{Y487A/Y487A}$ mice (Figure 5.8). Despite p53 stabilization in these tissues, changes p21 and CC-3 levels were less obvious, indicating the possibility that p53 targets may be differentially induced.

In order to further evaluate p53 activity in *Eμ-Myc;Mdm2*$^{Y487A/Y487A}$ mice following lymphoma development, qPCR analysis was performed. As expected, in spleen and lymph tissue, there appeared to be no change in p53 mRNA transcription (Figure 5.9), which suggests that changes in p53 protein levels are likely due to changes in protein stability or translation. In addition, p53-mediated transcription of several target genes, including *mdm2*, *bax*, and *apaf1*, is significantly upregulated in spleens from *Eμ-Myc;Mdm2*$^{Y487A/Y487A}$ mice compared to *Eμ-Myc;Mdm2*$^{+/+}$ mice. In lymph tissue, *mdm2* and *p21* transcription also appear to be elevated, but this difference is not statistically significant. Together these data suggest the possibility that the increased survival of *Eμ-Myc;Mdm2*$^{Y487A/Y487A}$ mice following lymphoma is because of increased p53 stability, allowing for increased p53 tumor suppressive activity. However, further analyses will be required to make more definitive conclusions.

DISCUSSION & FUTURE DIRECTIONS

Loss of MDM2 function allows for increased survival during c-MYC-induced lymphomagenesis

It is clear that the loss of MDM2 E3 ligase activity correlates with increased survival in a subset of mice overexpressing c-MYC (Figure 5.2). However, the reason for this increased survival is still unclear, and significantly more analyses are needed to elucidate this mechanism from several potential causes.

First, it is possible that loss of MDM2 E3 ligase activity and MDM2-mediated p53 degradation allows for low level increases in p53 stability and activity that benefit a subset of mice. Although this is not clear from the preliminary data, there are some indications that this may be the case, including the increased transcription of p53 target genes in spleen tissue of *Eμ-Myc;Mdm2*$^{Y487A/Y487A}$ mice, which has a large population of B cells (Figure 5.9). It will be important to compare tissues from *Eμ-Myc;Mdm2*$^{+/+}$ and *Eμ-Myc;Mdm2*$^{Y487A/Y487A}$ mice to mice lacking the *Eμ-Myc* transgene to determine whether p53 is truly differentially activated or stabilized. Although there are indications that loss of MDM2 E3 ligase activity could allow for increased p53 stability and activity in some tissues, there appears to be significant heterogeneity between *Eμ-Myc*-expressing mice. In order to extrapolate further, it will be necessary to analyze more samples. It will also be essential to analyze tumor growth, senescence, and apoptotic rates in *Eμ-Myc;Mdm2*$^{+/+}$ and *Eμ-Myc;Mdm2*$^{Y487A/Y487A}$ mice in order to determine if the MDM2^{Y487A} mutation correlates with decreased tumor growth and increased senescence or apoptosis, both of which are indicative of increased p53 activity.

Second, it is possible that p19ARF loss, which is common in *Eμ-Myc* mice (Eischen et al., 1999), may occur at different rates in these mice, possibly due to changes in the feedback loop of p53 to p19ARF signaling. It has been shown that p53 activation results in the downregulation of p19ARF through unknown mechanisms. It is possible that in *Eμ-Myc;Mdm2*$^{Y487A/Y487A}$ mice, increased p53 activity could cause p19ARF levels to be slightly reduced compared to *Eμ-Myc;Mdm2*$^{+/+}$ (prior to potential p19ARF deletion). Reducing p19ARF

expression could lessen oncogenic pressure for p19ARF deletion while still allowing for some p19ARF-mediated tumor suppressive functions. It is possible that p19ARF deletion occurs less frequently in *Eμ-Myc;Mdm2*$^{Y487A/Y487A}$ mice, allowing for increased latency to tumor formation. Analysis of p19ARF status in these mice will be critical to determine whether p19ARF signaling could be differentially regulated in the presence of the MDM2^{Y487A} mutation.

Third, it is possible that the loss of MDM2 E3 ligase could through unknown mechanisms bias oncogenic pressure against p53 deletion or mutation; however, this mechanism seems unlikely. For example, it has been previously shown that cell lines chronically treated with nutlin-3, a potent inhibitor of MDM2-p53 binding and non-genotoxic activator of p53, develop resistance to this drug and exhibit elevated rates of p53 mutation compared to vehicle treated cells (Aziz et al., 2011). This suggests that increased p53 stability and activity, which typically results in cell death or growth arrest, likely drives selection of p53 inactivation in cancer cells. This effect has also been observed in cancer patients with WT p53, who upon undergoing p53-activating chemotherapies acquire both resistance to the chemotherapy and either p53 deletion or mutation (Christiansen et al., 2001; Leonard et al., 2002). Disrupting MDM2 E3 ligase activity has been shown to allow for increased p53 protein stability and activity in response to DNA damage (Tollini et al., 2014). Thus, it is more likely that MDM2^{Y487A} mutation would bias p53 towards deletion or mutation, which could feasibly lead to decreased overall survival of *Eμ-Myc;Mdm2*$^{Y487A/Y487A}$ mice compared to *Eμ-Myc;Mdm2*$^{+/+}$ mice, which is the opposite of the observed survival phenotype. To investigate this possibility, the p53 mutational status of the tissues examined in this study will need to be determined.

Stress-specific necessity of MDM2 E3 ligase activity

The longer lifespan of *Eμ-Myc;Mdm2*$^{Y487A/Y487A}$ mice compared to *Eμ-Myc;Mdm2*$^{+/+}$ mice does support certain conclusions pertaining to stress-related p53 regulation. First, while it is clear that MDM2 E3 ligase activity is necessary for *in vivo* p53 regulation following acute, sub

lethal DNA damage-induced stress (Tollini et al., 2014), it is dispensable to organismal survival in the presence of chronic oncogenic stress. In fact, loss of MDM2 E3 ligase function appears to provide a survival advantage in this situation.

The reason for this differential necessity for MDM2 E3 ligase activity is likely due to the intensity and location of the stress. In the case of acute DNA damage, p53 is rapidly stabilized. Although c-MYC overexpression is capable of inducing a p53-dependent apoptotic program in cells (Hermeking and Eick, 1994), transgenic c-MYC overexpression in the mouse likely promotes p53 stabilization more slowly than irradiation. In addition, the sub lethal IR treatment described in the first study of the MDM2^{Y487A} mouse was a whole body treatment, while the *Eμ-Myc* transgene is only expressed in B cells (Harris et al., 1988; Tollini et al., 2014). While undue p53 activation throughout the body clearly causes lethality (de Oca Luna et al., 1995; Jones et al., 1995; Ringshausen et al., 2006), in the absence of extrinsic apoptotic stress to other tissues p53-mediated B cell death is unlikely to promote organismal demise. For example, patients undergoing chimeric antigen receptor (CAR) T cell therapy commonly (and intentionally) ablate B cells (Kochenderfer and Rosenberg, 2013). In the presence of chronic stress, it is also possible that other p53-regulating proteins could cooperate towards regulating p53 stability. Although it remains clear that MDM2 is the primary E3 ubiquitin ligase for p53, other E3 ubiquitin ligases targeting p53 have been described (Dornan et al., 2004; Leng et al., 2003). It is possible that during acute stress, MDM2-mediated p53 degradation is required to rapidly bring p53 to safe levels following resolution of the stress to prevent organismal death. On the other hand, in the presence of chronic oncogenic stress, it is possible that p53 is not stabilized to these same levels that require MDM2 E3 ligase activity, which would allow for p53 to be degraded by other E3 ligases instead. It will be important to determine whether p53 is still degraded in *Eμ-Myc;Mdm2*$^{Y487A/Y487A}$ mice. Although much work remains to be done, these preliminary data are encouraging towards demonstrating a stress-specific role for MDM2 E3 ligase activity in p53 regulation.

EXPERIMENTAL PROCEDURES

Mouse experiments

All mice were bred and maintained on a 12 h light and dark cycle. *Mdm2*^{Y487A} mutant mice were generated as previously described (Tollini et al., 2014). To generate *Eμ-Myc;Mdm2*$^{Y487A/Y487A}$ mice, *Eμ-Myc* male mice were bred with *Mdm2*$^{Y487A/Y487A}$ female mice. The resultant *Eμ-Myc;Mdm2*$^{Y487A/+}$ or *Eμ-Myc;Mdm2*$^{Y487A/Y487A}$ male mice were then bred with *Mdm2*$^{Y487A/Y487A}$ female mice. *Eμ-Myc* mice on C57BL/6 J background were purchased from The Jackson Laboratory (Bar Harbor, ME, USA) (stock number 002728). For survival studies, mice were examined regularly for early signs of lymphoma and monitored for tumor progression and signs of morbidity. Moribund mice were humanely euthanized. All mice were handled in strict accordance with protocols approved by the Institutional Animal Care and Use Committee at The University of North Carolina at Chapel Hill.

Protein analysis

For western blotting, proteins were extracted from tissues as previously described (Liu et al., 2016a). Briefly, mouse tissue was homogenized and lysed in 0.5% NP-40 lysis buffer. Proteins were detected using either ECL and Dura enhanced chemiluminescence systems (Thermo Scientific, SuperSignal West Dura Substrate). The following primary antibodies were used: mouse monoclonal anti-p53 (PAb 122, Thermo Scientific), mouse monoclonal anti-MDM2 (2A10, homemade), and rabbit polyclonal anti p19ARF (Ab80, Abcam) Rabbit polyclonal antibodies to p21 were gifts from Dr. Yue Xiong (University of North Carolina at Chapel Hill, Chapel Hill, NC).

Quantitative PCR

Total RNA was prepared from mouse tissues using QuickRNA™ MiniPrep Kit (Zymo Research, Irvine, CA, USA, #11-328). RNA concentration was determined using a NanoDrop spectrophotometer (Thermo Scientific, Waltham, MA, USA, NanoDrop 2000c). Complementary DNA was synthesized using iScript™ DNA Synthesis Kit (Bio-Rad, Hercules, CA, USA, #1708889). qPCR was performed with SYBR Green probes using the Applied Biosystems (Carlsbad, CA, USA) 7900HT Fast Real-Time PCR system. Thermal cycling conditions were 50 °C for 2 min, 95 °C for 5 min, followed by 40 cycles of 95 °C for 15 s and 60 °C for 1 min. Target gene transcript levels were normalized to *gapdh* transcript levels obtained in each sample via the subtraction of the Ct value of *gapdh* from the Ct value for each target gene. Results were expressed as the fold-change in transcript levels. Primers used for qPCR were as follows: *gapdh*, 5'-GAAAGCTGTGGCGTGATGG-3' and 5'-AGTGAGCTTCCCGTTCAGC-3'; *p53*, 5'-TGAACCGCCGACCTATCCTTA-3' and 5'-GGCACAAACACGAACCTCAAA-3'; *mdm2*, 5′-TGTGTGAGCTGAGGGAGATG-3′ and 5′-CACTTACGCCATCGTCAAGA-3'; *p21*, 5'-TCCACAGCGATATCCAGACA-3' and 5'-AGACAACGGCACACTTTGCT-3'; *bax*, 5'-GGACAGCAATATGGAGCTGCAGAGG-3' and 5'-GGAGGAAGTCCAGTGTCCAGCC-3'; *apaf1*, 5'- CGGTGAAGGTTGTGGAATGTCATTACCG-3' and 5'-GGATTTCTCCATTGTCATCTCCAGTTGC-3'; *tigar*, 5'-CGATCTCACGAGGACTAAGCAGACC-3' and 5'-GCGCCATGGCTCACAACTAAGATGC-3'.

Cell culture

Primary MEFs were isolated on embryonic (E) day 13.5 and grown in a 37°C incubator with 5% CO_2 in Dulbecco's modified Eagle's medium supplied with 10% fetal bovine serum and penicillin-streptomycin. For retroviral infections, *WT*, and *Mdm2*$^{Y487A/Y487A}$ MEFs were infected with retroviruses expressing c-MYC or pBabe control vector, and selected with puromycin (2.5

μg/ml) for 3 days. Infected MEFs were then allowed to recover for 48 h before harvesting for analysis.

Statistical analysis

Statistical analysis was carried out using GraphPad Prism 5 Software (GraphPad Software). Kaplan-Meier survival curves were generated to assess lifespan. Quantitative PCR data are represented as mean ±SEM, and were analyzed by the Student's *t* test.

Ethics statement

This investigation has been conducted in accordance with ethical standards, the Declaration of Helsinki, national and international guidelines, and has been approved by the authors' institutional review board.

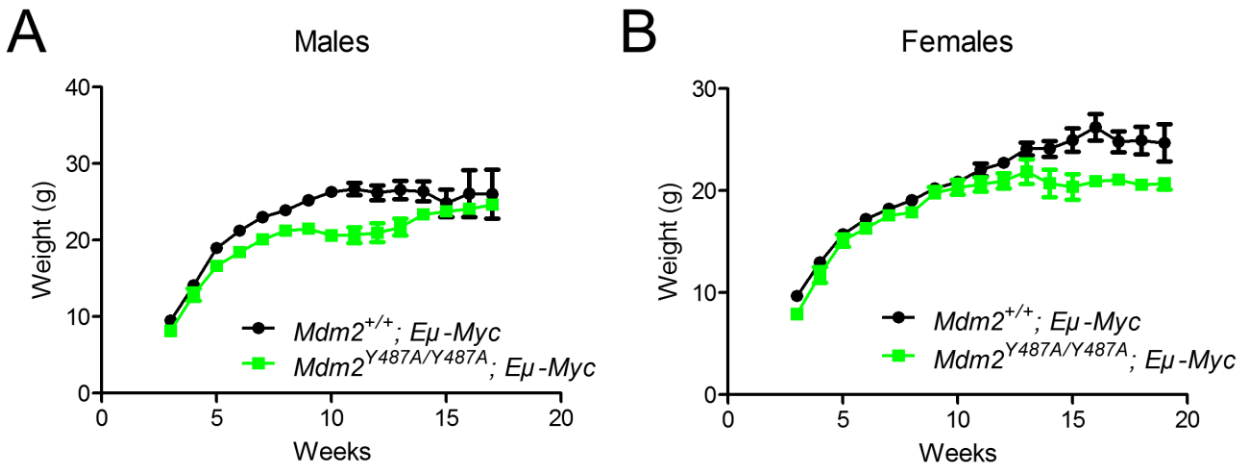

Figure 5.1 MDM2^{Y487A} mutation correlates with slightly lower body weight
Eμ-Myc;Mdm2$^{+/+}$ male (n=21) and female (n=21) as well as *Eμ-Myc;Mdm2*$^{Y487A/Y487A}$ male (n=16) and female (n=13) mice were weighed and observed weekly. Data represent means ±SEM.

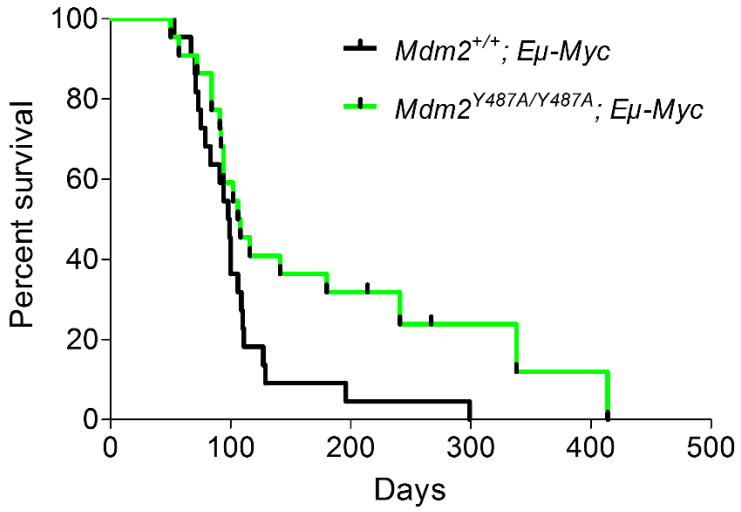

Figure 5.2 Disruption of MDM2 E3 ligase activity prolongs survival during c-MYC-induced lymphomagenesis.

Kaplan-Meier survival curves for *Eμ-Myc;Mdm2*$^{+/+}$ (n=22) and *Eμ-Myc;Mdm2*$^{Y487A/Y487A}$ (n=22) mice are shown. There was a significant difference between survival curves for *Eμ-Myc;Mdm2*$^{+/+}$ and *Eμ-Myc;Mdm2*$^{Y487A/Y487A}$ mice (analyzed by log-rank test; P=0.0255).

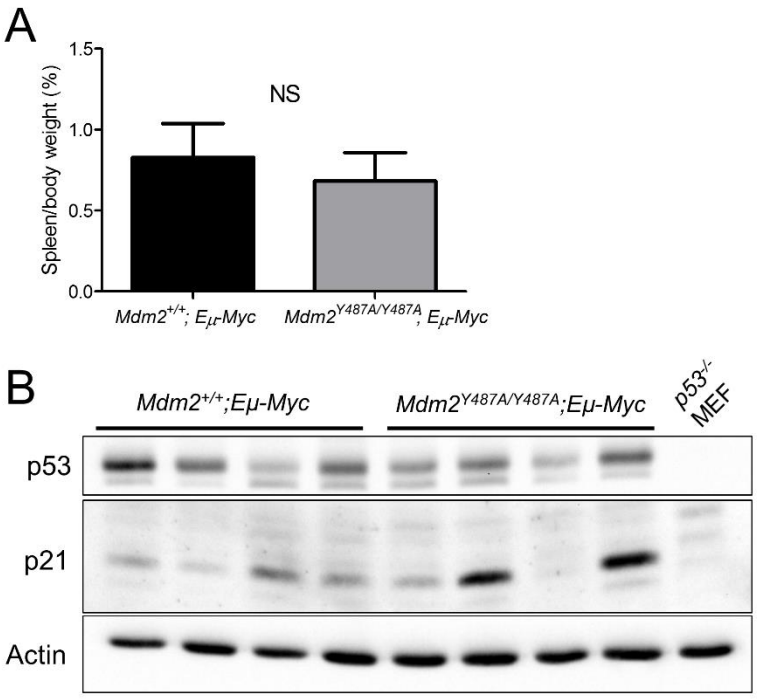

Figure 5.3 *Eμ-Myc;Mdm2$^{Y487A/Y487A}$* spleens do not display increased p53 stabilization prior to lymphoma development

A. Spleens from 8 week old *Eμ-Myc;Mdm2$^{+/+}$* (n=4) and *Eμ-Myc;Mdm2$^{Y487A/Y487A}$* (n=4) mice were harvested, weighed, and normalized to body weight. Data are represented as mean ±SEM. NS means no significant difference.

B. Spleens from 8 week old *Eμ-Myc;Mdm2$^{+/+}$* (n=4) and *Eμ-Myc;Mdm2$^{Y487A/Y487A}$* (n=4) mice were harvested and analyzed by WB.

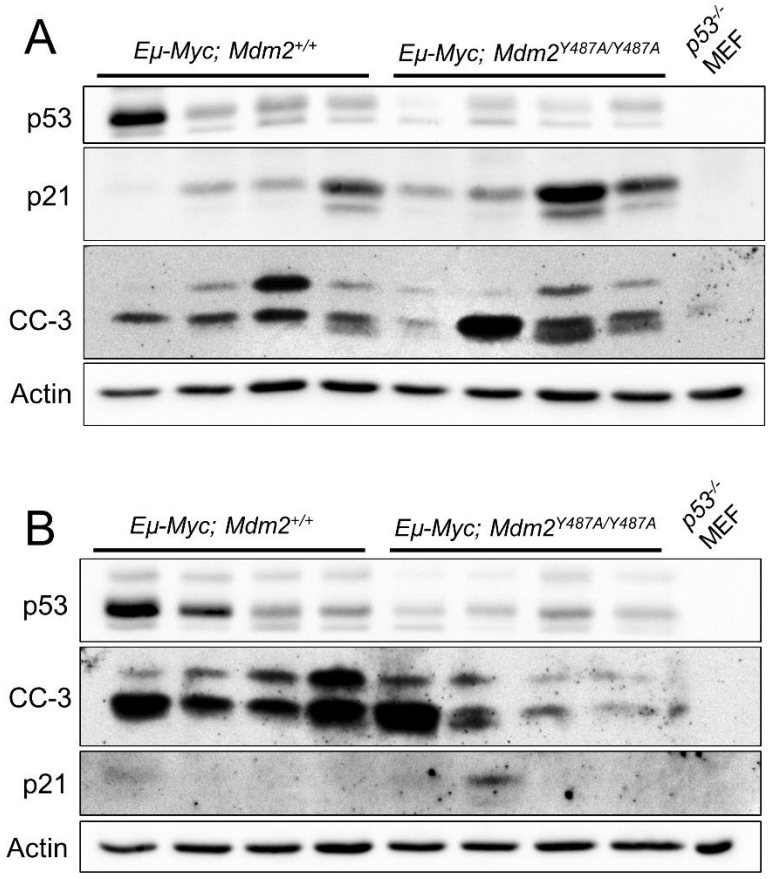

Figure 5.4 *Eμ-Myc;Mdm2*$^{Y487A/Y487A}$ thymic tissue and lymph nodes do not display increased p53 stabilization prior to lymphoma development.

A. Thymic tissue from 8 week old *Eμ-Myc;Mdm2*$^{+/+}$ (n=4) and *Eμ-Myc;Mdm2*$^{Y487A/Y487A}$ (n=4) mice were harvested and analyzed by WB.

B. Lymph nodes from 8 week old *Eμ-Myc;Mdm2*$^{+/+}$ (n=4) and *Eμ-Myc;Mdm2*$^{Y487A/Y487A}$ (n=4) mice were harvested and analyzed by WB.

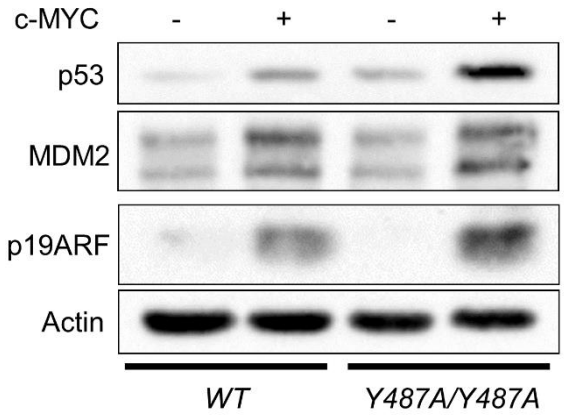

Figure 5.5 *Mdm2*$^{Y487A/Y487A}$ MEFs display increased p53 stabilization following c-MYC overexpression

WT and *Mdm2*$^{Y487A/Y487A}$ MEFs were infected with retrovirus containing either c-MYC (+) or a pBABE vector (-). Following infection, the cells were selected with puromycin and then harvested for analysis by western blot.

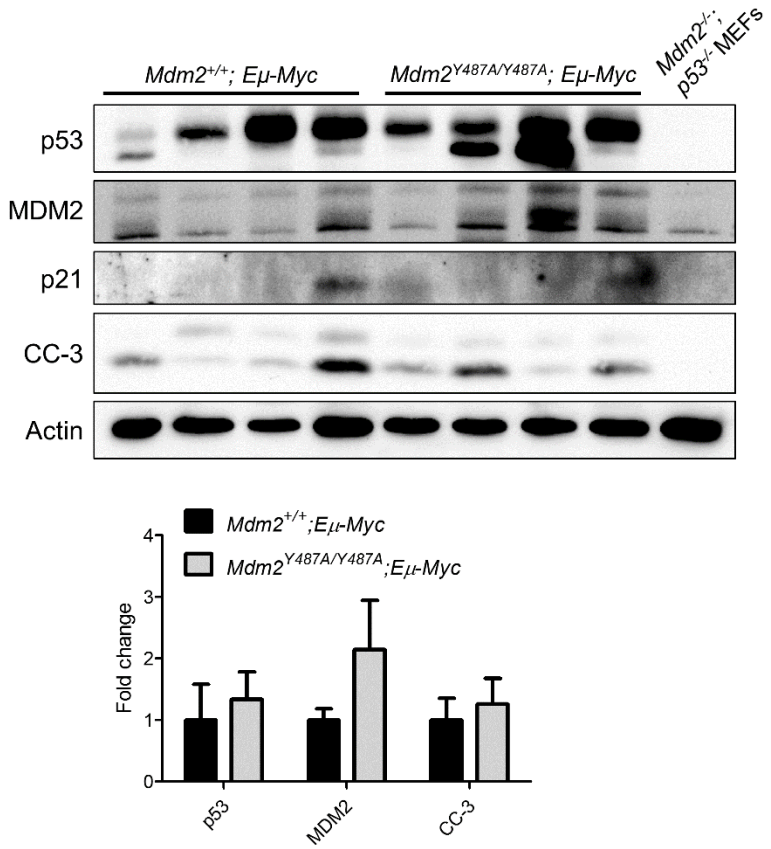

Figure 5.6 Following lymphoma onset, spleens isolated from *Eμ-Myc;Mdm2*$^{Y487A/Y487A}$ mice display increased p53 stability.

Spleens from age-matched *Eμ-Myc;Mdm2*$^{+/+}$ (n=4) and *Eμ-Myc;Mdm2*$^{Y487A/Y487A}$ (n=4) mice with symptoms of lymphoma were harvested and analyzed by WB. Quantification of protein levels relative to *Eμ-Myc;Mdm2*$^{+/+}$ mice is shown below the blot.

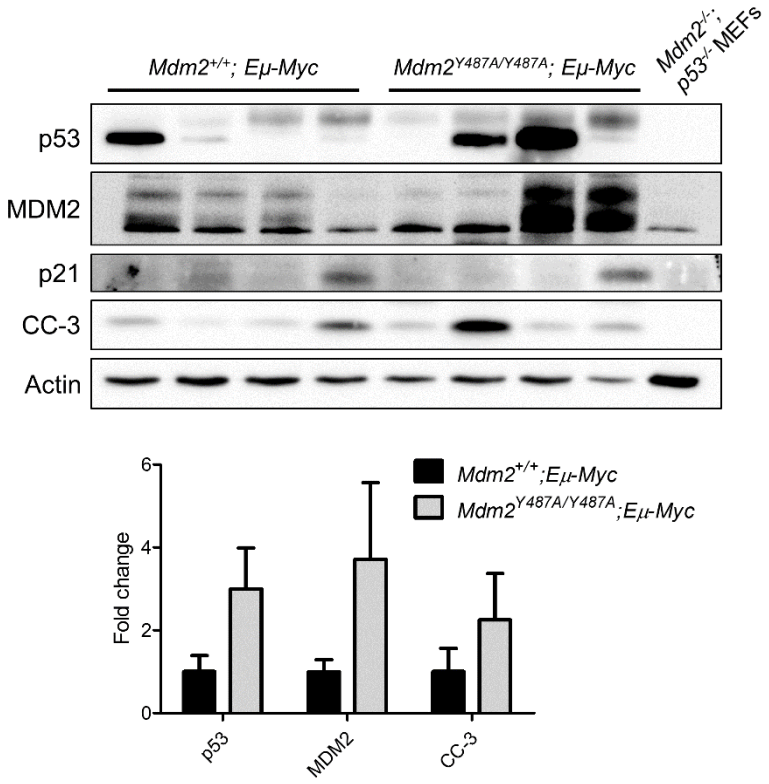

Figure 5.7 Following lymphoma onset, lymph nodes isolated from *Eμ-Myc;Mdm2*$^{Y487A/Y487A}$ mice display variable p53 stability.

Lymph nodes from age-matched *Eμ-Myc;Mdm2*$^{+/+}$ (n=4) and *Eμ-Myc;Mdm2*$^{Y487A/Y487A}$ (n=4) mice with symptoms of lymphoma were harvested and analyzed by WB. Quantification of protein levels relative to *Eμ-Myc;Mdm2*$^{+/+}$ mice is shown below the blot.

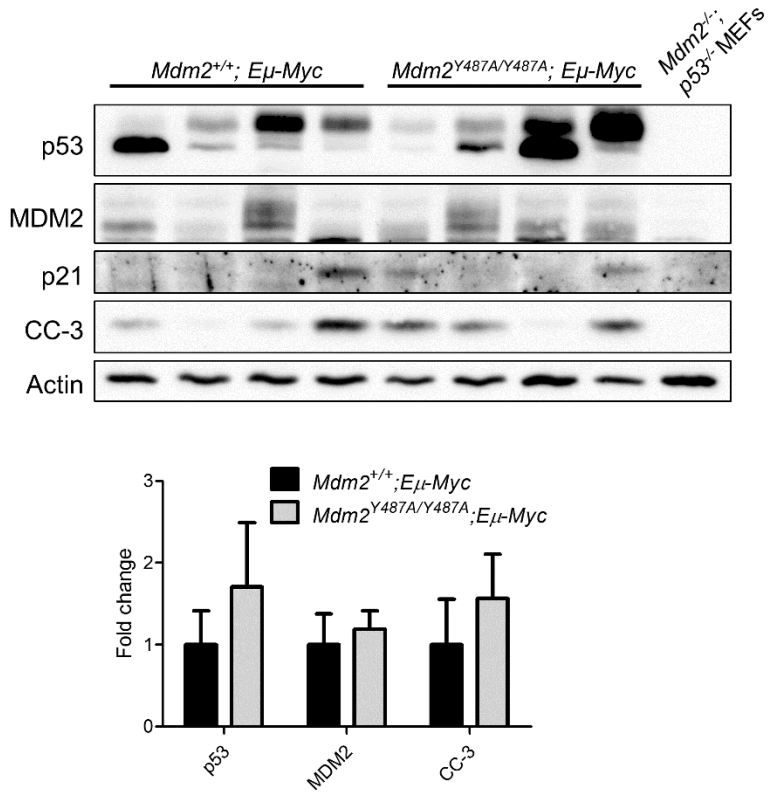

Figure 5.8 Following lymphoma onset, thymi isolated from *Eμ-Myc;Mdm2$^{Y487A/Y487A}$* mice display slightly increased p53 stability.

Thymic tissue from age-matched *Eμ-Myc;Mdm2$^{+/+}$* (n=4) and *Eμ-Myc;Mdm2$^{Y487A/Y487A}$* (n=4) mice with symptoms of lymphoma were harvested and analyzed by WB. Quantification of protein levels relative to *Eμ-Myc;Mdm2$^{+/+}$* mice is shown below the blot.

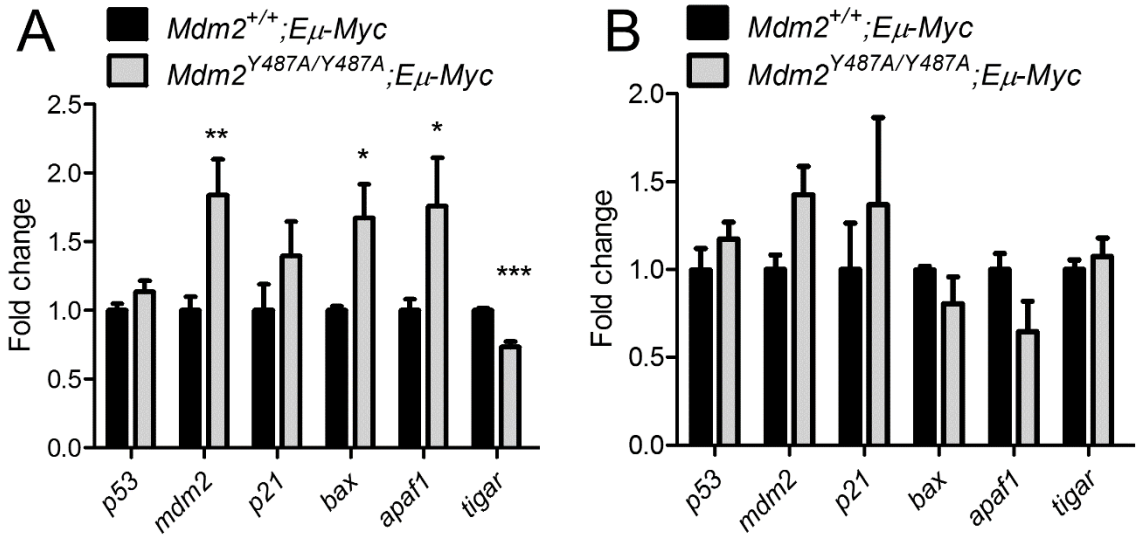

Figure 5.9 Following lymphoma onset, *Eμ-Myc;Mdm2*$^{Y487A/Y487A}$ mice display slightly increased p53 activity in spleen but not lymph node tissue.

A. Spleens from age-matched *Eμ-Myc;Mdm2*$^{+/+}$ (n=4) and *Eμ-Myc;Mdm2*$^{Y487A/Y487A}$ (n=4) mice with symptoms of lymphoma were harvested and analyzed by qPCR. Data are represented as mean ±SEM. *, P<0.05; **, P<0.01; ***, P<0.001.

B. Lymph nodes from age-matched *Eμ-Myc;Mdm2*$^{+/+}$ (n=4) and *Eμ-Myc;Mdm2*$^{Y487A/Y487A}$ (n=4) mice with symptoms of lymphoma were harvested and analyzed by qPCR. Data are represented as mean ±SEM.

CHAPTER 6: CONCLUSIONS AND FUTURE DIRECTIONS

Though p53 continues to be one of the most well-studied proteins due to its wide-ranging stress-response functions, our understanding of p53 and its regulation is continuously evolving. These changes in our understanding are in part due to the progression of *in vivo* modeling, which has allowed us to delineate the physiologically relevant conditions contributing to p53-mediated activation and tumor suppression.

It has been clearly demonstrated that MDM2 and MDMX are master regulators of p53 (Wade et al., 2010). It is also known that many upstream signals contribute to inhibition of MDM2 and/or MDMX to allow for p53 stabilization and activation, including p19ARF and RPs. However, mapping the relative contributions of these upstream signals to the inhibition of MDM2 or MDMX has been a difficult challenge within the field. Further, determining the signals that reestablish p53 inhibition following its activation will be important towards understanding p53 biology. The characterization of the $MDM2^{C305F}$ mouse has allowed for numerous advances in our understanding of RP-MDM2-p53 regulation in the presence of cancer-inducing transgenes. Meanwhile, the $MDM2^{Y487A}$ mouse has allowed us to further understand p53 regulation following the resolution of stress.

Evolving views of the RP-MDM2-p53 pathway in tumor prevention

RPs work independently of p19ARF to inhibit MDM2

Ribosomal biogenesis is a highly-coordinated process in which small perturbations can have big consequences. RPs have been shown to inhibit MDM2 E3 ligase activity in the presence of nucleolar and oncogenic stresses, which contributes to p53 stabilization and activation. Although it has been demonstrated *in vitro* that approximately 16 RPs bind to MDM2

(Liu et al., 2016b), very few of these interactions have been examined *in vivo*. The MDM2^{C305F} mouse was the first (and so far only) *in vivo* model to disrupt RP-MDM2 interaction without directly altering RPs, and this mouse demonstrated that RP-MDM2 signaling was critical for tumor prevention driven by c-MYC (Macias et al., 2010). However, the general heterogeneity of cancer and tumor driver signaling warrants further exploration of RP-MDM2-p53-mediated tumor prevention.

In response to c-MYC overexpression, both p19ARF and RPs bind to MDM2 and inhibit its ubiquitination of p53 (Eischen et al., 1999; Macias et al., 2010). Meanwhile, p19ARF regulates ribosomal biogenesis at multiple steps (Lessard et al., 2010; Saporita et al., 2011; Sugimoto et al., 2003). These findings allowed for the possibility that p19ARF contributes to p53 activation via disrupting ribosomal biogenesis and facilitating RP-mediated MDM2 inhibition. The work presented here demonstrates that this is not the case. Specifically, Chapters 2 and 3 show that RP-MDM2 binding is not dependent on the presence of p19ARF in its ability to regulate p53 and prevent tumorigenesis. This is principally demonstrated by reduced latency to death upon concomitant RP-MDM2 interaction disruption and p19ARF deletion (Figure 2.3). However, this work does not completely rule out the possibility that p19ARF-mediated regulation of ribosomal biogenesis enhances its p53-activating functions.

This work further explored the relative necessity of either RP or p19ARF signaling towards p53 activation, which appears to be dependent on the upstream oncogenic signal. For example, in the presence of the *Eμ-Myc* transgene, disruption of either p19ARF-MDM2 or RP-MDM2 interaction resulted in early tumorigenesis (Eischen et al., 1999; Macias et al., 2010), while concomitant disruption further increased the speed of tumor formation (Figure 2.3). In contrast, *Hras*^{G12V} transgene overexpression only allowed for tumor formation in the absence of p19ARF, but not upon RP-MDM2 binding disruption (Figure 3.1). This work confirms that p19ARF signaling through MDM2 is critical for p53 activation in the context of *Eμ-Myc* and *Hras*^{G12V} transgenic overexpression. In contrast, work presented here and published by others

has indicated that p19ARF is not required for p53-mediated activation and tumor suppression in all contexts. In the presence of the *Apc*^{Min} allele, RP-MDM2 interaction appears to serve a more protective role than p19ARF-MDM2 interaction, as p19ARF deletion does not alter APC-loss induced tumorigenesis (Gibson et al., 2005), while loss of RP-MDM2 interaction increases colon tumor formation (Figure 4.3). Together, these studies solidify the notion that though p19ARF regulates ribosomal biogenesis and participates in p53 regulation, these likely represent two independent MDM2-regulating protein interactions.

RP expression and RP-MDM2 interaction is differentially regulated by upstream signals

Ribosomal proteins are often upregulated in cancer. It has been previously shown that that the c-MYC oncogene is a master regulator of ribosomal biogenesis and RP protein expression, but the work presented here also demonstrates that RPs are upregulated in response to other oncogenic drivers. Specifically, this work shows that RPL23, but not RPL11 or RPL5, is upregulated in response to HRAS^{G12V} overexpression (Figure 3.6-8). To my knowledge, this work is the first report of a RAS-upregulated ribosomal protein. Interestingly, the regulation of RPL23 by RAS occurs both through increased *rpl23* transcription (Figure 3.7), and mTOR-dependent translation (Figure 3.12). RPL11 and RPL5 are also transcriptionally upregulated in APC-loss-induced colon tumors (Figure 4.3).

It is important to recognize that oncogenic signals do not occur in isolation. For example, some activating RAS mutations have been shown to contribute to c-MYC stabilization, further facilitating cancer progression (Sears et al., 1999; Sears et al., 2000). It is therefore likely that c-MYC signaling is also altered in the context of *Hras*^{G12V} transgene expression, possibly contributing to the differential RPL23 protein production. It is also unsurprising that RPs would be upregulated in APC-loss-induced tumors (Figure 4.3), given that c-MYC has been shown to be an important driver of cancer in these tumors (Sansom et al., 2007).

There are some indications that tissue specific RP-regulation occurs, though it is difficult to make direct comparisons between the models used in these studies. For example, in the presence of the *Apc*^{Min} allele, which induces tumor formation throughout the intestinal tract upon loss of APC heterozygosity, ribosomal protein RPL11 and RPL5 expression were increased in colon tumor tissue, but not in small intestinal tumor tissue (Figure 4.8). From this, it is possible to speculate that local tissue signaling dictates RP expression and RP-MDM2 interaction, even in the presence of the same driver mutation. This result is particularly meaningful in the context of human cancers. In humans, deletion of the *Apc* gene is the cause of a familial disorder linked to increased colorectal tumor formation, and the *Apc*^{Min} mouse models this deletion. Interestingly, *Apc*^{Min} mice develop small intestinal tumors with almost 100% penetrance, but small intestinal tumors are relatively rare in humans, even in the presence of *Apc* deletion (Pan and Morrison, 2011). However, it is particularly interesting that the presence of the MDM2^{C305F} mutation accelerates colon tumor formation in *Apc*^{Min} mice, as in combination with the tissue-specific induction of RPL11 and RPL5, this indicates that RP-MDM2-p53 signaling may be a more important modulator of colon tumor progression than what had been previously appreciated. Importantly, as RPs are abundantly expressed in almost all cells, this also suggests that upstream signaling dictates when and where RP-MDM2 interactions occur, and the degree to which they alter p53 signaling.

This work also contributes to the well-supported notion that MDM2 requires different signals to inhibit p53 during the presence of specific stimuli. Ribosomal proteins are present in almost all cell types, and though in the context of protein translation it is likely that they are acting similarly, it is possible that free RPs interact with MDM2 in a stress-specific manner. For instance, in RAS-expressing MEFs, both p19ARF and RPL23 were required for MDM2 inhibition (Figure 3.14), while RPL11 and RPL5 contributed to MDM2 inhibition in colon tissues bearing APC deletion (Figures 4.9-10). It is unknown why multiple RPs bind to MDM2. From these

studies, it is possible to speculate that individual RPs may respond either to unique oncogenic signals or in a tissue dependent manner to confer varying degrees of p53 stabilization.

Further investigation will be required to parse out the specific signals dictating differential RP-MDM2-p53 signaling. Although much work remains to be done in order to fully understand the contexts for RP-mediated p53 regulation, the MDM2^{C305F} mouse model remains a useful tool for characterizing the circumstances under which RPL5/RPL11-MDM2 interaction is required.

Relative necessity of MDM2 E3 ligase activity towards p53 regulation

In addition to altering our perception about how p53 is activated in response to oncogenic stress, this work has also contributed to our understanding about how p53 is regulated following the resolution of stress. Previously held views in the field advocated that MDM2-mediated p53 ubiquitination/degradation is important for preventing lethal p53 activation, and this idea is well-supported by *in vitro* studies (Haupt et al., 1997; Honda et al., 1997). Surprisingly, the MDM2^{Y487A} mouse, in which MDM2 E3 ligase activity is disrupted while MDM2-MDMX interaction is maintained, clearly demonstrated that MDM2 E3 ligase activity is not required for regulating basal p53 levels throughout the lifespan (Tollini et al., 2014). In contrast, mouse models bearing targeted disruption of the MDM2-MDMX heterodimer have largely demonstrated p53-dependent embryonic lethality (Huang et al., 2011; Itahana et al., 2007; Pant et al., 2011), indicating that the MDM2-MDMX heterodimer may be the primary mechanism of basal p53 regulation. Although it has been proposed that the MDM2-MDMX heterodimer is required for MDM2 E3 ligase activity towards p53 (Kawai et al., 2007), the MDM2^{Y487A} mouse suggests that the other functions of this heterodimer are critical for basal p53 regulation, including MDM2- or MDMX-p53 binding and transactivation inhibition. Although not definitively proven, results from several studies suggest that the MDM2-MDMX heterodimer promotes more efficient p53 binding and transactivation inhibition than individual MDM family proteins alone. For instance, Pant et al. observed decreased binding of MDMX$^{\Delta RING}$ to p53^{R172H} (Pant et al.,

2011), which harbors a missense mutation rendering it transcriptionally inactive (Lang et al., 2004). Others in the Zhang lab have also observed that MDM2- and MDMX-p53 binding is impaired in *Mdm2*$^{-/-}$;*p53*$^{ER/-}$ and *MdmX*$^{-/-}$;*p53*$^{ER/-}$ MEFS compared to *p53*$^{ER/-}$ MEFs (unpublished observations). Other functions of the heterodimer, including recruitment of post-translational p53 modifiers like p300, could also play a role in p53 regulation.

While MDM2 E3 ligase activity appears to be dispensable for basal p53 regulation *in vivo*, both *in vitro* and *in vivo* studies agree that it is critical for p53 regulation following stress-induced p53 stabilization. The specific necessity of MDM2 E3 ligase activity was first demonstrated in adult MDM2^{Y487A} mice, which suffer increased sensitivity to sub lethal IR-induced DNA damage, evidenced by p53-dependent lethality and hematopoietic failure. Clarifying these studies further, the work presented in Chapter 5 offers the possibility that MDM2 E3 ligase activity may only be required for degrading p53 after certain types of stress or in certain tissues. In contrast to demonstrating p53 dependent lethality in response to sub lethal DNA damage, MDM2^{Y487A} mice demonstrate increased survival in response to c-MYC-overexpression-induced tumorigenesis (Figure 5.2). c-MYC overexpression has been shown to initiate an endogenous apoptotic program (Evan et al., 1992), in part mediated by p53 (Hermeking and Eick, 1994). c-MYC overexpression also promotes the inhibition of MDM2 E3 ligase activity through the induction of p19ARF- and RP-MDM2 interactions. It was unknown whether oncogene activation would promote robust stabilization of p53 in the absence of MDM2 E3 ligase function. The *Eμ-Myc* model is well-known to engage p53, and the absence of MDM2 E3 ligase function further promotes p53 stabilization, allowing for p53 activation and tumor suppression via cell cycle arrest, metabolic, or apoptotic mechanisms. Although MDM2^{Y487A} mice demonstrate increased survival (Figure 5.2), it remains to be determined if the loss of MDM2 E3 ligase activity drives the increased p53 stabilization observed in these mice. Combined, these studies point to the idea that, while dispensable under normal conditions, MDM2-mediated p53 degradation is essential following the resolution of stress. Further,

different stresses may induce p53 stabilization to varying degrees, which may dictate the necessity of MDM2 E3 ligase-mediated p53 degradation.

MDM2 is often overexpressed in tumors bearing WT p53, contributing to its functional silencing. It is therefore conceivable that p53 reactivation via MDM2 inhibition could promote tumor regression. In fact, several non-genotoxic small molecule inhibitors of MDM2-p53 binding have shown significant tumor suppressing capabilities in tumor xenografts (Shangary et al., 2008; Vassilev et al., 2004). However, mouse models have suggested that complete restoration of p53 function should be used with caution, as abundant p53 activity is especially toxic (Ringshausen et al., 2006; Tollini et al., 2014; Zhang et al., 2014a). The relative normalcy of the $MDM2^{Y487A}$ mouse points to the fact that MDM2 E3 ligase inhibition on its own does not promote lethal p53 activation *in vivo*. The work presented in this dissertation is also suggestive that MDM2 E3 ligase inhibition could be a safe way to promote p53 stabilization, activation, and tumor suppression without promoting overt toxicity. In fact, several small molecule inhibitors of MDM2 E3 ligase activity have already been developed. The first, HLI98, was identified through a high throughput screen probing for inhibitors of MDM2 autoubiquitination (Yang et al., 2005). In cells, HLI98 decreased p53 ubiquitination and promoted subsequent p53 activation. However, HLI98 appears to lack specificity for MDM2, and may affect E2 loading on other E3 ligases. HLI98 derivative compounds, including MPD, MEL23 and MEL24, have been developed in an attempt to increase the specificity of inhibition, but these compounds also appear to have MDM2 and p53-independent activity (Herman et al., 2011; Roxburgh et al., 2012). Although MDM2 E3 ligase inhibition may be a feasible strategy for WT p53 activation, the pharmacology of MDM2 E3 ligase inhibitors must be further improved if they are to be used in the clinic.

On the other hand, studies in the $MDM2^{Y487A}$ mouse also suggest that MDM2 E3 ligase inhibition could promote extreme toxicity in combination with whole body DNA damaging chemotherapies, as this would increase whole-body p53 activation. Tissue-targeted therapies, such as targeted radiation, could be used to avoid this problem. However, further exploration of

p53 and its regulation in cancer will be important to understand the uses or repercussions of p53-reactivating therapies.

Future Directions

RP-MDM2-mediated p53 regulation

The studies presented in this dissertation relied heavily on the MDM2^{C305F} mouse to examine under which conditions certain RP-MDM2 interactions are required for p53-mediated tumor suppression. Although useful, this model only allows us to test the effects of RPL11- and RPL5-MDM2 binding. Although it has been postulated that RPL11 and RPL5 are uniquely important for RP-mediated p53 activation, the work presented in Chapter 3 points to a novel role for RPL23 in p19ARF, RPL11, and RPL5 independent tumor prevention. Interestingly, the MDM2^{C305F} mouse presents with elevated levels of RPL23, which appear to protect the mice from HRAS-induced tumorigenesis (Figure 3.1).

Although the MDM2^{C305F} mouse allowed us to discover a role for RPL23 in HRAS-mediated tumorigenesis, the *in vivo* consequences of RPL23-MDM2 interaction were not able to be directly tested in this study. In the future, it would be useful to examine mice in which other RP-MDM2 interactions are disrupted, while RPL11 and RPL5 interactions are maintained. This could be possible through mutation of the MDM2 central acidic domain *in vivo*. Systematic mutation of the MDM2 acidic domain and overexpression *in vitro*, coupled with immunoprecipitation of RPs could allow for the identification of mutations disrupting specific RP-MDM2 interactions. Further, generating *in vivo* models using these identified mutations could allow us to directly test the idea that specific RP-MDM2 interactions are respondent to specific upstream signals.

This work also demonstrates that activated RAS overexpression can drive the expression of RPL23, but this mechanism has not been elucidated. We have demonstrated that *rpl23* transcription is upregulated in response to HRAS^{G12V} overexpression (Figure 3.7), but

determining the downstream transcription factors required for this transactivation will be important for future studies. Several RPs have been demonstrated to be downstream p53 targets, but thus far RPL23 has not been identified as such (He and Sun, 2007; Xiong et al., 2011; Zhang et al., 2013c). Further, the studies presented here suggest that HRAS-induced RPL23 expression does not require p53 (Figure 3.14). In order to identify chromatin binding transcription factors contributing to increased RAS-induced rpl23 transcription, it may be useful to perform reverse ChIP assays in cells overexpressing RAS. This method combines immunoprecipitated DNA probes (specific for the promoter region of interest) with mass spectroscopic analysis to identify chromatin binding proteins in an unbiased manner (Rusk, 2009). Elucidating novel regulators of ribosomal proteins and ribosome biosynthesis will allow us to further understand how oncogenes promote increased proliferation as well as p53 activation. Further, $HRAS^{G12V}$ mutation is not the most common RAS alteration found in melanomas. The NRAS isoform is much more commonly altered in melanoma (Chin et al., 1997), and in the future it may be interesting and more clinically relevant to examine RP-MDM2-p53 interaction in a mutated NRAS setting.

MDM2 E3 ligase activity and MDM2-MDMX interaction

The relative contributions of MDM2 E3 ligase activity and MDM2/MDMX heterodimer formation to p53 regulation are still being investigated. The normal survival of the $MDM2^{Y487A}$ mouse directly contrasts with mice bearing alterations disrupting MDM2-MDMX heterodimerization, which present with embryonic lethality (Table 1.2). However, disruption of MDM2-MDMX binding has also been shown to have less severe consequences in adult mice. Mice bearing a Cre-inducible MDMX RING deletion allele ($MdmX^{flxRING}$) were healthy following MDMX RING deletion, suggesting that MDM2-MDMX heterodimer formation is dispensable for the regulation of p53 activity in adult mice. Whether p53 stability is affected by this loss has not been determined in adult mice and remains an interesting question. In addition, MDMX deletion

coupled with p53 reactivation in adult mice is also relatively well-tolerated (Garcia et al., 2011). From these studies, it is unclear whether the MDM2-MDMX heterodimer directly participates in p53 regulation following stress *in vivo*. As such, it would be interesting to examine the p53-dependent stress response in adult mice bearing MDMX RING domain deletion. This could be achieved by examining $MdmX^{flxRING/flxRING}$ mice following Cre-mediated recombination and RING domain deletion. Interestingly, following sub lethal IR treatment $MdmX^{+/-}$ mice demonstrated lethality, and $MdmX^{\Delta RING/+}$ mice did not (Pant et al., 2011). While not conclusive, these data are suggestive that MDM2-MDMX heterodimer formation may not be required for stress-induced p53 regulation *in vivo*. Understanding the individual necessities of these MDM family protein functions in different contexts is imperative to understanding p53 regulation.

Concluding Remarks

Mouse modeling has proven to be an important tool in the study of p53. It has facilitated the understanding of both the upstream modifying factors that contribute to p53 activation (like RPs and p19ARF), as well as mechanisms responsible for p53 regulation following stress-induced activation. Continued innovation and exploration is necessary towards understanding p53 regulation in cancer as amazingly the tens of thousands of p53 studies have yet to yield clinically relevant diagnostics or therapeutics. This increased knowledge will help to inform novel cancer therapies with the end goal of improving patient outcomes.

REFERENCES

Adams, J., Harris, A., Pinkert, C., Corcoran, L., Alexander, W., Cory, S., Palmiter, R.D., and Brinster, R. (1985). The c-myc oncogene driven by immunoglobulin enhancers induces lymphoid malignancy in transgenic mice. Nature *318*, 533-538.

Arabi, A., Wu, S., Ridderstråle, K., Bierhoff, H., Shiue, C., Fatyol, K., Fahlén, S., Hydbring, P., Söderberg, O., and Grummt, I. (2005). c-Myc associates with ribosomal DNA and activates RNA polymerase I transcription. Nature Cell Biology *7*, 303-310.

Astle, M., Hannan, K., Ng, P., Lee, R., George, A., Hsu, A., Haupt, Y., Hannan, R., and Pearson, R. (2012). AKT induces senescence in human cells via mTORC1 and p53 in the absence of DNA damage: implications for targeting mTOR during malignancy. Oncogene *31*, 1949-1962.

Aziz, M.H., Shen, H., and Maki, C.G. (2011). Acquisition of p53 mutations in response to the non-genotoxic p53 activator Nutlin-3. Oncogene *30*, 4678-4686.

Badciong, J.C., and Haas, A.L. (2002). MdmX is a RING finger ubiquitin ligase capable of synergistically enhancing Mdm2 ubiquitination. Journal of Biological Chemistry *277*, 49668-49675.

Bai, D., Zhang, J., Xiao, W., and Zheng, X. (2014). Regulation of the HDM2-p53 pathway by ribosomal protein L6 in response to ribosomal stress. Nucleic Acids Research *42*, 1799-1811.

Barak, Y., Juven, T., Haffner, R., and Oren, M. (1993). mdm2 expression is induced by wild type p53 activity. The EMBO Journal *12*, 461.

Bardot, B., Bouarich-Bourimi, R., Leemput, J., Lejour, V., Hamon, A., Plancke, L., Jochemsen, A., Simeonova, I., Fang, M., and Toledo, F. (2015). Mice engineered for an obligatory Mdm4 exon skipping express higher levels of the Mdm4-S isoform but exhibit increased p53 activity. Oncogene *34*, 2943-2948.

Barlev, N.A., Liu, L., Chehab, N.H., Mansfield, K., Harris, K.G., Halazonetis, T.D., and Berger, S.L. (2001). Acetylation of p53 activates transcription through recruitment of coactivators/histone acetyltransferases. Molecular Cell *8*, 1243-1254.

Barna, M., Pusic, A., Zollo, O., Costa, M., Kondrashov, N., Rego, E., Rao, P.H., and Ruggero, D. (2008). Suppression of Myc oncogenic activity by ribosomal protein haploinsufficiency. Nature *456*, 971-975.

Ben-Shem, A., Jenner, L., Yusupova, G., and Yusupov, M. (2010). Crystal Structure of the Eukaryotic Ribosome. Science *330*, 1203-1209.

Bensaad, K., Tsuruta, A., Selak, M.A., Vidal, M.N.C., Nakano, K., Bartrons, R., Gottlieb, E., and Vousden, K.H. (2006). TIGAR, a p53-inducible regulator of glycolysis and apoptosis. Cell *126*, 107-120.

Bertwistle, D., Sugimoto, M., and Sherr, C.J. (2004). Physical and Functional Interactions of the Arf Tumor Suppressor Protein with Nucleophosmin/B23. Molecular and Cellular Biology *24*, 985-996.

Bhat, K.P., Itahana, K., Jin, A., and Zhang, Y. (2004). Essential role of ribosomal protein L11 in mediating growth inhibition-induced p53 activation. The EMBO Journal *23*, 2402-2412.

Blandino, G., Levine, A.J., and Oren, M. (1999). Mutant p53 gain of function: differential effects of different p53 mutants on resistance of cultured cells to chemotherapy. Oncogene *18*, 477-485.

Boesten, L., Zadelaar, S., De Clercq, S., Francoz, S., van Nieuwkoop, A., Biessen, E., Hofmann, F., Feil, S., Feil, R., and Jochemsen, A. (2006). Mdm2, but not Mdm4, protects terminally differentiated smooth muscle cells from p53-mediated caspase-3-independent cell death. Cell Death & Differentiation *13*, 2089-2098.

Bond, G.L., Hu, W., Bond, E.E., Robins, H., Lutzker, S.G., Arva, N.C., Bargonetti, J., Bartel, F., Taubert, H., Wuerl, P.*, et al.* (2004). A Single Nucleotide Polymorphism in the *MDM2* Promoter Attenuates the p53 Tumor Suppressor Pathway and Accelerates Tumor Formation in Humans. Cell *119*, 591-602.

Boulon, S., Westman, B.J., Hutten, S., Boisvert, F.-M., and Lamond, A.I. (2010). The Nucleolus under Stress. Molecular Cell *40*, 216-227.

Brady, S.N., Yu, Y., Maggi, L.B., and Weber, J.D. (2004). ARF impedes NPM/B23 shuttling in an Mdm2-sensitive tumor suppressor pathway. Molecular and Cellular Biology *24*, 9327-9338.

Burgess, A., Chia, K.M., Haupt, S., Thomas, D., Haupt, Y., and Lim, E. (2016). Clinical Overview of MDM2/X-Targeted Therapies. Frontiers in Oncology *6*.

Carr, M.I., Roderick, J.E., Gannon, H.S., Kelliher, M.A., and Jones, S.N. (2016). Mdm2 Phosphorylation Regulates Its Stability and Has Contrasting Effects on Oncogene and Radiation-Induced Tumorigenesis. Cell Reports *16*, 2618-2629.

Chen, D., Kon, N., Zhong, J., Zhang, P., Yu, L., and Gu, W. (2013). Differential effects on ARF stability by normal versus oncogenic levels of c-Myc expression. Molecular Cell *51*, 46-56.

Chen, D., Zhang, Z., Li, M., Wang, W., Li, Y., Rayburn, E., Hill, D., Wang, H., and Zhang, R. (2007). Ribosomal protein S7 as a novel modulator of p53–MDM2 interaction: binding to MDM2, stabilization of p53 protein, and activation of p53 function. Oncogene *26*, 5029-5037.

Chen, J., Marechal, V., and Levine, A.J. (1993). Mapping of the p53 and mdm-2 interaction domains. Molecular and Cellular Biology *13*, 4107-4114.

Chen, L., Gilkes, D.M., Pan, Y., Lane, W.S., and Chen, J. (2005). ATM and Chk2-dependent phosphorylation of MDMX contribute to p53 activation after DNA damage. The EMBO Journal *24*, 3411-3422.

Cheng, Q., Chen, L., Li, Z., Lane, W.S., and Chen, J. (2009). ATM activates p53 by regulating MDM2 oligomerization and E3 processivity. The EMBO Journal *28*, 3857-3867.

Cheng, Q., Cross, B., Li, B., Chen, L., Li, Z., and Chen, J. (2011). Regulation of MDM2 E3 ligase activity by phosphorylation after DNA damage. Molecular and Cellular Biology *31*, 4951-4963.

Cheng, X., Xia, W., Yang, J.-Y., Hsu, J.L., Lang, J.-Y., Chou, C.-K., Du, Y., Sun, H.-L., Wyszomierski, S.L., and Mills, G.B. (2010). Activation of murine double minute 2 by Akt in mammary epithelium delays mammary involution and accelerates mammary tumorigenesis. Cancer Research *70*, 7684-7689.

Chin, L., Pomerantz, J., Polsky, D., Jacobson, M., Cohen, C., Cordon-Cardo, C., Horner, J.W., and DePinho, R.A. (1997). Cooperative effects of INK4a and ras in melanoma susceptibility in vivo. Genes & Development *11*, 2822-2834.

Chipuk, J.E., Kuwana, T., Bouchier-Hayes, L., Droin, N.M., Newmeyer, D.D., Schuler, M., and Green, D.R. (2004). Direct activation of Bax by p53 mediates mitochondrial membrane permeabilization and apoptosis. Science *303*, 1010-1014.

Christiansen, D.H., Andersen, M.K., and Pedersen-Bjergaard, J. (2001). Mutations with loss of heterozygosity of p53 are common in therapy-related myelodysplasia and acute myeloid leukemia after exposure to alkylating agents and significantly associated with deletion or loss of 5q, a complex karyotype, and a poor prognosis. Journal of clinical oncology : official journal of the American Society of Clinical Oncology *19*, 1405-1413.

Claypool, J.A., French, S.L., Johzuka, K., Eliason, K., Vu, L., Dodd, J.A., Beyer, A.L., and Nomura, M. (2004). Tor pathway regulates Rrn3p-dependent recruitment of yeast RNA polymerase I to the promoter but does not participate in alteration of the number of active genes. Molecular Biology of the Cell *15*, 946-956.

Coller, H.A., Grandori, C., Tamayo, P., Colbert, T., Lander, E.S., Eisenman, R.N., and Golub, T.R. (2000). Expression analysis with oligonucleotide microarrays reveals that MYC regulates genes involved in growth, cell cycle, signaling, and adhesion. Proceedings of the National Academy of Sciences *97*, 3260-3265.

Dai, M.-S., and Lu, H. (2004). Inhibition of MDM2-mediated p53 ubiquitination and degradation by ribosomal protein L5. Journal of Biological Chemistry *279*, 44475-44482.

Dai, M.-S., Zeng, S.X., Jin, Y., Sun, X.-X., David, L., and Lu, H. (2004). Ribosomal protein L23 activates p53 by inhibiting MDM2 function in response to ribosomal perturbation but not to translation inhibition. Molecular and Cellular Biology *24*, 7654-7668.

Dai, M.S., Arnold, H., Sun, X.X., Sears, R., and Lu, H. (2007). Inhibition of c-Myc activity by ribosomal protein L11. The EMBO Journal *26*, 3332-3345.

Dang, C.V. (2013). MYC, metabolism, cell growth, and tumorigenesis. Cold Spring Harbor Perspectives in Medicine *3*, a014217.

Dang, C.V., O'Donnell, K.A., Zeller, K.I., Nguyen, T., Osthus, R.C., and Li, F. (2006). The c-Myc target gene network. Paper presented at: Seminars in Cancer Biology (Elsevier).

De Marval, P.L.M., and Zhang, Y. (2011). The RP-Mdm2-p53 pathway and tumorigenesis. Oncotarget *2*, 234-238.

de Oca Luna, R.M., Wagner, D.S., and Lozano, G. (1995). Rescue of early embryonic lethality in mdm2-deficient mice by deletion of p53. Nature *378*, 203-206.

de Stanchina, E., McCurrach, M.E., Zindy, F., Shieh, S.-Y., Ferbeyre, G., Samuelson, A.V., Prives, C., Roussel, M.F., Sherr, C.J., and Lowe, S.W. (1998). E1A signaling to p53 involves the p19ARFtumor suppressor. Genes & Development *12*, 2434-2442.

DeLeo, A.B., Jay, G., Appella, E., Dubois, G.C., Law, L.W., and Old, L.J. (1979). Detection of a transformation-related antigen in chemically induced sarcomas and other transformed cells of the mouse. Proceedings of the National Academy of Sciences *76*, 2420-2424.

Dittmer, D., Pati, S., Zambetti, G., Chu, S., Teresky, A.K., Moore, M., Finlay, C., and Levine, A.J. (1993). Gain of function mutations in p53. Nature Genetics *4*, 42-46.

Donati, G., Peddigari, S., Mercer, Carol A., and Thomas, G. (2013). 5S Ribosomal RNA Is an Essential Component of a Nascent Ribosomal Precursor Complex that Regulates the Hdm2-p53 Checkpoint. Cell Reports *4*, 87-98.

Donehower, L.A., Harvey, M., Slagle, B.L., McArthuri, M.J., and Montgomery Jr, C.A. (1992). Mice deficient for p53 are developmentally normal but susceptible to spontaneous. Nature *356*, 19.

Dornan, D., Wertz, I., Shimizu, H., Arnott, D., Frantz, G.D., Dowd, P., O'rourke, K., Koeppen, H., and Dixit, V.M. (2004). The ubiquitin ligase COP1 is a critical negative regulator of p53. Nature *429*, 86-92.

Eberharter, A., and Becker, P.B. (2002). Histone acetylation: a switch between repressive and permissive chromatin. EMBO Reports *3*, 224-229.

Efeyan, A., and Serrano, M. (2007). p53: guardian of the genome and policeman of the oncogenes. Cell Cycle *6*, 1006-1010.

Eilers, M., and Eisenman, R.N. (2008). Myc's broad reach. Genes & Development *22*, 2755-2766.

Eischen, C.M., Alt, J.R., and Wang, P. (2004). Loss of one allele of ARF rescues Mdm2 haploinsufficiency effects on apoptosis and lymphoma development. Oncogene *23*, 8931-8940.

Eischen, C.M., Weber, J.D., Roussel, M.F., Sherr, C.J., and Cleveland, J.L. (1999). Disruption of the ARF–Mdm2–p53 tumor suppressor pathway in Myc-induced lymphomagenesis. Genes & Development *13*, 2658-2669.

el-Deiry, W.S., Tokino, T., Velculescu, V.E., Levy, D.B., Parsons, R., Trent, J.M., Lin, D., Mercer, W.E., Kinzler, K.W., and Vogelstein, B. (1993). WAF1, a potential mediator of p53 tumor suppression. Cell *75*, 817-825.

Elyada, E., Pribluda, A., Goldstein, R., Morgenstern, Y., Brachya, G., Cojocaru, G., Snir-Alkalay, I., Burstain, I., Haffner-Krausz, R., and Jung, S. (2011). CKIα ablation highlights a critical role for p53 in invasiveness control. Nature *470*, 409-413.

Evan, G.I., Wyllie, A.H., Gilbert, C.S., Littlewood, T.D., Land, H., Brooks, M., Waters, C.M., Penn, L.Z., and Hancock, D.C. (1992). Induction of apoptosis in fibroblasts by c-myc protein. Cell *69*, 119-128.

Fakharzadeh, S., Trusko, S.P., and George, D.L. (1991). Tumorigenic potential associated with enhanced expression of a gene that is amplified in a mouse tumor cell line. The EMBO Journal *10*, 1565.

Farmer, G., Colgan, J., Nakatani, Y., Manley, J.L., and Prives, C. (1996). Functional interaction between p53, the TATA-binding protein (TBP), andTBP-associated factors in vivo. Mol Cell Biol *16*, 4295-4304.

Feng, Y., Sentani, K., Wiese, A., Sands, E., Green, M., Bommer, G.T., Cho, K.R., and Fearon, E.R. (2013). Sox9 Induction, Ectopic Paneth Cells, and Mitotic Spindle Axis Defects in Mouse Colon Adenomatous Epithelium Arising From Conditional Biallelic Apc Inactivation. The American Journal of Pathology *2*, 493-503.

Feng, Z., Hu, W., Teresky, A.K., Hernando, E., Cordon-Cardo, C., and Levine, A.J. (2007). Declining p53 function in the aging process: a possible mechanism for the increased tumor incidence in older populations. Proceedings of the National Academy of Sciences *104*, 16633-16638.

Francoz, S., Froment, P., Bogaerts, S., De Clercq, S., Maetens, M., Doumont, G., Bellefroid, E., and Marine, J.-C. (2006). Mdm4 and Mdm2 cooperate to inhibit p53 activity in proliferating and quiescent cells in vivo. Proceedings of the National Academy of Sciences of the United States of America *103*, 3232-3237.

Franklin, D.A., He, Y., Leslie, P.L., Tikunov, A.P., Fenger, N., Macdonald, J.M., and Zhang, Y. (2016). p53 coordinates DNA repair with nucleotide synthesis by suppressing PFKFB3 expression and promoting the pentose phosphate pathway. Scientific Reports *6*.

Fumagalli, S., Di Cara, A., Neb-Gulati, A., Natt, F., Schwemberger, S., Hall, J., Babcock, G.F., Bernardi, R., Pandolfi, P.P., and Thomas, G. (2009a). Absence of nucleolar disruption after impairment of 40S ribosome biogenesis reveals an rpL11-translation-dependent mechanism of p53 induction. Nature Cell Biology *11*.

Fumagalli, S., Di Cara, A., Neb-Gulati, A., Natt, F., Schwemberger, S., Hall, J., Babcock, G.F., Bernardi, R., Pandolfi, P.P., and Thomas, G. (2009b). Absence of nucleolar disruption after impairment of 40S ribosome biogenesis reveals an rpL11-translation-dependent mechanism of p53 induction. Nature Cell Biology *11*, 501-508.

Fumagalli, S., Ivanenkov, V.V., Teng, T., and Thomas, G. (2012). Suprainduction of p53 by disruption of 40S and 60S ribosome biogenesis leads to the activation of a novel G2/M checkpoint. Genes & Development *26*, 1028.

Funk, W.D., Pak, D.T., Karas, R.H., Wright, W.E., and Shay, J.W. (1992). A transcriptionally active DNA-binding site for human p53 protein complexes. Molecular and Cellular Biology *12*, 2866-2871.

Gannon, H.S., Donehower, L.A., Lyle, S., and Jones, S.N. (2011). Mdm2–p53 signaling regulates epidermal stem cell senescence and premature aging phenotypes in mouse skin. Developmental Biology *353*, 1-9.

Gannon, H.S., Woda, B.A., and Jones, S.N. (2012). ATM phosphorylation of Mdm2 Ser394 regulates the amplitude and duration of the DNA damage response in mice. Cancer Cell *21*, 668-679.

Garcia, D., Warr, M.R., Martins, C.P., Swigart, L.B., Passegué, E., and Evan, G.I. (2011). Validation of MdmX as a therapeutic target for reactivating p53 in tumors. Genes & Development *25*, 1746-1757.

Geyer, R.K., Zhong, K.Y., and Maki, C.G. (2000). The MDM2 RING-finger domain is required to promote p53 nuclear export. Nature Cell Biology *2*, 569-573.

Gibson, S.L., Boquoi, A., Chen, T., Sharpless, N.E., Brensinger, C., and Enders, G.H. (2005). p16Ink4a inhibits histologic progression and angiogenic signaling in Min colon tumors. Cancer Biology & Therapy *4*, 1389-1394.

Gilkes, D.M., Chen, L., and Chen, J. (2006). MDMX regulation of p53 response to ribosomal stress. The EMBO Journal *25*, 5614-5625.

Gingras, A.-C., Gygi, S.P., Raught, B., Polakiewicz, R.D., Abraham, R.T., Hoekstra, M.F., Aebersold, R., and Sonenberg, N. (1999). Regulation of 4E-BP1 phosphorylation: a novel two-step mechanism. Genes & Development *13*, 1422-1437.

Gomez-Herreros, F., Rodriguez-Galan, O., Morillo-Huesca, M., Maya, D., Arista-Romero, M., de la Cruz, J., Chavez, S., and Munoz-Centeno, M.C. (2013). Balanced production of ribosome components is required for proper G1/S transition in Saccharomyces cerevisiae. The Journal of biological chemistry *288*, 31689-31700.

Gomez-Roman, N., Grandori, C., Eisenman, R.N., and White, R.J. (2003). Direct activation of RNA polymerase III transcription by c-Myc. Nature *421*, 290-294.

Grier, J.D., Xiong, S., Elizondo-Fraire, A.C., Parant, J.M., and Lozano, G. (2006). Tissue-specific differences of p53 inhibition by Mdm2 and Mdm4. Molecular and Cellular Biology *26*, 192-198.

Grier, J.D., Yan, W., and Lozano, G. (2002). Conditional allele of mdm2 which encodes a p53 inhibitor. Genesis *32*, 145-147.

Groden, J., Thliveris, A., Samowitz, W., Carlson, M., Gelbert, L., Albertsen, H., Joslyn, G., Stevens, J., Spirio, L., and Robertson, M. (1991). Identification and characterization of the familial adenomatous polyposis coli gene. Cell *66*, 589-600.

Gu, J., Kawai, H., Nie, L., Kitao, H., Wiederschain, D., Jochemsen, A.G., Parant, J., Lozano, G., and Yuan, Z.-M. (2002). Mutual dependence of MDM2 and MDMX in their functional inactivation of p53. Journal of Biological Chemistry *277*, 19251-19254.

Guo, Q.M., Malek, R.L., Kim, S., Chiao, C., He, M., Ruffy, M., Sanka, K., Lee, N.H., Dang, C.V., and Liu, E.T. (2000). Identification of c-myc responsive genes using rat cDNA microarray. Cancer Research *60*, 5922-5928.

Halberg, R.B., Katzung, D.S., Hoff, P.D., Moser, A.R., Cole, C.E., Lubet, R.A., Donehower, L.A., Jacoby, R.F., and Dove, W.F. (2000). Tumorigenesis in the multiple intestinal neoplasia mouse:

redundancy of negative regulators and specificity of modifiers. Proceedings of the National Academy of Sciences *97*, 3461-3466.

Hannan, K.M., Brandenburger, Y., Jenkins, A., Sharkey, K., Cavanaugh, A., Rothblum, L., Moss, T., Poortinga, G., McArthur, G.A., and Pearson, R.B. (2003). mTOR-dependent regulation of ribosomal gene transcription requires S6K1 and is mediated by phosphorylation of the carboxy-terminal activation domain of the nucleolar transcription factor UBF. Molecular and Cellular Biology *23*, 8862-8877.

Hara, K., Yonezawa, K., Weng, Q.-P., Kozlowski, M.T., Belham, C., and Avruch, J. (1998). Amino acid sufficiency and mTOR regulate p70 S6 kinase and eIF-4E BP1 through a common effector mechanism. Journal of Biological Chemistry *273*, 14484-14494.

Harris, A.W., Pinkert, C.A., Crawford, M., Langdon, W., Brinster, R., and Adams, J. (1988). The E mu-myc transgenic mouse. A model for high-incidence spontaneous lymphoma and leukemia of early B cells. J Exp Med *167*, 353-371.

Haupt, Y., Maya, R., Kazaz, A., and Oren, M. (1997). Mdm2 promotes therapid degradation of p53. Nature *387*, 296-299.

He, H., and Sun, Y. (2007). Ribosomal protein S27L is a direct p53 target that regulates apoptosis. Oncogene *26*, 2707-2716.

He, T.-C., Sparks, A.B., Rago, C., Hermeking, H., Zawel, L., da Costa, L.T., Morin, P.J., Vogelstein, B., and Kinzler, K.W. (1998). Identification of c-MYC as a target of the APC pathway. Science *281*, 1509-1512.

Herman, A.G., Hayano, M., Poyurovsky, M.V., Shimada, K., Skouta, R., Prives, C., and Stockwell, B.R. (2011). Discovery of Mdm2-MdmX E3 ligase inhibitors using a cell-based ubiquitination assay. Cancer Discovery *1*, 312-325.

Hermeking, H., and Eick, D. (1994). Mediation of c-Myc-induced apoptosis by p53. Science, 2091-2091.

Hill, R.M., Kuijper, S., Lindsey, J.C., Petrie, K., Schwalbe, E.C., Barker, K., Boult, J.K., Williamson, D., Ahmad, Z., and Hallsworth, A. (2015). Combined MYC and P53 defects emerge at medulloblastoma relapse and define rapidly progressive, therapeutically targetable disease. Cancer Cell *27*, 72-84.

Hoag, W.G. (1963). Spontaneous cancer in mice. Annals of the New York Academy of Sciences *108*, 805-831.

Hoffman, B., and Liebermann, D. (2008). Apoptotic signaling by c-MYC. Oncogene *27*, 6462-6472.

Honda, R., Tanaka, H., and Yasuda, H. (1997). Oncoprotein MDM2 is a ubiquitin ligase E3 for tumor suppressor p53. FEBS letters *420*, 25-27.

Honda, R., and Yasuda, H. (2000). Activity of MDM2, a ubiquitin ligase, toward p53 or itself is dependent on the RING finger domain of the ligase. Oncogene *19*, 1473-1476.

Hsu, B., Marin, M.C., El-Naggar, A.K., Stephens, L.C., Brisbay, S., and McDonnell, T.J. (1995). Evidence that c-myc mediated apoptosis does not require wild-type p53 during lymphomagenesis. Oncogene *11*, 175-179.

Hu, B., Gilkes, D.M., and Chen, J. (2007). Efficient p53 activation and apoptosis by simultaneous disruption of binding to MDM2 and MDMX. Cancer Research *67*, 8810-8817.

Hu, W., Zhang, C., Wu, R., Sun, Y., Levine, A., and Feng, Z. (2010). Glutaminase 2, a novel p53 target gene regulating energy metabolism and antioxidant function. Proceedings of the National Academy of Sciences *107*, 7455-7460.

Huang, L., Yan, Z., Liao, X., Li, Y., Yang, J., Wang, Z.-G., Zuo, Y., Kawai, H., Shadfan, M., and Ganapathy, S. (2011). The p53 inhibitors MDM2/MDMX complex is required for control of p53 activity in vivo. Proceedings of the National Academy of Sciences *108*, 12001-12006.

Iadevaia, V., Zhang, Z., Jan, E., and Proud, C.G. (2011). mTOR signaling regulates the processing of pre-rRNA in human cells. Nucleic Acids Research, gkr1040.

Itahana, K., Bhat, K.P., Jin, A., Itahana, Y., Hawke, D., Kobayashi, R., and Zhang, Y. (2003). Tumor suppressor ARF degrades B23, a nucleolar protein involved in ribosome biogenesis and cell proliferation. Molecular Cell *12*, 1151-1164.

Itahana, K., Mao, H., Jin, A., Itahana, Y., Clegg, H.V., Lindström, M.S., Bhat, K.P., Godfrey, V.L., Evan, G.I., and Zhang, Y. (2007). Targeted inactivation of Mdm2 RING finger E3 ubiquitin ligase activity in the mouse reveals mechanistic insights into p53 regulation. Cancer Cell *12*, 355-366.

Jackson, M.W., and Berberich, S.J. (2000). MdmX protects p53 from Mdm2-mediated degradation. Molecular and Cellular Biology *20*, 1001-1007.

Jemal, A., Siegel, R., Ward, E., Hao, Y., Xu, J., and Thun, M.J. (2009). Cancer statistics, 2009. CA: A Cancer Journal for Clinicians *59*, 225-249.

Ji, H., Wu, G., Zhan, X., Nolan, A., Koh, C., De Marzo, A., Doan, H.M., Fan, J., Cheadle, C., and Fallahi, M. (2011). Cell-type independent MYC target genes reveal a primordial signature involved in biomass accumulation. PloS One *6*, e26057.

Jin, A., Itahana, K., O'Keefe, K., and Zhang, Y. (2004). Inhibition of HDM2 and activation of p53 by ribosomal protein L23. Molecular and Cellular Biology *24*, 7669-7680.

Jones, S.N., Hancock, A.R., Vogel, H., Donehower, L.A., and Bradley, A. (1998). Overexpression of Mdm2 in mice reveals a p53-independent role for Mdm2 in tumorigenesis. Proceedings of the National Academy of Sciences *95*, 15608-15612.

Jones, S.N., Roe, A.E., Donehower, L.A., and Bradley, A. (1995). Rescue of embryonic lethality in Mdm2-deficient mice by absence of p53. Nature *378*, 206-208.

Jordan, J.J., Menendez, D., Inga, A., Nourredine, M., Bell, D., and Resnick, M.A. (2008). Noncanonical DNA motifs as transactivation targets by wild type and mutant p53. PLoS Genet *4*, e1000104.

Kamangar, F., Dores, G.M., and Anderson, W.F. (2006). Patterns of cancer incidence, mortality, and prevalence across five continents: defining priorities to reduce cancer disparities in different geographic regions of the world. Journal of Clinical Oncology *24*, 2137-2150.

Kamijo, T., Bodner, S., Van De Kamp, E., Randle, D.H., and Sherr, C.J. (1999). Tumor spectrum in ARF-deficient mice. Cancer Research *59*, 2217-2222.

Kamijo, T., Weber, J.D., Zambetti, G., Zindy, F., Roussel, M.F., and Sherr, C.J. (1998). Functional and physical interactions of the ARF tumor suppressor with p53 and Mdm2. Proceedings of the National Academy of Sciences *95*, 8292-8297.

Kamijo, T., Zindy, F., Roussel, M.F., Quelle, D.E., Downing, J.R., Ashmun, R.A., Grosveld, G., and Sherr, C.J. (1997). Tumor suppression at the mouse INK4a locus mediated by the alternative reading frame product p19 ARF. Cell *91*, 649-659.

Kawai, H., Lopez-Pajares, V., Kim, M.M., Wiederschain, D., and Yuan, Z.-M. (2007). RING Domain–Mediated Interaction Is a Requirement for MDM2's E3 Ligase Activity. Cancer Research *67*, 6026-6030.

Kawai, H., Wiederschain, D., Kitao, H., Stuart, J., Tsai, K.K., and Yuan, Z.-M. (2003). DNA damage-induced MDMX degradation is mediated by MDM2. Journal of Biological Chemistry *278*, 45946-45953.

Kim, H., Tu, H.-C., Ren, D., Takeuchi, O., Jeffers, J.R., Zambetti, G.P., Hsieh, J.J.-D., and Cheng, E.H.-Y. (2009). Stepwise activation of BAX and BAK by tBID, BIM, and PUMA initiates mitochondrial apoptosis. Molecular Cell *36*, 487-499.

Kim, S., Li, Q., Dang, C.V., and Lee, L.A. (2000). Induction of ribosomal genes and hepatocyte hypertrophy by adenovirus-mediated expression of c-Myc in vivo. Proceedings of the National Academy of Sciences *97*, 11198-11202.

Kim, T.-H., Leslie, P., and Zhang, Y. (2014). Ribosomal proteins as unrevealed caretakers for cellular stress and genomic instability. Oncotarget *5*, 860-871.

Kim, Y., Girard, L., Giacomini, C., Wang, P., Hernandez-Boussard, T., Tibshirani, R., Minna, J., and Pollack, J. (2006). Combined microarray analysis of small cell lung cancer reveals altered apoptotic balance and distinct expression signatures of MYC family gene amplification. Oncogene *25*, 130-138.

Kinzler, K., Nilbert, M., Su, L., Vogelstein, B., Bryan, T., Levy, D., Smith, K., Preisinger, A., Hedge, P., and McKechnie, D. (1991). Identification of FAP locus genes from chromosome 5q21. Science *253*, 661-665.

Kinzler, K.W., and Vogelstein, B. (1996). Lessons from hereditary colorectal cancer. Cell *87*, 159-170.

Kochenderfer, J.N., and Rosenberg, S.A. (2013). Treating B-cell cancer with T cells expressing anti-CD19 chimeric antigen receptors. Nature reviews Clinical oncology *10*, 267-276.

Kress, M., May, E., Cassingena, R., and May, P. (1979). Simian virus 40-transformed cells express new species of proteins precipitable by anti-simian virus 40 tumor serum. Journal of Virology *31*, 472-483.

Kubbutat, M.H.G., Jones, S.N., and Vousden, K.H. (1997). Regulation of p53 stability by Mdm2. Nature *387*, 299-303.

Kussie, P.H., Gorina, S., Marechal, V., and Elenbaas, B. (1996). Structure of the MDM2 oncoprotein bound to the p53 tumor suppressor transactivation domain. Science *274*, 948.

Lane, D., and Crawford, L. (1979). T antigen is bound to a host protein in SY40-transformed cells. Nature *278*, 261-263.

Lane, D.P. (1992). Cancer. p53, guardian of the genome. Nature *358*, 15-16.

Lang, G.A., Iwakuma, T., Suh, Y.-A., Liu, G., Rao, V.A., Parant, J.M., Valentin-Vega, Y.A., Terzian, T., Caldwell, L.C., Strong, L.C.*, et al.* (2004). Gain of Function of a p53 Hot Spot Mutation in a Mouse Model of Li-Fraumeni Syndrome. Cell *119*, 861-872.

LeBron, C., Chen, L., Gilkes, D.M., and Chen, J. (2006). Regulation of MDMX nuclear import and degradation by Chk2 and 14-3-3. The EMBO Journal *25*, 1196-1206.

Leng, R.P., Lin, Y., Ma, W., Wu, H., Lemmers, B., Chung, S., Parant, J.M., Lozano, G., Hakem, R., and Benchimol, S. (2003). Pirh2, a p53-Induced Ubiquitin-Protein Ligase, Promotes p53 Degradation. Cell *112*, 779-791.

Lengner, C.J., Steinman, H.A., Gagnon, J., Smith, T.W., Henderson, J.E., Kream, B.E., Stein, G.S., Lian, J.B., and Jones, S.N. (2006). Osteoblast differentiation and skeletal development are regulated by Mdm2–p53 signaling. The Journal of Cell Biology *172*, 909-921.

Leonard, D.G., Travis, L.B., Addya, K., Dores, G.M., Holowaty, E.J., Bergfeldt, K., Malkin, D., Kohler, B.A., Lynch, C.F., Wiklund, T.*, et al.* (2002). p53 mutations in leukemia and myelodysplastic syndrome after ovarian cancer. Clinical cancer research : an official journal of the American Association for Cancer Research *8*, 973-985.

Lessard, F., Morin, F., Ivanchuk, S., Langlois, F., Stefanovsky, V., Rutka, J., and Moss, T. (2010). The ARF tumor suppressor controls ribosome biogenesis by regulating the RNA polymerase I transcription factor TTF-I. Molecular Cell *38*, 539-550.

Li, H., Tsang, C.K., Watkins, M., Bertram, P.G., and Zheng, X.F. (2006). Nutrient regulates Tor1 nuclear localization and association with rDNA promoter. Nature *442*, 1058-1061.

Li, P., Nijhawan, D., Budihardjo, I., Srinivasula, S.M., Ahmad, M., Alnemri, E.S., and Wang, X. (1997). Cytochrome c and dATP-dependent formation of Apaf-1/caspase-9 complex initiates an apoptotic protease cascade. Cell *91*, 479-489.

Li, Q., Zhang, Y., El-Naggar, A.K., Xiong, S., Yang, P., Jackson, J.G., Chau, G., and Lozano, G. (2014). Therapeutic efficacy of p53 restoration in Mdm2-overexpressing tumors. Molecular cancer research : MCR *12*, 901-911.

Li, T., Kon, N., Jiang, L., Tan, M., Ludwig, T., Zhao, Y., Baer, R., and Gu, W. (2012). Tumor suppression in the absence of p53-mediated cell-cycle arrest, apoptosis, and senescence. Cell *149*, 1269-1283.

Liao, J.-M., Zhou, X., Gatignol, A., and Lu, H. (2014). Ribosomal proteins L5 and L11 co-operatively inactivate c-Myc via RNA-induced silencing complex. Oncogene *33*, 4916-4923.

Lill, N.L., Grossman, S.R., Ginsberg, D., DeCaprio, J., and Livingston, D.M. (1997). Binding and modulation of p53 by p300/CBP coactivators. Nature *387*, 823.

Lin, A.W., and Lowe, S.W. (2001). Oncogenic ras activates the ARF-p53 pathway to suppress epithelial cell transformation. Proceedings of the National Academy of Sciences *98*, 5025-5030.

Linares, L.K., Hengstermann, A., Ciechanover, A., Müller, S., and Scheffner, M. (2003). HdmX stimulates Hdm2-mediated ubiquitination and degradation of p53. Proceedings of the National Academy of Sciences *100*, 12009-12014.

Lindström, M.S. (2010). NPM1/B23: a multifunctional chaperone in ribosome biogenesis and chromatin remodeling. Biochemistry research international *2011*.

Lindström, M.S., Jin, A., Deisenroth, C., Wolf, G.W., and Zhang, Y. (2007). Cancer-associated mutations in the MDM2 zinc finger domain disrupt ribosomal protein interaction and attenuate MDM2-induced p53 degradation. Molecular and Cellular Biology *27*, 1056-1068.

Linke, K., Mace, P., Smith, C., Vaux, D., Silke, J., and Day, C.L. (2008). Structure of the MDM2/MDMX RING domain heterodimer reveals dimerization is required for their ubiquitylation in trans. Cell Death & Differentiation *15*, 841-848.

Linzer, D.I., and Levine, A.J. (1979). Characterization of a 54K dalton cellular SV40 tumor antigen present in SV40-transformed cells and uninfected embryonal carcinoma cells. Cell *17*, 43-52.

Littlewood, T.D., Kreuzaler, P., and Evan, G.I. (2012). All things to all people. Cell *151*, 11-13.

Liu, J., Zhang, C., Lin, M., Zhu, W., Liang, Y., Hong, X., Zhao, Y., Young, K.H., Hu, W., and Feng, Z. (2014a). Glutaminase 2 negatively regulates the PI3K/AKT signaling and shows tumor suppression activity in human hepatocellular carcinoma. Oncotarget *5*, 2635-2647.

Liu, S., Kim, T.-H., Franklin, D.A., and Zhang, Y. (2017). Protection against High-Fat-Diet-Induced Obesity in MDM2 C305F Mice Due to Reduced p53 Activity and Enhanced Energy Expenditure. Cell Reports *18*, 1005-1018.

Liu, S., Tackmann, N., Yang, J., and Zhang, Y. (2016a). Disruption of the RP-MDM2-p53 pathway accelerates APC loss-induced colorectal tumorigenesis. Oncogene.

Liu, Y., Deisenroth, C., and Zhang, Y. (2016b). RP–MDM2–p53 Pathway: Linking Ribosomal Biogenesis and Tumor Surveillance. Trends in Cancer *2*, 191-204.

Liu, Y., He, Y., Jin, A., Tikunov, A.P., Zhou, L., Tollini, L.A., Leslie, P., Kim, T.-H., Li, L.O., and Coleman, R.A. (2014b). Ribosomal protein–Mdm2–p53 pathway coordinates nutrient stress with

lipid metabolism by regulating MCD and promoting fatty acid oxidation. Proceedings of the National Academy of Sciences *111*, E2414-E2422.

Lohrum, M.A., Ludwig, R.L., Kubbutat, M.H., Hanlon, M., and Vousden, K.H. (2003). Regulation of HDM2 activity by the ribosomal protein L11. Cancer Cell *3*, 577-587.

Lohrum, M.A., Woods, D.B., Ludwig, R.L., Bálint, É., and Vousden, K.H. (2001). C-terminal ubiquitination of p53 contributes to nuclear export. Molecular and cellular biology *21*, 8521-8532.

Macias, E., Jin, A., Deisenroth, C., Bhat, K., Mao, H., Lindström, M.S., and Zhang, Y. (2010). An ARF-independent c-MYC-activated tumor suppression pathway mediated by ribosomal protein-Mdm2 Interaction. Cancer Cell *18*, 231-243.

Maetens, M., Doumont, G., De Clercq, S., Francoz, S., Froment, P., Bellefroid, E., Klingmuller, U., Lozano, G., and Marine, J.-C. (2007). Distinct roles of Mdm2 and Mdm4 in red cell production. Blood *109*, 2630-2633.

Mahajan, P.B. (1994). Modulation of transcription of rRNA genes by rapamycin. International Journal of Immunopharmacology *16*, 711-721.

Mamane, Y., Petroulakis, E., Martineau, Y., Sato, T.-A., Larsson, O., Rajasekhar, V.K., and Sonenberg, N. (2007). Epigenetic activation of a subset of mRNAs by eIF4E explains its effects on cell proliferation. PLoS One *2*, e242.

Martin, D., Munoz, R., Subler, M., and Deb, S. (1993). p53 binds to the TATA-binding protein-TATA complex. Journal of Biological Chemistry *268*, 13062-13067.

Mateyak, M.K., Obaya, A.J., Adachi, S., and Sedivy, J.M. (1997). Phenotypes of c-myc deficient rat fibroblasts isolated by targeted homologous recombination.". Detail *36*, 38.

Mayer, C., Zhao, J., Yuan, X., and Grummt, I. (2004). mTOR-dependent activation of the transcription factor TIF-IA links rRNA synthesis to nutrient availability. Genes & Development *18*, 423-434.

McMahon, S.B., Wood, M.A., and Cole, M.D. (2000). The essential cofactor TRRAP recruits the histone acetyltransferase hGCN5 to c-Myc. Molecular and Cellular Biology *20*, 556-562.

Mendrysa, S.M., McElwee, M.K., Michalowski, J., O'Leary, K.A., Young, K.M., and Perry, M.E. (2003). mdm2 Is critical for inhibition of p53 during lymphopoiesis and the response to ionizing irradiation. Molecular and Cellular Biology *23*, 462-472.

Menendez, D., Inga, A., and Resnick, M.A. (2009). The expanding universe of p53 targets. Nature Reviews Cancer *9*, 724-737.

Meng, X., Carlson, N., Dong, J., and Zhang, Y. (2015a). Oncogenic c-Myc-induced lymphomagenesis is inhibited non-redundantly by the p19Arf–Mdm2–p53 and RP–Mdm2–p53 pathways. Oncogene *34*, 5709-5717.

Meng, X., Carlson, N., Dong, J., and Zhang, Y. (2015b). Oncogenic c-Myc-induced lymphomagenesis is inhibited non-redundantly by the p19Arf–Mdm2–p53 and RP–Mdm2–p53 pathways. Oncogene.

Meng, X., Leslie, P., Zhang, Y., and Dong, J. (2014). Stem cells in a three-dimensional scaffold environment. Springerplus *3*, 1.

Meng, X., Tackmann, N.R., Liu, S., Yang, J., Dong, J., Wu, C., Cox, A.D., and Zhang, Y. (2016). RPL23 links oncogenic RAS signaling to p53-mediated tumor suppression. Cancer Research *76*, 5030-5039.

Menssen, A., and Hermeking, H. (2002). Characterization of the c-MYC-regulated transcriptome by SAGE: identification and analysis of c-MYC target genes. Proceedings of the National Academy of Sciences *99*, 6274-6279.

Meyer, N., and Penn, L.Z. (2008). Reflecting on 25 years with MYC. Nature Reviews Cancer *8*, 976-990.

Momand, J., Villegas, A., and Belyi, V.A. (2011). The evolution of MDM2 family genes. Gene *486*, 23-30.

Morin, P.J., Sparks, A.B., Korinek, V., Barker, N., Clevers, H., Vogelstein, B., and Kinzler, K.W. (1997). Activation of β-catenin-Tcf signaling in colon cancer by mutations in β-catenin or APC. Science *275*, 1787-1790.

Moroni, M.C., Hickman, E.S., Denchi, E.L., Caprara, G., Colli, E., Cecconi, F., Müller, H., and Helin, K. (2001). Apaf-1 is a transcriptional target for E2F and p53. Nature Cell Biology *3*, 552-558.

Moser, A.R., Dove, W.F., Roth, K.A., and Gordon, J.I. (1992). The Min (multiple intestinal neoplasia) mutation: its effect on gut epithelial cell differentiation and interaction with a modifier system. The Journal of Cell Biology *116*, 1517-1526.

Moser, A.R., Pitot, H.C., and Dove, W.F. (1990). A dominant mutation that predisposes to multiple intestinal neoplasia in the mouse. Science *247*, 322-324.

Muller, P.A., and Vousden, K.H. (2013). p53 mutations in cancer. Nature Cell Biology *15*, 2-8.

Muller, P.A., and Vousden, K.H. (2014). Mutant p53 in cancer: new functions and therapeutic opportunities. Cancer Cell *25*, 304-317.

Murphy, D., Junttila, M., Pouyet, L., Karnezis, A., Shchors, K., Bui, D., Brown-Swigart, L., Johnson, L., and Evan, G. (2008). Distinct thresholds govern Myc's biological output In vivo. Cancer Cell *14*, 447-457.

Nakano, K., and Vousden, K.H. (2001). PUMA, a novel proapoptotic gene, is induced by p53. Molecular Cell *7*, 683-694.

Narla, A., and Ebert, B.L. (2010). Ribosomopathies: human disorders of ribosome dysfunction. Blood *115*, 3196-3205.

Network, C.G.A. (2012). Comprehensive molecular characterization of human colon and rectal cancer. Nature *487*, 330-337.

Nishisho, I., Nakamura, Y., Miyoshi, Y., Miki, Y., Ando, H., Horii, A., Koyama, K., Utsunomiya, J., Baba, S., and Hedge, P. (1991). Mutations of Chromosome 5q21 Genes in FAP and Colorectal Cancer Patients. Science *253*, 665-669.

Oda, E., Ohki, R., Murasawa, H., Nemoto, J., Shibue, T., Yamashita, T., Tokino, T., Taniguchi, T., and Tanaka, N. (2000). Noxa, a BH3-only member of the Bcl-2 family and candidate mediator of p53-induced apoptosis. Science *288*, 1053-1058.

Odintsova, T.I., Müller, E.-C., Ivanov, A.V., Egorov, T.A., Bienert, R., Vladimirov, S.N., Kostka, S., Otto, A., Wittmann-Liebold, B., and Karpova, G.G. (2003). Characterization and analysis of posttranslational modifications of the human large cytoplasmic ribosomal subunit proteins by mass spectrometry and Edman sequencing. Journal of Protein Chemistry *22*, 249-258.

Okamoto, K., Kashima, K., Pereg, Y., Ishida, M., Yamazaki, S., Nota, A., Teunisse, A., Migliorini, D., Kitabayashi, I., and Marine, J.-C. (2005). DNA damage-induced phosphorylation of MdmX at serine 367 activates p53 by targeting MdmX for Mdm2-dependent degradation. Molecular and Cellular Biology *25*, 9608-9620.

Oliner, J.D., Pietenpol, J.A., Thiagalingam, S., Gyuris, J., Kinzler, K.W., and Vogelstein, B. (1993). Oncoprotein MDM2 conceals the activation domain of tumour suppressor p53.

Olive, K.P., Tuveson, D.A., Ruhe, Z.C., Yin, B., Willis, N.A., Bronson, R.T., Crowley, D., and Jacks, T. (2004). Mutant p53 gain of function in two mouse models of Li-Fraumeni syndrome. Cell *119*, 847-860.

Ouelle, D.E., Zindy, F., Ashmun, R.A., and Sherr, C.J. (1995). Alternative reading frames of the INK4a tumor suppressor gene encode two unrelated proteins capable of inducing cell cycle arrest. Cell *83*, 993-1000.

Packham, G., and Cleveland, J.L. (1995). c-Myc and apoptosis. Biochimica et Biophysica Acta (BBA)-Reviews on Cancer *1242*, 11-28.

Palmero, I., Pantoja, C., and Serrano, M. (1998). p19ARF links the tumour suppressor p53 to Ras. Nature *395*, 125-126.

Pan, S.Y., and Morrison, H. (2011). Epidemiology of cancer of the small intestine. World Journal of Gastrointestinal Oncology *3*, 33-42.

Pan, Y., and Chen, J. (2003). MDM2 promotes ubiquitination and degradation of MDMX. Molecular and Cellular Biology *23*, 5113-5121.

Pant, V., and Lozano, G. (2014). Dissecting the p53-Mdm2 feedback loop in vivo: uncoupling the role in p53 stability and activity. Oncotarget *5*, 1149-1156.

Pant, V., Xiong, S., Iwakuma, T., Quintás-Cardama, A., and Lozano, G. (2011). Heterodimerization of Mdm2 and Mdm4 is critical for regulating p53 activity during embryogenesis but dispensable for p53 and Mdm2 stability. Proceedings of the National Academy of Sciences *108*, 11995-12000.

Parant, J., Chavez-Reyes, A., Little, N.A., Yan, W., Reinke, V., Jochemsen, A.G., and Lozano, G. (2001). Rescue of embryonic lethality in Mdm4-null mice by loss of Trp53 suggests a nonoverlapping pathway with MDM2 to regulate p53. Nature Genetics *29*, 92-95.

Pastorino, J.G., Chen, S.-T., Tafani, M., Snyder, J.W., and Farber, J.L. (1998). The overexpression of Bax produces cell death upon induction of the mitochondrial permeability transition. Journal of Biological Chemistry *273*, 7770-7775.

Pavletich, N.P., Chambers, K.A., and Pabo, C.O. (1993). The DNA-binding domain of p53 contains the four conserved regions and the major mutation hot spots. Genes & Development *7*, 2556-2564.

Pereg, Y., Lam, S., Teunisse, A., Biton, S., Meulmeester, E., Mittelman, L., Buscemi, G., Okamoto, K., Taya, Y., and Shiloh, Y. (2006). Differential roles of ATM-and Chk2-mediated phosphorylations of Hdmx in response to DNA damage. Molecular and Cellular Biology *26*, 6819-6831.

Pereg, Y., Shkedy, D., de Graaf, P., Meulmeester, E., Edelson-Averbukh, M., Salek, M., Biton, S., Teunisse, A.F., Lehmann, W.D., and Jochemsen, A.G. (2005). Phosphorylation of Hdmx mediates its Hdm2-and ATM-dependent degradation in response to DNA damage. Proceedings of the National Academy of Sciences of the United States of America *102*, 5056-5061.

Perry, R.P., and Kelley, D.E. (1970). Inhibition of RNA synthesis by actinomycin D: characteristic dose-response of different RNA species. Journal of Cellular Physiology *76*, 127-139.

Pomerantz, J., Schreiber-Agus, N., Liégeois, N.J., Silverman, A., Alland, L., Chin, L., Potes, J., Chen, K., Orlow, I., and Lee, H.-W. (1998). The Ink4a tumor suppressor gene product, p19 Arf, interacts with MDM2 and neutralizes MDM2's inhibition of p53. Cell *92*, 713-723.

Post, S.M., Quintás-Cardama, A., Pant, V., Iwakuma, T., Hamir, A., Jackson, J.G., Maccio, D.R., Bond, G.L., Johnson, D.G., and Levine, A.J. (2010). A high-frequency regulatory polymorphism in the p53 pathway accelerates tumor development. Cancer Cell *18*, 220-230.

Powers, T., and Walter, P. (1999). Regulation of ribosome biogenesis by the rapamycin-sensitive TOR-signaling pathway in Saccharomyces cerevisiae. Molecular Biology of the Cell *10*, 987-1000.

Pullen, N., and Thomas, G. (1997). The modular phosphorylation and activation of p70s6k. FEBS letters *410*, 78-82.

Qi, Y., Gregory, M.A., Li, Z., Brousal, J.P., West, K., and Hann, S.R. (2004). p19ARF directly and differentially controls the functions of c-Myc independently of p53. Nature *431*, 712-717.

Radfar, A., Unnikrishnan, I., Lee, H.-W., DePinho, R.A., and Rosenberg, N. (1998). p19Arf induces p53-dependent apoptosis during Abelson virus-mediated pre-B cell transformation. Proceedings of the National Academy of Sciences *95*, 13194-13199.

Ringshausen, I., O'Shea, C.C., Finch, A.J., Swigart, L.B., and Evan, G.I. (2006). Mdm2 is critically and continuously required to suppress lethal p53 activity in vivo. Cancer Cell *10*, 501-514.

Robertson, K.D., and Jones, P.A. (1998). The human ARF cell cycle regulatory gene promoter is a CpG island which can be silenced by DNA methylation and down-regulated by wild-type p53. Molecular and Cellular Biology *18*, 6457-6473.

Roux, P.P., Shahbazian, D., Vu, H., Holz, M.K., Cohen, M.S., Taunton, J., Sonenberg, N., and Blenis, J. (2007). RAS/ERK signaling promotes site-specific ribosomal protein S6 phosphorylation via RSK and stimulates cap-dependent translation. Journal of Biological Chemistry *282*, 14056-14064.

Roxburgh, P., Hock, A.K., Dickens, M.P., Mezna, M., Fischer, P.M., and Vousden, K.H. (2012). Small molecules that bind the Mdm2 RING stabilize and activate p53. Carcinogenesis *33*, 791-798.

Rusk, N. (2009). Reverse ChIP. Nat Meth *6*, 187-187.

Ruvinsky, I., and Meyuhas, O. (2006). Ribosomal protein S6 phosphorylation: from protein synthesis to cell size. Trends in Biochemical Sciences *31*, 342-348.

Sabò, A., and Amati, B. (2014). Genome recognition by MYC. Cold Spring Harbor Perspectives in Medicine *4*, a014191.

Saitoh, M., Pullen, N., Brennan, P., Cantrell, D., Dennis, P.B., and Thomas, G. (2002). Regulation of an activated S6 kinase 1 variant reveals a novel mammalian target of rapamycin phosphorylation site. Journal of Biological Chemistry *277*, 20104-20112.

Sansom, O.J., Meniel, V.S., Muncan, V., Phesse, T.J., Wilkins, J.A., Reed, K.R., Vass, J.K., Athineos, D., Clevers, H., and Clarke, A.R. (2007). Myc deletion rescues Apc deficiency in the small intestine. Nature *446*, 676-679.

Sansom, O.J., Reed, K.R., Hayes, A.J., Ireland, H., Brinkmann, H., Newton, I.P., Batlle, E., Simon-Assmann, P., Clevers, H., and Nathke, I.S. (2004). Loss of Apc in vivo immediately perturbs Wnt signaling, differentiation, and migration. Genes & Development *18*, 1385-1390.

Saporita, A.J., Chang, H.-C., Winkeler, C.L., Apicelli, A.J., Kladney, R.D., Wang, J., Townsend, R.R., Michel, L.S., and Weber, J.D. (2011). RNA helicase DDX5 is a p53-independent target of ARF that participates in ribosome biogenesis. Cancer Research *71*, 6708-6717.

Sato, T., Vries, R.G., Snippert, H.J., van de Wetering, M., Barker, N., Stange, D.E., van Es, J.H., Abo, A., Kujala, P., and Peters, P.J. (2009). Single Lgr5 stem cells build crypt villus structures in vitro without a mesenchymal niche. Nature *459*, 262-265.

Schlosser, I., Hölzel, M., Hoffmann, R., Burtscher, H., Kohlhuber, F., Schuhmacher, M., Chapman, R., Weidle, U.H., and Eick, D. (2005). Dissection of transcriptional programmes in response to serum and c-Myc in a human B-cell line. Oncogene *24*, 520-524.

Schmitt, C.A., McCurrach, M.E., de Stanchina, E., Wallace-Brodeur, R.R., and Lowe, S.W. (1999). INK4a/ARF mutations accelerate lymphomagenesis and promote chemoresistance by disabling p53. Genes & Development *13*, 2670-2677.

Schuhmacher, M., Kohlhuber, F., Hölzel, M., Kaiser, C., Burtscher, H., Jarsch, M., Bornkamm, G.W., Laux, G., Polack, A., and Weidle, U.H. (2001). The transcriptional program of a human B cell line in response to Myc. Nucleic Acids Research *29*, 397-406.

Schwartzenberg-Bar-Yoseph, F., Armoni, M., and Karnieli, E. (2004). The tumor suppressor p53 down-regulates glucose transporters GLUT1 and GLUT4 gene expression. Cancer Research *64*, 2627-2633.

Schwitalla, S., Ziegler, P.K., Horst, D., Becker, V., Kerle, I., Begus-Nahrmann, Y., Lechel, A., Rudolph, K.L., Langer, R., and Slotta-Huspenina, J. (2013). Loss of p53 in Enterocytes Generates an Inflammatory Microenvironment Enabling Invasion and Lymph Node Metastasis of Carcinogen-Induced Colorectal Tumors. Cancer Cell *23*, 93-106.

Sears, R., Leone, G., DeGregori, J., and Nevins, J.R. (1999). Ras enhances Myc protein stability. Molecular Cell *3*, 169-179.

Sears, R., Nuckolls, F., Haura, E., Taya, Y., Tamai, K., and Nevins, J.R. (2000). Multiple Ras-dependent phosphorylation pathways regulate Myc protein stability. Genes & Development *14*, 2501-2514.

Serrano, M., Lin, A.W., McCurrach, M.E., Beach, D., and Lowe, S.W. (1997). Oncogenic ras provokes premature cell senescence associated with accumulation of p53 and p16 INK4a. Cell *88*, 593-602.

Seto, E., Usheva, A., Zambetti, G.P., Momand, J., Horikoshi, N., Weinmann, R., Levine, A.J., and Shenk, T. (1992). Wild-type p53 binds to the TATA-binding protein and represses transcription. Proceedings of the National Academy of Sciences *89*, 12028-12032.

Shangary, S., Qin, D., McEachern, D., Liu, M., Miller, R.S., Qiu, S., Nikolovska-Coleska, Z., Ding, K., Wang, G., and Chen, J. (2008). Temporal activation of p53 by a specific MDM2 inhibitor is selectively toxic to tumors and leads to complete tumor growth inhibition. Proceedings of the National Academy of Sciences *105*, 3933-3938.

Sherr, C.J. (2006). Divorcing ARF and p53: an unsettled case. Nature Reviews Cancer *6*, 663-673.

Shetty, S., Bruns, T., Weston, C.J., Stamataki, Z., Oo, Y.H., Long, H.M., Reynolds, G.M., Pratt, G., Moss, P., and Jalkanen, S. (2012). Recruitment mechanisms of primary and malignant B cells to the human liver. Hepatology *56*, 1521-1531.

Shvarts, A., Steegenga, W., Riteco, N., Van Laar, T., Dekker, P., Bazuine, M., Van Ham, R., Van Oordt, W.V.D.H., Hateboer, G., and Van der Eb, A. (1996). MDMX: a novel p53-binding protein with some functional properties of MDM2. The EMBO Journal *15*, 5349.

Sidman, C., Marshall, J., and Harris, A. (1988). Genetic Studies on Eμ-myc Transgenic Mice. In Mechanisms in B-Cell Neoplasia 1988 (Springer), pp. 94-99.

Smith, G.S., Walford, R.L., and Mickey, M.R. (1973). Lifespan and incidence of cancer and other diseases in selected long-lived inbred mice and their F1 hybrids. Journal of the National Cancer Institute *50*, 1195-1213.

Smith, M.L., Chen, I.-T., Zhan, Q., and Bae, I. (1994). Interaction of the p53-regulated protein Gadd45 with proliferating cell nuclear antigen. Science *266*, 1376.

Sobell, H.M., Jain, S., Sakore, T., and Nordman, C. (1971). Stereochemistry of actinomycin–DNA binding. Nature *231*, 200-205.

Song, H., Hollstein, M., and Xu, Y. (2007). p53 gain-of-function cancer mutants induce genetic instability by inactivating ATM. Nature Cell Biology *9*, 573-580.

Soragni, A., Janzen, D.M., Johnson, L.M., Lindgren, A.G., Nguyen, A.T.-Q., Tiourin, E., Soriaga, A.B., Lu, J., Jiang, L., and Faull, K.F. (2016). A designed inhibitor of p53 aggregation rescues p53 tumor suppression in ovarian carcinomas. Cancer Cell *29*, 90-103.

Steinman, H.A., Hoover, K.M., Keeler, M.L., Sands, A.T., and Jones, S.N. (2005). Rescue of Mdm4-deficient mice by Mdm2 reveals functional overlap of Mdm2 and Mdm4 in development. Oncogene *24*, 7935-7940.

Stommel, J.M., and Wahl, G.M. (2004). Accelerated MDM2 auto-degradation induced by DNA-damage kinases is required for p53 activation. The EMBO Journal *23*, 1547-1556.

Stott, F.J., Bates, S., James, M.C., McConnell, B.B., Starborg, M., Brookes, S., Palmero, I., Ryan, K., Hara, E., and Vousden, K.H. (1998). The alternative product from the human CDKN2A locus, p14ARF, participates in a regulatory feedback loop with p53 and MDM2. The EMBO Journal *17*, 5001-5014.

Sugimoto, M., Kuo, M.-L., Roussel, M.F., and Sherr, C.J. (2003). Nucleolar Arf tumor suppressor inhibits ribosomal RNA processing. Molecular Cell *11*, 415-424.

Szeliga, M., Bogacinska-Karas, M., Rozycka, A., Hilgier, W., Marquez, J., and Albrecht, J. (2014). Silencing of GLS and overexpression of GLS2 genes cooperate in decreasing the proliferation and viability of glioblastoma cells. Tumour biology : the journal of the International Society for Oncodevelopmental Biology and Medicine *35*, 1855-1862.

Tanimura, S., Ohtsuka, S., Mitsui, K., Shirouzu, K., Yoshimura, A., and Ohtsubo, M. (1999). MDM2 interacts with MDMX through their RING finger domains. FEBS letters *447*, 5-9.

Tao, W., and Levine, A.J. (1999). P19ARF stabilizes p53 by blocking nucleo-cytoplasmic shuttling of Mdm2. Proceedings of the National Academy of Sciences *96*, 6937-6941.

Teng, T., Mercer, C.A., Hexley, P., Thomas, G., and Fumagalli, S. (2013). Loss of tumor suppressor RPL5/RPL11 does not induce cell cycle arrest but impedes proliferation due to reduced ribosome content and translation capacity. Molecular and Cellular Biology *33*, 4660-4671.

Thut, C.J., Chen, J.-L., Klemm, R., and Tijan, R. (1995). p53 transcriptional activation mediated by coactivators TAF (II) 40 and TAF (II) 60. Science *267*, 100.

Tollini, L.A., Jin, A., Park, J., and Zhang, Y. (2014). Regulation of p53 by Mdm2 E3 ligase function is dispensable in embryogenesis and development, but essential in response to DNA damage. Cancer Cell *26*, 235-247.

Toshiyuki, M., and Reed, J.C. (1995). Tumor suppressor p53 is a direct transcriptional activator of the human bax gene. Cell *80*, 293-299.

Toth, P., Tucsek, Z., Tarantini, S., Sosnowska, D., Gautam, T., Mitschelen, M., Koller, A., Sonntag, W.E., Csiszar, A., and Ungvari, Z. (2014). IGF-1 deficiency impairs cerebral myogenic autoregulation in hypertensive mice. Journal of Cerebral Blood Flow & Metabolism *34*, 1887-1897.

Tovar, C., Rosinski, J., Filipovic, Z., Higgins, B., Kolinsky, K., Hilton, H., Zhao, X., Vu, B.T., Qing, W., and Packman, K. (2006). Small-molecule MDM2 antagonists reveal aberrant p53 signaling in cancer: implications for therapy. Proceedings of the National Academy of Sciences of the United States of America *103*, 1888-1893.

Valente, L.J., Gray, D.H., Michalak, E.M., Pinon-Hofbauer, J., Egle, A., Scott, C.L., Janic, A., and Strasser, A. (2013). p53 efficiently suppresses tumor development in the complete absence of its cell-cycle inhibitory and proapoptotic effectors p21, Puma, and Noxa. Cell Reports *3*, 1339-1345.

Valentin-Vega, Y., Okano, H., and Lozano, G. (2008). The intestinal epithelium compensates for p53-mediated cell death and guarantees organismal survival. Cell Death & Differentiation *15*, 1772-1781.

Valentin-Vega, Y.A., Box, N., Terzian, T., and Lozano, G. (2009). Mdm4 loss in the intestinal epithelium leads to compartmentalized cell death but no tissue abnormalities. Differentiation *77*, 442-449.

Van De Wetering, M., Sancho, E., Verweij, C., De Lau, W., Oving, I., Hurlstone, A., Van Der Horn, K., Batlle, E., Coudreuse, D., and Haramis, A.-P. (2002). The β-catenin/TCF-4 complex imposes a crypt progenitor phenotype on colorectal cancer cells. Cell *111*, 241-250.

van Riggelen, J., Yetil, A., and Felsher, D.W. (2010). MYC as a regulator of ribosome biogenesis and protein synthesis. Nature Reviews Cancer *10*.

Vassilev, L.T., Vu, B.T., Graves, B., Carvajal, D., Podlaski, F., Filipovic, Z., Kong, N., Kammlott, U., Lukacs, C., and Klein, C. (2004). In vivo activation of the p53 pathway by small-molecule antagonists of MDM2. Science *303*, 844-848.

Vladimirov, S.N., Ivanov, A.V., Karpova, G.G., Musolyamov, A.K., Egorov, T.A., Thiede, B., Wittmann-Liebold, B., and Otto, A. (1996). Characterization of the Human Small-Ribosomal-Subunit Proteins by N-Terminal and Internal Sequencing, and Mass Spectrometry. The FEBS Journal *239*, 144-149.

Vousden, K.H., and Ryan, K.M. (2009). p53 and metabolism. Nature Reviews Cancer *9*, 691-700.

Wade, M., Li, Y.-C., and Wahl, G.M. (2013). MDM2, MDMX and p53 in oncogenesis and cancer therapy. Nature Reviews Cancer *13*, 83-96.

Wade, M., Wang, Y.V., and Wahl, G.M. (2010). The p53 orchestra: Mdm2 and Mdmx set the tone. Trends in Cell Biology *20*, 299-309.

Wang, Y., Schwedes, J.F., Parks, D., Mann, K., and Tegtmeyer, P. (1995). Interaction of p53 with its consensus DNA-binding site. Molecular and Cellular Biology *15*, 2157-2165.

Wang, Y.V., Leblanc, M., Wade, M., Jochemsen, A.G., and Wahl, G.M. (2009). Increased radioresistance and accelerated B cell lymphomas in mice with Mdmx mutations that prevent modifications by DNA-damage-activated kinases. Cancer Cell *16*, 33-43.

Warner, J.R. (1999). The economics of ribosome biosynthesis in yeast. Trends in Biochemical Sciences *24*, 437-440.

Watson, J.D., Oster, S.K., Shago, M., Khosravi, F., and Penn, L.Z. (2002). Identifying genes regulated in a Myc-dependent manner. Journal of Biological Chemistry *277*, 36921-36930.

Weber, J.D., Taylor, L.J., Roussel, M.F., Sherr, C.J., and Bar-Sagi, D. (1999). Nucleolar Arf sequesters Mdm2 and activates p53. Nature Cell Biology *1*, 20-26.

White, P., Liebhaber, S.A., and Cooke, N.E. (2002). 129X1/SvJ mouse strain has a novel defect in inflammatory cell recruitment. The Journal of Immunology *168*, 869-874.

Wilkinson, D.S., Tlsty, T.D., and Hanas, R.J. (1975). The inhibition of ribosomal RNA synthesis and maturation in Novikoff hepatoma cells by 5-fluorouridine. Cancer Research *35*, 3014-3020.

Wu, X., Bayle, J.H., Olson, D., and Levine, A.J. (1993). The p53-mdm-2 autoregulatory feedback loop. Genes & Development *7*, 1126-1132.

Xiong, S., Pant, V., Suh, Y.-A., Van Pelt, C.S., Wang, Y., Valentin-Vega, Y.A., Post, S.M., and Lozano, G. (2010). Spontaneous tumorigenesis in mice overexpressing the p53-negative regulator Mdm4. Cancer Research *70*, 7148-7154.

Xiong, S., Van Pelt, C.S., Elizondo-Fraire, A.C., Liu, G., and Lozano, G. (2006). Synergistic roles of Mdm2 and Mdm4 for p53 inhibition in central nervous system development. Proceedings of the National Academy of Sciences of the United States of America *103*, 3226-3231.

Xiong, X., Zhao, Y., He, H., and Sun, Y. (2011). Ribosomal protein S27-like and S27 interplay with p53-MDM2 axis as a target, a substrate and a regulator. Oncogene *30*, 1798-1811.

Yang, Y., Ludwig, R.L., Jensen, J.P., Pierre, S.A., Medaglia, M.V., Davydov, I.V., Safiran, Y.J., Oberoi, P., Kenten, J.H., and Phillips, A.C. (2005). Small molecule inhibitors of HDM2 ubiquitin ligase activity stabilize and activate p53 in cells. Cancer Cell *7*, 547-559.

Zeller, K.I., Jegga, A.G., Aronow, B.J., O'Donnell, K.A., and Dang, C.V. (2003). An integrated database of genes responsive to the Myc oncogenic transcription factor: identification of direct genomic targets. Genome Biology *4*, 1.

Zhang, J., Wang, C., Chen, M., Cao, J., Zhong, Y., Chen, L., Shen, H.M., and Xia, D. (2013a). Epigenetic silencing of glutaminase 2 in human liver and colon cancers. BMC cancer *13*, 601.

Zhang, Q., He, X., Chen, L., Zhang, C., Gao, X., Yang, Z., and Liu, G. (2012). Synergistic regulation of p53 by Mdm2 and Mdm4 is critical in cardiac endocardial cushion morphogenesis during heart development. The Journal of Pathology *228*, 416-428.

Zhang, Q., Spears, E., Boone, D.N., Li, Z., Gregory, M.A., and Hann, S.R. (2013b). Domain-specific c-Myc ubiquitylation controls c-Myc transcriptional and apoptotic activity. Proceedings of the National Academy of Sciences *110*, 978-983.

Zhang, X.-d., Qin, Z.-h., and Wang, J. (2010). The role of p53 in cell metabolism. Acta Pharmacologica Sinica *31*, 1208-1212.

Zhang, X., Wang, W., Wang, H., Wang, M., Xu, W., and Zhang, R. (2013c). Identification of ribosomal protein S25 (RPS25)–MDM2–p53 regulatory feedback loop. Oncogene *32*, 2782-2791.

Zhang, Y., and Lu, H. (2009). Signaling to p53: ribosomal proteins find their way. Cancer Cell *16*, 369-377.

Zhang, Y., Wolf, G.W., Bhat, K., Jin, A., Allio, T., Burkhart, W.A., and Xiong, Y. (2003). Ribosomal protein L11 negatively regulates oncoprotein MDM2 and mediates a p53-dependent ribosomal-stress checkpoint pathway. Molecular and Cellular Biology *23*, 8902-8912.

Zhang, Y., Xiong, S., Li, Q., Hu, S., Tashakori, M., Van Pelt, C., You, M.J., Pageon, L., and Lozano, G. (2014a). Tissue-specific and age-dependent effects of global Mdm2 loss. The Journal of Pathology *233*, 380-391.

Zhang, Y., Xiong, Y., and Yarbrough, W.G. (1998). ARF promotes MDM2 degradation and stabilizes p53: ARF-INK4a locus deletion impairs both the Rb and p53 tumor suppression pathways. Cell *92*, 725-734.

Zhang, Y., Zhang, X., and Lu, H. (2014b). Aberrant activation of p53 due to loss of MDM2 or MDMX causes early lens dysmorphogenesis. Developmental Biology *396*, 19-30.

Zindy, F., Eischen, C.M., Randle, D.H., Kamijo, T., Cleveland, J.L., Sherr, C.J., and Roussel, M.F. (1998). Myc signaling via the ARF tumor suppressor regulates p53-dependent apoptosis and immortalization. Genes & Development *12*, 2424-2433.

Zoncu, R., Efeyan, A., and Sabatini, D.M. (2011). mTOR: from growth signal integration to cancer, diabetes and ageing. Nature reviews Molecular cell biology *12*, 21-35.

Zou, H., Henzel, W.J., Liu, X., Lutschg, A., and Wang, X. (1997). Apaf-1, a human protein homologous to C. elegans CED-4, participates in cytochrome c–dependent activation of caspase-3. Cell *90*, 405-413.